

A Combined Perfectly Matching Layer and  
Infinite Element Formulation for Unbounded  
Wave Problems

Joseph S. Pettigrew

Department of Mathematics and Statistics

University of Strathclyde

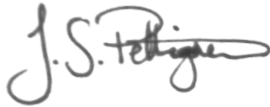
Glasgow, UK

April 23, 2019

This thesis is submitted to the University of Strathclyde for the  
degree of Doctor of Philosophy in the Faculty of Science.

This thesis is the result of the authors original research. It has been composed by the author and has not been previously submitted for examination which has led to the award of a degree.

The copyright of this thesis belongs to the author under the terms of the United Kingdom Copyright Acts as qualified by University of Strathclyde Regulation 3.50. Due acknowledgement must always be made of the use of any material contained in, or derived from, this thesis.

Signed:   
Date: 23/4/19

# Acknowledgements

I am sincerely grateful to my supervisor, Prof. Anthony J. Mulholland, for all the help, support, advice and time he has given me throughout my studies at Strathclyde. It has been invaluable.

I would like to thank my industrial sponsors, Weidlinger Associates, Inc., for allowing me the opportunity to pursue a further degree and, in particular, Gerry Harvey, Andrew Tweedie, John Mould, and Jeffrey Cipolla for their help.

I would also like to thank the staff at the Centre for Ultrasonic Engineering and everyone else in the Department of Mathematics and Statistics at the University of Strathclyde.

I would like to extend my thanks in a special way to my mother, my sister, and my wife, Emma, who have been unceasing in their support and encouragement throughout my studies. I could not have done it without them.

Finally, I would like to dedicate this thesis to my father, John Pettigrew, who sadly passed away during my second year of undergraduate studies and so never had the chance to see me graduate. This is for you, dad.

# Contents

<b>1</b>	<b>Introduction</b>	<b>1</b>
1.1	Background & Motivation . . . . .	1
1.1.1	Ultrasound . . . . .	2
1.1.2	Non-Destructive Evaluation . . . . .	3
1.1.3	Infinite Domains . . . . .	4
1.2	Outline of the Thesis . . . . .	7
<b>2</b>	<b>A Combined Perfectly Matching Layer and Infinite Element Formulation for Unbounded Wave Problems in the Frequency Domain</b>	<b>10</b>
2.1	Geometry and Governing Equations . . . . .	11
2.2	The Exact Solution . . . . .	13
2.3	The Variational Formulation in the Frequency Domain . . . . .	18
2.3.1	Perfectly Matching Layer Coordinate Transformation . . . . .	19
2.3.2	Formulation of the Discrete Problem . . . . .	20
2.3.3	Selection of Radial Basis Functions ( $f$ ) and Test Functions ( $w$ ) . . . . .	24
2.3.4	The Transverse Discretisation . . . . .	28
2.3.5	The Case $z = r$ . . . . .	33

2.4	Perfectly Matching Layer & Infinite Element Combination . . . . .	37
2.5	Results . . . . .	40
2.5.1	Unconjugated Burnett formulation . . . . .	40
2.5.2	Conjugated Burnett formulation . . . . .	46
2.5.3	Astley-Leis formulation . . . . .	49
2.6	Conclusion . . . . .	54

<b>3</b>	<b>A Combined Perfectly Matching Layer and Infinite Element For- mulation for the Three Dimensional Elastodynamic Wave Equa- tion</b>	<b>56</b>
3.1	Motivation . . . . .	56
3.2	Background . . . . .	57
3.3	Geometry and Governing Equations . . . . .	58
3.4	Constant stretching . . . . .	66
3.4.1	The velocity equations . . . . .	66
3.4.2	The stress equations . . . . .	86
3.4.3	The final solution . . . . .	101
3.5	Retaining a spatial dependency . . . . .	106
3.5.1	The velocity equations . . . . .	106
3.5.2	The stress equations . . . . .	116
3.5.3	The final solution . . . . .	130
3.6	Implementation . . . . .	133
3.7	Results . . . . .	136
3.7.1	Constant Stretching . . . . .	138
3.7.2	Spatially Dependent Stretching . . . . .	141
3.8	Conclusion . . . . .	146

<b>4</b>	<b>Conclusions</b>	<b>147</b>
4.1	Introduction . . . . .	147
4.2	Results . . . . .	149
4.3	Future Work . . . . .	151
4.4	Concluding Remarks . . . . .	152
<b>A</b>	<b>The stiffness tensor</b>	<b>160</b>

# Chapter 1

## Introduction

### 1.1 Background & Motivation

In many practical problems the spatial domain is much larger than the region of interest. When this happens it is useful to study a smaller domain containing the region of interest and simply assume that the outer domain extends to infinity [1]. This is particularly useful in numerical modelling and simulation, where resources are limited by memory and processing power [2]. These models and simulations have important roles in ultrasonic non-destructive evaluation/testing (NDE/NDT), a method of inspection using high frequency acoustic/elastic waves, often used in safety critical industries such as nuclear power and aerospace [3, 4].

One method of numerical simulation is the Finite Element Method (FEM), a process whereby a complicated region is reduced to a collection of smaller, simpler shapes, such as triangles, tetrahedrals, hexahedrals, etc., and within which the solution is described by a set of basis functions [5]. The problem can then be solved over each element and, by extension, over the whole domain. In order to simulate infinite domains, appropriate boundary conditions must be employed, at

the interface between the interior spatial domain and the outer (infinite) domain, that absorb without reflection any wave radiating from the interior domain [6]. A number of such boundary conditions have been developed for this purpose, each with their own advantages and disadvantages. These include Absorbing Boundary Conditions [7], Perfectly Matching Layers [8] and Infinite Elements [9].

### 1.1.1 Ultrasound

Acoustic waves with a frequency greater than 20kHz, the upper range of human hearing [10], can be classed as ultrasonic. These high frequency oscillating acoustic pressure waves are often found in use by animals and insects, such as dolphins, bats and moths, as a method of navigation and to locate predators or prey [11–14].

Ultrasound is also used within the field of medicine, most notably for obstetric sonography, wherein real-time images can be generated to monitor the health and development of a foetus in utero without any adverse effects and to aid in treatment of both foetus and mother [15–19]. It is also used as a medical imaging tool for other diagnostic purposes, including visualisations of organs such as the heart in echocardiograms and intravascular imaging [20–24]. While medical ultrasound is commonplace today, it took almost four decades from its inception in the 1920s until it began to flourish, with Professor Ian Donald of Glasgow playing no small part in its growth in the field [25–27]. Today the technology is used safely in a wide range of medical applications from ultrasound mammography in breast cancer imaging [28–31], assessment of osteoporosis [32–35], characterisation of abdominal aortic aneurisms [36–39], focused drug delivery for neurological conditions such as Parkinson’s, Alzheimer’s and glioblastoma [40–43], tissue characterisation in the vascular system to aid in the treatment of atherosclerosis and prevention of ischemic strokes [44–47], histotripsy, a method of mechanical tissue fractionation



using high intensity ultrasound pulses [48–51], and lithotripsy, whereby ultrasonic waves are used to break up kidney stones or other hard masses so that they may be easily passed through the body [52–55]. Ultrasound has even found use in dentistry, where it may be used for simple scaling of the teeth to cleaning inaccessible surfaces during root canal treatment, assessment of maxillofacial fractures, and implant dentistry [56–59].

Another use for the technology was advanced by the threat of the First World War and the use of submarines in combat for the first time. An early form of SONAR, an acronym for **SO**und **N**avigation **A**nd **R**anging, was in use by 1915 with British submarines fitted with Fessenden oscillator hydrophones to detect enemy vessels [60, 61]. While SONAR is still widely used in defence and civil applications, the study of ultrasound has even led to the development of acoustic cloaking techniques to effectively make vessels invisible to ultrasound waves [62–64].

Other modern applications include ultrasound assisted extraction (UAE) in the food, pharmaceutical, cosmetic and bioenergy industries [65–68], wastewater treatment [69–72], sanitary treatment of fresh produce to reduce the risk of microbial contamination such as *E. coli* and salmonella in the food industry [73–76], and the development of guidance systems for unmanned aerial vehicles (drones) with applications to the power industry [77].

### **1.1.2 Non-Destructive Evaluation**

Non-destructive evaluation (NDE), sometimes referred to as non-destructive testing (NDT), is the collective name for a number of techniques used to inspect safety critical structures such as nuclear power stations [78], oil pipelines [79], aerospace components [80], turbine blades [81], and many more. They are deployed to de-

tect defects, take measurements of thickness, and characterise the internal geometry of the structure. There are many types of NDE techniques, each with their own strengths and weaknesses, from the most basic visual inspection, to thermal imaging, electromagnetic testing, X-ray radiography, computed tomography and shearography testing [82,83]. Ultrasonic NDT, using high frequency elastic waves, is a popular method by which components can be inspected to ensure reliability without compromising their functionality. In recent years, this method has grown in popularity due to being relatively inexpensive and the portability of the necessary equipment, which can often be reduced to a hand-held device. Other benefits include the potential for automating processes and the possibility of real-time results [84].

### **1.1.3 Infinite Domains**

By infinite domains, we refer to spatial domains that have infinite length or area or volume. In real world modelling, infinite domains appear in many situations, and in others it is convenient to consider a large domain to be infinite. The problem arises in many fields including acoustics [85], geophysics [86], oceanography [87], meteorology [88], gas dynamics [89], hydrodynamics [90] and electromagnetics [91]. For instance, in earthquake engineering, the infinite domain would be the earth and the region of interest would be a much smaller region around a structure or seismic source; in underwater acoustics the infinite domain could be the ocean, while the region of interest is a smaller region around a submarine or other submerged body; and in aerospace problems, the infinite domain may be atmospheric air while the region of interest relates only to the flow around an airplane wing [92]. In cases such as this it is necessary to employ a boundary condition on the exterior of the computational domain to prevent outgoing waves reflecting back into the region

of interest.

A number of methods exist to deal with these reflections within numerical simulation, such as Absorbing Boundary Conditions (ABC) [7], Boundary Element Methods (BEM), Perfectly Matching Layers (PML) [8] and Infinite Elements (IE) [9]. A review of Finite Element Method (FEM) techniques for time-harmonic acoustics, and in particular for boundary conditions such as absorbing boundary conditions, infinite elements and absorbing layers, is carried out in [93, 94], while [95–97] also examine PMLs for time-harmonic acoustics with FEM. FEM methods for modelling the elastic wave equation with PMLs in both the time and frequency domain are presented in [98–101]. FEM has been used extensively in the modelling of ultrasound devices and systems [102–108], with many Finite Element Analysis software packages available, including PZFlex [109].

Three main categories of Absorbing Boundary Conditions can be considered: low order local ABCs, high order local ABCs and exact nonlocal ABCs. Low order local ABCs are the classical ABCs proposed in the 1970s and 1980s and are still in use today [110, 111]. They can be considered a generalisation of the Sommerfeld radiation condition, but are only effective with low order operators as the product-nature of the operators generate higher order derivatives making implementation impractical at higher orders. High order local ABCs are derived in the same way as low order local ABCs but with the introduction of an auxiliary variable in the transformed plane leading to no derivatives beyond second order and no normal derivatives of the auxiliary variables [112]. Exact nonlocal ABCs have the property that the solution obtained in the finite domain is identical to that in the unbounded domain, but the cost is an integral operator that couples all points on the boundary, making it powerful in frequency dependent problems, but difficult in the time-dependent case [113].

Boundary Integral Methods and Boundary Element Methods apply surface elements on the boundary of a finite domain, meaning they are often more efficient than domain-based methods due to the reduction of dimensions. An overview of the development of these techniques is provided in [114] alongside historical biographies of its chief proponents. BEMs are especially suited to problems in unbounded domains, since the problem is reduced to the physical boundary without the need for the introduction of an artificial boundary. However, BEMs often produce matrices which are dense and nonsymmetrical, resulting in large solution times and memory requirements for computational solutions.

The PML technique (first presented by Berenger [8]) is based on the use of an absorbing layer, with the matching medium designed to absorb without reflection and prevent any wave travelling back into the computational domain. While Berenger dealt with electromagnetic waves, Chew and Liu [115] proved there exists a fictitious elastic PML half-space in solids which completely absorbs elastic waves in spite of the coupling between compressional and shear waves. This was achieved by interpreting the PML as coordinate stretching in the frequency domain. In the same year, Lyons et al. [116] demonstrated the accuracy and future potential of the PML in a finite element formulation. The work of Liu and Tao [117] and Qi and Geers [118] extended the PML to simulate acoustic wave propagation in absorptive media and demonstrated its excellent absorbing ability. The PML was also shown to be effective in numerically solving the Helmholtz equation by Turkel and Yefet [119] and developed further for time harmonic elastodynamics by Basu and Chopra [120]. More recently, the performance of the PML has been improved with the use of adaptive meshing [121, 122]. Further work has included development of higher order PMLs [123] and formulation for the Finite Difference Time Domain (FDTD) simulation of acoustic scattering with PMLs [124].

An alternative approach is to use Infinite Elements at the boundary rather than truncating the finite element mesh. These Infinite Elements essentially extend the element domain to infinity, and are based on the shape functions used in the interior elements; the shape function is multiplied by an appropriate decay function to achieve the desired behaviour at infinity. The IE method is discussed in detail by Bettess [9] while Astley [125] provides a review of IE formulations with various element types and assesses their accuracy. Infinite Elements have been applied to the acoustic wave equation in the frequency domain [126–133] and in the time domain [134–137], as well as to the elastic wave equation in the time domain [138], while [139, 140] also explored transient infinite elements.

## 1.2 Outline of the Thesis

The aim of this thesis is to devise a new boundary condition for unbounded elastodynamic wave problems for use in the finite element modelling of ultrasound devices and systems. To do so the coordinate stretching transformation of a perfectly matching layer will be combined with infinite element test functions for what is believed to be the first time, and applied to both the acoustic and elastic wave equations. The problem of a radiating sphere will be examined in the frequency domain, while a three dimensional formulation capable of modelling elastodynamic waves in a volume will be examined in the time domain using the special case of a semi-infinite waveguide. Three types of infinite element will be assessed with a particular stretching function, the form of which has not been optimised. The original material in this thesis is as follows:

1. In Chapter 2 the problem of a vibrating sphere in the frequency domain is considered in order to provide an exact solution with which to assess the

accuracy of the new PML+IE formulation. The inertia and resistance are derived from the acoustic response in order to be used as a measure of accuracy. A variational formulation is used to introduce the infinite elements while, in section 2.3.1, a coordinate stretching function introduces the perfectly matching layer to the derivation for the first time. Three types of infinite element are considered: the unconjugated Burnett element, the conjugated Burnett element and the Astley-Leis element. It is shown that the infinite element only formulation can be derived via a particular choice of PML stretching function. An error measure is introduced as the difference between the PML+IE formulation and the exact solution for both inertia and resistance and integrated over a range of wavelengths for a number of acoustic modes. Finally, a set of stretching function parameters is assessed to show that it is possible to achieve greater accuracy using the new PML+IE formulation than by using the IE only method.

2. In Chapter 3 a method for studying elastodynamic waves in a three dimensional, heterogeneous volume is constructed with a PML+IE formulation at its boundary. For the present work, this method is used to conduct a numerical study of a semi-infinite one dimensional rectangular homogeneous waveguide, thereby allowing an empirical comparison of the method to an infinite element only approach. Section 3.3 introduces the elastodynamic wave equation. Fourier transforms in time are taken in order to introduce the coordinate stretching transformation. The variational formulation is again followed with the assumption that the material is locally isotropic. The problem is discretised with traditional hexahedral finite elements modelling the inner domain and infinite element test functions introduced in the exterior

domain. Two scenarios are considered: the case with constant PML stretching in all three directions and the case with stretching in only one direction. Mass lumping and diagonalisation is performed in order to provide an explicit scheme for implementation. A reflection coefficient is then defined and used to compare the new PML+IE formulation with the FE only implementation and used to find values for the PML stretching function parameters that maximise the reduction in the reflected wave.

## Chapter 2

# A Combined Perfectly Matching Layer and Infinite Element Formulation for Unbounded Wave Problems in the Frequency Domain

In this chapter, we will consider a scalar problem and propose a Perfectly Matching Layer [8] and Infinite Element [9] combination (PML+IE) for waves in a fluid. We will assess its performance by calculating the pressure exterior to a vibrating sphere in the frequency domain. The aim of this new PML+IE concept is to create an element that is able to absorb long-wavelength waves at all angles of incidence and also to converge to the correct low-frequency limit. The spherical radiator is considered as it has an exact solution and so a robust assessment of the new technique can be made. It allows a comparison to be made between the



PML+IE solution and the IE only solution via the surface inertia and resistance in the near field across a range of  $kR$  values (wavenumber  $\times$  radius of sphere). Results indicate that for certain modes there is a marked improvement (in the difference between the exact and approximate solutions) at lower frequencies for the PML+IE combination.

## 2.1 Geometry and Governing Equations

We consider the exterior Helmholtz problem with the geometry shown in Figure 2.1 as in [125] where  $\Gamma$  is an arbitrarily shaped radiating surface,  $\Omega_i$  is the inner domain, modelled by conventional Finite Element Method techniques, and  $\Omega_e$  is the outer domain, modelled by IE/PML combinations.

The complex pressure amplitude  $p(\mathbf{x}, k)$  satisfies the Helmholtz equation [125]

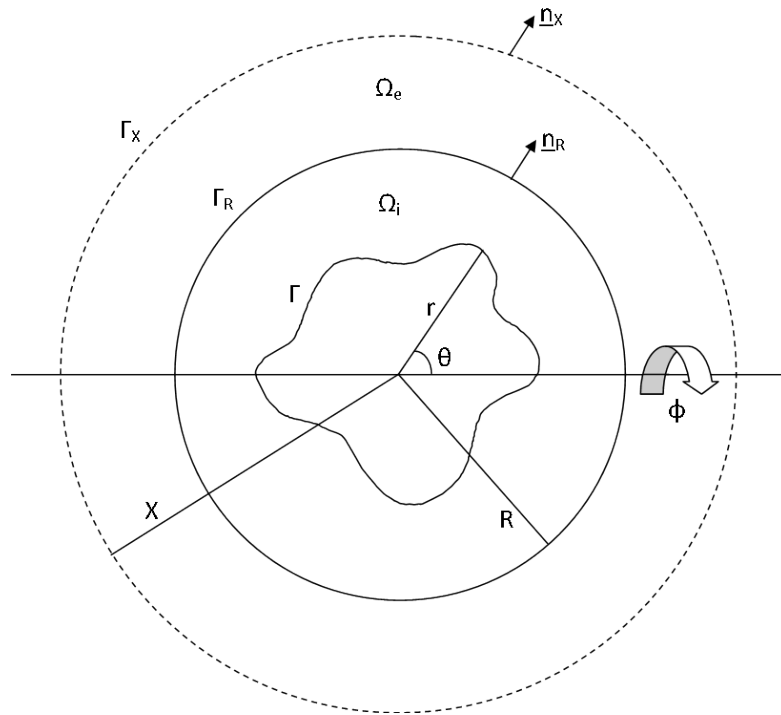
$$\nabla^2 p + k^2 p = 0 \quad \text{in } \Omega_e \quad (2.1)$$

where it is assumed that  $p$  is time harmonic,  $p = p(\mathbf{x}, k)e^{i\omega t}$ , with boundary conditions

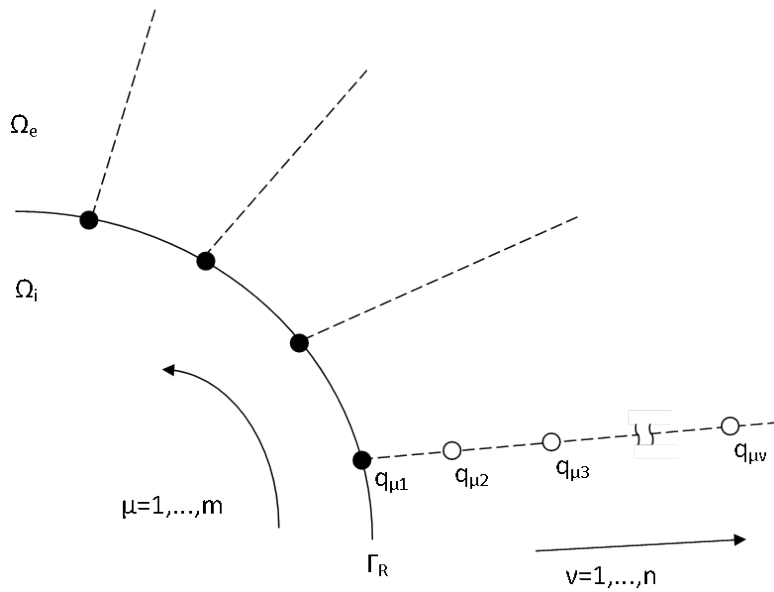
$$\nabla p \cdot \mathbf{n}_R = -\rho a(\theta, \phi) \quad \text{on } \Gamma_R, \quad (2.2)$$

$$\nabla p \cdot \mathbf{n}_X = -ikp + \epsilon \quad \text{on } \Gamma_X, \quad (2.3)$$

where  $\epsilon = O(\frac{1}{X^2})$  as  $X \rightarrow \infty$ , and where  $\Gamma_R$  is the boundary of  $\Omega_i$ ,  $\Gamma_X$  is the boundary of  $\Omega_e$  with radius  $X$ ,  $\mathbf{n}_R$  and  $\mathbf{n}_X$  are vectors normal to the surfaces of  $\Omega_i$  and  $\Omega_e$ , respectively,  $k$  is the wavenumber, and  $\theta$  and  $\phi$  are the angles shown in Figure 2.1. Equation (2.2) is the kinematic condition on  $\Gamma_R$  for a steady time harmonic normal acceleration  $a(\theta, \phi)e^{i\omega t}$  with fluid density  $\rho$ , and equation (2.3)



(a) Geometry of the exterior problem. The radius  $R$  of the domain  $\Omega_i$  is fixed and the domain is meshed by standard finite elements.



(b) Ordering of infinite element nodal parameters on the boundary of the meshed region  $\Omega_i$ .

Figure 2.1: A schematic showing the domain  $\Omega_e$  where the Perfectly Matching Layer and Infinite Element formulation is applied.

is the Sommerfeld radiation condition [141] in three dimensions.

## 2.2 The Exact Solution

For  $r > R$ , that is in the exterior domain  $\Omega_e$ , any wave satisfying the Sommerfeld radiation condition given by equation (2.3) can be expanded as an infinite series of multipole terms [125]

$$p(\mathbf{x}, k) = \left( \frac{\alpha_1(\theta, \phi)}{r} + \frac{\alpha_2(\theta, \phi)}{r^2} + \frac{\alpha_3(\theta, \phi)}{r^3} + \dots \right) e^{-ikr} \quad (2.4)$$

which we will see later in equation (2.24). Alternatively it can be regarded as consisting of outwardly propagating separable modes [142] of the form

$$p(\mathbf{x}, k) = \sum_{\mu=1}^{\infty} \sum_{\nu=1}^{\infty} A_{\mu\nu} h_{\mu-1}^{(2)}(kr) Y_{\mu\nu}(\theta, \phi), \quad (2.5)$$

where  $h_{\mu-1}^{(2)}$  is the spherical Hankel function of the second kind of order  $\mu - 1$ , and where

$$Y_{\mu\nu}(\theta, \phi) = P_{\mu-1}^{\nu-1}(\cos \theta) e^{\pm i(\nu-1)\phi},$$

wherein  $P_{\mu-1}^{\nu-1}$  denotes the Legendre function of order  $\nu - 1$  and degree  $\mu - 1$ .

For the axisymmetric case, the double summation in equation (2.5) reduces to

$$p(\mathbf{x}, k) = \sum_{\mu=1}^{\infty} A_{\mu} h_{\mu-1}^{(2)}(kr) P_{\mu-1}(\cos \theta). \quad (2.6)$$

From equation (2.2), the boundary condition becomes

$$\frac{\partial p}{\partial r} = -\rho \frac{\partial u}{\partial t},$$

where  $u$  is the velocity since  $a(\theta, \phi)$  is the acceleration. So we have

$$\sum_{\mu=1}^{\infty} A_{\mu} P_{\mu-1}(\cos \theta) h_{\mu-1}^{(2)'}(kr) k e^{i\omega t} = -\rho \frac{\partial u}{\partial t}.$$

Integrating with respect to  $t$  gives

$$u = \frac{i}{\rho c} \sum_{\mu=1}^{\infty} A_{\mu} P_{\mu-1}(\cos \theta) h_{\mu-1}^{(2)'}(kr) e^{i\omega t},$$

where  $c = \omega/k$ . Then the specific acoustic impedance of degree (multipole order)  $\mu$ , defined by  $\bar{Z}_{\mu} = p/u$ , is given by

$$\bar{Z}_{\mu} = -i\rho c \frac{h_{\mu-1}^{(2)}(kr)}{h_{\mu-1}^{(2)'}(kr)}.$$

The quantities acoustic resistance,  $\bar{R}(k, \theta)$ , and acoustic reactance,  $\bar{X}(k, \theta)$ , are defined by the relation  $\bar{Z} = \bar{R}(k, \theta) + i\bar{X}(k, \theta)$  [142]. We define the normalised acoustic impedance by  $Z_{\mu} = \bar{Z}/\rho c$ , thus, by extension, the normalised acoustic resistance,  $R_{\mu}$ , and the normalised acoustic reactance,  $X_{\mu}$ , are given by

$$R_{\mu} = \frac{\bar{R}_{\mu}}{\rho c} = \text{Re} \left\{ -\frac{i h_{\mu-1}^{(2)}(kr)}{h_{\mu-1}^{(2)'}(kr)} \right\} = \text{Im} \left\{ \frac{h_{\mu-1}^{(2)}(kr)}{h_{\mu-1}^{(2)'}(kr)} \right\} \quad (2.7)$$

and

$$X_{\mu} = \frac{\bar{X}_{\mu}}{\rho c} = \text{Im} \left\{ -\frac{i h_{\mu-1}^{(2)}(kr)}{h_{\mu-1}^{(2)'}(kr)} \right\} = \text{Re} \left\{ -\frac{h_{\mu-1}^{(2)}(kr)}{h_{\mu-1}^{(2)'}(kr)} \right\}. \quad (2.8)$$

for each multipole order  $\mu$ .

We introduce the acoustic response, as in [125], defined by  $p/a$ . From the definition of specific acoustic impedance, we have  $\bar{Z} = i\omega p/a$  since  $a = i\omega u$ . Then

$$\frac{p}{a} = \frac{\bar{R}}{ikc} + \frac{\bar{X}}{kc} = \frac{\bar{X}}{kc} - i\frac{\bar{R}}{kc} = \bar{S} - i\frac{\bar{R}}{kc}, \quad (2.9)$$

where

$$\bar{S} = \frac{\bar{X}(k, \theta)}{kc}$$

is called the acoustic inertia and

$$R_\mu = -\frac{k}{\rho} \text{Im} \left( \frac{p}{a} \right). \quad (2.10)$$

To obtain the specific acoustic inertia we follow the process outlined in [143] utilising recurrence relations in Chapter 10 of [144] for the spherical Hankel function of the second kind given by

$$h_{\mu-1}^{(2)'}(kr) = \frac{\mu-1}{kr} h_{\mu-1}^{(2)}(kr) - h_\mu^{(2)}(kr)$$

to give

$$Z_\mu = \frac{-i}{(\mu-1)/kr - h_\mu^{(2)}(kr)/h_{\mu-1}^{(2)}(kr)}.$$

Then from the limiting form of Bessel functions for small arguments [144] we have

$$h_\mu^{(2)}(kr) = \frac{(kr)^\mu}{(2\mu+1)!!} + i \frac{(2\mu-1)!!}{(kr)^{\mu+1}}$$

where  $0 < k \ll 1$ , and where !! denotes the double factorial defined as

$$(2k-1)!! = \prod_{i=1}^k (2i-1).$$

Then

$$\begin{aligned}
\frac{h_{\mu}^{(2)}(kr)}{h_{\mu-1}^{(2)}(kr)} &= \frac{\frac{(kr)^{\mu}}{(2\mu+1)!!} + i\frac{(2\mu-1)!!}{(kr)^{\mu+1}}}{\frac{(kr)^{\mu-1}}{(2\mu-1)!!} + i\frac{(2\mu-3)!!}{(kr)^{\mu}}} \\
&= \frac{((kr)^{4\mu} + (2\mu-1)!!^2(2\mu-3)!!(2\mu+1)!!)(2\mu-1)!!^2(kr)^{2\mu}}{(2\mu+1)!!(2\mu-1)!!(kr)^{2\mu+1}((kr)^{4\mu-2} + (2\mu-3)!!^2(2\mu-1)!!^2)} \\
&\quad - i\frac{((kr)^2 - (2\mu+1)(2\mu-1))(2\mu-1)!!^2(kr)^{2\mu}}{((kr)^{4\mu-2} + (2\mu-3)!!^2(2\mu-1)!!^2)(2\mu+1)(2\mu-1)(kr)^2} \\
&\approx \frac{(2\mu-1)!!^2(2\mu-3)!!(2\mu+1)!!(2\mu-1)}{(2\mu+1)(2\mu-3)!!^2(2\mu-1)!!^2(kr)} \\
&\quad + i\frac{(2\mu+1)(2\mu-1)(2\mu-1)!!^2(kr)^{2\mu}}{(2\mu-3)!!^2(2\mu-1)!!^2(2\mu+1)(2\mu-1)(kr)^2} \\
&\approx \frac{2\mu-1}{kr} + i\left(\frac{(kr)^{\mu-1}}{(2\mu-3)!!}\right)^2.
\end{aligned}$$

Therefore, for small arguments,

$$\begin{aligned}
Z_\mu &= - \frac{i}{\frac{\mu-1}{kr} - \frac{2\mu-1}{kr} - i \left( \frac{(kr)^{\mu-1}}{(2\mu-3)!!} \right)^2} \\
&= - \frac{i \left( \frac{-\mu}{kr} + i \left( \frac{(kr)^{\mu-1}}{(2\mu-3)!!} \right)^2 \right)}{\left( \frac{-\mu}{kr} \right)^2 + \left( \frac{(kr)^{\mu-1}}{(2\mu-3)!!} \right)^4} \\
&= \frac{(kr)^{2\mu} (2\mu-3)!!^2 + i\mu kr (2\mu-3)!!^4}{\mu^2 (2\mu-3)!!^4 + (kr)^{4\mu-2}} \\
&\approx \left( \frac{(kr)^\mu}{\mu(2\mu-3)!!} \right)^2 + i \frac{kr}{\mu}.
\end{aligned}$$

Then, from equation (2.9), we have that  $S^*$ , the asymptotic behaviour of  $\bar{S}$ , is given by

$$\begin{aligned}
S^* &= \operatorname{Re} \left( \frac{p}{a} \right) \\
&= \operatorname{Re} \left( \frac{\bar{Z}}{i\omega} \right) \\
&= \operatorname{Re} \left( \frac{Z\rho c}{i\omega} \right) \\
&= \frac{\rho r}{\mu},
\end{aligned}$$

so then the specific inertia is given by

$$S_\mu = \frac{\bar{S}}{S^*} = \frac{\mu}{\rho r} \bar{S}. \tag{2.11}$$

Therefore, from equations (2.8), (2.9) and (2.11), the normalised specific inertia is given by

$$S_\mu = \text{Re} \left\{ \frac{-\mu h_{\mu-1}^{(2)}(kr)}{(kr) h_{\mu-1}^{(2)'}(kr)} \right\}. \quad (2.12)$$

We will use these exact solutions for specific resistance and inertia, given by equations (2.7) and (2.12), respectively, to compare with the numerical values given by our PML+IE formulation.

## 2.3 The Variational Formulation in the Frequency Domain

In this chapter the variational formulation of the problem is presented with the introduction of a perfectly matching layer coordinate transformation. The discrete problem is then derived and a selection of basis functions and test functions in the radial and transverse directions are introduced with three forms of infinite element. From the discrete problem, the acoustic response is derived as a numerical measure with which to assess the accuracy of the PML+IE formulation contrasted with the IE only formulation in comparison to the acoustic response of the exact solution. Finally, the particular case for the perfectly matching layer coordinate transformation  $z = r$  is examined and shown to replicate the infinite element only case of [125].

Multiplying equation (2.1) by a test function  $w(\mathbf{x}, k)$  and integrating over  $\Omega_e$  gives

$$\int_{\Omega_e} (w \nabla^2 p + k^2 w p) d\Omega_e = 0.$$



Applying the divergence theorem, we have

$$-\int_{\Omega_e} (\nabla w \cdot \nabla p - k^2 w p) d\Omega_e + \int_{\Gamma} w \nabla p \cdot \mathbf{n} d\Gamma = 0,$$

and incorporating the boundary conditions given by equations (2.2) and (2.3) gives

$$\int_{\Omega_e} (\nabla w \cdot \nabla p - k^2 w p) d\Omega_e + \int_{\Gamma_X} w (ikp - \epsilon) d\Gamma_X - \int_{\Gamma_R} w (\rho a) d\Gamma_R = 0,$$

since  $\mathbf{n} = -\mathbf{n}_X$  on  $\Gamma_X$ . That is

$$\int_{\Omega_e} (\nabla w \cdot \nabla p - k^2 w p) d\Omega_e + \int_{\Gamma_X} (ikwp - w\epsilon) d\Gamma_X - \rho \int_{\Gamma_R} w a d\Gamma_R = 0. \quad (2.13)$$

### 2.3.1 Perfectly Matching Layer Coordinate Transformation

We introduce the stretching function  $z \in \mathbb{C}$  defined by

$$z(r) = \int_R^r \lambda(s) ds,$$

so that  $\partial z(r)/\partial r = \lambda(r)$ . At present, the choice of the function  $\lambda(r)$  is arbitrary.

In practice, it will be used to adjust and improve the performance of the PML element. Then  $\partial/\partial z = 1/\lambda(r)\partial/\partial r = 1/z'(r)\partial/\partial r$  and so

$$\begin{aligned} \nabla_z &= \left( \frac{1}{z} \frac{\partial}{\partial \theta}, \frac{1}{z \sin \theta} \frac{\partial}{\partial \phi}, \frac{1}{\lambda(r)} \frac{\partial}{\partial r} \right), \\ &= \left( \frac{r}{z} \left( \frac{1}{r} \frac{\partial}{\partial \theta} \right), \underbrace{\frac{r}{z} \left( \frac{1}{r \sin \theta} \frac{\partial}{\partial \phi} \right)}_{= \frac{r}{z} \nabla_{\theta\phi}}, \frac{1}{z'(r)} \frac{\partial}{\partial r} \right). \end{aligned}$$

Also,

$$\begin{aligned}
d\Omega_z &= z^2 \sin \theta dz d\theta d\phi, \\
&= \left(\frac{z}{r}\right)^2 z' r^2 \sin \theta dr d\theta d\phi, \\
&= \left(\frac{z}{r}\right)^2 z' d\Omega_e, \\
&= \left(\frac{z}{R}\right)^2 z' dr d\Gamma_R,
\end{aligned}$$

since  $d\Omega_e = r^2 \sin \theta dr d\theta d\phi$  and  $d\Gamma_R = R^2 \sin \theta d\theta d\phi$ . Now equation (2.13) becomes

$$\begin{aligned}
&\int_{\Omega_z} (\nabla_z w \cdot \nabla_z p - k^2 w p) d\Omega_z + \int_{\Gamma_X} (ikwp - w\epsilon) d\Gamma_X \\
&- \rho \int_{\Gamma_R} w a d\Gamma_R = 0
\end{aligned}$$

which gives

$$\begin{aligned}
&\int_{\Omega_z} \left[ \left(\frac{r}{z}\right)^2 \nabla_{\theta\phi} w \cdot \nabla_{\theta\phi} p + \frac{1}{(z')^2} \frac{\partial w}{\partial r} \frac{\partial p}{\partial r} - k^2 w p \right] \left(\frac{z}{R}\right)^2 z' dr d\Gamma_R \\
&+ \int_{\Gamma_X} (ikwp - w\epsilon) d\Gamma_X - \rho \int_{\Gamma_R} w a d\Gamma_R = 0.
\end{aligned} \tag{2.14}$$

### 2.3.2 Formulation of the Discrete Problem

A trial solution

$$p(\mathbf{x}, k) = \sum_{\mu=1}^m \sum_{\nu=1}^n q_{\mu\nu} f_{\nu}(r, k) g_{\mu}(\theta, \phi) \tag{2.15}$$

is proposed where  $q_{\mu\nu}$  are unknown coefficients ( $\nu = 1, \dots, n; \mu = 1, \dots, m$ ),  $g_{\mu}(\theta, \phi)$  are transverse basis functions ( $\mu = 1, \dots, m$ ), and  $f_{\nu}(r, k)$  are wavenumber dependent radial basis functions ( $\nu = 1, \dots, n$ ) as in Figure 2.1b. This can be

written as a single summation of  $N = (n \times m)$  terms

$$p(\mathbf{x}) = \sum_{\alpha=1}^N q_{\alpha}^* f_{\alpha}^*(r, \theta, \phi, k) \quad (2.16)$$

where

$$\mathbf{x} = (r, \theta, \phi, k), \quad q_{\alpha}^* = q_{\mu\nu}, \quad \text{and} \quad f_{\alpha}^*(r, \theta, \phi, k) = f_{\nu}(r, k)g_{\mu}(\theta, \phi). \quad (2.17)$$

The correspondence between  $\alpha$  and  $\mu$  and  $\nu$  is defined by

$$\begin{array}{c} \nu \\ 1 \quad 2 \quad \cdots \quad j \quad \cdots \quad n \\ \mu \begin{array}{c} 1 \\ 2 \\ 3 \\ \vdots \\ i \\ \vdots \\ m \end{array} \left[ \begin{array}{cccccc} 1 & 2 & \cdots & j & \cdots & n \\ 1 & 2 & \cdots & j & \cdots & n \\ n+1 & n+2 & \cdots & n+j & \cdots & 2n \\ 2n+1 & 2n+2 & \cdots & 2n+j & \cdots & 3n \\ \vdots & & & \vdots & & \vdots \\ (i-1)n+1 & \dots\dots\dots & & (i-1)n+j & \cdots & in \\ \vdots & & & \vdots & & \vdots \\ (m-1)n+1 & \dots\dots\dots & & (m-1)n+j & \cdots & nm \end{array} \right]. \end{array}$$

Selecting test functions  $w_\alpha^*(r, \theta, \phi, k)$  forms a set of algebraic equations for the unknowns  $q_\alpha^*$ . Substituting equation (2.16) into equation (2.14) gives

$$\begin{aligned} & \int_{\Omega_z} \left[ \left(\frac{r}{z}\right)^2 \nabla_{\theta\phi} w_\alpha^* \cdot \sum_{\beta=1}^N q_\beta^* \nabla_{\theta\phi} f_\beta^* + \frac{1}{(z')^2} \frac{\partial w_\alpha^*}{\partial r} \sum_{\beta=1}^N q_\beta^* \frac{\partial f_\beta^*}{\partial r} \right. \\ & \left. - k^2 w_\alpha^* \sum_{\beta=1}^N q_\beta^* f_\beta^* \right] \left(\frac{z}{R}\right)^2 z' dr d\Gamma_R \\ & + \int_{\Gamma_X} \left( ik w_\alpha^* \sum_{\beta=1}^N q_\beta^* f_\beta^* - w_\alpha^* \epsilon \right) d\Gamma_X \\ & - \rho \int_{\Gamma_R} w_\alpha^* a d\Gamma_R = 0, \end{aligned}$$

which gives

$$\begin{aligned} & \sum_{\beta=1}^N \left( \int_{\Omega_z} \left[ \left(\frac{r}{z}\right)^2 \nabla_{\theta\phi} w_\alpha^* \cdot \nabla_{\theta\phi} f_\beta^* + \frac{1}{(z')^2} \frac{\partial w_\alpha^*}{\partial r} \frac{\partial f_\beta^*}{\partial r} - k^2 w_\alpha^* f_\beta^* \right] \right. \\ & \quad \left. \times \left(\frac{z}{R}\right)^2 z' dr d\Gamma_R + ik \int_{\Gamma_X} w_\alpha^* f_\beta^* d\Gamma_X \right) q_\beta^* \\ & = \rho \int_{\Gamma_R} w_\alpha^* a d\Gamma_R + \int_{\Gamma_X} w_\alpha^* \epsilon d\Gamma_X. \end{aligned} \tag{2.18}$$

Even though  $f_\alpha^*$  and  $w_\alpha^*$  can be chosen independently, it is assumed that they have the same transverse basis so that

$$w_\alpha^*(r, \theta, \phi, k) = w_\nu(r, k) g_\mu(\theta, \phi). \tag{2.19}$$

Substituting equation (2.19) into equation (2.18), we get for each  $\alpha = 1, \dots, N$   
(with  $\mu, \nu$  relating to  $\alpha$  and  $\mu', \nu'$  relating to  $\beta$ )

$$\begin{aligned}
& \sum_{\beta=1}^N \left( \int_{\Omega_z} \left( \frac{1}{z^2} \frac{\partial g_\mu}{\partial \theta} \frac{\partial g_{\mu'}}{\partial \theta} w_\nu f_{\nu'} + \frac{1}{z^2 \sin^2 \theta} \frac{\partial g_\mu}{\partial \phi} \frac{\partial g_{\mu'}}{\partial \phi} w_\nu f_{\nu'} \right. \right. \\
& \quad \left. \left. + \frac{1}{(z')^2} \frac{\partial w_\nu}{\partial r} \frac{\partial f_{\nu'}}{\partial r} g_\mu g_{\mu'} - k^2 w_\nu f_{\nu'} g_\mu g_{\mu'} \right) \left( \frac{z}{R} \right)^2 z' dr d\Gamma_R \right. \\
& \quad \left. + \int_{\Gamma_X} ik w_\nu f_{\nu'} g_\mu g_{\mu'} d\Gamma_X \right) q_\beta^* \\
& = \rho \int_{\Gamma_R} w_\nu g_\mu a d\Gamma_R + \int_{\Gamma_X} w_\nu g_\mu \epsilon d\Gamma_X
\end{aligned}$$

which yields

$$\begin{aligned}
& \sum_{\beta=1}^N \left( \int_R^X \left( \frac{1}{R} \right)^2 z' w_\nu f_{\nu'} dr \int_{\Gamma_R} \left( \frac{\partial g_\mu}{\partial \theta} \frac{\partial g_{\mu'}}{\partial \theta} + \frac{1}{\sin^2 \theta} \frac{\partial g_\mu}{\partial \phi} \frac{\partial g_{\mu'}}{\partial \phi} \right) d\Gamma_R \right. \\
& \quad \left. + \int_R^X \left( \left( \frac{z}{R} \right)^2 \frac{1}{z'} \frac{\partial w_\nu}{\partial r} \frac{\partial f_{\nu'}}{\partial r} - k^2 \left( \frac{z}{R} \right)^2 z' w_\nu f_{\nu'} \right) dr \int_{\Gamma_R} g_\mu g_{\mu'} d\Gamma_R \right. \\
& \quad \left. + ik w_\nu(X) f_{\nu'}(X) \int_{\Gamma_X} g_\mu g_{\mu'} d\Gamma_X \right) q_\beta^* \\
& = \rho w_\nu(R) \int_{\Gamma_R} g_\mu a d\Gamma_R + w_\nu(X) \int_{\Gamma_X} g_\mu \epsilon d\Gamma_X,
\end{aligned}$$

which can be written as

$$A_{\alpha\beta}^* q_\beta^* = h_\alpha^*. \quad (2.20)$$

Now noticing that  $d\Gamma_X = (X/R)^2 d\Gamma_R$ , we can write this as

$$A_{\alpha\beta}^* = B_{\nu\nu'}^{(1)} C_{\mu\mu'}^{(1)} + B_{\nu\nu'}^{(2)} C_{\mu\mu'}^{(2)}, \quad (2.21)$$

where

$$B_{\nu\nu'}^{(1)} = \int_R^X \left( \frac{z}{R} \right)^2 \left( \frac{1}{z'} \frac{\partial w_\nu}{\partial r} \frac{\partial f_{\nu'}}{\partial r} - k^2 z' w_\nu f_{\nu'} \right) dr + ik \left( \frac{X}{R} \right)^2 w_\nu(X) f_{\nu'}(X), \quad (2.22a)$$

$$C_{\mu\mu'}^{(1)} = \int_{\Gamma_R} g_\mu g_{\mu'} d\Gamma_R, \quad (2.22b)$$

$$B_{\nu\nu'}^{(2)} = \int_R^X \left( \frac{1}{R} \right)^2 z' w_\nu f_{\nu'} dr, \quad (2.22c)$$

$$C_{\mu\mu'}^{(2)} = \int_{\Gamma_R} \left( \frac{\partial g_\mu}{\partial \theta} \frac{\partial g_{\mu'}}{\partial \theta} + \frac{1}{\sin^2 \theta} \frac{\partial g_\mu}{\partial \phi} \frac{\partial g_{\mu'}}{\partial \phi} \right) d\Gamma_R. \quad (2.22d)$$

and

$$h_\alpha^* = \rho w_\nu(R) \int_{\Gamma_R} g_\mu a d\Gamma_R + w_\nu(X) \int_{\Gamma_X} g_\mu \epsilon d\Gamma_X. \quad (2.22e)$$

### 2.3.3 Selection of Radial Basis Functions ( $f$ ) and Test Functions ( $w$ )

In each case, the basis functions (with radial basis function/Infinite Element order  $\nu$ ) are defined as [125]

$$f_\nu(r, k) = \left( \frac{R}{r} \right)^\nu e^{-ik(r-R)}, \quad \nu = 1, \dots, n. \quad (2.23)$$

So the trial solution given by equation (2.15) becomes

$$\begin{aligned} p(\mathbf{x}) &= \sum_{\mu=1}^m \sum_{\nu=1}^n q_{\mu\nu} f_\nu g_\mu, \\ &= \sum_{\mu=1}^m g_\mu \sum_{\nu=1}^n q_{\mu\nu} \left( \frac{R}{r} \right)^\nu e^{-ik(r-R)}, \\ &= e^{ikR} \left( \sum_{\mu=1}^m \frac{q_{\mu 1} g_\mu R}{r} + \sum_{\mu=1}^m \frac{q_{\mu 2} g_\mu R^2}{r^2} + \dots + \sum_{\mu=1}^m \frac{q_{\mu n} g_\mu R^n}{r^n} \right) e^{-ikr}, \end{aligned} \quad (2.24)$$

which is of the form of the multipole expansion in equation (2.4) taking

$$\sum_{\mu=1}^m e^{ikR} q_{\mu\nu} g_{\mu} R^{\nu} \equiv \alpha_{\nu}(\theta, \phi)$$

and truncating after  $n$  terms.

We will examine three choices of radial test functions (Infinite Elements)  $w_{\nu}(r, k)$ ,  $\nu = 1, \dots, n$ :

(i) unconjugated Burnett [145]

$$w_{\nu}(r, k) = \left(\frac{R}{r}\right)^{\nu} e^{-ik(r-R)} \equiv f_{\nu}(r, k), \quad (2.25a)$$

(ii) conjugated Burnett [146]

$$w_{\nu}(r, k) = \left(\frac{R}{r}\right)^{\nu} e^{ik(r-R)} \equiv \text{conj}\{f_{\nu}(r, k)\}, \quad (2.25b)$$

(iii) Astley-Leis [135]

$$w_{\nu}(r, k) = \left(\frac{R}{r}\right)^{\nu+2} e^{ik(r-R)} \equiv \left(\frac{R}{r}\right)^2 \text{conj}\{f_{\nu}(r, k)\}. \quad (2.25c)$$

Substituting each of these into (2.22a) and (2.22c) in the limit  $X \rightarrow \infty$  then gives

(i) unconjugated Burnett

$$\begin{aligned}
B_{\nu\nu'}^{(1)} &= \lim_{X \rightarrow \infty} \int_R^X \left(\frac{z}{R}\right)^2 \left\{ \frac{1}{z'} \left[ \nu \left(\frac{R}{r}\right)^{\nu-1} \left(-\frac{R}{r^2}\right) e^{-ik(r-R)} - ik \left(\frac{R}{r}\right)^\nu e^{-ik(r-R)} \right] \right. \\
&\quad \times \left[ \nu' \left(\frac{R}{r}\right)^{\nu'-1} \left(-\frac{R}{r^2}\right) e^{-ik(r-R)} - ik \left(\frac{R}{r}\right)^{\nu'} e^{-ik(r-R)} \right] \\
&\quad \left. - k^2 z' \left(\frac{R}{r}\right)^\nu e^{-ik(r-R)} \left(\frac{R}{r}\right)^{\nu'} e^{-ik(r-R)} \right\} dr \\
&\quad + ik \left(\frac{X}{R}\right)^2 \left(\frac{R}{X}\right)^\nu e^{-ik(X-R)} \left(\frac{R}{X}\right)^{\nu'} e^{-ik(X-R)} \\
&= \lim_{X \rightarrow \infty} \int_R^X e^{-2ik(r-R)} \left(\frac{z}{R}\right)^2 \left\{ \frac{1}{z'} \left[ \frac{\nu\nu'}{R^2} \left(\frac{R}{r}\right)^{\nu+\nu'+2} - k^2 \left(\frac{R}{r}\right)^{\nu+\nu'} \right. \right. \\
&\quad \left. \left. + \frac{ik}{R} \left(\frac{R}{r}\right)^{\nu+\nu'+1} (\nu + \nu') \right] - k^2 z' \left(\frac{R}{r}\right)^{\nu+\nu'} \right\} dr \\
&\quad + ik \left(\frac{R}{X}\right)^{\nu+\nu'-2} e^{-2ik(X-R)} \tag{2.26a}
\end{aligned}$$

$$\begin{aligned}
B_{\nu\nu'}^{(2)} &= \lim_{X \rightarrow \infty} \int_R^X \left(\frac{1}{R}\right)^2 z' \left(\frac{R}{r}\right)^\nu \left(\frac{R}{r}\right)^{\nu'} e^{-2ik(r-R)} dr \\
&= \lim_{X \rightarrow \infty} \int_R^X \left(\frac{1}{R}\right)^2 z' \left(\frac{R}{r}\right)^{\nu+\nu'} e^{-2ik(r-R)} dr \tag{2.26b}
\end{aligned}$$



(ii) conjugated Burnett

$$\begin{aligned}
B_{\nu\nu'}^{(1)} &= \lim_{X \rightarrow \infty} \int_R^X \left(\frac{z}{R}\right)^2 \left\{ \frac{1}{z'} \left[ \nu \left(\frac{R}{r}\right)^{\nu-1} \left(-\frac{R}{r^2}\right) e^{ik(r-R)} + ik \left(\frac{R}{r}\right)^\nu e^{ik(r-R)} \right] \right. \\
&\quad \times \left. \left[ \nu' \left(\frac{R}{r}\right)^{\nu'-1} \left(-\frac{R}{r^2}\right) e^{-ik(r-R)} - ik \left(\frac{R}{r}\right)^{\nu'} e^{-ik(r-R)} \right] \right. \\
&\quad \left. - k^2 z' \left(\frac{R}{r}\right)^{\nu+\nu'} \right\} dr + ik \left(\frac{X}{R}\right)^2 \left(\frac{R}{X}\right)^{\nu+\nu'} \\
&= \lim_{X \rightarrow \infty} \int_R^X \left(\frac{z}{R}\right)^2 \left\{ \frac{1}{z'} \left[ \frac{\nu\nu'}{R^2} \left(\frac{R}{r}\right)^{\nu+\nu'+2} + k^2 \left(\frac{R}{r}\right)^{\nu+\nu'} \right. \right. \\
&\quad \left. \left. + \frac{ik}{R} \left(\frac{R}{r}\right)^{\nu+\nu'+1} (\nu - \nu') \right] - k^2 z' \left(\frac{R}{r}\right)^{\nu+\nu'} \right\} dr \\
&\quad + ik \left(\frac{R}{X}\right)^{\nu+\nu'-2} \tag{2.27a}
\end{aligned}$$

$$\begin{aligned}
B_{\nu\nu'}^{(2)} &= \lim_{X \rightarrow \infty} \int_R^X \left(\frac{1}{R}\right)^2 z' \left(\frac{R}{r}\right)^\nu \left(\frac{R}{r}\right)^{\nu'} dr \\
&= \lim_{X \rightarrow \infty} \int_R^X \left(\frac{1}{R}\right)^2 z' \left(\frac{R}{r}\right)^{\nu+\nu'} dr \tag{2.27b}
\end{aligned}$$

(iii) Astley-Leis

$$\begin{aligned}
B_{\nu\nu'}^{(1)} &= \lim_{X \rightarrow \infty} \int_R^X \left(\frac{z}{R}\right)^2 \left\{ \frac{1}{z'} \left[ (\nu+2) \left(\frac{R}{r}\right)^{\nu+1} \left(-\frac{R}{r^2}\right) e^{ik(r-R)} + ik \left(\frac{R}{r}\right)^{\nu+2} e^{ik(r-R)} \right] \right. \\
&\quad \times \left[ \nu' \left(\frac{R}{r}\right)^{\nu'-1} \left(-\frac{R}{r^2}\right) e^{-ik(r-R)} - ik \left(\frac{R}{r}\right)^{\nu'} e^{-ik(r-R)} \right] \\
&\quad \left. - k^2 z' \left(\frac{R}{r}\right)^{\nu+\nu'+2} \right\} dr + ik \left(\frac{X}{R}\right)^2 \left(\frac{R}{X}\right)^{\nu+\nu'+2} \\
&= \lim_{X \rightarrow \infty} \int_R^X \left(\frac{z}{R}\right)^2 \left\{ \frac{1}{z'} \left[ \frac{(\nu+2)\nu'}{R^2} \left(\frac{R}{r}\right)^{\nu+\nu'+4} + k^2 \left(\frac{R}{r}\right)^{\nu+\nu'+2} \right. \right. \\
&\quad \left. \left. + \frac{ik}{R} \left(\frac{R}{r}\right)^{\nu+\nu'+3} (\nu-\nu'+2) \right] - k^2 z' \left(\frac{R}{r}\right)^{\nu+\nu'+2} \right\} dr \\
&\quad + ik \left(\frac{R}{X}\right)^{\nu+\nu'} \tag{2.28a}
\end{aligned}$$

$$\begin{aligned}
B_{\nu\nu'}^{(2)} &= \lim_{X \rightarrow \infty} \int_R^X \left(\frac{1}{R}\right)^2 z' \left(\frac{R}{r}\right)^{\nu+2} \left(\frac{R}{r}\right)^{\nu'} dr \\
&= \lim_{X \rightarrow \infty} \int_R^X \left(\frac{1}{R}\right)^2 z' \left(\frac{R}{r}\right)^{\nu+\nu'+2} dr \tag{2.28b}
\end{aligned}$$

### 2.3.4 The Transverse Discretisation

In practice, the transverse discretisation for infinite elements is chosen to be conventional isoparametric Finite Element Method polynomials. Here, to investigate accuracy, we choose the transverse basis functions using the separable exact solution of the Helmholtz equation on a sphere from equation (2.6). The result is the same as in [125] and for the axisymmetric case,

$$g_\mu(\theta, \phi) = P_{\mu-1}(\cos \theta), \quad \mu = 1, \dots, m. \tag{2.29}$$

Then from equation (2.22b)

$$\begin{aligned}
C_{\mu\mu'}^{(1)} &= \int_{\Gamma_R} P_{\mu-1}(\cos \theta) P_{\mu'-1}(\cos \theta) d\Gamma_R, \\
&= \int_0^{2\pi} \int_0^\pi P_{\mu-1}(\cos \theta) P_{\mu'-1}(\cos \theta) R^2 \sin \theta d\theta d\phi, \\
&= 2\pi R^2 \int_0^\pi P_{\mu-1}(\cos \theta) P_{\mu'-1}(\cos \theta) \sin \theta d\theta,
\end{aligned}$$

and using the substitution  $u = \cos \theta$ , we have

$$C_{\mu\mu'}^{(1)} = 2\pi R^2 \int_{-1}^1 P_{\mu-1}(x) P_{\mu'-1}(x) dx.$$

Then by the orthogonality of Legendre polynomials [142],

$$\begin{aligned}
C_{\mu\mu'}^{(1)} &= 2\pi R^2 \frac{2}{2(\mu-1)+1} \delta_{\mu\mu'}, \\
&= \frac{4\pi R^2}{2\mu-1} \delta_{\mu\mu'}.
\end{aligned} \tag{2.30}$$

From equation (2.22d)

$$C_{\mu\mu'}^{(2)} = \int_{\Gamma_R} \frac{dP_{\mu-1}}{d\theta} \frac{dP_{\mu'-1}}{d\theta} R^2 \sin \theta d\theta d\phi,$$

and again using the substitution  $x = \cos \theta$ ,

$$C_{\mu\mu'}^{(2)} = 2\pi R^2 \int_{-1}^1 \frac{dP_{\mu-1}(x)}{dx} \frac{dP_{\mu'-1}(x)}{dx} (1-x^2) dx.$$

The associated Legendre polynomial ( $P_{\mu-1}^1$ ) of order 1 satisfies

$$P_{\mu-1}^1 = -(1-x^2)^{\frac{1}{2}} dP_{\mu-1}/dx$$

[144] (Chapter 8) and so using the orthogonality of that function, we get

$$\begin{aligned}
C_{\mu\mu'}^{(2)} &= 2\pi R^2 \int_{-1}^1 P_{\mu-1}^1(x) P_{\mu'-1}^1(x) dx, \\
&= 2\pi R^2 \frac{2(\mu' - 1 + 1)!}{(2(\mu' - 1) + 1)(\mu' - 1 - 1)!} \delta_{\mu\mu'}, \\
&= 4\pi R^2 \frac{\mu'!}{(2\mu' - 1)(\mu' - 2)!} \delta_{\mu\mu'}, \\
&= 4\pi R^2 \frac{\mu'(\mu' - 1)}{2\mu' - 1} \delta_{\mu\mu'}.
\end{aligned} \tag{2.31}$$

So  $C^{(1)}$  and  $C^{(2)}$  are diagonal and so equation (2.20) becomes

$$\begin{bmatrix} A^{(1)} & 0 & \cdots & 0 \\ 0 & A^{(2)} & & \vdots \\ \vdots & & \ddots & 0 \\ 0 & \cdots & 0 & A^{(m)} \end{bmatrix} \begin{bmatrix} q^{(1)} \\ \vdots \\ \vdots \\ q^{(m)} \end{bmatrix} = \begin{bmatrix} h^{(1)} \\ \vdots \\ \vdots \\ h^{(m)} \end{bmatrix},$$

where

$$A_{n \times n}^{(\mu)} = B_{\nu\nu'}^{(1)} C_{\mu\mu}^{(1)} + B_{\nu\nu'}^{(2)} C_{\mu\mu}^{(2)}, \quad (\nu, \nu' = 1, \dots, n), \tag{2.32}$$

$q_{n \times 1}^{(\mu)} = [q_{\mu 1}, q_{\mu 2}, \dots, q_{\mu n}]^\top$ , and  $h_{n \times 1}^{(\mu)} = h_\mu [1, \dots, 1]^\top$ ,  $\mu = 1, \dots, m$ . By letting  $\epsilon \rightarrow 0$  in equation (2.22e) and since  $w_\nu(R, k) = 1$  then using equation (2.29),

$$h_\mu = \rho \int_{\Gamma_R} P_{\mu-1}(\cos \theta) a(\theta) d\Gamma_R, \quad \mu = 1, \dots, m. \tag{2.33}$$

Using the block structure of  $A$  then we have that

$$q^{(\mu)} = (A^{(\mu)})^{-1} h^{(\mu)}.$$

That is

$$q_\nu^{(\mu)} = h_\mu \sum_{j=1}^n (A^{(\mu)})_{\nu j}^{-1}, \quad \nu = 1, \dots, n. \quad (2.34)$$

Then from equations (2.16) and (2.17), we have

$$p = \sum_{\alpha=1}^N q_\alpha^* f_\alpha^* = \sum_{\mu=1}^m \sum_{\nu=1}^n q_\nu^{(\mu)} f_\nu g_\mu.$$

From equation (2.9) we have for each multipole order  $\mu$ ,

$$p_\mu = \left( S_\mu - i \frac{R_\mu}{kc} \right) a(\theta),$$

so then

$$g_\mu \sum_{\nu=1}^n q_\nu^{(\mu)} f_\nu = \left( S_\mu - i \frac{R_\mu}{kc} \right) a(\theta).$$

Multiplying by  $\rho$  and  $g_j$  and integrating over  $\Gamma_R$  gives

$$\rho \int_{\Gamma_R} g_j g_\mu \sum_{\nu=1}^n q_\nu^{(\mu)} f_\nu d\Gamma_R = \rho \int_{\Gamma_R} \left( S_\mu - i \frac{R_\mu}{kc} \right) g_j a(\theta) d\Gamma_R.$$

We will calculate the acoustic response on the surface of the sphere, that is where  $r = R$ . Since  $f_\nu(r = R) = 1$ , and  $q_\nu^{(\mu)}$ ,  $S_\mu$ , and  $R_\mu$  are independent of  $\theta$  (and  $\phi$ ), then we have

$$\begin{aligned} \rho \sum_{\nu=1}^n q_\nu^{(\mu)} \int_{\Gamma_R} g_j g_\mu d\Gamma_R &= \left( S_\mu - i \frac{R_\mu}{kc} \right) \rho \int_{\Gamma_R} g_j a(\theta) d\Gamma_R \\ &= \left( S_\mu - i \frac{R_\mu}{kc} \right) h_j, \end{aligned}$$

from equation (2.33). By the orthogonality of the Legendre polynomials we have from equation (2.30) that

$$\int_{\Gamma_R} g_j g_\mu d\Gamma_R = \begin{cases} \frac{4\pi R^2}{2\mu - 1} & j = \mu \\ 0 & \text{otherwise.} \end{cases}$$

So then

$$\rho \frac{4\pi R^2}{2\mu - 1} \sum_{\nu=1}^n q_\nu^{(\mu)} = h_\mu \left( S_\mu - i \frac{R_\mu}{kc} \right), \quad (2.35)$$

and so from equation (2.34)

$$\begin{aligned} S_\mu - i \frac{R_\mu}{kc} &= \rho \frac{4\pi R^2}{2\mu - 1} \sum_{\nu=1}^n \frac{q_\nu^{(\mu)}}{h_\mu}, \\ &= \rho \frac{4\pi R^2}{2\mu - 1} \sum_{\nu=1}^n \sum_{j=1}^n (A^{(\mu)})_{\nu j}^{-1}, \\ &= \frac{\rho 4\pi R^2}{2\mu - 1} \bar{A}^{(\mu)} \end{aligned}$$

where

$$\bar{A}^{(\mu)} = \sum_{j,\nu=1}^n (A^{(\mu)})_{\nu j}^{-1}. \quad (2.36)$$

By equation (2.11) we have that

$$S_\mu = \frac{4\mu\pi R}{2\mu - 1} \operatorname{Re} \{ \bar{A}^{(\mu)} \}, \quad (2.37)$$

and from equations (2.7) and (2.10)

$$R_\mu = -\frac{4\pi k R^2}{2\mu - 1} \operatorname{Im} \{ \bar{A}^{(\mu)} \}. \quad (2.38)$$

### 2.3.5 The Case $z = r$

Choosing the PML stretching function to be  $z(r) = r$  yields the infinite element form of the solution given in [125]. Here we carry out the procedure with each (infinite element) test function in turn.

(i) Unconjugated Burnett: from equation (2.26a)

$$\begin{aligned}
B_{\nu\nu'}^{(1)} &= \lim_{X \rightarrow \infty} \int_R^X e^{-2ik(r-R)} \left(\frac{r}{R}\right)^2 \left\{ \frac{\nu\nu'}{R^2} \left(\frac{R}{r}\right)^{\nu+\nu'+2} - k^2 \left(\frac{R}{r}\right)^{\nu+\nu'} \right. \\
&\quad \left. + \frac{ik}{R} \left(\frac{R}{r}\right)^{\nu+\nu'+1} (\nu + \nu') - k^2 \left(\frac{R}{r}\right)^{\nu+\nu'} \right\} dr \\
&\quad + ik \left(\frac{R}{X}\right)^{\nu+\nu'-2} e^{-2ik(X-R)} \\
&= \lim_{X \rightarrow \infty} \int_R^X e^{-2ik(r-R)} \left\{ \frac{\nu\nu'}{R^2} \left(\frac{R}{r}\right)^{\nu+\nu'} - 2k^2 \left(\frac{R}{r}\right)^{\nu+\nu'-2} \right. \\
&\quad \left. + \frac{ik}{R} \left(\frac{R}{r}\right)^{\nu+\nu'-1} (\nu + \nu') \right\} dr \\
&\quad + ik \left(\frac{R}{X}\right)^{\nu+\nu'-2} e^{-2ik(X-R)}
\end{aligned}$$

If the order of the radial basis function satisfies  $\nu \neq 1$ , or  $\nu' \neq 1$ , then the last term tends to zero and

$$\begin{aligned}
B_{\nu\nu'}^{(1)} &= \frac{1}{R} \left( \nu\nu' \int_R^\infty \left(\frac{R}{r}\right)^{\nu+\nu'} e^{-2ik(r-R)} \frac{1}{R} dr \right. \\
&\quad \left. + ikR(\nu + \nu') \int_R^\infty \left(\frac{R}{r}\right)^{\nu+\nu'-1} e^{-2ik(r-R)} \frac{1}{R} dr \right. \\
&\quad \left. - 2(kR)^2 \int_R^\infty \left(\frac{R}{r}\right)^{\nu+\nu'-2} e^{-2ik(r-R)} \frac{1}{R} dr \right) \\
&= \frac{1}{R} (\nu\nu' I_{\nu+\nu'} + ikR(\nu + \nu') I_{\nu+\nu'-1} - 2(kR)^2 I_{\nu+\nu'-2})
\end{aligned}$$

where

$$I_j = \int_R^\infty \left(\frac{R}{r}\right)^j e^{-2ik(r-R)} \frac{1}{R} dr.$$

If  $\nu = \nu' = 1$  then

$$\begin{aligned} B_{11}^{(1)} &= \lim_{X \rightarrow \infty} \int_R^X e^{-2ik(r-R)} \left\{ \frac{1}{R^2} \left(\frac{R}{r}\right)^2 - 2k^2 + \frac{2ik}{R} \left(\frac{R}{r}\right) \right\} dr + ik e^{-2ik(X-R)} \\ &= \lim_{X \rightarrow \infty} \frac{1}{R} \left( \int_R^X \left(\frac{R}{r}\right)^2 e^{-2ik(r-R)} \frac{1}{R} dr + 2ikR \int_R^X \left(\frac{R}{r}\right) e^{-2ik(r-R)} \frac{1}{R} dr \right. \\ &\quad \left. - 2k^2 R \int_R^X e^{-2ik(r-R)} dr \right) + ik e^{-2ik(X-R)} \\ &= \frac{1}{R} (I_2 + 2ikRI_1) + \lim_{X \rightarrow \infty} \left( -2k^2 \int_R^X e^{-2ik(r-R)} dr + ik e^{-2ik(X-R)} \right) \\ &= \frac{1}{R} (I_2 + 2ikRI_1) + \lim_{X \rightarrow \infty} \left( -2k^2 \left[ \frac{e^{-2ik(r-R)}}{-2ik} \right]_R^X + ik e^{-2ik(X-R)} \right) \\ &= \frac{1}{R} (I_2 + 2ikRI_1) + \lim_{X \rightarrow \infty} \left( -ike^{-2ik(X-R)} + ik + ik e^{-2ik(X-R)} \right) \\ &= \frac{1}{R} (I_2 + 2ikRI_1 + ikR). \end{aligned} \tag{2.39}$$

Now using integration by parts we have

$$\begin{aligned} I_2 &= \left[ -\frac{R^2}{r} e^{-2ik(r-R)} \frac{1}{R} \right]_R^\infty - R \int_R^\infty \left(\frac{R}{r}\right) e^{-2ik(r-R)} 2ik \frac{1}{R} dr \\ &= 1 - 2ikRI_1. \end{aligned}$$

So then

$$\begin{aligned} B_{11}^{(1)} &= \frac{1}{R} (1 - 2ikRI_1 + 2ikRI_1 + ikR) \\ &= \frac{1}{R} (1 + ikR). \end{aligned}$$



Similarly from equation (2.26b) we have

$$\begin{aligned} B_{\nu\nu'}^{(2)} &= \lim_{X \rightarrow \infty} \int_R^X \left(\frac{1}{R}\right)^2 \left(\frac{R}{r}\right)^{\nu+\nu'} e^{-2ik(r-R)} dr \\ &= \frac{1}{R} I_{\nu+\nu'} \quad \forall \nu, \nu' \geq 1. \end{aligned}$$

(ii) Conjugated Burnett: from equation (2.27a) we have

$$\begin{aligned} B_{\nu\nu'}^{(1)} &= \lim_{X \rightarrow \infty} \int_R^X \left(\frac{r}{R}\right)^2 \left\{ \frac{\nu\nu'}{R^2} \left(\frac{R}{r}\right)^{\nu+\nu'+2} + k^2 \left(\frac{R}{r}\right)^{\nu+\nu'} \right. \\ &\quad \left. + \frac{ik}{R} \left(\frac{R}{r}\right)^{\nu+\nu'+1} (\nu - \nu') - k^2 \left(\frac{R}{r}\right)^{\nu+\nu'} \right\} dr + ik \left(\frac{R}{X}\right)^{\nu+\nu'-2} \\ &= \lim_{X \rightarrow \infty} \int_R^X \left\{ \frac{\nu\nu'}{R^2} \left(\frac{R}{r}\right)^{\nu+\nu'} + \frac{ik}{R} \left(\frac{R}{r}\right)^{\nu+\nu'-1} (\nu - \nu') \right\} dr + ik \left(\frac{R}{X}\right)^{\nu+\nu'-2} \\ &= \lim_{X \rightarrow \infty} \left[ \frac{\nu\nu' R^{\nu+\nu'-2}}{-(\nu + \nu' - 1)r^{\nu+\nu'-1}} + \frac{ik(\nu - \nu')R^{\nu+\nu'-2}}{-(\nu + \nu' - 2)r^{\nu+\nu'-2}} \right]_R^X + ik \left(\frac{R}{X}\right)^{\nu+\nu'-2} \end{aligned}$$

If  $\nu \neq 1$ , or  $\nu' \neq 1$ , then

$$\begin{aligned} B_{\nu\nu'}^{(1)} &= \frac{\nu\nu'}{(\nu + \nu' - 1)R} + \frac{ik(\nu - \nu')}{\nu + \nu' - 2} \\ &= \frac{1}{R} \left( \frac{\nu\nu'}{\nu + \nu' - 1} + \frac{ikR(\nu - \nu')}{\nu + \nu' - 2} \right). \end{aligned}$$

If  $\nu = \nu' = 1$ , then

$$\begin{aligned} B_{11}^{(1)} &= \lim_{X \rightarrow \infty} \left[ \frac{-1}{r} \right]_R^X + ik \\ &= \frac{1}{R} (1 + ikR). \end{aligned}$$

And similarly from equation (2.27b)

$$\begin{aligned}
B_{\nu\nu'}^{(2)} &= \lim_{X \rightarrow \infty} \int_R^X \left(\frac{R}{r}\right)^{\nu+\nu'} \frac{1}{R^2} dr \\
&= \lim_{X \rightarrow \infty} \left[ \frac{R^{\nu+\nu'-2}}{-(\nu+\nu'-1)r^{\nu+\nu'-1}} \right]_R^X \\
&= \frac{1}{R} \left( \frac{1}{\nu+\nu'-1} \right) \quad \forall \nu, \nu' \geq 1.
\end{aligned}$$

(iii) Astley-Leis: from equation (2.28a)

$$\begin{aligned}
B_{\nu\nu'}^{(1)} &= \lim_{X \rightarrow \infty} \int_R^X \left(\frac{r}{R}\right)^2 \left\{ \frac{(\nu+2)\nu'}{R^2} \left(\frac{R}{r}\right)^{\nu+\nu'+4} + k^2 \left(\frac{R}{r}\right)^{\nu+\nu'+2} \right. \\
&\quad \left. + \frac{ik}{R} \left(\frac{R}{r}\right)^{\nu+\nu'+3} (\nu-\nu'+2) \right\} - k^2 \left(\frac{R}{r}\right)^{\nu+\nu'+2} \Big\} dr \\
&\quad + ik \left(\frac{R}{X}\right)^{\nu+\nu'} \\
&= \lim_{X \rightarrow \infty} \int_R^X \left\{ \frac{(\nu+2)\nu'}{R^2} \left(\frac{R}{r}\right)^{\nu+\nu'+2} + \frac{ik}{R} \left(\frac{R}{r}\right)^{\nu+\nu'+1} (\nu-\nu'+2) \right\} dr \\
&\quad + ik \left(\frac{R}{X}\right)^{\nu+\nu'} \\
&= \lim_{X \rightarrow \infty} \left[ \frac{(\nu+2)\nu'R^{\nu+\nu'}}{-(\nu+\nu'+1)r^{\nu+\nu'+1}} + \frac{ik(\nu-\nu'+2)R^{\nu+\nu'}}{-(\nu+\nu')r^{\nu+\nu'}} \right]_R^X + ik \left(\frac{R}{X}\right)^{\nu+\nu'} \\
&= \frac{1}{R} \left[ \frac{(\nu+2)\nu'}{\nu+\nu'+1} + \frac{ikR(\nu-\nu'+2)}{\nu+\nu'} \right].
\end{aligned}$$

Note that if  $\nu = \nu' = 1$ , then

$$B_{11}^{(1)} = \frac{1}{R} (1 + ikR),$$

as was found above for the previous two cases. Similarly, from equation

(2.28b)

$$\begin{aligned}
B_{\nu\nu'}^{(1)} &= \lim_{X \rightarrow \infty} \int_R^X \left(\frac{R}{r}\right)^{\nu+\nu'+2} \frac{1}{R^2} dr \\
&= \lim_{X \rightarrow \infty} \left[ \frac{R^{\nu+\nu'}}{-(\nu+\nu'+1)r^{\nu+\nu'+1}} \right]_R^X \\
&= \frac{1}{R} \left( \frac{1}{\nu+\nu'+1} \right) \quad \forall \nu, \nu' \geq 1.
\end{aligned}$$

## 2.4 Perfectly Matching Layer & Infinite Element Combination

We have seen that the case  $z(r) \equiv r$  reduces to the infinite element solution of [125]. We now look at a particular PML+IE formulation informed by the choice of stretching function in the elastodynamic case (see Chapter 3). We take

$$z(r) = r + \frac{4i\beta}{5k} (r - R)^{\frac{5}{4}} + \frac{\alpha}{2} (r - R)^2 + \frac{4i\alpha\beta}{9k} (r - R)^{\frac{9}{4}} \quad (2.40)$$

where  $\alpha$  and  $\beta$  are constants that may be used to fine tune the PML+IE. We examine each infinite element formulation in turn in order to assess the possible advantages of this PML+IE combination.

We first define the following error functions:

$$\epsilon_1^{\mu,\nu}(kR, \alpha, \beta) = |S_\mu^{PML+IE}(kR, \alpha, \beta) - S_\mu^{exact}(kR)|, \quad (2.41)$$

$$\epsilon_2^{\mu,\nu}(kR) = |S_\mu^{IE}(kR) - S_\mu^{exact}(kR)|, \quad (2.42)$$

$$\epsilon_3^{\mu,\nu}(kR, \alpha, \beta) = |R_\mu^{PML+IE}(kR, \alpha, \beta) - R_\mu^{exact}(kR)|, \quad (2.43)$$

$$\epsilon_4^{\mu,\nu}(kR) = |R_\mu^{IE}(kR) - R_\mu^{exact}(kR)|, \quad (2.44)$$

where  $S_\mu^{exact}$  and  $R_\mu^{exact}$  are given by equations (2.12) and (2.7), respectively,  $S_\mu^{PML+IE}$  and  $S_\mu^{IE}$  are given by equation (2.37), and  $R_\mu^{PML+IE}$  and  $R_\mu^{IE}$  are given by equation (2.38). Here the superscript PML+IE refers to the choice of PML stretching function given by equation (2.40), while IE refers to the choice  $z = r$ , replicating the infinite element only formulation.

Then we may define an overall error function,  $Q(\alpha, \beta)$ , that takes account of the total error integrated across an appropriate range of  $kR$  values and across a range of modes. Therefore,

$$\begin{aligned}
Q(\alpha, \beta) &= \sum_{\mu, \nu=1}^N \int (\epsilon_1^{\mu, \nu}(kR, \alpha, \beta) - \epsilon_2^{\mu, \nu}(kR) + \epsilon_3^{\mu, \nu}(kR, \alpha, \beta) - \epsilon_4^{\mu, \nu}(kR)) d(kR), \\
&= \sum_{\mu, \nu=1}^N \int (\epsilon_1^{\mu, \nu}(kR, \alpha, \beta) + \epsilon_3^{\mu, \nu}(kR, \alpha, \beta)) d(kR) \\
&\quad - \sum_{\mu, \nu=1}^N \int (\epsilon_2^{\mu, \nu}(kR) + \epsilon_4^{\mu, \nu}(kR)) d(kR), \\
&= \sum_{\mu, \nu=1}^N \int (\epsilon_1^{\mu, \nu}(kR, \alpha, \beta) + \epsilon_3^{\mu, \nu}(kR, \alpha, \beta)) d(kR) - E_{\mu, \nu}. \tag{2.45}
\end{aligned}$$

We can then numerically calculate  $E_{\mu, \nu}$  for the first few modes of  $\mu$  and  $\nu$  for illustrative purposes. Then we can plot  $Q(\alpha, \beta)$  against  $\alpha$  and  $\beta$  respectively in order to find  $(\alpha^*, \beta^*)$  such that

$$(\alpha^*, \beta^*) = \arg \min_{\alpha, \beta} Q(\alpha, \beta).$$

In order to show an advantage of the PML+IE formulation over the IE only formulation,  $Q(\alpha, \beta)$  must be negative.

For clarity a summary of the equations that feed into the calculation of equation (2.45) are now provided in the pseudo code below.

1. Choose a form for  $z(r)$  (and hence its derivative  $z'(r)$ ). Here equation (2.40) is employed.
2. Choose an Infinite Element form. For illustration we choose the Unconjugated Burnett form.
3. Calculate
  - $B^{(1)}$  using equation (2.26a)
  - $B^{(2)}$  using equation (2.26b)
  - $C^{(1)}$  using equation (2.30)
  - $C^{(2)}$  using equation (2.31)
4. Calculate  $A^\mu$  using equation (2.32)
5. Calculate  $A^{\bar{(\mu)}}$  using equation (2.36)
6. Calculate
  - $S_\mu^{PML+IE}$  using equation (2.37)
  - $S_\mu^{IE}$  using equation (2.37) (with  $z = r$  i.e.  $\alpha = \beta = 0$ )
  - $R_\mu^{PML+IE}$  using equation (2.38)
  - $R_\mu^{IE}$  using equation (2.38) (with  $z = r$  i.e.  $\alpha = \beta = 0$ )
7. Calculate
  - $S_\mu^{exact}$  using equation (2.12)
  - $R_\mu^{exact}$  using equation (2.7)
8. Calculate
  - $\epsilon_1$  using equation (2.41)

- $\epsilon_2$  using equation (2.42)
- $\epsilon_3$  using equation (2.43)
- $\epsilon_4$  using equation (2.44)

9. Calculate  $Q$  using equation (2.45)

## 2.5 Results

### 2.5.1 Unconjugated Burnett formulation

In order to show that the PML+IE formulation has an advantage over the IE only formulation, it is necessary to find values for  $\alpha$  and  $\beta$  such that the error function,  $Q(\alpha, \beta)$  given by equation (2.45), is negative, thereby showing better agreement between the PML+IE formulation and the exact solution than between the IE only formulation and the exact solution. To do so, the  $E_{\mu, \nu}$  term must first be calculated as this does not depend on  $\alpha$  or  $\beta$  and so need only be calculated once.

Taking first the unconjugated Burnett infinite element, for  $kR \in [0.01, 0.42]$ , directed by a particular interest in large wavelength problems wherein this parameter space provided greatest scope for improvement in a numerical solution, and with  $N = 3$  giving the first few modes of  $\mu$  and  $\nu$  where there is least attenuation and therefore where the boundary will have most effect, we have from equation (2.45),

$$E_{\mu, \nu} \approx \sum_{\mu, \nu=1}^3 \int (\epsilon_2^{\mu, \nu}(kR) + \epsilon_4^{\mu, \nu}(kR)) d(kR),$$

$$\approx 2.77063.$$

Figure 2.2 shows the error function given by equation (2.45) for the PML+IE

formulation with the unconjugated Burnett infinite element, with  $\beta = 0.01$  informed by numerical experimentation,  $X = 10$  (a sufficiently large boundary due to computational restrictions),  $kR = 0.1, \dots, 0.4$ , and  $m, n = 1, \dots, 3$ , with varying  $\alpha$ . As stated, for the PML+IE formulation to show advantage over the IE only formulation,  $Q(\alpha, \beta)$  must be negative. From the figure, it can be seen that there are a range of values for  $\alpha$  in  $[-1, 1]$  that give a negative value for  $Q(\alpha, \beta)$ . In figure 2.2a, it can be seen that the choice  $\alpha = -0.7$  would not result in a negative value for  $Q(\alpha, \beta)$ , while figure 2.2b shows that all positive values between 0 and 1 result in better agreement between the PML+IE formulation and the exact solution. Figures 2.2c and 2.2d look more closely at the ranges for  $\alpha$  that could provide greatest improvement, that is between  $-0.1$  and  $-0.01$ , and between  $0.01$  and  $0.1$ . From figure 2.2c, the value that produces the largest negative value for  $Q(\alpha, \beta)$  is  $\alpha = -0.07$ .

Figure 2.3 shows the error function given by equation (2.45) for the PML+IE formulation with the unconjugated Burnett infinite element, with  $\alpha = -0.07$ ,  $X = 10$ ,  $kR = 0.1, \dots, 0.4$ , and  $m, n = 1, \dots, 3$ , with varying  $\beta$ . It can be seen that any of the values for beta between  $-1$  and  $1$  results in a negative value for  $Q(\alpha, \beta)$ , meaning that the PML+IE formulation outperforms the IE only formulation overall. Figures 2.3a and 2.3b show that  $\beta$  closer to zero results in a more negative  $Q(\alpha, \beta)$ . Figures 2.3c and 2.3d examine values for  $\beta < |0.1|$ , with  $\beta = 0.01$  resulting in  $Q(\alpha, \beta) = -2.494$ , the lowest value for the range of  $\beta$  values explored.

Figure 2.4 shows the specific inertia for the exact solution,  $S_{\mu}^{exact}$  given by equation 2.12), and the numerical values of the specific inertia for the PML+IE formulation with the unconjugated Burnett infinite element,  $S_{\mu}^{PML+IE}$ , and the infinite element only formulation,  $S_{\mu}^{IE}$ , given by equation (2.37), plotted against  $kR$ , with  $\alpha = -0.07$  and  $\beta = 0.01$ , for varying modes of  $\mu$  and  $\nu$ . There is very

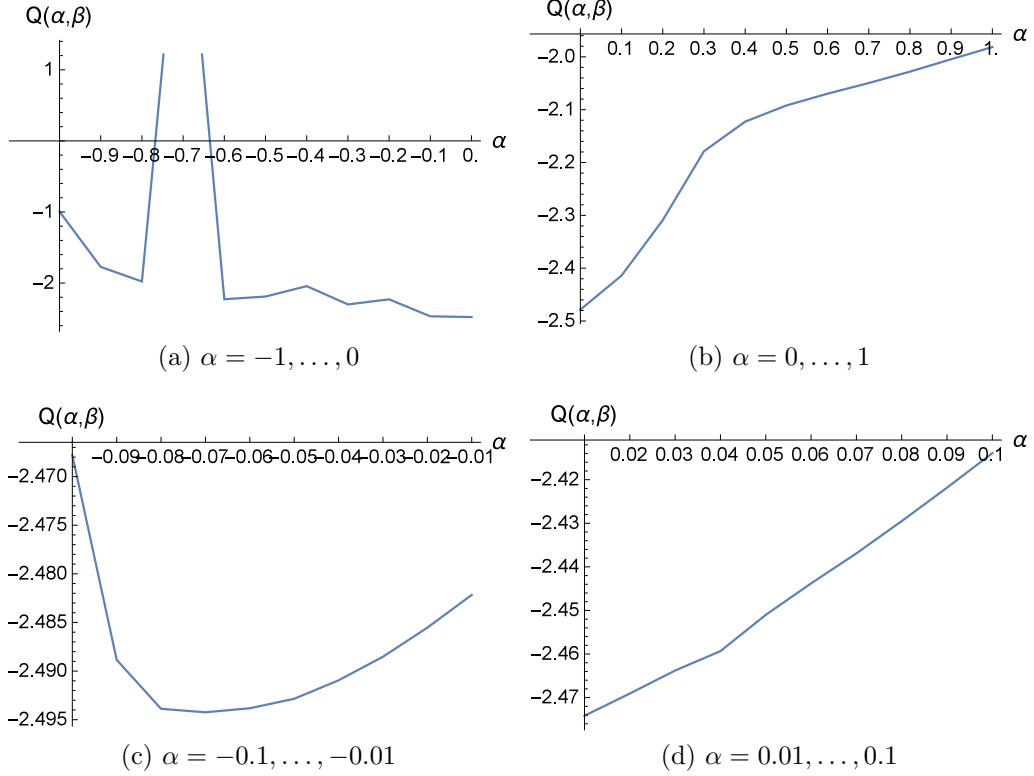


Figure 2.2: Plots of the error  $Q(\alpha, \beta)$  given by equation (2.45) for the PML+IE formulation using the unconjugated Burnett element with varying  $\alpha$  and  $\beta = 0.01$ . A negative value for  $Q(\alpha, \beta)$  indicates that the PML+IE formulation has more agreement with the exact solution than does the IE only formulation.

little difference between the PML+IE formulation and the IE only formulation for specific inertia for any of the modes shown, although in figure 2.4e, the PML+IE formulation does agree with the exact solution for more  $kR$  values than does the IE only formulation.

Figure 2.5 shows the exact specific resistance,  $R_\mu^{exact}$  given by equation (2.7), and the numerical values of the specific resistance for the PML+IE formulation with the unconjugated Burnett infinite element,  $R_\mu^{PML+IE}$ , and the infinite element only formulation,  $R_\mu^{IE}$ , given by equation (2.38), plotted against  $kR$ , with  $\alpha = -0.07$  and  $\beta = 0.01$ , for varying modes of  $\mu$  and  $\nu$ . As with the inertia in figure 2.4, there is little difference to be seen between the PML+IE and IE only formulations



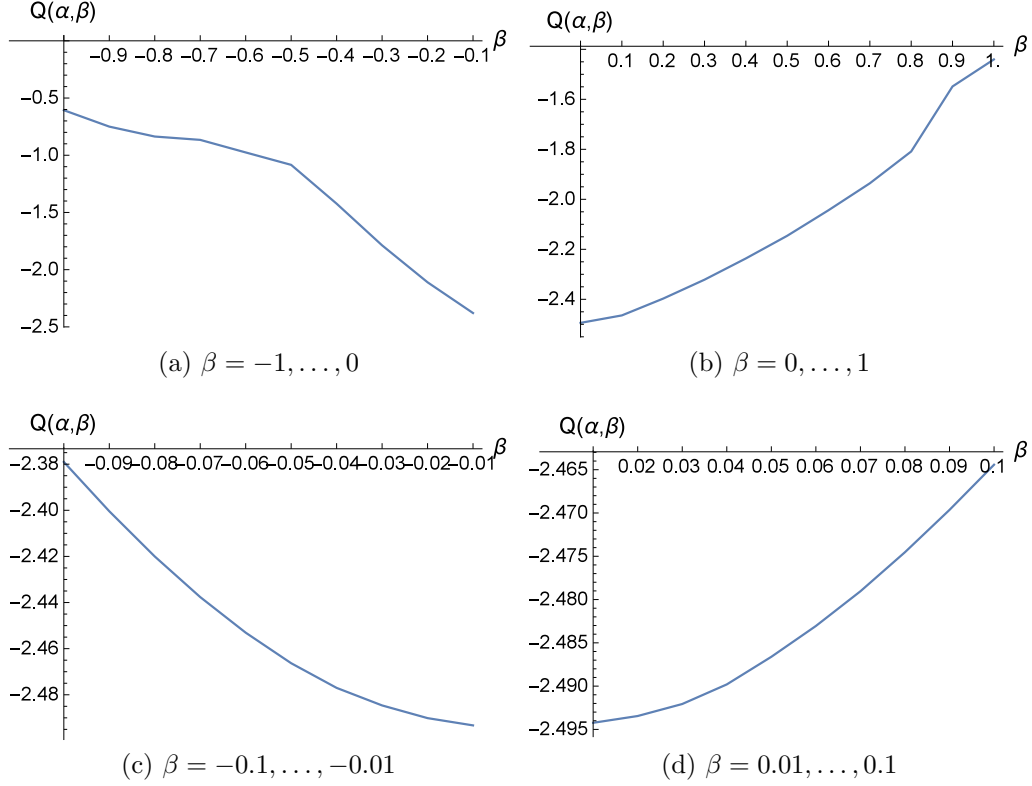


Figure 2.3: Plots of the error  $Q(\alpha, \beta)$  given by equation (2.45) for the PML+IE formulation using the unconjugated Burnett element with varying  $\beta$  and  $\alpha = -0.07$ . A negative value for  $Q(\alpha, \beta)$  indicates that the PML+IE formulation has more agreement with the exact solution than does the IE only formulation.

for the nodes shown in figure 2.5, with both being a good approximation to the exact solution, except in the cases  $\mu = 2$ ,  $\nu = 3$  (figure 2.5d) where the inertia in the PML+IE formulation briefly becomes negative around  $kR = 0.35$ . In figure 2.5e, both the PML+IE and IE only formulations do not show as good agreement with the exact solution, however, the PML+IE formulation does lie closer to the exact solution for the majority of the range of  $kR$  values shown.

Figures 2.2 and 2.3 suggest that  $Q(\alpha, \beta)$  is a non-convex function of  $\alpha$  and  $\beta$  and therefore finding the global minimum  $(\alpha^*, \beta^*)$  would require the use of a global optimisation methodology. This is a nontrivial task and so, due to time constraints, such an investigation was not undertaken. The aim of the thesis

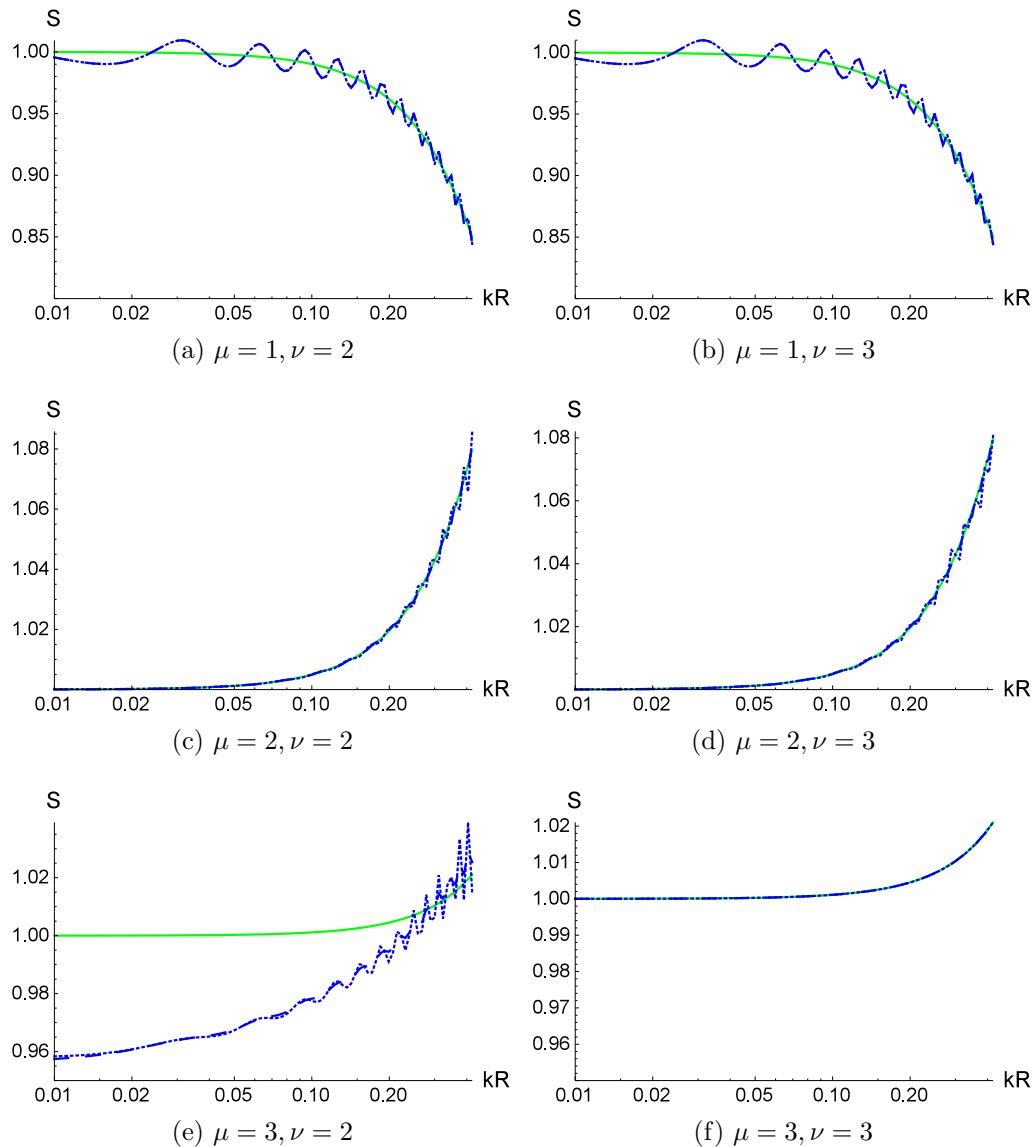


Figure 2.4: Plots of the specific inertia for the exact solution,  $S_\mu^{exact}$  given by equation (2.12) (solid line), and the numerical values of the specific inertia for the infinite element only formulation,  $S_\mu^{IE}$  (dashed), and for the PML+IE formulation using the unconjugated Burnett element,  $S_\mu^{PML+IE}$  (dotted) given by equation (2.37) with  $(\alpha, \beta) = (-0.07, 0.01)$ , where  $kR$  is plotted on a logarithmic scale.

was to investigate whether or not a PML+IE scheme could be constructed for this elasticity model and whether or not there was any advantage in doing so in terms of the errors that arise. We have shown that it is indeed possible to have a PML+IE formulation for this setting and also that there is a reduction in the

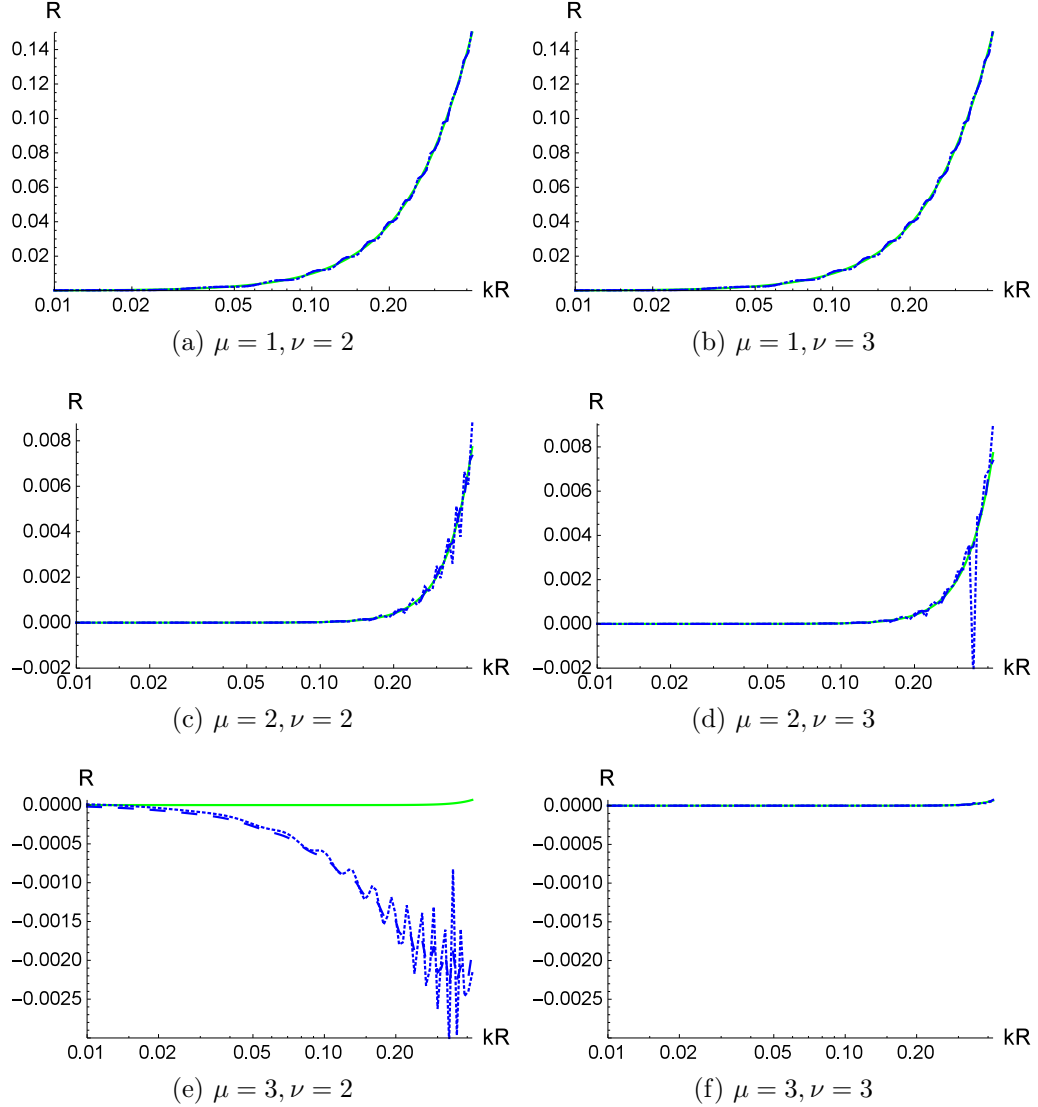


Figure 2.5: Plots of the specific resistance for the exact solution,  $R_\mu^{exact}$  given by equation (2.7) (solid line), and the numerical values of the specific resistance for the infinite element only formulation,  $R_\mu^{IE}$  (dashed), and for the PML+IE formulation using the unconjugated Burnett element,  $R_\mu^{PML+IE}$  (dotted) given by equation (2.38) with  $(\alpha, \beta) = (-0.07, 0.01)$ , where  $kR$  is plotted on a logarithmic scale.

error. So Figures 2.2 and 2.3 should be viewed as being merely illustrative of the level of benefit in using the PML+IE approach and they also convey the non-convex nature of  $Q(\alpha, \beta)$ . The evaluation of equation (2.45) involves a series of nested functions stemming from equations (2.12) and (2.26a) and is therefore quite involved. One can observe a sharp peak in Figure 2.2a and the cause of this has

yet to be identified: exhaustive numerical tests have been undertaken to confirm the veracity of the numerical implementation of these equations. These limited observations suggest that automating the identification of the optimal parameter set will be a difficult task and so this is left for a future study.

## 2.5.2 Conjugated Burnett formulation

Now taking the conjugated Burnett infinite element, for  $kR \in [0.01, 0.42]$ , with  $N = 3$ , we have

$$E_{\mu,\nu} \approx \sum_{\mu,\nu=1}^3 \int (\epsilon_2^{\mu,\nu}(kR) + \epsilon_4^{\mu,\nu}(kR)) d(kR),$$

$$\approx 4.13463.$$

Figure 2.6 shows the error function given by equation (2.45) for the PML+IE formulation with the unconjugated Burnett infinite element, with  $\beta = 0.01$ ,  $X = 10$ ,  $kR = 0.1, \dots, 0.4$ , and  $m, n = 1, \dots, 3$ , with varying  $\alpha$ . Once again, a negative value for  $Q(\alpha, \beta)$  would indicate an advantage of the PML+IE formulation over the IE only formulation. The plots are less monotonic than with the unconjugated Burnett infinite element of figure 2.2, although from figure 2.6a and 2.6b, the largest negative values still seem to occur around  $\alpha = 0$ . Taking a closer look at this range in figures 2.6c and 2.6d, the best value for  $\alpha$  would appear to be 0.07.

Figure 2.7 shows the error function given by equation (2.45) for the PML+IE formulation with the unconjugated Burnett infinite element, with  $\alpha = 0.07$ ,  $X = 10$ ,  $kR = 0.1, \dots, 0.4$ , and  $m, n = 1, \dots, 3$ , with varying  $\beta$ . In figures 2.6a and 2.6b, it is again clear that there is a range of values for  $\beta$  that will give a negative value for  $Q(\alpha, \beta)$  within this range, but the best value again lies close to zero. From figures 2.6c and 2.6d, the value that gives the largest negative  $Q(\alpha, \beta)$  is

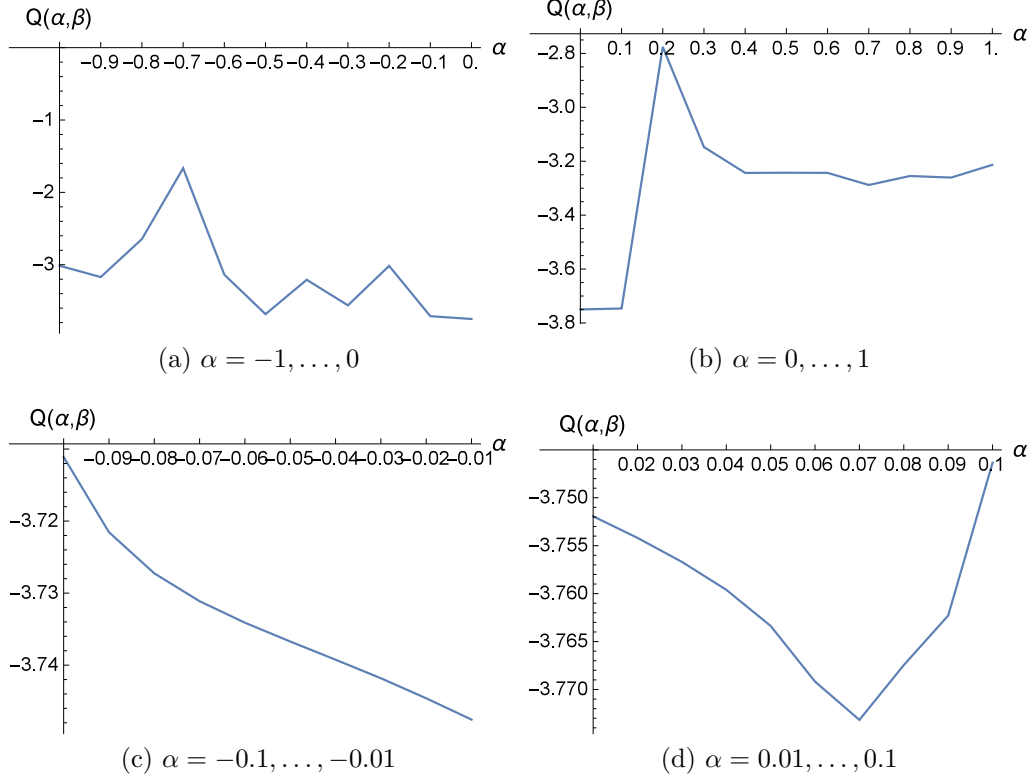


Figure 2.6: Plots of the error  $Q(\alpha, \beta)$  given by equation (2.45) for the PML+IE formulation using the conjugated Burnett element with varying  $\alpha$  and  $\beta = 0.01$ . A negative value for  $Q(\alpha, \beta)$  indicates that the PML+IE formulation has more agreement with the exact solution than does the IE only formulation.

$\beta = 0.01$ .

Figure 2.8 shows the specific inertia for the exact solution,  $S_\mu^{exact}$ , and the numerical values of the specific inertia for the PML+IE formulation with the conjugated Burnett infinite element,  $S_\mu^{PML+IE}$ , and the infinite element only formulation,  $S_\mu^{IE}$ , plotted against  $kR$ , with  $\alpha = 0.07$  and  $\beta = 0.01$ , for varying modes of  $\mu$  and  $\nu$ . Despite the error and  $Q(\alpha, \beta)$  being negative for all the values of  $\alpha$  and  $\beta$  examined, the PML+IE formulation does not, at a glance, appear to outperform the IE only formulation for the modes shown with  $kR$  in the range shown, however, the difference in figures 2.8c and 2.8d is small compared with the difference in the modes with lower  $\mu$  values.

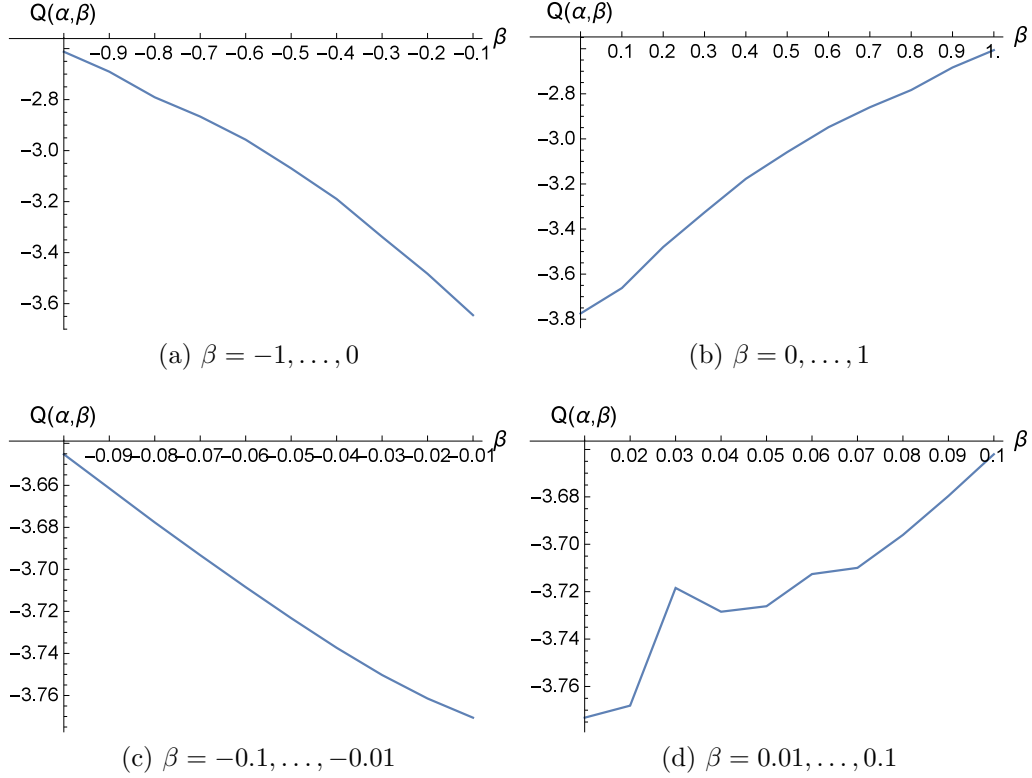


Figure 2.7: Plots of the error  $Q(\alpha, \beta)$  given by equation (2.45) for the PML+IE formulation using the conjugated Burnett element with varying  $\beta$  and  $\alpha = 0.07$ . A negative value for  $Q(\alpha, \beta)$  indicates that the PML+IE formulation has more agreement with the exact solution than does the IE only formulation.

Figure 2.9 shows the specific resistance for the exact solution,  $R_\mu^{exact}$ , and the numerical values of the specific resistance for the PML+IE formulation with the unconjugated Burnett infinite element,  $S_\mu^{PML+IE}$ , and the infinite element only formulation,  $S_\mu^{IE}$ , plotted against  $kR$ , with  $\alpha = 0.07$  and  $\beta = 0.01$ , for varying modes of  $\mu$  and  $\nu$ . Similar to the inertia, the resistance in the PML+IE formulation does not appear to outperform the IE only formulation, and in fact appears worse in figures 2.9c-2.9f, however, the difference here is much smaller than that in the inertia.

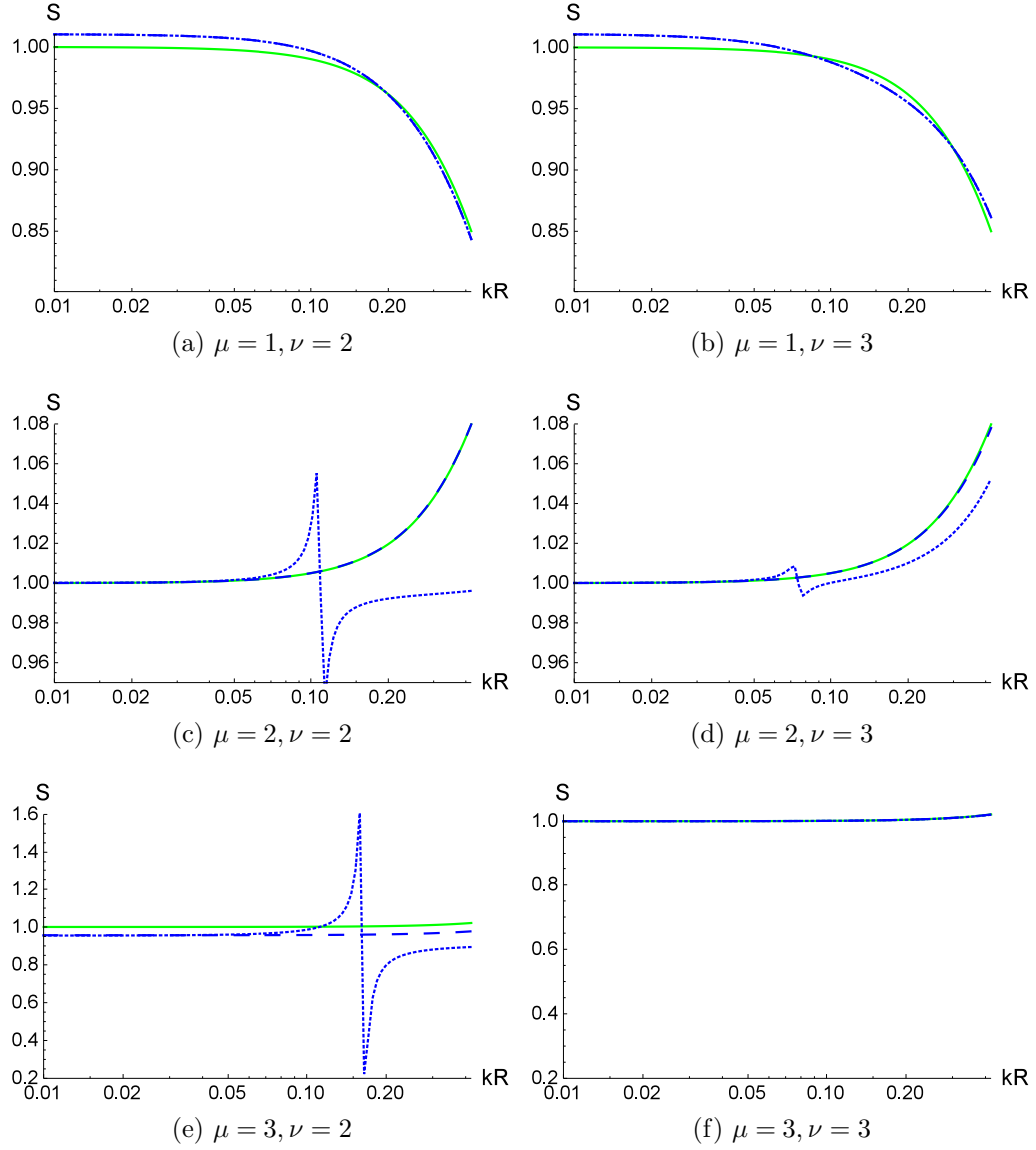


Figure 2.8: Plots of the specific inertia for the exact solution,  $S_\mu^{exact}$  (solid line), given by equation (2.12), and the numerical values for the specific inertia for the infinite element only formulation,  $S_\mu^{IE}$  (dashed), and for the PML+IE formulation using the conjugated Burnett element,  $S_\mu^{PML+IE}$  (dotted), given by equation (2.37), with  $(\alpha, \beta) = (0.07, 0.01)$ , where  $kR$  is plotted on a logarithmic scale.

### 2.5.3 Astley-Leis formulation

Finally, taking the Astley-Leis infinite element, for  $kR \in [0.01, 0.42]$ , with  $N = 3$ , we have

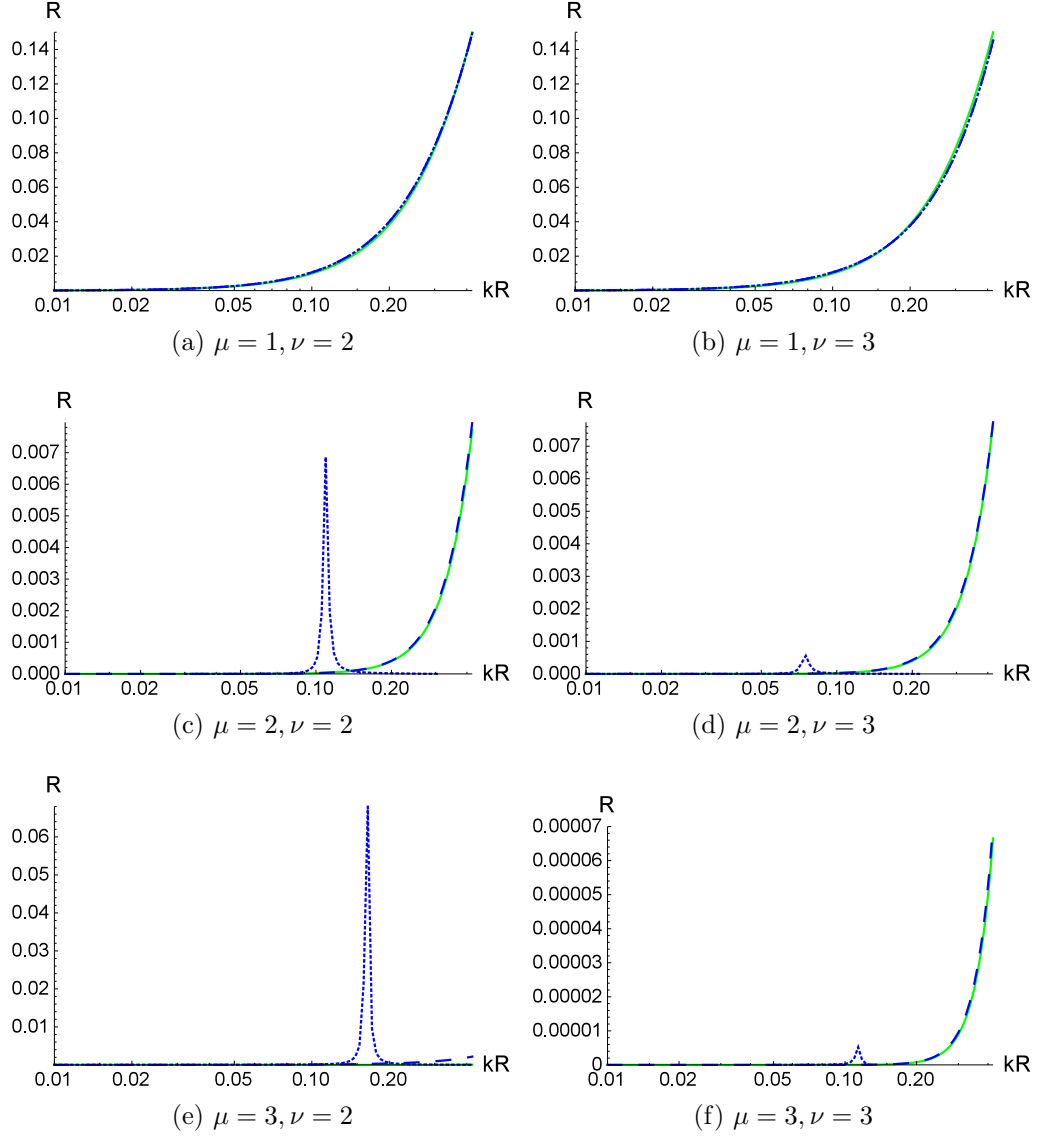


Figure 2.9: Plots of the specific resistance for the exact solution,  $R_\mu^{exact}$  (solid line), given by equation (2.7), and the numerical values of the specific resistance for the infinite element only formulation,  $R_\mu^{IE}$  (dashed), and for the PML+IE formulation using the conjugated Burnett element,  $R_\mu^{PML+IE}$  (dotted), given by equation (2.38), with  $(\alpha, \beta) = (0.07, 0.01)$ , where  $kR$  is plotted on a logarithmic scale.

$$\begin{aligned}
 E_{\mu,\nu} &\approx \sum_{\mu,\nu=1}^3 \int (\epsilon_2^{\mu,\nu}(kR) + \epsilon_4^{\mu,\nu}(kR)) d(kR), \\
 &\approx 0.788019.
 \end{aligned}$$



Figure 2.10 shows the error function given by equation (2.45) for the PML+IE formulation with the Astley-Leis infinite element, with  $\beta = 0.01$ ,  $X = 10$ ,  $kR = 0.1, \dots, 0.4$ , and  $m, n = 1, \dots, 3$ , with varying  $\alpha$ . The error  $Q(\alpha, \beta)$  for the Astley-Leis infinite element bears a resemblance to that of the unconjugated Burnett infinite element, with positive values appearing in figures 2.10a and 2.10b. As with each of the other types of infinite element, the best value for  $\alpha$  has appeared close to zero. From figure 2.10c the optimum value for  $\alpha$  in this case is  $-0.02$ .

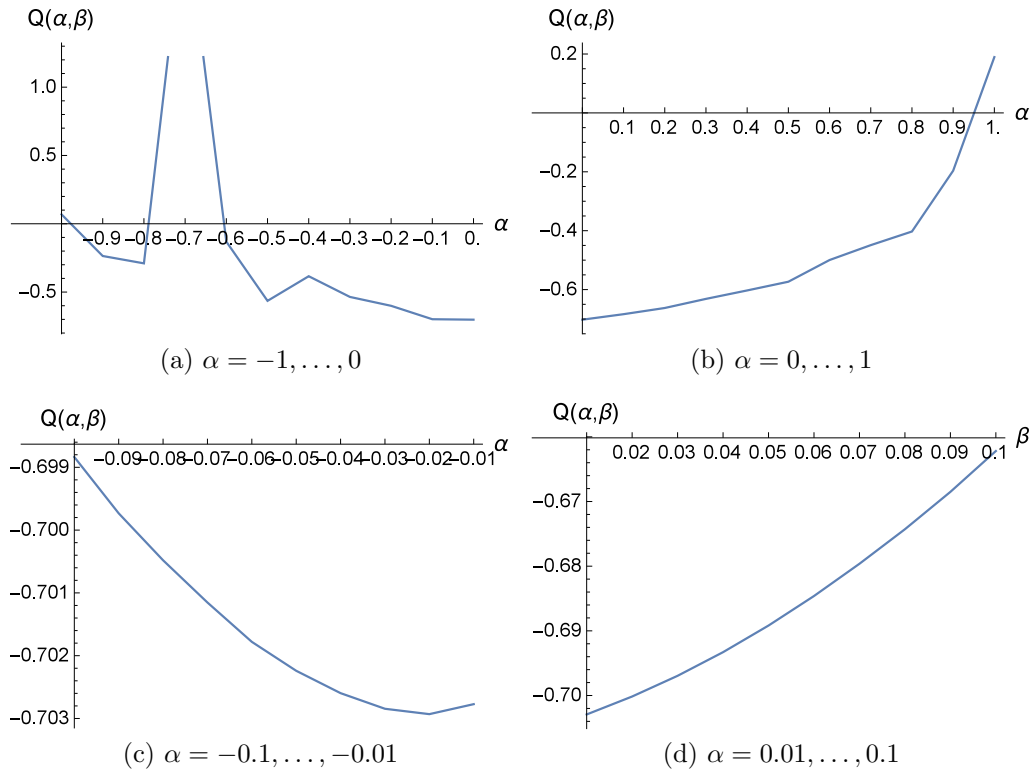


Figure 2.10: Plots of the error  $Q(\alpha, \beta)$  given by equation (2.45), for the PML+IE formulation using the Astley-Leis element with varying  $\alpha$  and  $\beta = 0.01$ .

Figure 2.11 shows the error function given by equation (2.45) for the PML+IE formulation with the Astley-Leis infinite element, with  $\alpha = -0.02$ ,  $X = 10$ ,  $kR = 0.1, \dots, 0.4$ , and  $m, n = 1, \dots, 3$ , with varying  $\beta$ . This is the first infinite element to give a positive value for  $Q(\alpha, \beta)$  when varying  $\beta$ , as can be seen in figures 2.10a and 2.10b, however, these also show once again that the optimum value for  $\beta$  lies

close to zero. From figures 2.10c and 2.10d it is apparent that the value that gives the best error  $Q(\alpha, \beta)$  and therefore the best improvement in PML+IE over IE only formulation is  $\beta = 0.01$ .

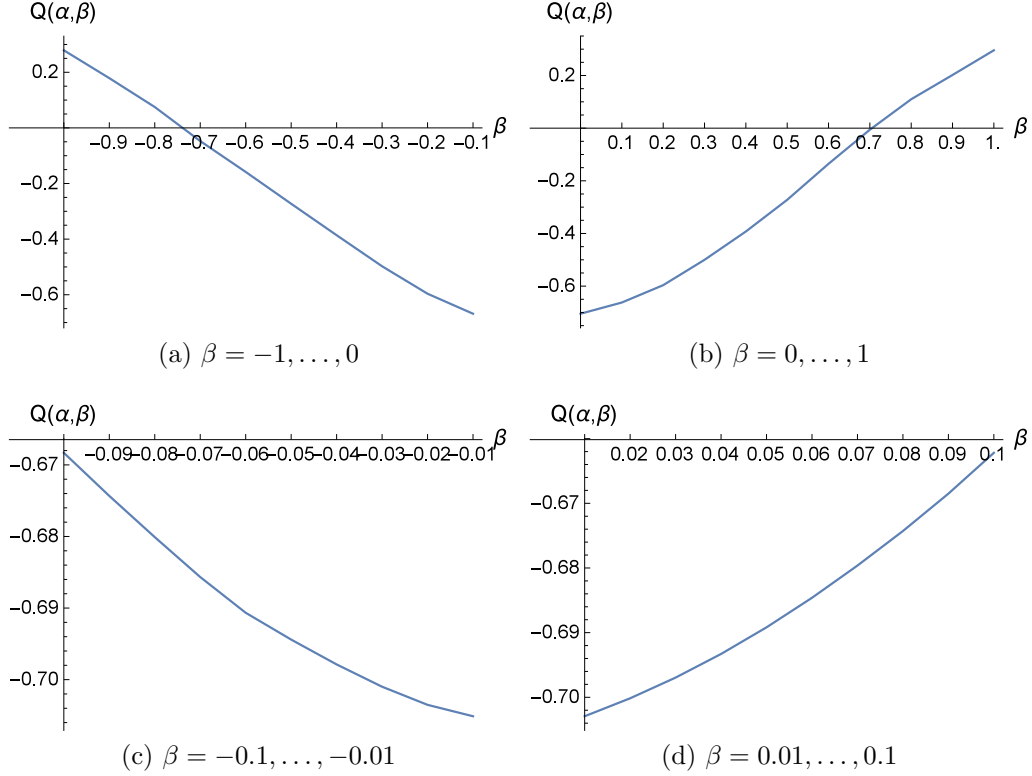


Figure 2.11: Plots of the error  $Q(\alpha, \beta)$  given by equation (2.45), for the PML+IE formulation using the Astley-Leis element with varying  $\beta$  and  $\alpha = -0.02$ .

Figure 2.12 shows the specific inertia for the exact solution,  $S_\mu^{exact}$ , and the numerical values of the specific inertia for the PML+IE formulation with the Astley-Leis infinite element,  $S_\mu^{PML+IE}$ , and for the infinite element only formulation,  $S_\mu^{IE}$ , plotted against  $kR$ , with  $\alpha = -0.02$  and  $\beta = 0.01$ , for varying modes of  $\mu$  and  $\nu$ . From figures 2.12a-2.12d and 2.12f, it can be seen that both the PML+IE and IE only formulations show good agreement with the exact solution. In figure 2.12e, both formulations differ slightly from the exact solution, but agree with each other very well, so it is not apparent that one formulation performs any better than the other for inertia.

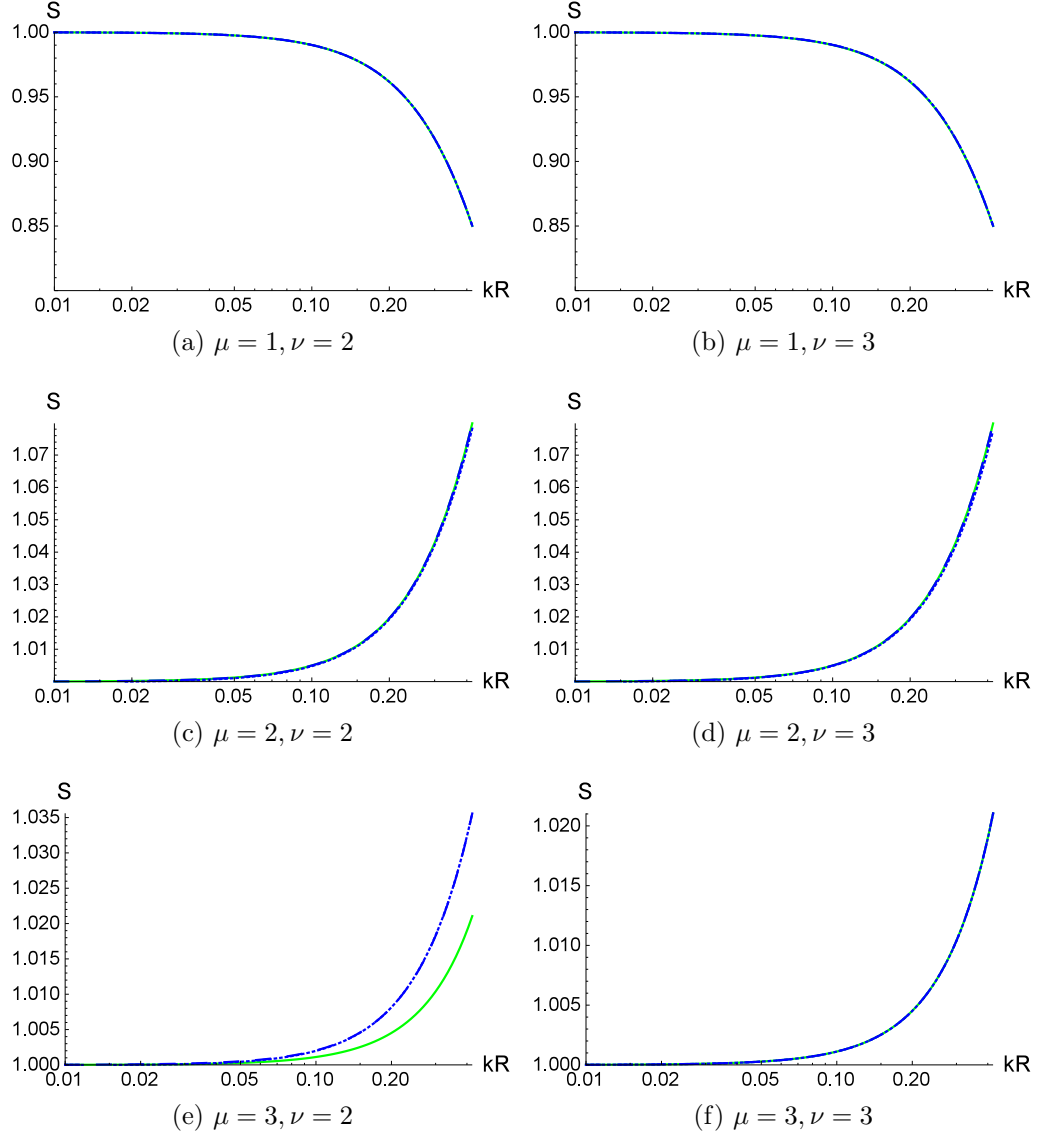


Figure 2.12: Plots of the specific inertia for the exact solution,  $S_\mu^{exact}$  (solid line), given by equation (2.12), and the numerical values of the specific inertia for the infinite element only formulation,  $S_\mu^{IE}$  (dashed), and for the PML+IE formulation using the Astley-Leis element,  $S_\mu^{PML+IE}$  (dotted), given by equation (2.37), with  $(\alpha, \beta) = (-0.02, 0.01)$ , where  $kR$  is plotted on a logarithmic scale.

Figure 2.13 shows the specific resistance for the exact solution,  $R_\mu^{exact}$ , and the numerical values of the specific resistance for the PML+IE formulation with the Astley-Leis infinite element,  $R_\mu^{PML+IE}$ , and the infinite element only formulation,  $R_\mu^{IE}$ , plotted against  $kR$ , with  $\alpha = -0.02$  and  $\beta = 0.01$ , for varying modes of

$\mu$  and  $\nu$ . As with the inertia for the Astley-Leis element, it can be seen from figures 2.13a-2.13d and 2.13f, that both the PML+IE and IE only formulations show good agreement with the exact solution. In figure 2.13e, both formulations differ slightly from the exact solution, agreeing with each other rather well, until around  $kR = 0.35$ , where the PML+IE formulation becomes closer to the exact solution than does the IE only formulation.

## 2.6 Conclusion

A new absorbing boundary layer has been formulated for unbounded wave problems by combining the Perfectly Matching Layer of Berenger [8] and the Infinite Element of Bettess [9]. Derivations have been presented using the unconjugated Burnett, the conjugated Burnett and the Astley-Leis infinite elements. The modal response of a spherical radiator in the frequency domain has been calculated with the new PML+IE method and the results have been contrasted with the IE only method. Finally, a particular choice of the PML stretching function has been presented for use with each type of test function and it has been demonstrated that the PML+IE technique can have an improvement at low wavenumbers in the approximation to the exact solution. This chapter represents a first attempt to combine the PML and IE formulations and it is clear that there is much room for improvement beyond the choice of PML made in equation (2.40).

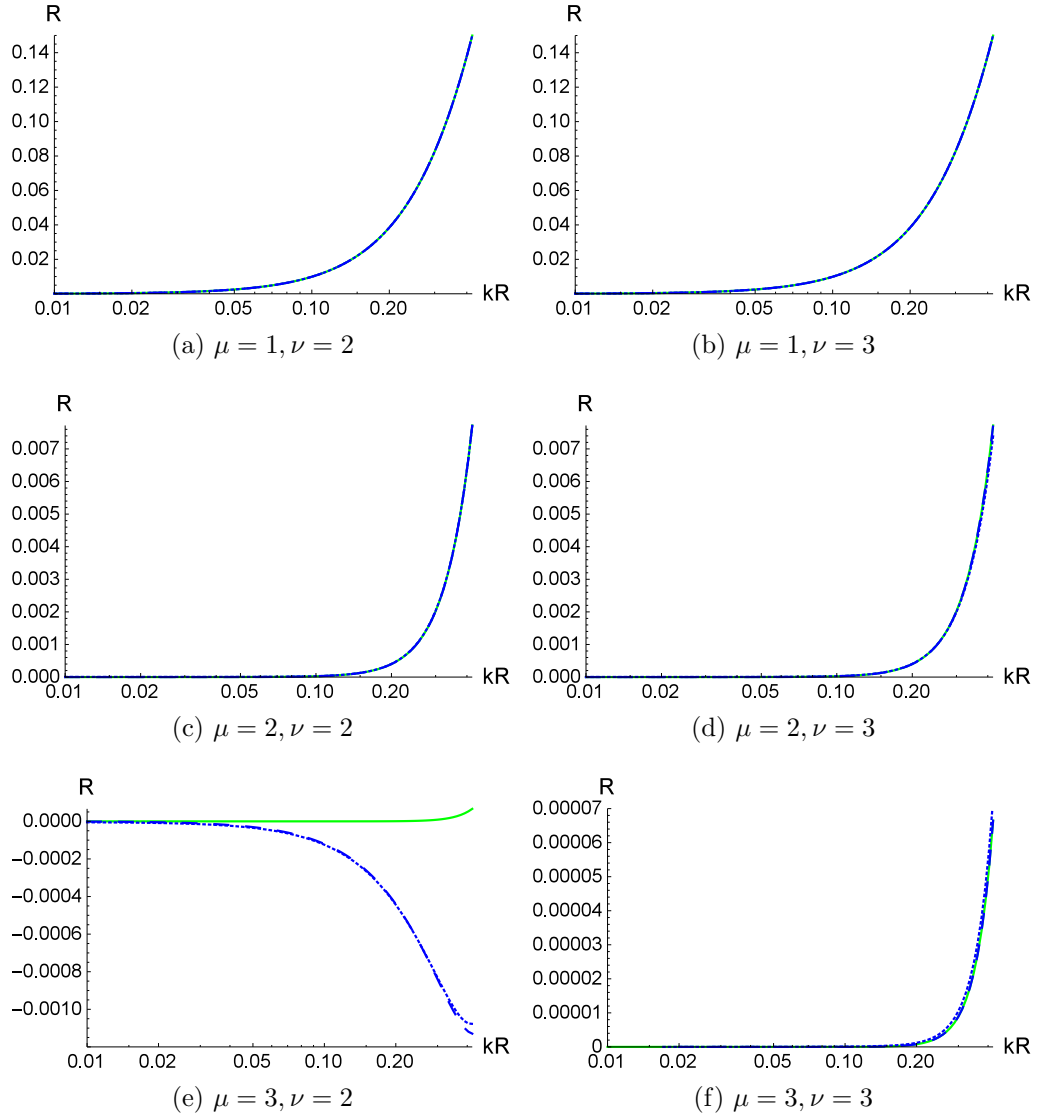


Figure 2.13: Plots of the specific resistance for the exact solution,  $R_\mu^{exact}$  (solid line), given by equation (2.7), and the numerical values of the specific resistance for the infinite element only formulation,  $R_\mu^{IE}$  (dashed), and for the PML+IE formulation using the Astley-Leis element,  $R_\mu^{PML+IE}$  (dotted), given by equation (2.38), with  $(\alpha, \beta) = (-0.02, 0.01)$ , where  $kR$  is plotted on a logarithmic scale.

## **Chapter 3**

# **A Combined Perfectly Matching Layer and Infinite Element Formulation for the Three Dimensional Elastodynamic Wave Equation**

### **3.1 Motivation**

In the previous chapter, Berenger's Perfectly Matching Layer (PML) and Bettess' Infinite Element (IE) schemes were combined to create a new type of element for unbounded acoustic wave problems. In this chapter, the PML and Astley-Leis IE schemes are combined within a finite element framework for elastodynamic wave problems. Where the new element formulation was previously assessed through its use in the calculation of the acoustic modal response of a spherical radiator in the

frequency domain, the present formulation is assessed through its use in a three-dimensional elastic waveguide in the time domain, using a reflection coefficient as a measure of accuracy.

## 3.2 Background

A time domain finite element formulation for elastic wave propagation in an unbounded two-dimensional anisotropic solid using a Perfectly Matching Layer (PML) was proposed in [147], while a PML/Infinite Element (IE) combination was derived in [148] for the scalar wave equation in the time domain and for the frequency domain in [149]. The present work is believed to be the first finite element implementation of a combined PML/IE formulation for the vector elastic wave equation in the time domain. In addition, mass lumping and diagonalisation are used to produce an explicit time domain formulation. The formulation is presented in a pseudo-one-dimensional way by considering a semi-infinite rectangular waveguide for ease of exposition, however, it could naturally extend to reflect fully three-dimensional problems by having PML+IE boundary conditions at all domain boundaries.

In section 3.3, the geometry and governing equations of the problem are introduced and attention is restricted to a locally isotropic material. The system is taken into the frequency domain, through Fourier transforms, in order to introduce the PML stretching, which is frequency dependent. A variational formulation is followed before introducing a finite element discretisation. In section 3.4 the PML stretching function is assumed to be spatially independent. With this assumption, the velocity and stress equations are derived for both finite and infinite elements. The global velocity equations are described by recombining the elemental descrip-

tions. In section 3.5 the PML stretching function has coefficients dependent only on the spatial variable  $x_1$ . The velocity and stress equations for the finite elements are found to be the same as in section 3.4, while infinite integral terms appear in the infinite element equations. An analysis of these integrals for particular forms of the stretching function coefficients is presented before the velocity and stress equations for the infinite elements are derived. Finally, an explicit scheme in the time domain for the global velocity equations is described by recombining the finite and infinite element equations. Section 3.7 presents the results for both the constant stretching case and the spatially dependent stretching case, in comparison with the finite element only method for a steel waveguide. A reflection coefficient is devised as a measure of accuracy and is used to explore possible values for the stretching function parameters.

### 3.3 Geometry and Governing Equations

Consider the problem of a semi-infinite rectangular waveguide with the geometry shown in Figure 3.1 where  $\Gamma_X$  is a notional face at  $x_1 = X_1$  which will later be allowed to tend to infinity,  $\Omega_F$  is the inner domain, modelled by conventional Finite Element Method techniques, and  $\Omega_I$  is the outer domain, modelled by Perfectly Matching Layer (PML)/Infinite Element (IE) combinations.

The governing elastodynamic equations are [150]

$$\rho \frac{\partial v_i}{\partial t} = \sum_{j=1}^3 \frac{\partial \sigma_{ij}}{\partial x_j}, \quad (3.1)$$



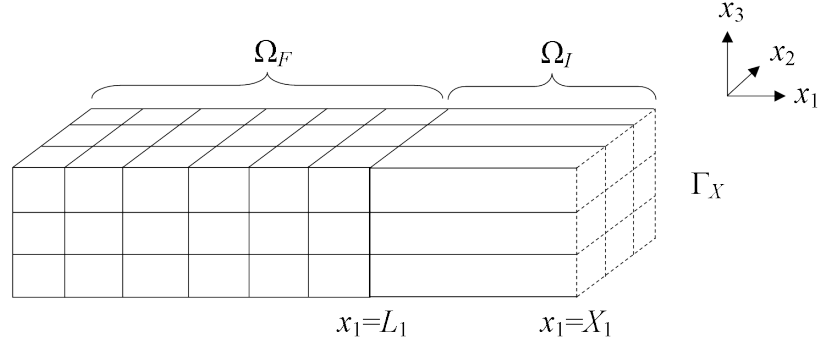


Figure 3.1: The geometry of the semi-infinite rectangular waveguide. The interior domain  $\Omega_F$  is of fixed length  $L_1$  and is meshed using standard finite elements. The exterior domain  $\Omega_I$  is the semi-infinite part of the domain and uses the PML/IE combination. The face  $\Gamma_X$  at  $x_1 = X_1$  is a notional face that will later be allowed to tend to infinity.

where

$$\sigma_{ij} = \sum_{k,l=1}^3 C_{ijkl} \frac{\partial u_k}{\partial x_l}.$$

That is

$$\frac{\partial \sigma_{ij}}{\partial t} = \sum_{k,l=1}^3 C_{ijkl} \frac{\partial v_k}{\partial x_l}, \quad (3.2)$$

with stress free boundary conditions on all faces except  $\Gamma_X$  where the Sommerfeld radiation condition is employed. Taking Fourier transforms in time of equations (3.1) and (3.2), then switching to stretched coordinates  $\tilde{x}_j$  gives (assuming  $v_i(\mathbf{x}, 0) = 0$  and  $\sigma_{ij}(\mathbf{x}, 0) = 0$ )

$$-i\omega\rho\hat{v}_i = \sum_{j=1}^3 \frac{\partial \hat{\sigma}_{ij}}{\partial \tilde{x}_j}, \quad (3.3)$$

$$-i\omega\hat{\sigma}_{ij} = \sum_{k,l=1}^3 C_{ijkl} \frac{\partial \hat{v}_k}{\partial \tilde{x}_l}. \quad (3.4)$$

Then using the transformation

$$\frac{\partial}{\partial \tilde{x}_j} = \frac{1}{s_j} \frac{\partial}{\partial x_j} \quad (3.5)$$

where

$$s_j(x_j) = \begin{cases} 1 & \text{in } \Omega_F \\ \alpha_j(x_j) \left(1 + \frac{i}{\omega} \beta_j(x_j)\right) & \text{in } \Omega_I \end{cases} \quad (3.6)$$

yields

$$-i\omega \rho \hat{v}_i = \sum_{j=1}^3 \frac{1}{s_j} \frac{\partial \hat{\sigma}_{ij}}{\partial \tilde{x}_j}, \quad (3.7)$$

$$-i\omega \hat{\sigma}_{ij} = \sum_{k,l=1}^3 \frac{C_{ijkl}}{s_l} \frac{\partial \hat{v}_k}{\partial \tilde{x}_l}. \quad (3.8)$$

Now multiplying both sides of equations (3.7) and (3.8) by a test function  $w$  and integrating over the whole domain  $\Omega = \Omega_F \cup \Omega_I$  gives

$$\int_{\Omega} -i\omega \rho \hat{v}_i w d\Omega = \int_{\Omega} \sum_{j=1}^3 \frac{1}{s_j} \frac{\partial \hat{\sigma}_{ij}}{\partial x_j} w d\Omega, \quad (3.9)$$

and

$$\int_{\Omega} -i\omega \hat{\sigma}_{ij} w d\Omega = \int_{\Omega} \sum_{k,l=1}^3 \frac{C_{ijkl}}{s_l} \frac{\partial \hat{v}_k}{\partial x_l} w d\Omega. \quad (3.10)$$

Now applying the divergence theorem to equation (3.9) and noting that all the boundaries of  $\Omega$  are stress-free *except*  $\Gamma_X$ ,

$$\int_{\Omega} -i\omega \rho \hat{v}_i w d\Omega = \int_{\Gamma_X} \sum_{j=1}^3 \frac{1}{s_j} \hat{\sigma}_{ij} w d\Gamma_X - \int_{\Omega} \sum_{j=1}^3 \frac{1}{s_j} \hat{\sigma}_{ij} \frac{\partial w}{\partial x_j} d\Omega. \quad (3.11)$$

Now substitute equation (3.8) into the  $\Gamma_X$  integral in equation (3.11) giving

$$\int_{\Omega} -i\omega\rho\hat{v}_i w d\Omega = \int_{\Gamma_X} \sum_{j,k,l=1}^3 \frac{1}{-i\omega s_j} \frac{C_{ijkl}}{s_l} \frac{\partial \hat{v}_k}{\partial x_l} w d\Gamma_X - \int_{\Omega} \sum_{j=1}^3 \frac{1}{s_j} \hat{\sigma}_{ij} \frac{\partial w}{\partial x_j} d\Omega. \quad (3.12)$$

Then by the Sommerfeld radiation condition

$$\nabla \hat{v}_i = -i\bar{k}\hat{v}_i + \epsilon \quad \text{on } \Gamma_X \quad (3.13)$$

where  $\epsilon = O(1/X_1^2)$  and where  $\bar{k}$  indicates that a choice of  $\bar{k}$  can be made as either the wavenumber of a compression wave or a shear wave, equation (3.12) becomes

$$\int_{\Omega} -i\omega\rho\hat{v}_i w d\Omega = \int_{\Gamma_X} \sum_{j,k,l=1}^3 \frac{C_{ijkl}}{s_j s_l} \left( \frac{1}{\bar{c}} \hat{v}_k + \frac{\epsilon}{-i\omega} \right) w d\Gamma_X - \int_{\Omega} \sum_{j=1}^3 \frac{1}{s_j} \hat{\sigma}_{ij} \frac{\partial w}{\partial x_j} d\Omega. \quad (3.14)$$

For an isotropic material with stiffness tensor  $C$  given by (switching to Voigt notation)

$$C = \begin{bmatrix} \lambda + 2\mu & \lambda & \lambda & 0 & 0 & 0 \\ \lambda & \lambda + 2\mu & \lambda & 0 & 0 & 0 \\ \lambda & \lambda & \lambda + 2\mu & 0 & 0 & 0 \\ 0 & 0 & 0 & \mu & 0 & 0 \\ 0 & 0 & 0 & 0 & \mu & 0 \\ 0 & 0 & 0 & 0 & 0 & \mu \end{bmatrix},$$

so from equation (3.8)

$$-i\omega\hat{\sigma}_{11} = \frac{\lambda + 2\mu}{s_1}\hat{v}_{1,1} + \frac{\lambda}{s_2}\hat{v}_{2,2} + \frac{\lambda}{s_3}\hat{v}_{3,3}, \quad (3.15)$$

$$-i\omega\hat{\sigma}_{22} = \frac{\lambda}{s_1}\hat{v}_{1,1} + \frac{\lambda + 2\mu}{s_2}\hat{v}_{2,2} + \frac{\lambda}{s_3}\hat{v}_{3,3}, \quad (3.16)$$

$$-i\omega\hat{\sigma}_{33} = \frac{\lambda}{s_1}\hat{v}_{1,1} + \frac{\lambda}{s_2}\hat{v}_{2,2} + \frac{\lambda + 2\mu}{s_3}\hat{v}_{3,3}, \quad (3.17)$$

$$-i\omega\hat{\sigma}_{23} = \frac{\mu}{s_2}\hat{v}_{3,2} + \frac{\mu}{s_3}\hat{v}_{2,3}, \quad (3.18)$$

$$-i\omega\hat{\sigma}_{13} = \frac{\mu}{s_1}\hat{v}_{3,1} + \frac{\mu}{s_3}\hat{v}_{1,3}, \quad (3.19)$$

and

$$-i\omega\hat{\sigma}_{12} = \frac{\mu}{s_1}\hat{v}_{2,1} + \frac{\mu}{s_2}\hat{v}_{1,2}. \quad (3.20)$$

Then letting  $\hat{\mathbf{v}} = (\hat{p}, \hat{q}, \hat{r})$ , equation (3.14) gives

$$\begin{aligned} \int_{\Omega} -i\omega\rho\hat{p}w\,d\Omega &= \int_{\Gamma_X} \left\{ \frac{\lambda + 2\mu}{s_1^2} \left( \frac{\hat{p}}{\bar{c}} + \frac{\epsilon}{-i\omega} \right) + \frac{\lambda}{s_1s_2} \left( \frac{\hat{q}}{\bar{c}} + \frac{\epsilon}{-i\omega} \right) \right. \\ &\quad + \frac{\lambda}{s_1s_3} \left( \frac{\hat{r}}{\bar{c}} + \frac{\epsilon}{-i\omega} \right) + \frac{\mu}{s_1s_2} \left( \frac{\hat{q}}{\bar{c}} + \frac{\epsilon}{-i\omega} \right) + \frac{\mu}{s_2^2} \left( \frac{\hat{p}}{\bar{c}} + \frac{\epsilon}{-i\omega} \right) \\ &\quad \left. + \frac{\mu}{s_1s_3} \left( \frac{\hat{r}}{\bar{c}} + \frac{\epsilon}{-i\omega} \right) + \frac{\mu}{s_3^2} \left( \frac{\hat{p}}{\bar{c}} + \frac{\epsilon}{-i\omega} \right) \right\} w\,d\Gamma_X \\ &\quad - \int_{\Omega} \left\{ \frac{\hat{\sigma}_{11}}{s_1} \frac{\partial w}{\partial x_1} + \frac{\hat{\sigma}_{12}}{s_2} \frac{\partial w}{\partial x_2} + \frac{\hat{\sigma}_{13}}{s_3} \frac{\partial w}{\partial x_3} \right\} d\Omega, \end{aligned} \quad (3.21)$$

$$\begin{aligned}
\int_{\Omega} -i\omega\rho\hat{q}wd\Omega &= \int_{\Gamma_X} \left\{ \frac{\mu}{s_1^2} \left( \frac{\hat{q}}{\bar{c}} + \frac{\epsilon}{-i\omega} \right) + \frac{\mu}{s_1s_2} \left( \frac{\hat{p}}{\bar{c}} + \frac{\epsilon}{-i\omega} \right) \right. \\
&\quad + \frac{\lambda}{s_1s_2} \left( \frac{\hat{p}}{\bar{c}} + \frac{\epsilon}{-i\omega} \right) + \frac{\lambda+2\mu}{s_2^2} \left( \frac{\hat{q}}{\bar{c}} + \frac{\epsilon}{-i\omega} \right) + \frac{\lambda}{s_2s_3} \left( \frac{\hat{r}}{\bar{c}} + \frac{\epsilon}{-i\omega} \right) \\
&\quad \left. + \frac{\mu}{s_2s_3} \left( \frac{\hat{r}}{\bar{c}} + \frac{\epsilon}{-i\omega} \right) + \frac{\mu}{s_3^2} \left( \frac{\hat{q}}{\bar{c}} + \frac{\epsilon}{-i\omega} \right) \right\} wd\Gamma_X \\
&\quad - \int_{\Omega} \left\{ \frac{\hat{\sigma}_{21}}{s_1} \frac{\partial w}{\partial x_1} + \frac{\hat{\sigma}_{22}}{s_2} \frac{\partial w}{\partial x_2} + \frac{\hat{\sigma}_{23}}{s_3} \frac{\partial w}{\partial x_3} \right\} d\Omega, \tag{3.22}
\end{aligned}$$

$$\begin{aligned}
\int_{\Omega} -i\omega\rho\hat{r}wd\Omega &= \int_{\Gamma_X} \left\{ \frac{\mu}{s_1^2} \left( \frac{\hat{r}}{\bar{c}} + \frac{\epsilon}{-i\omega} \right) + \frac{\mu}{s_1s_3} \left( \frac{\hat{p}}{\bar{c}} + \frac{\epsilon}{-i\omega} \right) \right. \\
&\quad + \frac{\mu}{s_2^2} \left( \frac{\hat{r}}{\bar{c}} + \frac{\epsilon}{-i\omega} \right) + \frac{\mu}{s_2s_3} \left( \frac{\hat{q}}{\bar{c}} + \frac{\epsilon}{-i\omega} \right) + \frac{\lambda}{s_1s_3} \left( \frac{\hat{p}}{\bar{c}} + \frac{\epsilon}{-i\omega} \right) \\
&\quad \left. + \frac{\lambda}{s_2s_3} \left( \frac{\hat{q}}{\bar{c}} + \frac{\epsilon}{-i\omega} \right) + \frac{\lambda+2\mu}{s_3^2} \left( \frac{\hat{r}}{\bar{c}} + \frac{\epsilon}{-i\omega} \right) \right\} wd\Gamma_X \\
&\quad - \int_{\Omega} \left\{ \frac{\hat{\sigma}_{13}}{s_1} \frac{\partial w}{\partial x_1} + \frac{\hat{\sigma}_{23}}{s_2} \frac{\partial w}{\partial x_2} + \frac{\hat{\sigma}_{33}}{s_3} \frac{\partial w}{\partial x_3} \right\} d\Omega, \tag{3.23}
\end{aligned}$$

Now discretise by letting  $p = \sum_{j=1}^N \phi_j(x_1, x_2, x_3)p_j(t)$ , for example, then

$$\begin{aligned}
\hat{p} &= \sum_{j=1}^N \phi_j(x_1, x_2, x_3) \hat{p}_j(\omega), \\
\hat{q} &= \sum_{j=1}^N \phi_j(x_1, x_2, x_3) \hat{q}_j(\omega), \\
\hat{r} &= \sum_{j=1}^N \phi_j(x_1, x_2, x_3) \hat{r}_j(\omega),
\end{aligned} \tag{3.24}$$

$$\begin{aligned}
\hat{\sigma}_1 &= \sum_{j=1}^N \phi_j(x_1, x_2, x_3) \hat{\gamma}_{1j}(\omega), \\
&\vdots \\
\hat{\sigma}_6 &= \sum_{j=1}^N \phi_j(x_1, x_2, x_3) \hat{\gamma}_{6j}(\omega),
\end{aligned} \tag{3.25}$$

(converting to Voigt notation meaning that  $\hat{\sigma}_1 \equiv \hat{\sigma}_{11}$ ,  $\hat{\sigma}_2 \equiv \hat{\sigma}_{22}$ ,  $\hat{\sigma}_3 \equiv \hat{\sigma}_{33}$ ,  $\hat{\sigma}_4 \equiv \hat{\sigma}_{23} = \hat{\sigma}_{32}$ ,  $\hat{\sigma}_5 \equiv \hat{\sigma}_{13} = \hat{\sigma}_{31}$ ,  $\hat{\sigma}_6 \equiv \hat{\sigma}_{12} = \hat{\sigma}_{21}$ ) where subscript  $j$  refers to the nodes in the finite element discretisation and where the  $\phi_j$  are basis functions defined as

$$\phi_j(x_1, x_2, x_3) = \begin{cases} N_j(x_1, x_2, x_3) & \text{in } \Omega_F \\ f_j(x_1, \omega)g_j(x_2, x_3) & \text{in } \Omega_I \end{cases} \quad (j = 1, \dots, N) \quad (3.26)$$

and the test function  $w$  is replaced by a series of test functions  $\theta_i$  of compact support, defined as

$$\theta_i(x_1, x_2, x_3) = \begin{cases} N_i(x_1, x_2, x_3) & \text{in } \Omega_F \\ w_i(x_1, \omega)g_i(x_2, x_3) & \text{in } \Omega_I \end{cases} \quad (i = 1, \dots, N). \quad (3.27)$$

Defining the test function in this way, means that there are now  $N$  test functions and equations (3.21)-(3.23) must be satisfied for all  $i = 1, \dots, N$ . Therefore, with the definitions given in equations (3.24)-(3.27), equations (3.21)-(3.23) become

$$\begin{aligned} & \sum_{j=1}^N \left\{ \int_{\Omega_F} -i\omega\rho N_i N_j d\Omega_F \hat{p}_j \right. \\ & + \left. \int_{\Omega_F} \left\{ \frac{1}{s_1} \frac{\partial N_i}{\partial x_1} N_j \hat{\gamma}_{1j} + \frac{1}{s_2} \frac{\partial N_i}{\partial x_2} N_j \hat{\gamma}_{6j} + \frac{1}{s_3} \frac{\partial N_i}{\partial x_3} N_j \hat{\gamma}_{5j} \right\} d\Omega_F \right\} \\ & = \sum_{j=1}^N \left\{ \frac{1}{\bar{c}} \left( \int_{\Gamma_X} \left( \frac{\lambda + 2\mu}{s_1^2} + \frac{\mu}{s_2^2} + \frac{\mu}{s_3^2} \right) w_i f_j g_i g_j d\Gamma_X \hat{p}_j \right. \right. \\ & + \left. \int_{\Gamma_X} \frac{\lambda + \mu}{s_1 s_2} w_i f_j g_i g_j d\Gamma_X \hat{q}_j + \int_{\Gamma_X} \frac{\lambda + \mu}{s_1 s_3} w_i f_j g_i g_j d\Gamma_X \hat{r}_j \right) \\ & + \frac{\epsilon}{-i\omega} \int_{\Gamma_X} \left( \frac{\lambda + 2\mu}{s_1^2} + \frac{\mu}{s_2^2} + \frac{\mu}{s_3^2} + \frac{\lambda + \mu}{s_1} \left( \frac{1}{s_2} + \frac{1}{s_3} \right) \right) w_i g_i d\Gamma_X \\ & - \int_{\Omega_I} \left\{ \frac{1}{s_1} \frac{\partial w_i}{\partial x_1} f_j g_i g_j \hat{\gamma}_{1j} + \frac{1}{s_2} w_i f_j \frac{\partial g_i}{\partial x_2} g_j \hat{\gamma}_{6j} + \frac{1}{s_3} w_i f_j \frac{\partial g_i}{\partial x_3} g_j \hat{\gamma}_{5j} \right\} d\Omega_I \\ & \left. - \int_{\Omega_I} -i\omega\rho w_i f_j g_i g_j d\Omega_I \hat{p}_j \right\} \quad (i = 1, \dots, N) \quad (3.28) \end{aligned}$$

$$\begin{aligned}
& \sum_{j=1}^N \left\{ \int_{\Omega_F} -i\omega\rho N_i N_j d\Omega_F \hat{q}_j \right. \\
& + \int_{\Omega_F} \left\{ \frac{1}{s_1} \frac{\partial N_i}{\partial x_1} N_j \hat{\gamma}_{6j} + \frac{1}{s_2} \frac{\partial N_i}{\partial x_2} N_j \hat{\gamma}_{2j} + \frac{1}{s_3} \frac{\partial N_i}{\partial x_3} N_j \hat{\gamma}_{4j} \right\} d\Omega_F \left. \right\} \\
& = \sum_{j=1}^N \left\{ \frac{1}{\bar{c}} \left( \int_{\Gamma_X} \left( \frac{\mu}{s_1^2} + \frac{\lambda + 2\mu}{s_2^2} + \frac{\mu}{s_3^2} \right) w_i f_j g_i g_j d\Gamma_X \hat{q}_j \right. \right. \\
& + \int_{\Gamma_X} \frac{\lambda + \mu}{s_1 s_2} w_i f_j g_i g_j d\Gamma_X \hat{p}_j + \int_{\Gamma_X} \frac{\lambda + \mu}{s_2 s_3} w_i f_j g_i g_j d\Gamma_X \hat{r}_j \left. \right) \\
& + \frac{\epsilon}{-i\omega} \int_{\Gamma_X} \left( \frac{\mu}{s_1^2} + \frac{\lambda + 2\mu}{s_2^2} + \frac{\mu}{s_3^2} + \frac{\lambda + \mu}{s_2} \left( \frac{1}{s_1} + \frac{1}{s_3} \right) \right) w_i g_i d\Gamma_X \\
& - \int_{\Omega_I} \left\{ \frac{1}{s_1} \frac{\partial w_i}{\partial x_1} f_j g_i g_j \hat{\gamma}_{6j} + \frac{1}{s_2} w_i f_j \frac{\partial g_i}{\partial x_2} g_j \hat{\gamma}_{2j} + \frac{1}{s_3} w_i f_j \frac{\partial g_i}{\partial x_3} g_j \hat{\gamma}_{4j} \right\} d\Omega_I \\
& \left. - \int_{\Omega_I} -i\omega\rho w_i f_j g_i g_j d\Omega_I \hat{q}_j \right\} \quad (i = 1, \dots, N) \tag{3.29}
\end{aligned}$$

$$\begin{aligned}
& \sum_{j=1}^N \left\{ \int_{\Omega_F} -i\omega\rho N_i N_j d\Omega_F \hat{r}_j \right. \\
& + \int_{\Omega_F} \left\{ \frac{1}{s_1} \frac{\partial N_i}{\partial x_1} N_j \hat{\gamma}_{5j} + \frac{1}{s_2} \frac{\partial N_i}{\partial x_2} N_j \hat{\gamma}_{4j} + \frac{1}{s_3} \frac{\partial N_i}{\partial x_3} N_j \hat{\gamma}_{3j} \right\} d\Omega_F \left. \right\} \\
& = \sum_{j=1}^N \left\{ \frac{1}{\bar{c}} \left( \int_{\Gamma_X} \left( \frac{\mu}{s_1^2} + \frac{\mu}{s_2^2} + \frac{\lambda + 2\mu}{s_3^2} \right) w_i f_j g_i g_j d\Gamma_X \hat{r}_j \right. \right. \\
& + \int_{\Gamma_X} \frac{\lambda + \mu}{s_1 s_3} w_i f_j g_i g_j d\Gamma_X \hat{p}_j + \int_{\Gamma_X} \frac{\lambda + \mu}{s_2 s_3} w_i f_j g_i g_j d\Gamma_X \hat{q}_j \left. \right) \\
& + \frac{\epsilon}{-i\omega} \int_{\Gamma_X} \left( \frac{\mu}{s_1^2} + \frac{\mu}{s_2^2} + \frac{\lambda + 2\mu}{s_3^2} + \frac{\lambda + \mu}{s_3} \left( \frac{1}{s_1} + \frac{1}{s_2} \right) \right) w_i g_i d\Gamma_X \\
& - \int_{\Omega_I} \left\{ \frac{1}{s_1} \frac{\partial w_i}{\partial x_1} f_j g_i g_j \hat{\gamma}_{5j} + \frac{1}{s_2} w_i f_j \frac{\partial g_i}{\partial x_2} g_j \hat{\gamma}_{4j} + \frac{1}{s_3} w_i f_j \frac{\partial g_i}{\partial x_3} g_j \hat{\gamma}_{3j} \right\} d\Omega_I \\
& \left. - \int_{\Omega_I} -i\omega\rho w_i f_j g_i g_j d\Omega_I \hat{r}_j \right\} \quad (i = 1, \dots, N) \tag{3.30}
\end{aligned}$$

Now in order to progress, some decisions must be made about the stretching function. Two scenarios will be considered: the first has constant stretching in all three directions, that is,  $s_1 = s_2 = s_3 \equiv s$ ; while the second scenario has stretching in

only one direction, with a spatial dependency retained, that is, set  $s_2 = s_3 \equiv 1$  and  $s_1$  remains a function of  $x_1$ . Note however that in both cases  $s$  is still a function of frequency.

## 3.4 Constant stretching

### 3.4.1 The velocity equations

In this case the aim is to simplify the integrals involved and so it is assumed that  $s_j$  is independent of  $x_j$ , that is,  $s_1 = s_2 = s_3 \equiv s$ . Then multiplying throughout equations (3.28)-(3.30) by  $s$  gives

$$\begin{aligned}
& \sum_{j=1}^N \left\{ \int_{\Omega_F} -i\omega\rho N_i N_j d\Omega_F s \hat{p}_j \right. \\
& \left. + \int_{\Omega_F} \left\{ \frac{\partial N_i}{\partial x_1} N_j \hat{\gamma}_{1j} + \frac{\partial N_i}{\partial x_2} N_j \hat{\gamma}_{6j} + \frac{\partial N_i}{\partial x_3} N_j \hat{\gamma}_{5j} \right\} d\Omega_F \right\} \\
& = \sum_{j=1}^N \left\{ \frac{1}{\bar{c}} \left( \int_{\Gamma_X} (\lambda + 4\mu) w_i f_j g_i g_j d\Gamma_X \frac{1}{s} \hat{p}_j \right. \right. \\
& \left. \left. + \int_{\Gamma_X} (\lambda + \mu) w_i f_j g_i g_j d\Gamma_X \frac{1}{s} \hat{q}_j + \int_{\Gamma_X} (\lambda + \mu) w_i f_j g_i g_j d\Gamma_X \frac{1}{s} \hat{r}_j \right) \right. \\
& \left. - \frac{\epsilon}{i\omega s} \int_{\Gamma_X} (3\lambda + 6\mu) w_i g_i d\Gamma_X \right. \\
& \left. - \int_{\Omega_I} \left\{ \frac{\partial w_i}{\partial x_1} f_j g_i g_j \hat{\gamma}_{1j} + w_i f_j \frac{\partial g_i}{\partial x_2} g_j \hat{\gamma}_{6j} + w_i f_j \frac{\partial g_i}{\partial x_3} g_j \hat{\gamma}_{5j} \right\} d\Omega_I \right. \\
& \left. + \int_{\Omega_I} i\omega\rho w_i f_j g_i g_j d\Omega_I s \hat{p}_j \right\} \quad (i = 1, \dots, N) \tag{3.31}
\end{aligned}$$



$$\begin{aligned}
& \sum_{j=1}^N \left\{ \int_{\Omega_F} -i\omega\rho N_i N_j d\Omega_F s \hat{q}_j \right. \\
& + \int_{\Omega_F} \left\{ \frac{\partial N_i}{\partial x_1} N_j \hat{\gamma}_{6j} + \frac{\partial N_i}{\partial x_2} N_j \hat{\gamma}_{2j} + \frac{\partial N_i}{\partial x_3} N_j \hat{\gamma}_{4j} \right\} d\Omega_F \left. \right\} \\
& = \sum_{j=1}^N \left\{ \frac{1}{\bar{c}} \left( \int_{\Gamma_X} (\lambda + 4\mu) w_i f_j g_i g_j d\Gamma_X \frac{1}{s} \hat{q}_j \right. \right. \\
& + \int_{\Gamma_X} (\lambda + \mu) w_i f_j g_i g_j d\Gamma_X \frac{1}{s} \hat{p}_j + \int_{\Gamma_X} (\lambda + \mu) w_i f_j g_i g_j d\Gamma_X \frac{1}{s} \hat{r}_j \left. \right. \\
& - \frac{\epsilon}{i\omega s} \int_{\Gamma_X} (3\lambda + 6\mu) w_i g_i d\Gamma_X \\
& - \int_{\Omega_I} \left\{ \frac{\partial w_i}{\partial x_1} f_j g_i g_j \hat{\gamma}_{6j} + w_i f_j \frac{\partial g_i}{\partial x_2} g_j \hat{\gamma}_{2j} + w_i f_j \frac{\partial g_i}{\partial x_3} g_j \hat{\gamma}_{4j} \right\} d\Omega_I \\
& \left. + \int_{\Omega_I} i\omega\rho w_i f_j g_i g_j d\Omega_I s \hat{q}_j \right\} \quad (i = 1, \dots, N) \tag{3.32}
\end{aligned}$$

$$\begin{aligned}
& \sum_{j=1}^N \left\{ \int_{\Omega_F} -i\omega\rho N_i N_j d\Omega_F s \hat{r}_j \right. \\
& + \int_{\Omega_F} \left\{ \frac{\partial N_i}{\partial x_1} N_j \hat{\gamma}_{5j} + \frac{\partial N_i}{\partial x_2} N_j \hat{\gamma}_{4j} + \frac{\partial N_i}{\partial x_3} N_j \hat{\gamma}_{3j} \right\} d\Omega_F \left. \right\} \\
& = \sum_{j=1}^N \left\{ \frac{1}{\bar{c}} \left( \int_{\Gamma_X} (\lambda + 4\mu) w_i f_j g_i g_j d\Gamma_X \frac{1}{s} \hat{r}_j \right. \right. \\
& + \int_{\Gamma_X} (\lambda + \mu) w_i f_j g_i g_j d\Gamma_X \frac{1}{s} \hat{p}_j + \int_{\Gamma_X} (\lambda + \mu) w_i f_j g_i g_j d\Gamma_X \frac{1}{s} \hat{q}_j \left. \right. \\
& - \frac{\epsilon}{i\omega s} \int_{\Gamma_X} (3\lambda + 6\mu) w_i g_i d\Gamma_X \\
& - \int_{\Omega_I} \left\{ \frac{\partial w_i}{\partial x_1} f_j g_i g_j \hat{\gamma}_{5j} + w_i f_j \frac{\partial g_i}{\partial x_2} g_j \hat{\gamma}_{4j} + w_i f_j \frac{\partial g_i}{\partial x_3} g_j \hat{\gamma}_{3j} \right\} d\Omega_I \\
& \left. + \int_{\Omega_I} i\omega\rho w_i f_j g_i g_j d\Omega_I s \hat{r}_j \right\} \quad (i = 1, \dots, N) \tag{3.33}
\end{aligned}$$

Now define the basis functions as functions of a local coordinate system  $(\xi, \eta, \zeta)$

which is centred on the node  $j$  and so

$$N_{j'}(\xi, \eta, \zeta) = \frac{1}{8}(1 + \xi\xi_{j'})(1 + \eta\eta_{j'})(1 + \zeta\zeta_{j'}) \quad \text{in } \Omega_F \quad (3.34)$$

$$f_{j'}(x_1, \omega) = \left(\frac{L_1}{x_1}\right) e^{-i\bar{k}(x_1-L_1)} \quad \text{in } \Omega_I \quad (3.35)$$

$$g_{j'}(\eta, \zeta) = \frac{1}{4}(1 + \eta\eta_{j'})(1 + \zeta\zeta_{j'}) \quad \text{in } \Omega_I \quad (3.36)$$

where  $(\xi_{j'}, \eta_{j'}, \zeta_{j'})$  are the local coordinates of node  $j'$ .

Now introduce a parameterisation in terms of these local coordinates of the finite and infinite elements. In  $\Omega_I$  this parameterisation is only used in the  $x_2$  and  $x_3$  directions. The mappings are shown in figures 3.4 and 3.6.

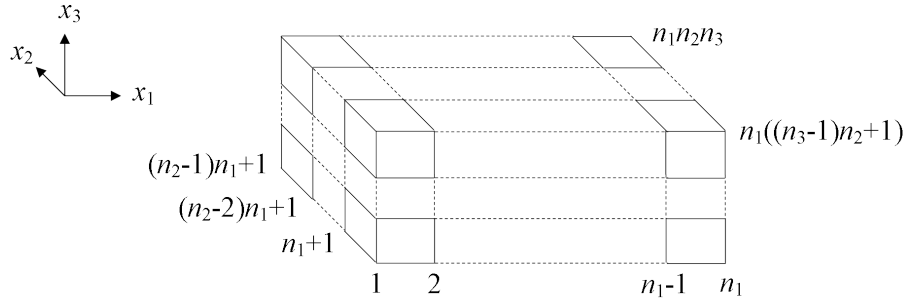


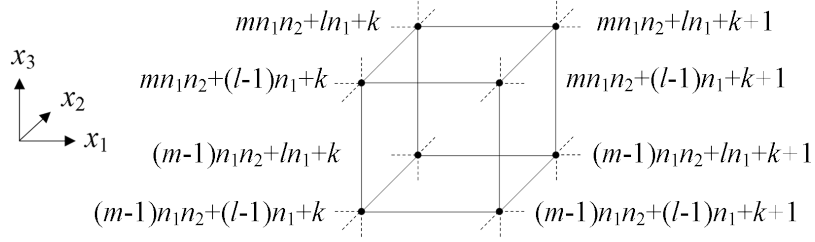
Figure 3.2: The global node numbering scheme (in  $\Omega_F$ ) is illustrated where  $n_1$ ,  $n_2$ , and  $n_3$ , are the number of nodes in the  $x_1$ ,  $x_2$ , and  $x_3$  directions respectively. The numbering sequence begins at the bottom front corner of the waveguide (position 1 above) where  $(x_1, x_2, x_3) = (0, 0, 0)$  and traverses the  $x_1$  direction first, the  $x_2$  direction second, and the  $x_3$  direction third.

The test functions are now chosen as

$$N_{i'}(\xi, \eta, \zeta) = \frac{1}{8}(1 + \xi\xi_{i'})(1 + \eta\eta_{i'})(1 + \zeta\zeta_{i'}) \quad \text{in } \Omega_F \quad (3.37)$$

$$w_{i'}(x_1, \omega) = \left(\frac{L_1}{x_1}\right)^3 e^{i\bar{k}(x_1-L_1)} \equiv \left(\frac{L_1}{x_1}\right)^2 \text{conj}\{f_{j'}\} \quad \text{in } \Omega_I \quad (3.38)$$

where the choice of  $w_{i'}$  is based on the Astley-Leis infinite element [125]. So the



$$\text{Finite Element number } e = (m-1)(n_1n_2-1) + (l-1)(n_1-1) + k$$

$$k=1, \dots, n_1-1, \quad l=1, \dots, n_2-1, \quad m=1, \dots, n_3-1$$

Figure 3.3: The global node numbers for a finite element  $e$  (in  $\Omega_F$ ) are shown, where  $k$ ,  $l$ , and  $m$  are indices rather than coordinates, and where  $n_1$ ,  $n_2$ , and  $n_3$ , again denote the number of nodes in the  $x_1$ ,  $x_2$ , and  $x_3$  directions respectively.

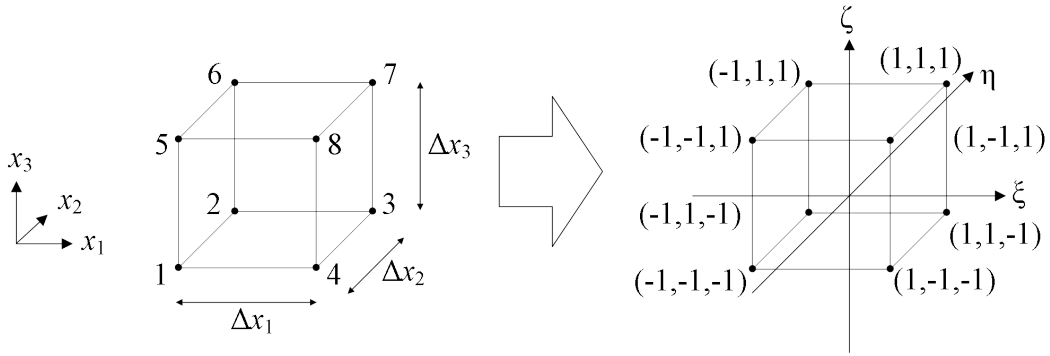


Figure 3.4: The mapping of the finite elements (in  $\Omega_F$ ) in global coordinates  $(x_1, x_2, x_3)$  to local coordinates  $(\xi, \eta, \zeta)$  with node numbering indicated as shown. The local node numbering  $i' = 1, \dots, 8$ , is used in the figure on the left.

basis function at node  $i$  corresponding to the vertex labelled 1 in the left-hand element in figure 3.4 corresponds to  $(\xi, \eta, \zeta) = (-1, -1, -1)$  in the right-hand element in figure 3.4.

Now with the mappings given as above, choose

$$\xi(x_1) = \frac{2}{\Delta x_1} \left( |x_1 - x_{1j'}| - \frac{\Delta x_1}{2} \right), \quad (3.39)$$

$$\eta(x_2) = \frac{2}{\Delta x_2} \left( |x_2 - x_{2j'}| - \frac{\Delta x_2}{2} \right),$$

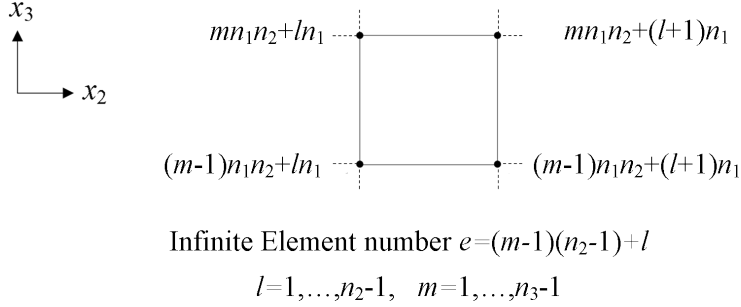


Figure 3.5: The global node numbers for an infinite element  $e$  (in  $\Omega_I$ ) are shown, where  $l$  and  $m$  are indices rather than coordinates, and where  $n_1$ ,  $n_2$ , and  $n_3$ , again denote the number of nodes in the  $x_1$ ,  $x_2$ , and  $x_3$  directions respectively.

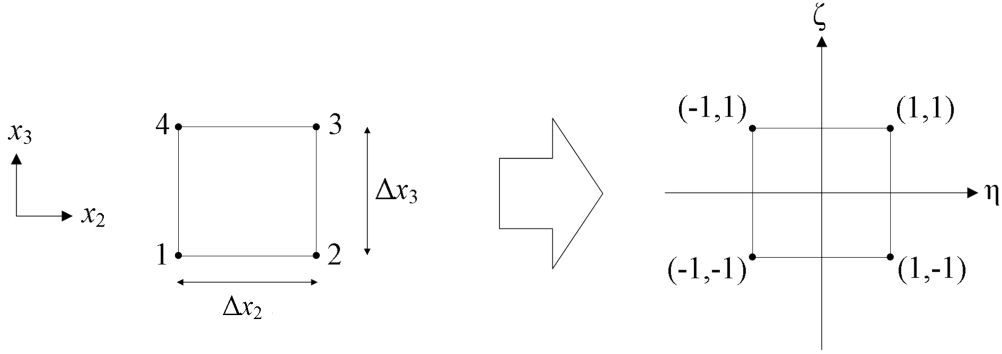


Figure 3.6: The mapping of the infinite elements (in  $\Omega_I$ ) in global coordinates  $(x_2, x_3)$  to local coordinates  $(\eta, \zeta)$  with node numbering indicated as shown. The local node numbering  $i' = 1, \dots, 4$ , is used in the figure on the left and the  $x_1$  direction (the infinite element direction) points out of the plane of the page.

and

$$\zeta(x_3) = \frac{2}{\Delta x_3} \left( |x_3 - x_{3j'}| - \frac{\Delta x_3}{2} \right).$$

Hence the  $N_{i'}$  have value 1 at node  $i'$  and value 0 at all other nodes, and the  $N_{i'}$  form a continuous function whose support is in the elements of which node  $i'$

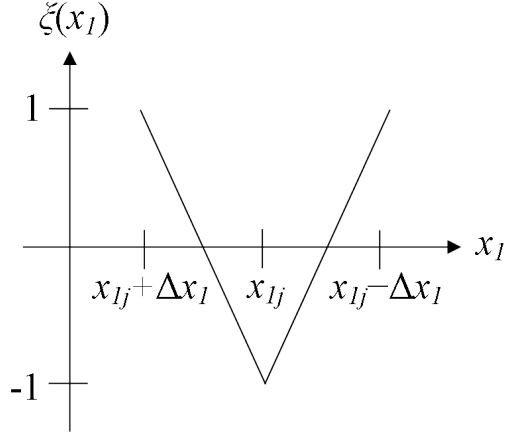


Figure 3.7: Local coordinate  $\xi$  is plotted as a function of global coordinate  $x_1$ . The other local coordinates  $\eta(x_2)$  and  $\zeta(x_3)$  follow similarly.

is a vertex. Hence, from equation (3.37)

$$\frac{\partial N_{j'}}{\partial \xi} = \frac{\xi_{j'}}{8} (1 + \eta\eta_{j'}) (1 + \zeta\zeta_{j'}), \quad (3.40)$$

and from equation (3.39)

$$\frac{\partial \xi}{\partial x_1} = \frac{2}{\Delta x_1}.$$

Then

$$\frac{\partial N_{j'}}{\partial x_1} = \frac{\partial N_{j'}}{\partial \xi} \frac{\partial \xi}{\partial x_1} = \frac{2}{\Delta x_1} \frac{\partial N_{j'}}{\partial \xi}. \quad (3.41)$$

Similarly

$$\frac{\partial N_{j'}}{\partial x_2} = \frac{2}{\Delta x_2} \frac{\partial N_{j'}}{\partial \eta}, \quad \frac{\partial N_{j'}}{\partial x_3} = \frac{2}{\Delta x_3} \frac{\partial N_{j'}}{\partial \zeta}, \quad \frac{\partial g_{j'}}{\partial x_2} = \frac{2}{\Delta x_2} \frac{\partial g_{j'}}{\partial \eta}, \quad \frac{\partial g_{j'}}{\partial x_3} = \frac{2}{\Delta x_3} \frac{\partial g_{j'}}{\partial \zeta}, \quad (3.42)$$

and similarly

$$\frac{\partial \eta}{\partial x_2} = \frac{2}{\Delta x_2} \quad \text{and} \quad \frac{\partial \zeta}{\partial x_3} = \frac{2}{\Delta x_3}. \quad (3.43)$$

The integrals over the finite part of the domain,  $\Omega_F$ , are then split into integrals over each finite element,  $\Omega_{FE}$ , and the integrals over the infinite part of the domain,  $\Omega_I$ , are split into integrals over each infinite element,  $\Omega_{IE}$ . These integrals will later be recombined such that  $\sum_{FE} \left( \int_{\Omega_{FE}} d\Omega_{FE} \right) = \int_{\Omega_F} d\Omega_F$  and  $\sum_{IE} \left( \int_{\Omega_{IE}} d\Omega_{IE} \right) = \int_{\Omega_I} d\Omega_I$ . Equations (3.41)-(3.43) will therefore be needed to evaluate the integrals over the finite elements or infinite elements.

So, switching to the local coordinate system as shown in figure 3.4, from the left-hand side of equations (3.31)-(3.33) with  $s = 1$ , define for each finite element (in  $\Omega_F$ )

$$A_{1i'}^{(F)} = \sum_{j'=1}^8 \left\{ -i\omega\rho \int_{\Omega_{FE}} N_{i'} N_{j'} d\Omega_{FE} \hat{p}_{j'} + \int_{\Omega_{FE}} \left\{ \frac{\partial N_{i'}}{\partial x_1} N_{j'} \hat{\gamma}_{1j'} + \frac{\partial N_{i'}}{\partial x_2} N_{j'} \hat{\gamma}_{6j'} + \frac{\partial N_{i'}}{\partial x_3} N_{j'} \hat{\gamma}_{5j'} \right\} d\Omega_{FE} \right\} \quad (i' = 1, \dots, 8), \quad (3.44)$$

$$A_{2i'}^{(F)} = \sum_{j'=1}^8 \left\{ -i\omega\rho \int_{\Omega_{FE}} N_{i'} N_{j'} d\Omega_{FE} \hat{q}_{j'} + \int_{\Omega_{FE}} \left\{ \frac{\partial N_{i'}}{\partial x_1} N_{j'} \hat{\gamma}_{6j'} + \frac{\partial N_{i'}}{\partial x_2} N_{j'} \hat{\gamma}_{2j'} + \frac{\partial N_{i'}}{\partial x_3} N_{j'} \hat{\gamma}_{4j'} \right\} d\Omega_{FE} \right\} \quad (i' = 1, \dots, 8), \quad (3.45)$$

$$A_{3i'}^{(F)} = \sum_{j'=1}^8 \left\{ -i\omega\rho \int_{\Omega_{FE}} N_{i'} N_{j'} d\Omega_{FE} \hat{r}_{j'} + \int_{\Omega_{FE}} \left\{ \frac{\partial N_{i'}}{\partial x_1} N_{j'} \hat{\gamma}_{5j'} + \frac{\partial N_{i'}}{\partial x_2} N_{j'} \hat{\gamma}_{4j'} + \frac{\partial N_{i'}}{\partial x_3} N_{j'} \hat{\gamma}_{3j'} \right\} d\Omega_{FE} \right\} \quad (i' = 1, \dots, 8), \quad (3.46)$$

and from the right-hand side of equations (3.31)-(3.33) (taking the negative in order to emphasise the similarity with the finite element case), define for each infinite element (in  $\Omega_I$ )

$$\begin{aligned}
A_{1i'}^{(I)} = & \sum_{j'=1}^4 \left\{ -i\omega\rho \int_{\Omega_{IE}} w_{i'} f_{j'} g_{i'} g_{j'} d\Omega_{IE} \hat{p}_{j'} \right. \\
& - \frac{1}{\bar{c}} \left( \frac{\lambda + 4\mu}{s} \hat{p}_{j'} + \frac{\lambda + \mu}{s} \hat{q}_{j'} + \frac{\lambda + \mu}{s} \hat{r}_{j'} \right) \int_{\Gamma_X} w_{i'} f_{j'} g_{i'} g_{j'} d\Gamma_X \\
& - \frac{\epsilon}{-i\omega s} (3\lambda + 6\mu) \int_{\Gamma_X} w_{i'} g_{i'} d\Gamma_X \\
& \left. + \int_{\Omega_{IE}} \left\{ \frac{\partial w_{i'}}{\partial x_1} f_{j'} g_{i'} g_{j'} \hat{\gamma}_{1j'} + w_{i'} f_{j'} \frac{\partial g_{i'}}{\partial x_2} g_{j'} \hat{\gamma}_{6j'} + w_{i'} f_{j'} \frac{\partial g_{i'}}{\partial x_3} g_{j'} \hat{\gamma}_{5j'} \right\} d\Omega_{IE} \right\} \\
& (i' = 1, \dots, 4),
\end{aligned} \tag{3.47}$$

$$\begin{aligned}
A_{2i'}^{(I)} = & \sum_{j'=1}^4 \left\{ -i\omega\rho \int_{\Omega_{IE}} w_{i'} f_{j'} g_{i'} g_{j'} d\Omega_{IE} \hat{q}_{j'} \right. \\
& - \frac{1}{\bar{c}} \left( \frac{\lambda + 4\mu}{s} \hat{q}_{j'} + \frac{\lambda + \mu}{s} \hat{p}_{j'} + \frac{\lambda + \mu}{s} \hat{r}_{j'} \right) \int_{\Gamma_X} w_{i'} f_{j'} g_{i'} g_{j'} d\Gamma_X \\
& - \frac{\epsilon}{-i\omega s} (3\lambda + 6\mu) \int_{\Gamma_X} w_{i'} g_{i'} d\Gamma_X \\
& \left. + \int_{\Omega_{IE}} \left\{ \frac{\partial w_{i'}}{\partial x_1} f_{j'} g_{i'} g_{j'} \hat{\gamma}_{6j'} + w_{i'} f_{j'} \frac{\partial g_{i'}}{\partial x_2} g_{j'} \hat{\gamma}_{2j'} + w_{i'} f_{j'} \frac{\partial g_{i'}}{\partial x_3} g_{j'} \hat{\gamma}_{4j'} \right\} d\Omega_{IE} \right\} \\
& (i' = 1, \dots, 4),
\end{aligned} \tag{3.48}$$

$$\begin{aligned}
A_{3i'}^{(I)} = & \sum_{j'=1}^4 \left\{ -i\omega\rho \int_{\Omega_{IE}} w_{i'} f_{j'} g_{i'} g_{j'} d\Omega_{IE} s \hat{r}_{j'} \right. \\
& - \frac{1}{\bar{c}} \left( \frac{\lambda + 4\mu}{s} \hat{r}_{j'} + \frac{\lambda + \mu}{s} \hat{p}_{j'} + \frac{\lambda + \mu}{s} \hat{q}_{j'} \right) \int_{\Gamma_X} w_{i'} f_{j'} g_{i'} g_{j'} d\Gamma_X \\
& - \frac{\epsilon}{-i\omega s} (3\lambda + 6\mu) \int_{\Gamma_X} w_{i'} g_{i'} d\Gamma_X \\
& \left. + \int_{\Omega_{IE}} \left\{ \frac{\partial w_{i'}}{\partial x_1} f_{j'} g_{i'} g_{j'} \hat{\gamma}_{5j'} + w_{i'} f_{j'} \frac{\partial g_{i'}}{\partial x_2} g_{j'} \hat{\gamma}_{4j'} + w_{i'} f_{j'} \frac{\partial g_{i'}}{\partial x_3} g_{j'} \hat{\gamma}_{3j'} \right\} d\Omega_{IE} \right\} \\
& (i' = 1, \dots, 4).
\end{aligned} \tag{3.49}$$

The integrals that must be evaluated are then (using equation (3.43))

$$\begin{aligned}
\int_{\Omega_{FE}} N_{i'} N_{j'} d\Omega_{FE} &= \int_{-1}^1 \int_{-1}^1 \int_{-1}^1 \frac{1}{8} (1 + \xi \xi_{i'}) (1 + \eta \eta_{i'}) (1 + \zeta \zeta_{i'}) \\
& \quad \times \frac{1}{8} (1 + \xi \xi_{j'}) (1 + \eta \eta_{j'}) (1 + \zeta \zeta_{j'}) \\
& \quad \times \frac{\Delta x_1 \Delta x_2 \Delta x_3}{8} d\xi d\eta d\zeta \\
&= \frac{\Delta x_1 \Delta x_2 \Delta x_3}{512} \int_{-1}^1 (1 + \xi \xi_{i'}) (1 + \xi \xi_{j'}) d\xi \\
& \quad \times \int_{-1}^1 (1 + \eta \eta_{i'}) (1 + \eta \eta_{j'}) d\eta \\
& \quad \times \int_{-1}^1 (1 + \zeta \zeta_{i'}) (1 + \zeta \zeta_{j'}) d\zeta \\
&= \frac{\Delta x_1 \Delta x_2 \Delta x_3}{512} \left[ \xi + \frac{\xi^2}{2} (\xi_{i'} + \xi_{j'}) + \frac{\xi^3}{3} \xi_{i'} \xi_{j'} \right]_{-1}^1 \\
& \quad \times \left[ \eta + \frac{\eta^2}{2} (\eta_{i'} + \eta_{j'}) + \frac{\eta^3}{3} \eta_{i'} \eta_{j'} \right]_{-1}^1 \\
& \quad \times \left[ \zeta + \frac{\zeta^2}{2} (\zeta_{i'} + \zeta_{j'}) + \frac{\zeta^3}{3} \zeta_{i'} \zeta_{j'} \right]_{-1}^1 \\
&= \frac{\Delta x_1 \Delta x_2 \Delta x_3}{512} \left( 2 + \frac{2\xi_{i'} \xi_{j'}}{3} \right) \left( 2 + \frac{2\eta_{i'} \eta_{j'}}{3} \right) \left( 2 + \frac{2\zeta_{i'} \zeta_{j'}}{3} \right) \\
&= \frac{\Delta x_1 \Delta x_2 \Delta x_3}{64} \left( 1 + \frac{\xi_{i'} \xi_{j'}}{3} \right) \left( 1 + \frac{\eta_{i'} \eta_{j'}}{3} \right) \left( 1 + \frac{\zeta_{i'} \zeta_{j'}}{3} \right), \tag{3.50}
\end{aligned}$$



and using equations (3.42), (3.37) and (3.40),

$$\begin{aligned}
\int_{\Omega_{FE}} \frac{\partial N_{i'}}{\partial x_1} N_{j'} d\Omega_{FE} &= \int_{-1}^1 \int_{-1}^1 \int_{-1}^1 \frac{2}{\Delta x_1} \frac{\partial N_{i'}}{\partial \xi} N_{j'} \frac{\Delta x_1 \Delta x_2 \Delta x_3}{8} d\xi d\eta d\zeta \\
&= \int_{-1}^1 \int_{-1}^1 \int_{-1}^1 \frac{\xi_{i'}}{8} (1 + \eta \eta_{i'}) (1 + \zeta \zeta_{i'}) \\
&\quad \times \frac{1}{8} (1 + \xi \xi_{j'}) (1 + \eta \eta_{j'}) (1 + \zeta \zeta_{j'}) \\
&\quad \times \frac{\Delta x_2 \Delta x_3}{4} d\xi d\eta d\zeta \\
&= \frac{\Delta x_2 \Delta x_3}{32} \xi_i \left(1 + \frac{\eta_{i'} \eta_{j'}}{3}\right) \left(1 + \frac{\zeta_{i'} \zeta_{j'}}{3}\right). \tag{3.51}
\end{aligned}$$

Similarly,

$$\int_{\Omega_{FE}} \frac{\partial N_{i'}}{\partial x_2} N_{j'} d\Omega_{FE} = \frac{\Delta x_1 \Delta x_3}{32} \eta_i \left(1 + \frac{\xi_{i'} \xi_{j'}}{3}\right) \left(1 + \frac{\zeta_{i'} \zeta_{j'}}{3}\right), \tag{3.52}$$

and

$$\int_{\Omega_{FE}} \frac{\partial N_{i'}}{\partial x_3} N_{j'} d\Omega_{FE} = \frac{\Delta x_1 \Delta x_2}{32} \zeta_i \left(1 + \frac{\xi_{i'} \xi_{j'}}{3}\right) \left(1 + \frac{\eta_{i'} \eta_{j'}}{3}\right). \tag{3.53}$$

That takes care of equations (3.44) to (3.46) and using equations (3.35), (3.36),

(3.38) and (3.43), for equation (3.47) gives

$$\begin{aligned}
\int_{\Omega_{IE}} w_{i'} f_{j'} g_{i'} g_{j'} d\Omega_{IE} &= \lim_{X_1 \rightarrow \infty} \int_{L_1}^{X_1} \left( \frac{L_1}{x_1} \right)^4 dx_1 \int_{-1}^1 \int_{-1}^1 \frac{1}{4} (1 + \eta \eta_{i'}) (1 + \zeta \zeta_{i'}) \\
&\quad \times \frac{1}{4} (1 + \eta \eta_{j'}) (1 + \zeta \zeta_{j'}) \\
&\quad \times \frac{\Delta x_2 \Delta x_3}{4} d\eta d\zeta \\
&= \frac{\Delta x_2 \Delta x_3}{64} \left( 2 + \frac{2\eta_{i'} \eta_{j'}}{3} \right) \left( 2 + \frac{2\zeta_{i'} \zeta_{j'}}{3} \right) \lim_{X_1 \rightarrow \infty} \left[ -\frac{L_1^4}{3x_1^3} \right]_{L_1}^{X_1} \\
&= \frac{\Delta x_2 \Delta x_3}{16} \left( 1 + \frac{\eta_{i'} \eta_{j'}}{3} \right) \left( 1 + \frac{\zeta_{i'} \zeta_{j'}}{3} \right) \lim_{X_1 \rightarrow \infty} \left( -\frac{L_1^4}{3X_1^3} + \frac{L_1}{3} \right) \\
&= \frac{\Delta x_2 \Delta x_3}{16} \left( 1 + \frac{\eta_{i'} \eta_{j'}}{3} \right) \left( 1 + \frac{\zeta_{i'} \zeta_{j'}}{3} \right) \frac{L_1}{3}. \tag{3.54}
\end{aligned}$$

Also

$$\begin{aligned}
\int_{\Gamma_X} w_{i'} f_{j'} g_{i'} g_{j'} d\Gamma_X &= \lim_{X_1 \rightarrow \infty} w_{i'}(X_1) f_{j'}(X_1) \int_{-1}^1 \int_{-1}^1 g_{i'} g_{j'} \frac{\Delta x_2 \Delta x_3}{4} d\eta d\zeta \\
&= \frac{\Delta x_2 \Delta x_3}{16} \left( 1 + \frac{\eta_{i'} \eta_{j'}}{3} \right) \left( 1 + \frac{\zeta_{i'} \zeta_{j'}}{3} \right) \lim_{X_1 \rightarrow \infty} \left( \frac{L_1}{X_1} \right)^4 \\
&= 0, \tag{3.55}
\end{aligned}$$

and

$$\begin{aligned}
\int_{\Gamma_X} w_{i'} g_{i'} d\Gamma_X &= \lim_{X_1 \rightarrow \infty} w_{i'}(X_1) \int_{-1}^1 \int_{-1}^1 g_{i'} \frac{\Delta x_2 \Delta x_3}{4} d\eta d\zeta \\
&= \frac{\Delta x_2 \Delta x_3}{4} \lim_{X_1 \rightarrow \infty} \left( \frac{L_1}{X_1} \right)^3 e^{i\bar{k}(X_1 - L_1)} \\
&= 0, \tag{3.56}
\end{aligned}$$

and, by differentiating equation (3.38),

$$\begin{aligned}
\int_{\Omega_{IE}} \frac{\partial w_{i'}}{\partial x_1} f_{j'} g_{i'} g_{j'} d\Omega_{IE} &= \lim_{X_1 \rightarrow \infty} \int_{L_1}^{X_1} \left( \frac{L_1}{x_1} \right)^4 \left( i\bar{k} - \frac{1}{x_1} \right) dx_1 \\
&\quad \times \int_{-1}^1 \int_{-1}^1 g_{i'} g_{j'} \frac{\Delta x_2 \Delta x_3}{4} d\eta d\zeta \\
&= \frac{\Delta x_2 \Delta x_3}{16} \left( 1 + \frac{\eta_{i'} \eta_{j'}}{3} \right) \left( 1 + \frac{\zeta_{i'} \zeta_{j'}}{3} \right) \\
&\quad \times \lim_{X_1 \rightarrow \infty} \left[ -\frac{i\bar{k} L_1^4}{3x_1^3} + \frac{L_1^4}{4x_1^4} \right]_{L_1}^{X_1} \\
&= \frac{\Delta x_2 \Delta x_3}{16} \left( 1 + \frac{\eta_{i'} \eta_{j'}}{3} \right) \left( 1 + \frac{\zeta_{i'} \zeta_{j'}}{3} \right) \\
&\quad \times \lim_{X_1 \rightarrow \infty} \left( -\frac{i\bar{k} L_1^4}{3X_1^3} + \frac{L_1^4}{4X_1^4} + \frac{i\bar{k} L_1}{3} - \frac{1}{4} \right) \\
&= \frac{\Delta x_2 \Delta x_3}{16} \left( 1 + \frac{\eta_{i'} \eta_{j'}}{3} \right) \left( 1 + \frac{\zeta_{i'} \zeta_{j'}}{3} \right) \left( \frac{i\bar{k} L_1}{3} - \frac{1}{4} \right). \quad (3.57)
\end{aligned}$$

Finally, from differentiating equation (3.36), from equations (3.42) and (3.43), and following a similar derivation to that in equation (3.54),

$$\begin{aligned}
\int_{\Omega_{IE}} w_{i'} f_{j'} \frac{\partial g_{i'}}{\partial x_2} g_{j'} d\Omega_{IE} &= \frac{L_1}{3} \int_{-1}^1 \int_{-1}^1 \frac{\partial g_{i'}}{\partial \eta} g_{j'} \frac{\Delta x_3}{2} d\eta d\zeta \\
&= \frac{L_1}{3} \frac{\Delta x_3}{8} \eta_i \left( 1 + \frac{\zeta_{i'} \zeta_{j'}}{3} \right), \quad (3.58)
\end{aligned}$$

and

$$\int_{\Omega_{IE}} w_{i'} f_{j'} \frac{\partial g_{i'}}{\partial x_3} g_{j'} d\Omega_{IE} = \frac{L_1}{3} \frac{\Delta x_2}{8} \zeta_{i'} \left( 1 + \frac{\eta_{i'} \eta_{j'}}{3} \right). \quad (3.59)$$

Then from equations (3.44)-(3.46) with the integrals given by equations (3.50)-

(3.53), for each finite element

$$\begin{aligned}
A_{1i'}^{(F)} = \sum_{j'=1}^8 \left\{ & -i\omega\rho \frac{\Delta x_1 \Delta x_2 \Delta x_3}{64} \left(1 + \frac{\xi_{i'} \xi_{j'}}{3}\right) \left(1 + \frac{\eta_{i'} \eta_{j'}}{3}\right) \left(1 + \frac{\zeta_{i'} \zeta_{j'}}{3}\right) \hat{p}_{j'} \right. \\
& + \frac{\Delta x_2 \Delta x_3}{32} \xi_{i'} \left(1 + \frac{\eta_{i'} \eta_{j'}}{3}\right) \left(1 + \frac{\zeta_{i'} \zeta_{j'}}{3}\right) \hat{\gamma}_{1j'} \\
& + \frac{\Delta x_1 \Delta x_3}{32} \eta_{i'} \left(1 + \frac{\xi_{i'} \xi_{j'}}{3}\right) \left(1 + \frac{\zeta_{i'} \zeta_{j'}}{3}\right) \hat{\gamma}_{6j'} \\
& \left. + \frac{\Delta x_1 \Delta x_2}{32} \zeta_{i'} \left(1 + \frac{\xi_{i'} \xi_{j'}}{3}\right) \left(1 + \frac{\eta_{i'} \eta_{j'}}{3}\right) \hat{\gamma}_{5j'} \right\} \quad (i' = 1, \dots, 8),
\end{aligned} \tag{3.60}$$

$$\begin{aligned}
A_{2i'}^{(F)} = \sum_{j'=1}^8 \left\{ & -i\omega\rho \frac{\Delta x_1 \Delta x_2 \Delta x_3}{64} \left(1 + \frac{\xi_{i'} \xi_{j'}}{3}\right) \left(1 + \frac{\eta_{i'} \eta_{j'}}{3}\right) \left(1 + \frac{\zeta_{i'} \zeta_{j'}}{3}\right) \hat{q}_{j'} \right. \\
& + \frac{\Delta x_2 \Delta x_3}{32} \xi_{i'} \left(1 + \frac{\eta_{i'} \eta_{j'}}{3}\right) \left(1 + \frac{\zeta_{i'} \zeta_{j'}}{3}\right) \hat{\gamma}_{6j'} \\
& + \frac{\Delta x_1 \Delta x_3}{32} \eta_{i'} \left(1 + \frac{\xi_{i'} \xi_{j'}}{3}\right) \left(1 + \frac{\zeta_{i'} \zeta_{j'}}{3}\right) \hat{\gamma}_{2j'} \\
& \left. + \frac{\Delta x_1 \Delta x_2}{32} \zeta_{i'} \left(1 + \frac{\xi_{i'} \xi_{j'}}{3}\right) \left(1 + \frac{\eta_{i'} \eta_{j'}}{3}\right) \hat{\gamma}_{4j'} \right\} \quad (i' = 1, \dots, 8),
\end{aligned} \tag{3.61}$$

$$\begin{aligned}
A_{3i'}^{(F)} = \sum_{j'=1}^8 \left\{ & -i\omega\rho \frac{\Delta x_1 \Delta x_2 \Delta x_3}{64} \left(1 + \frac{\xi_{i'} \xi_{j'}}{3}\right) \left(1 + \frac{\eta_{i'} \eta_{j'}}{3}\right) \left(1 + \frac{\zeta_{i'} \zeta_{j'}}{3}\right) \hat{r}_{j'} \right. \\
& + \frac{\Delta x_2 \Delta x_3}{32} \xi_{i'} \left(1 + \frac{\eta_{i'} \eta_{j'}}{3}\right) \left(1 + \frac{\zeta_{i'} \zeta_{j'}}{3}\right) \hat{\gamma}_{5j'} \\
& + \frac{\Delta x_1 \Delta x_3}{32} \eta_{i'} \left(1 + \frac{\xi_{i'} \xi_{j'}}{3}\right) \left(1 + \frac{\zeta_{i'} \zeta_{j'}}{3}\right) \hat{\gamma}_{4j'} \\
& \left. + \frac{\Delta x_1 \Delta x_2}{32} \zeta_{i'} \left(1 + \frac{\xi_{i'} \xi_{j'}}{3}\right) \left(1 + \frac{\eta_{i'} \eta_{j'}}{3}\right) \hat{\gamma}_{3j'} \right\} \quad (i' = 1, \dots, 8),
\end{aligned} \tag{3.62}$$

and from equations (3.47)-(3.49) with integrals given by equations (3.54)-(3.59), for each infinite element

$$\begin{aligned}
A_{1i'}^{(I)} = \sum_{j'=1}^4 \left\{ & -i\omega\rho \frac{\Delta x_2 \Delta x_3}{16} \left(1 + \frac{\eta_{i'} \eta_{j'}}{3}\right) \left(1 + \frac{\zeta_{i'} \zeta_{j'}}{3}\right) \frac{L_1}{3} s \hat{p}_{j'} \right. \\
& + \frac{\Delta x_2 \Delta x_3}{16} \left(1 + \frac{\eta_{i'} \eta_{j'}}{3}\right) \left(1 + \frac{\zeta_{i'} \zeta_{j'}}{3}\right) \left(\frac{i\bar{k}L_1}{3} - \frac{1}{4}\right) \hat{\gamma}_{1j'} \\
& + \frac{L_1}{3} \frac{\Delta x_3}{8} \eta_{i'} \left(1 + \frac{\zeta_{i'} \zeta_{j'}}{3}\right) \hat{\gamma}_{6j'} \\
& \left. + \frac{L_1}{3} \frac{\Delta x_2}{8} \zeta_{i'} \left(1 + \frac{\eta_{i'} \eta_{j'}}{3}\right) \hat{\gamma}_{5j'} \right\} \quad (i' = 1, \dots, 4), \tag{3.63}
\end{aligned}$$

$$\begin{aligned}
A_{2i'}^{(I)} = \sum_{j'=1}^4 \left\{ & -i\omega\rho \frac{\Delta x_2 \Delta x_3}{16} \left(1 + \frac{\eta_{i'} \eta_{j'}}{3}\right) \left(1 + \frac{\zeta_{i'} \zeta_{j'}}{3}\right) \frac{L_1}{3} s \hat{q}_{j'} \right. \\
& + \frac{\Delta x_2 \Delta x_3}{16} \left(1 + \frac{\eta_{i'} \eta_{j'}}{3}\right) \left(1 + \frac{\zeta_{i'} \zeta_{j'}}{3}\right) \left(\frac{i\bar{k}L_1}{3} - \frac{1}{4}\right) \hat{\gamma}_{6j'} \\
& + \frac{L_1}{3} \frac{\Delta x_3}{8} \eta_{i'} \left(1 + \frac{\zeta_{i'} \zeta_{j'}}{3}\right) \hat{\gamma}_{2j'} \\
& \left. + \frac{L_1}{3} \frac{\Delta x_2}{8} \zeta_{i'} \left(1 + \frac{\eta_{i'} \eta_{j'}}{3}\right) \hat{\gamma}_{4j'} \right\} \quad (i' = 1, \dots, 4), \quad (3.64)
\end{aligned}$$

$$\begin{aligned}
A_{3i'}^{(I)} = \sum_{j'=1}^4 \left\{ & -i\omega\rho \frac{\Delta x_2 \Delta x_3}{16} \left(1 + \frac{\eta_{i'} \eta_{j'}}{3}\right) \left(1 + \frac{\zeta_{i'} \zeta_{j'}}{3}\right) \frac{L_1}{3} s \hat{r}_{j'} \right. \\
& + \frac{\Delta x_2 \Delta x_3}{16} \left(1 + \frac{\eta_{i'} \eta_{j'}}{3}\right) \left(1 + \frac{\zeta_{i'} \zeta_{j'}}{3}\right) \left(\frac{i\bar{k}L_1}{3} - \frac{1}{4}\right) \hat{\gamma}_{5j'} \\
& + \frac{L_1}{3} \frac{\Delta x_3}{8} \eta_{i'} \left(1 + \frac{\zeta_{i'} \zeta_{j'}}{3}\right) \hat{\gamma}_{4j'} \\
& \left. + \frac{L_1}{3} \frac{\Delta x_2}{8} \zeta_{i'} \left(1 + \frac{\eta_{i'} \eta_{j'}}{3}\right) \hat{\gamma}_{3j'} \right\} \quad (i' = 1, \dots, 4). \quad (3.65)
\end{aligned}$$

The assumption is made that the stress components at a local node  $i'$ , given by  $\hat{\gamma}_{ni'}$  for  $n = 1, \dots, 6$ , is equal to the stress components at local node  $j'$ , given by  $\hat{\gamma}_{nj'}$  for  $n = 1, \dots, 6$ , when nodes  $i'$  and  $j'$  belong to the same element. Therefore

$$\hat{\gamma}_{ni'} = \hat{\gamma}_{nj'} \equiv \hat{\psi}_n \quad i', j' \in \Omega_e$$

where  $\Omega_e$  is either a finite or infinite element. Then  $\hat{\gamma}_{ni'}$ , the stress components at a local node  $i'$ , can be replaced by  $\hat{\psi}_n$ , the stress component for the element under consideration. Now expanding the summations in equations (3.60)-(3.65) with  $(\xi_{i'}, \eta_{i'}, \zeta_{i'})$  and  $(\xi_{j'}, \eta_{j'}, \zeta_{j'})$  given as in figure 3.4 for the finite elements and

in figure 3.6 for the infinite elements yields,

$$\sum_{j'=1}^8 \left(1 + \frac{\xi_{i'}\xi_{j'}}{3}\right) \left(1 + \frac{\eta_{i'}\eta_{j'}}{3}\right) \left(1 + \frac{\zeta_{i'}\zeta_{j'}}{3}\right) \hat{p}_{j'}$$

$$= \begin{cases} \frac{1}{27} (64\hat{p}_1 + 32\hat{p}_2 + 16\hat{p}_3 + 32\hat{p}_4 + 32\hat{p}_5 + 16\hat{p}_6 + 8\hat{p}_7 + 16\hat{p}_8) & i' = 1, \\ \frac{1}{27} (32\hat{p}_1 + 64\hat{p}_2 + 32\hat{p}_3 + 16\hat{p}_4 + 16\hat{p}_5 + 32\hat{p}_6 + 16\hat{p}_7 + 8\hat{p}_8) & i' = 2, \\ \frac{1}{27} (16\hat{p}_1 + 32\hat{p}_2 + 64\hat{p}_3 + 32\hat{p}_4 + 8\hat{p}_5 + 16\hat{p}_6 + 32\hat{p}_7 + 16\hat{p}_8) & i' = 3, \\ \frac{1}{27} (32\hat{p}_1 + 16\hat{p}_2 + 32\hat{p}_3 + 64\hat{p}_4 + 16\hat{p}_5 + 8\hat{p}_6 + 16\hat{p}_7 + 32\hat{p}_8) & i' = 4, \\ \frac{1}{27} (32\hat{p}_1 + 16\hat{p}_2 + 8\hat{p}_3 + 16\hat{p}_4 + 64\hat{p}_5 + 32\hat{p}_6 + 16\hat{p}_7 + 32\hat{p}_8) & i' = 5, \\ \frac{1}{27} (16\hat{p}_1 + 32\hat{p}_2 + 16\hat{p}_3 + 8\hat{p}_4 + 32\hat{p}_5 + 64\hat{p}_6 + 32\hat{p}_7 + 16\hat{p}_8) & i' = 6, \\ \frac{1}{27} (8\hat{p}_1 + 16\hat{p}_2 + 32\hat{p}_3 + 16\hat{p}_4 + 16\hat{p}_5 + 32\hat{p}_6 + 64\hat{p}_7 + 32\hat{p}_8) & i' = 7, \\ \frac{1}{27} (16\hat{p}_1 + 8\hat{p}_2 + 16\hat{p}_3 + 32\hat{p}_4 + 32\hat{p}_5 + 16\hat{p}_6 + 32\hat{p}_7 + 64\hat{p}_8) & i' = 8, \end{cases}$$

$$\sum_{j'=1}^8 \xi_{i'} \left(1 + \frac{\eta_{i'}\eta_{j'}}{3}\right) \left(1 + \frac{\zeta_{i'}\zeta_{j'}}{3}\right) = \begin{cases} -8 & i' \in \{1, 2, 5, 6\}, \\ 8 & i' \in \{3, 4, 7, 8\}, \end{cases}$$

$$\sum_{j'=1}^8 \eta_{i'} \left(1 + \frac{\xi_{i'}\xi_{j'}}{3}\right) \left(1 + \frac{\zeta_{i'}\zeta_{j'}}{3}\right) = \begin{cases} -8 & i' \in \{1, 4, 5, 8\}, \\ 8 & i' \in \{2, 3, 6, 7\}, \end{cases}$$

$$\sum_{j'=1}^8 \zeta_{i'} \left(1 + \frac{\xi_{i'}\xi_{j'}}{3}\right) \left(1 + \frac{\eta_{i'}\eta_{j'}}{3}\right) = \begin{cases} -8 & i' \in \{1, 2, 3, 4\}, \\ 8 & i' \in \{5, 6, 7, 8\}, \end{cases}$$

$$\sum_{j'=1}^4 \left(1 + \frac{\eta_{i'}\eta_{j'}}{3}\right) \left(1 + \frac{\zeta_{i'}\zeta_{j'}}{3}\right) \hat{p}_{j'} = \begin{cases} \frac{1}{9} (16\hat{p}_1 + 8\hat{p}_2 + 4\hat{p}_3 + 8\hat{p}_4) & i' = 1, \\ \frac{1}{9} (8\hat{p}_1 + 16\hat{p}_2 + 8\hat{p}_3 + 4\hat{p}_4) & i' = 2, \\ \frac{1}{9} (4\hat{p}_1 + 8\hat{p}_2 + 16\hat{p}_3 + 8\hat{p}_4) & i' = 3, \\ \frac{1}{9} (8\hat{p}_1 + 4\hat{p}_2 + 8\hat{p}_3 + 16\hat{p}_4) & i' = 4, \end{cases}$$

$$\sum_{j'=1}^4 \eta_{i'} \left(1 + \frac{\zeta_{i'}\zeta_{j'}}{3}\right) = \begin{cases} -4 & i' \in \{1, 4\}, \\ 4 & i' \in \{2, 3\}, \end{cases}$$

$$\sum_{j'=1}^4 \zeta_{i'} \left(1 + \frac{\eta_{i'}\eta_{j'}}{3}\right) = \begin{cases} -4 & i' \in \{1, 2\}, \\ 4 & i' \in \{3, 4\}, \end{cases}$$

and therefore, for each finite element, for example

$$A_{11}^{(F)} = \frac{\rho\Delta x_1\Delta x_2\Delta x_3}{216} (-i\omega) (8\hat{p}_1 + 4\hat{p}_2 + 2\hat{p}_3 + 4\hat{p}_4 + 4\hat{p}_5 + 2\hat{p}_6 + \hat{p}_7 + 2\hat{p}_8) \\ + \chi_1^{0,2} \frac{\Delta x_2\Delta x_3}{4} \hat{\psi}_1 + \chi_1^{1,2} \frac{\Delta x_1\Delta x_3}{4} \hat{\psi}_6 + \chi_1^{0,4} \frac{\Delta x_1\Delta x_2}{4} \hat{\psi}_5, \quad (3.66)$$

with similar expressions for  $A_{12}^{(F)}, \dots, A_{18}^{(F)}$ , and for each infinite element, for example

$$A_{11}^{(I)} = \frac{\rho\Delta x_2\Delta x_3L_1}{108} (-i\omega s) (4\hat{p}_1 + 2\hat{p}_2 + \hat{p}_3 + 2\hat{p}_4) \\ + \frac{\Delta x_2\Delta x_3}{4} \left(\frac{i\bar{k}L_1}{3} - \frac{1}{4}\right) \hat{\psi}_1 + \chi_1^{1,2} \frac{\Delta x_3L_1}{6} \hat{\psi}_6 + \chi_1^{0,2} \frac{\Delta x_2L_1}{6} \hat{\psi}_5, \quad (3.67)$$

with similar expressions for  $A_{12}^{(I)}, \dots, A_{14}^{(I)}$ . For computational speed we want to derive an explicit scheme to solve the discretised elastodynamic equations. Equations (3.60) to (3.62) form the discretised version of the left hand side of equations



(3.31) to (3.33) and in their current form will lead to an implicit set of algebraic equations in the unknowns. Deriving an explicit scheme would then require the inversion of a very large coefficient matrix which could only be conducted numerically and would be computationally expensive. One approach is to approximate this matrix by a diagonal one whose inversion can then be conducted by hand calculation. This approximation is made by performing mass lumping”, that is to say, summing the entries within a row of the velocity coefficient matrix and replacing the diagonal entry with this sum, setting all other entries to zero. This approximation is predicated on the assumption that there are no sharp changes in the velocities and so adjacent nodes have very similar values and hence one can approximate the value at one node by the value at its neighbour. Then for each finite element

$$\begin{aligned}
A_{1i'}^{(F)} &= \frac{\rho \Delta x_1 \Delta x_2 \Delta x_3}{8} (-i\omega \hat{p}_{i'}) \\
&\quad + \chi_{i'}^{0,2} \frac{\Delta x_2 \Delta x_3}{4} \hat{\psi}_1 + \chi_{i'}^{1,2} \frac{\Delta x_1 \Delta x_3}{4} \hat{\psi}_6 + \chi_{i'}^{0,4} \frac{\Delta x_1 \Delta x_2}{4} \hat{\psi}_5 \quad (i' = 1, \dots, 8),
\end{aligned} \tag{3.68}$$

$$\begin{aligned}
A_{2i'}^{(F)} &= \frac{\rho \Delta x_1 \Delta x_2 \Delta x_3}{8} (-i\omega \hat{q}_{i'}) \\
&\quad + \chi_{i'}^{0,2} \frac{\Delta x_2 \Delta x_3}{4} \hat{\psi}_6 + \chi_{i'}^{1,2} \frac{\Delta x_1 \Delta x_3}{4} \hat{\psi}_2 + \chi_{i'}^{0,4} \frac{\Delta x_1 \Delta x_2}{4} \hat{\psi}_4 \quad (i' = 1, \dots, 8),
\end{aligned} \tag{3.69}$$

$$\begin{aligned}
A_{3i'}^{(F)} &= \frac{\rho \Delta x_1 \Delta x_2 \Delta x_3}{8} (-i\omega \hat{r}_{i'}) \\
&\quad + \chi_{i'}^{0,2} \frac{\Delta x_2 \Delta x_3}{4} \hat{\psi}_5 + \chi_{i'}^{1,2} \frac{\Delta x_1 \Delta x_3}{4} \hat{\psi}_4 + \chi_{i'}^{0,4} \frac{\Delta x_1 \Delta x_2}{4} \hat{\psi}_3 \quad (i' = 1, \dots, 8),
\end{aligned} \tag{3.70}$$

and for each infinite element

$$\begin{aligned}
A_{1i'}^{(I)} &= \frac{\rho\Delta x_2\Delta x_3L_1}{12}(-i\omega s\hat{p}_{i'}) \\
&+ \frac{\Delta x_2\Delta x_3}{4}\left(\frac{i\bar{k}L_1}{3} - \frac{1}{4}\right)\hat{\psi}_1 + \chi_{i'}^{1,2}\frac{\Delta x_3L_1}{6}\hat{\psi}_6 + \chi_{i'}^{0,2}\frac{\Delta x_2L_1}{6}\hat{\psi}_5 \quad (i' = 1, \dots, 4),
\end{aligned} \tag{3.71}$$

$$\begin{aligned}
A_{2i'}^{(I)} &= \frac{\rho\Delta x_2\Delta x_3L_1}{12}(-i\omega s\hat{q}_{i'}) \\
&+ \frac{\Delta x_2\Delta x_3}{4}\left(\frac{i\bar{k}L_1}{3} - \frac{1}{4}\right)\hat{\psi}_6 + \chi_{i'}^{1,2}\frac{\Delta x_3L_1}{6}\hat{\psi}_2 + \chi_{i'}^{0,2}\frac{\Delta x_2L_1}{6}\hat{\psi}_4 \quad (i' = 1, \dots, 4),
\end{aligned} \tag{3.72}$$

$$\begin{aligned}
A_{3i'}^{(I)} &= \frac{\rho\Delta x_2\Delta x_3L_1}{12}(-i\omega s\hat{r}_{i'}) \\
&+ \frac{\Delta x_2\Delta x_3}{4}\left(\frac{i\bar{k}L_1}{3} - \frac{1}{4}\right)\hat{\psi}_5 + \chi_{i'}^{1,2}\frac{\Delta x_3L_1}{6}\hat{\psi}_4 + \chi_{i'}^{0,2}\frac{\Delta x_2L_1}{6}\hat{\psi}_3 \quad (i' = 1, \dots, 4),
\end{aligned} \tag{3.73}$$

where

$$\chi_{i'}^{m,n} = (-1)^\varphi \text{ with } \varphi = \left\lceil \frac{i' + m}{2n} \right\rceil, \tag{3.74}$$

and where  $\lceil \cdot \rceil$  denotes the ceiling function.

Now substituting for  $s(\omega)$  in equations (3.71)-(3.73) using equation (3.6) and taking inverse Fourier transforms in time of equations (3.68)-(3.73) gives, for each

finite element

$$\begin{aligned}
A_{1i'}^{(F)} &= \frac{\rho \Delta x_1 \Delta x_2 \Delta x_3}{8} \dot{p}_{i'} \\
&\quad + \chi_{i'}^{0,2} \frac{\Delta x_2 \Delta x_3}{4} \psi_1 + \chi_{i'}^{1,2} \frac{\Delta x_1 \Delta x_3}{4} \psi_6 + \chi_{i'}^{0,4} \frac{\Delta x_1 \Delta x_2}{4} \psi_5 \quad (i' = 1, \dots, 8),
\end{aligned} \tag{3.75}$$

$$\begin{aligned}
A_{2i'}^{(F)} &= \frac{\rho \Delta x_1 \Delta x_2 \Delta x_3}{8} \dot{q}_{i'} \\
&\quad + \chi_{i'}^{0,2} \frac{\Delta x_2 \Delta x_3}{4} \psi_6 + \chi_{i'}^{1,2} \frac{\Delta x_1 \Delta x_3}{4} \psi_2 + \chi_{i'}^{0,4} \frac{\Delta x_1 \Delta x_2}{4} \psi_4 \quad (i' = 1, \dots, 8),
\end{aligned} \tag{3.76}$$

$$\begin{aligned}
A_{3i'}^{(F)} &= \frac{\rho \Delta x_1 \Delta x_2 \Delta x_3}{8} \dot{r}_{i'} \\
&\quad + \chi_{i'}^{0,2} \frac{\Delta x_2 \Delta x_3}{4} \psi_5 + \chi_{i'}^{1,2} \frac{\Delta x_1 \Delta x_3}{4} \psi_4 + \chi_{i'}^{0,4} \frac{\Delta x_1 \Delta x_2}{4} \psi_3 \quad (i' = 1, \dots, 8),
\end{aligned} \tag{3.77}$$

and for each infinite element

$$\begin{aligned}
A_{1i'}^{(I)} &= \frac{\rho \Delta x_2 \Delta x_3 L_1}{12} \alpha (\dot{p}_{i'} + \beta p_{i'}) \\
&\quad - \frac{\Delta x_2 \Delta x_3}{4} \left( \frac{L_1}{3\bar{c}} \dot{\psi}_1 + \frac{1}{4} \psi_1 \right) + \chi_{i'}^{1,2} \frac{\Delta x_3 L_1}{6} \psi_6 + \chi_{i'}^{0,2} \frac{\Delta x_2 L_1}{6} \psi_5 \quad (i' = 1, \dots, 4),
\end{aligned} \tag{3.78}$$

$$\begin{aligned}
A_{2i'}^{(I)} &= \frac{\rho \Delta x_2 \Delta x_3 L_1}{12} \alpha (\dot{q}_{i'} + \beta q_{i'}) \\
&\quad - \frac{\Delta x_2 \Delta x_3}{4} \left( \frac{L_1}{3\bar{c}} \dot{\psi}_6 + \frac{1}{4} \psi_6 \right) + \chi_{i'}^{1,2} \frac{\Delta x_3 L_1}{6} \psi_2 + \chi_{i'}^{0,2} \frac{\Delta x_2 L_1}{6} \psi_4 \quad (i' = 1, \dots, 4),
\end{aligned} \tag{3.79}$$

$$\begin{aligned}
A_{3i'}^{(I)} &= \frac{\rho \Delta x_2 \Delta x_3 L_1}{12} \alpha (\dot{r}_{i'} + \beta r_{i'}) \\
&\quad - \frac{\Delta x_2 \Delta x_3}{4} \left( \frac{L_1}{3\bar{c}} \dot{\psi}_5 + \frac{1}{4} \psi_5 \right) + \chi_{i'}^{1,2} \frac{\Delta x_3 L_1}{6} \psi_4 + \chi_{i'}^{0,2} \frac{\Delta x_2 L_1}{6} \psi_3 \quad (i' = 1, \dots, 4).
\end{aligned} \tag{3.80}$$

### 3.4.2 The stress equations

Now from the stress equation (3.10) with equations (3.15)-(3.20)

$$\int_{\Omega} -i\omega \hat{\sigma}_1 w d\Omega = \int_{\Omega} \left\{ \frac{\lambda + 2\mu}{s_1} \frac{\partial \hat{p}}{\partial x_1} + \frac{\lambda}{s_2} \frac{\partial \hat{q}}{\partial x_2} + \frac{\lambda}{s_3} \frac{\partial \hat{r}}{\partial x_3} \right\} w d\Omega, \tag{3.81}$$

$$\int_{\Omega} -i\omega \hat{\sigma}_2 w d\Omega = \int_{\Omega} \left\{ \frac{\lambda}{s_1} \frac{\partial \hat{p}}{\partial x_1} + \frac{\lambda + 2\mu}{s_2} \frac{\partial \hat{q}}{\partial x_2} + \frac{\lambda}{s_3} \frac{\partial \hat{r}}{\partial x_3} \right\} w d\Omega, \tag{3.82}$$

$$\int_{\Omega} -i\omega \hat{\sigma}_3 w d\Omega = \int_{\Omega} \left\{ \frac{\lambda}{s_1} \frac{\partial \hat{p}}{\partial x_1} + \frac{\lambda}{s_2} \frac{\partial \hat{q}}{\partial x_2} + \frac{\lambda + 2\mu}{s_3} \frac{\partial \hat{r}}{\partial x_3} \right\} w d\Omega, \tag{3.83}$$

$$\int_{\Omega} -i\omega \hat{\sigma}_4 w d\Omega = \int_{\Omega} \left\{ \frac{\mu}{s_2} \frac{\partial \hat{r}}{\partial x_2} + \frac{\mu}{s_3} \frac{\partial \hat{q}}{\partial x_3} \right\} w d\Omega, \tag{3.84}$$

$$\int_{\Omega} -i\omega \hat{\sigma}_5 w d\Omega = \int_{\Omega} \left\{ \frac{\mu}{s_1} \frac{\partial \hat{r}}{\partial x_1} + \frac{\mu}{s_3} \frac{\partial \hat{p}}{\partial x_3} \right\} w d\Omega, \tag{3.85}$$

$$\int_{\Omega} -i\omega \hat{\sigma}_6 w d\Omega = \int_{\Omega} \left\{ \frac{\mu}{s_1} \frac{\partial \hat{q}}{\partial x_1} + \frac{\mu}{s_2} \frac{\partial \hat{p}}{\partial x_2} \right\} w d\Omega. \tag{3.86}$$

Then with the solution expressed in terms of the basis function expansion in equations (3.24) and (3.25), with the basis functions and test functions given by equations (3.26) and (3.27), assuming as before that  $s = 1$  in  $\Omega_F$  and  $s_1 = s_2 = s_3 \equiv s$

in  $\Omega_I$ , and multiplying throughout by  $s$ , from equations (3.81)-(3.86)

$$\begin{aligned}
& \sum_{j=1}^N \left\{ \int_{\Omega_F} -i\omega N_i N_j \hat{\gamma}_{1j} d\Omega_F \right. \\
& \quad \left. - \int_{\Omega_F} \left\{ (\lambda + 2\mu) N_i \frac{\partial N_j}{\partial x_1} \hat{p}_j + \lambda N_i \frac{\partial N_j}{\partial x_2} \hat{q}_j + \lambda N_i \frac{\partial N_j}{\partial x_3} \hat{r}_j \right\} d\Omega_F \right\} \\
& = \sum_{j=1}^N \left\{ \int_{\Omega_I} \left\{ (\lambda + 2\mu) w_i \frac{\partial f_j}{\partial x_1} g_i g_j \hat{p}_j + \lambda w_i f_j g_i \frac{\partial g_j}{\partial x_2} \hat{q}_j + \lambda w_i f_j g_i \frac{\partial g_j}{\partial x_3} \hat{r}_j \right\} d\Omega_I \right. \\
& \quad \left. - \int_{\Omega_I} -i\omega w_i f_j g_i g_j s \hat{\gamma}_{1j} d\Omega_I \right\} \quad (i = 1, \dots, N), \tag{3.87}
\end{aligned}$$

$$\begin{aligned}
& \sum_{j=1}^N \left\{ \int_{\Omega_F} -i\omega N_i N_j \hat{\gamma}_{2j} d\Omega_F \right. \\
& \quad \left. - \int_{\Omega_F} \left\{ \lambda N_i \frac{\partial N_j}{\partial x_1} \hat{p}_j + (\lambda + 2\mu) N_i \frac{\partial N_j}{\partial x_2} \hat{q}_j + \lambda N_i \frac{\partial N_j}{\partial x_3} \hat{r}_j \right\} d\Omega_F \right\} \\
& = \sum_{j=1}^N \left\{ \int_{\Omega_I} \left\{ \lambda w_i \frac{\partial f_j}{\partial x_1} g_i g_j \hat{p}_j + (\lambda + 2\mu) w_i f_j g_i \frac{\partial g_j}{\partial x_2} \hat{q}_j + \lambda w_i f_j g_i \frac{\partial g_j}{\partial x_3} \hat{r}_j \right\} d\Omega_I \right. \\
& \quad \left. - \int_{\Omega_I} -i\omega w_i f_j g_i g_j s \hat{\gamma}_{2j} d\Omega_I \right\} \quad (i = 1, \dots, N), \tag{3.88}
\end{aligned}$$

$$\begin{aligned}
& \sum_{j=1}^N \left\{ \int_{\Omega_F} -i\omega N_i N_j \hat{\gamma}_{3j} d\Omega_F \right. \\
& \quad \left. - \int_{\Omega_F} \left\{ \lambda N_i \frac{\partial N_j}{\partial x_1} \hat{p}_j + \lambda N_i \frac{\partial N_j}{\partial x_2} \hat{q}_j + (\lambda + 2\mu) N_i \frac{\partial N_j}{\partial x_3} \hat{r}_j \right\} d\Omega_F \right\} \\
& = \sum_{j=1}^N \left\{ \int_{\Omega_I} \left\{ \lambda w_i \frac{\partial f_j}{\partial x_1} g_i g_j \hat{p}_j + \lambda w_i f_j g_i \frac{\partial g_j}{\partial x_2} \hat{q}_j + (\lambda + 2\mu) w_i f_j g_i \frac{\partial g_j}{\partial x_3} \hat{r}_j \right\} d\Omega_I \right. \\
& \quad \left. - \int_{\Omega_I} -i\omega w_i f_j g_i g_j s \hat{\gamma}_{3j} d\Omega_I \right\} \quad (i = 1, \dots, N), \tag{3.89}
\end{aligned}$$

$$\begin{aligned}
& \sum_{j=1}^N \left\{ \int_{\Omega_F} -i\omega N_i N_j \hat{\gamma}_{4j} d\Omega_F - \int_{\Omega_F} \left\{ \mu N_i \frac{\partial N_j}{\partial x_2} \hat{r}_j + \mu N_i \frac{\partial N_j}{\partial x_3} \hat{q}_j \right\} d\Omega_F \right\} \\
&= \sum_{j=1}^N \left\{ \int_{\Omega_I} \left\{ \mu w_i f_j g_i \frac{\partial g_j}{\partial x_2} \hat{r}_j + \mu w_i f_j g_i \frac{\partial g_j}{\partial x_3} \hat{q}_j \right\} d\Omega_I \right. \\
&\quad \left. - \int_{\Omega_I} -i\omega w_i f_j g_i g_j s \hat{\gamma}_{4j} d\Omega_I \right\} \quad (i = 1, \dots, N), \tag{3.90}
\end{aligned}$$

$$\begin{aligned}
& \sum_{j=1}^N \left\{ \int_{\Omega_F} -i\omega N_i N_j \hat{\gamma}_{5j} d\Omega_F - \int_{\Omega_F} \left\{ \mu N_i \frac{\partial N_j}{\partial x_1} \hat{r}_j + \mu N_i \frac{\partial N_j}{\partial x_3} \hat{p}_j \right\} d\Omega_F \right\} \\
&= \sum_{j=1}^N \left\{ \int_{\Omega_I} \left\{ \mu w_i \frac{\partial f_j}{\partial x_1} g_i g_j \hat{r}_j + \mu w_i f_j g_i \frac{\partial g_j}{\partial x_3} \hat{p}_j \right\} d\Omega_I \right. \\
&\quad \left. - \int_{\Omega_I} -i\omega w_i f_j g_i g_j s \hat{\gamma}_{5j} d\Omega_I \right\} \quad (i = 1, \dots, N), \tag{3.91}
\end{aligned}$$

$$\begin{aligned}
& \sum_{j=1}^N \left\{ \int_{\Omega_F} -i\omega N_i N_j \hat{\gamma}_{6j} d\Omega_F - \int_{\Omega_F} \left\{ \mu N_i \frac{\partial N_j}{\partial x_1} \hat{q}_j + \mu N_i \frac{\partial N_j}{\partial x_2} \hat{p}_j \right\} d\Omega_F \right\} \\
&= \sum_{j=1}^N \left\{ \int_{\Omega_I} \left\{ \mu w_i \frac{\partial f_j}{\partial x_1} g_i g_j \hat{q}_j + \mu w_i f_j g_i \frac{\partial g_j}{\partial x_2} \hat{p}_j \right\} d\Omega_I \right. \\
&\quad \left. - \int_{\Omega_I} -i\omega w_i f_j g_i g_j s \hat{\gamma}_{6j} d\Omega_I \right\} \quad (i = 1, \dots, N). \tag{3.92}
\end{aligned}$$

Proceeding as before in treating these equations element by element in the local coordinate system  $(\xi, \eta, \zeta)$  with local node numbering  $(i', j')$ , then, given the choice of basis functions in equations (3.34)-(3.36) and test functions in equations (3.37) and (3.38), from the left-hand side of equation (3.87) with the integrals in equations

(3.50), (3.51), and (3.57)-(3.59), define for each finite element

$$\begin{aligned}
B_{1i'}^{(F)} = & \sum_{j'=1}^8 \left\{ \frac{\Delta x_1 \Delta x_2 \Delta x_3}{64} \left( 1 + \frac{\xi_{i'} \xi_{j'}}{3} \right) \left( 1 + \frac{\eta_{i'} \eta_{j'}}{3} \right) \left( 1 + \frac{\zeta_{i'} \zeta_{j'}}{3} \right) (-i\omega \hat{\gamma}_{1j'}) \right. \\
& - (\lambda + 2\mu) \frac{\Delta x_2 \Delta x_3}{32} \xi_{j'} \left( 1 + \frac{\eta_{i'} \eta_{j'}}{3} \right) \left( 1 + \frac{\zeta_{i'} \zeta_{j'}}{3} \right) \hat{p}_{j'} \\
& - \lambda \frac{\Delta x_1 \Delta x_3}{32} \eta_{j'} \left( 1 + \frac{\xi_{i'} \xi_{j'}}{3} \right) \left( 1 + \frac{\zeta_{i'} \zeta_{j'}}{3} \right) \hat{q}_{j'} \\
& \left. - \lambda \frac{\Delta x_1 \Delta x_2}{32} \zeta_{j'} \left( 1 + \frac{\xi_{i'} \xi_{j'}}{3} \right) \left( 1 + \frac{\eta_{i'} \eta_{j'}}{3} \right) \hat{r}_{j'} \right\} \quad (i' = 1, \dots, 8).
\end{aligned}$$

Again, since time derivatives of  $\gamma_{nj'}$  will otherwise result, in order to provide an explicit scheme the assumption is made that  $\hat{\gamma}_{ni'} = \hat{\gamma}_{nj'} \equiv \hat{\psi}_n$  when  $i', j'$  are nodes of the same element, then expanding the summations over  $j'$  gives

$$\begin{aligned}
B_1^{(F)} = & \Delta x_1 \Delta x_2 \Delta x_3 (-i\omega \hat{\psi}_1) \\
& - (\lambda + 2\mu) \frac{\Delta x_2 \Delta x_3}{4} (-\hat{p}_1 - \hat{p}_2 + \hat{p}_3 + \hat{p}_4 - \hat{p}_5 - \hat{p}_6 + \hat{p}_7 + \hat{p}_8) \\
& - \lambda \frac{\Delta x_1 \Delta x_3}{4} (-\hat{q}_1 + \hat{q}_2 + \hat{q}_3 - \hat{q}_4 - \hat{q}_5 + \hat{q}_6 + \hat{q}_7 - \hat{q}_8) \\
& - \lambda \frac{\Delta x_1 \Delta x_2}{4} (-\hat{r}_1 - \hat{r}_2 - \hat{r}_3 - \hat{r}_4 + \hat{r}_5 + \hat{r}_6 + \hat{r}_7 + \hat{r}_8).
\end{aligned}$$

Therefore

$$\begin{aligned}
\frac{B_1^{(F)}}{\Delta x_1 \Delta x_2 \Delta x_3} = & -i\omega \hat{\psi}_1 - \frac{\lambda + 2\mu}{4\Delta x_1} (-\hat{p}_1 - \hat{p}_2 + \hat{p}_3 + \hat{p}_4 - \hat{p}_5 - \hat{p}_6 + \hat{p}_7 + \hat{p}_8) \\
& - \frac{\lambda}{4\Delta x_2} (-\hat{q}_1 + \hat{q}_2 + \hat{q}_3 - \hat{q}_4 - \hat{q}_5 + \hat{q}_6 + \hat{q}_7 - \hat{q}_8) \\
& - \frac{\lambda}{4\Delta x_3} (-\hat{r}_1 - \hat{r}_2 - \hat{r}_3 - \hat{r}_4 + \hat{r}_5 + \hat{r}_6 + \hat{r}_7 + \hat{r}_8). \quad (3.93)
\end{aligned}$$

Then in the same way, from equations (3.88)-(3.92),

$$\begin{aligned} \frac{B_2^{(F)}}{\Delta x_1 \Delta x_2 \Delta x_3} &= -i\omega\hat{\psi}_2 - \frac{\lambda}{4\Delta x_1}(-\hat{p}_1 - \hat{p}_2 + \hat{p}_3 + \hat{p}_4 - \hat{p}_5 - \hat{p}_6 + \hat{p}_7 + \hat{p}_8) \\ &\quad - \frac{\lambda + 2\mu}{4\Delta x_2}(-\hat{q}_1 + \hat{q}_2 + \hat{q}_3 - \hat{q}_4 - \hat{q}_5 + \hat{q}_6 + \hat{q}_7 - \hat{q}_8) \\ &\quad - \frac{\lambda}{4\Delta x_3}(-\hat{r}_1 - \hat{r}_2 - \hat{r}_3 - \hat{r}_4 + \hat{r}_5 + \hat{r}_6 + \hat{r}_7 + \hat{r}_8), \end{aligned} \quad (3.94)$$

$$\begin{aligned} \frac{B_3^{(F)}}{\Delta x_1 \Delta x_2 \Delta x_3} &= -i\omega\hat{\psi}_3 - \frac{\lambda}{4\Delta x_1}(-\hat{p}_1 - \hat{p}_2 + \hat{p}_3 + \hat{p}_4 - \hat{p}_5 - \hat{p}_6 + \hat{p}_7 + \hat{p}_8) \\ &\quad - \frac{\lambda}{4\Delta x_2}(-\hat{q}_1 + \hat{q}_2 + \hat{q}_3 - \hat{q}_4 - \hat{q}_5 + \hat{q}_6 + \hat{q}_7 - \hat{q}_8) \\ &\quad - \frac{\lambda + 2\mu}{4\Delta x_3}(-\hat{r}_1 - \hat{r}_2 - \hat{r}_3 - \hat{r}_4 + \hat{r}_5 + \hat{r}_6 + \hat{r}_7 + \hat{r}_8), \end{aligned} \quad (3.95)$$

$$\begin{aligned} \frac{B_4^{(F)}}{\Delta x_1 \Delta x_2 \Delta x_3} &= -i\omega\hat{\psi}_4 - \frac{\mu}{4\Delta x_2}(\hat{r}_7 - \hat{r}_1 + \hat{r}_2 - \hat{r}_8 + \hat{r}_3 - \hat{r}_5 + \hat{r}_6 - \hat{r}_4) \\ &\quad - \frac{\mu}{4\Delta x_3}(\hat{q}_7 - \hat{q}_1 + \hat{q}_8 - \hat{q}_2 + \hat{q}_5 - \hat{q}_3 + \hat{q}_6 - \hat{q}_4), \end{aligned} \quad (3.96)$$

$$\begin{aligned} \frac{B_5^{(F)}}{\Delta x_1 \Delta x_2 \Delta x_3} &= -i\omega\hat{\psi}_5 - \frac{\mu}{4\Delta x_1}(\hat{r}_7 - \hat{r}_1 + \hat{r}_8 - \hat{r}_2 + \hat{r}_3 - \hat{r}_5 + \hat{r}_4 - \hat{r}_6) \\ &\quad - \frac{\mu}{4\Delta x_3}(\hat{p}_7 - \hat{p}_1 + \hat{p}_8 - \hat{p}_2 + \hat{p}_5 - \hat{p}_3 + \hat{p}_6 - \hat{p}_4), \end{aligned} \quad (3.97)$$

$$\begin{aligned} \frac{B_6^{(F)}}{\Delta x_1 \Delta x_2 \Delta x_3} &= -i\omega\hat{\psi}_6 - \frac{\mu}{4\Delta x_1}(\hat{q}_7 - \hat{q}_1 + \hat{q}_8 - \hat{q}_2 + \hat{q}_3 - \hat{q}_5 + \hat{q}_4 - \hat{q}_6) \\ &\quad - \frac{\mu}{4\Delta x_2}(\hat{p}_7 - \hat{p}_1 + \hat{p}_2 - \hat{p}_8 + \hat{p}_3 - \hat{p}_5 + \hat{p}_6 - \hat{p}_4). \end{aligned} \quad (3.98)$$

Then from the right-hand side of equation (3.87) (again taking the negative to emphasise the parallels with the finite element case), with the integrals in equations (3.54) and (3.57)-(3.59), define for each infinite element

$$\begin{aligned} B_{1i'}^{(I)} &= \sum_{j'=1}^4 \frac{\Delta x_2 \Delta x_3}{16} \left(1 + \frac{\eta_{i'} \eta_{j'}}{3}\right) \left(1 + \frac{\zeta_{i'} \zeta_{j'}}{3}\right) \frac{L_1}{3} (-i\omega s \hat{\gamma}_{1j'}) \\ &\quad - (\lambda + 2\mu) \frac{\Delta x_2 \Delta x_3}{16} \left(1 + \frac{\eta_{i'} \eta_{j'}}{3}\right) \left(1 + \frac{\zeta_{i'} \zeta_{j'}}{3}\right) \left(-\frac{i\bar{k}L_1}{3} - \frac{1}{4}\right) \hat{p}_{j'} \\ &\quad - \lambda \frac{L_1}{3} \frac{\Delta x_3}{8} \eta_{j'} \left(1 + \frac{\zeta_{i'} \zeta_{j'}}{3}\right) \hat{q}_{j'} - \lambda \frac{L_1}{3} \frac{\Delta x_2}{8} \zeta_{j'} \left(1 + \frac{\eta_{i'} \eta_{j'}}{3}\right) \hat{r}_{j'} \quad (i' = 1, \dots, 4). \end{aligned}$$



Again, expanding the summation over  $j'$  and summing over  $i' = 1, \dots, 4$  gives

$$\begin{aligned}
B_1^{(I)} &= -i\omega \frac{\Delta x_2 \Delta x_3 L_1}{3} s\hat{\psi}_1 - (\lambda + 2\mu) \frac{\Delta x_2 \Delta x_3}{4} \left( -\frac{i\bar{k}L_1}{3} - \frac{1}{4} \right) (\hat{p}_1 + \hat{p}_2 + \hat{p}_3 + \hat{p}_4) \\
&\quad - \lambda \frac{\Delta x_3 L_1}{6} (\hat{q}_3 - \hat{q}_1 + \hat{q}_2 - \hat{q}_4) - \lambda \frac{\Delta x_2 L_1}{6} (\hat{r}_3 - \hat{r}_1 + \hat{r}_4 - \hat{r}_2), \tag{3.99}
\end{aligned}$$

and similarly from equations (3.88)-(3.92) we have

$$\begin{aligned}
B_2^{(I)} &= -i\omega \frac{\Delta x_2 \Delta x_3 L_1}{3} s\hat{\psi}_2 - \lambda \frac{\Delta x_2 \Delta x_3}{4} \left( -\frac{i\bar{k}L_1}{3} - \frac{1}{4} \right) (\hat{p}_1 + \hat{p}_2 + \hat{p}_3 + \hat{p}_4) \\
&\quad - (\lambda + 2\mu) \frac{\Delta x_3 L_1}{6} (\hat{q}_3 - \hat{q}_1 + \hat{q}_2 - \hat{q}_4) \\
&\quad - \lambda \frac{\Delta x_2 L_1}{6} (\hat{r}_3 - \hat{r}_1 + \hat{r}_4 - \hat{r}_2), \tag{3.100}
\end{aligned}$$

$$\begin{aligned}
B_3^{(I)} &= -i\omega \frac{\Delta x_2 \Delta x_3 L_1}{3} s\hat{\psi}_3 - \lambda \frac{\Delta x_2 \Delta x_3}{4} \left( -\frac{i\bar{k}L_1}{3} - \frac{1}{4} \right) (\hat{p}_1 + \hat{p}_2 + \hat{p}_3 + \hat{p}_4) \\
&\quad - \lambda \frac{\Delta x_3 L_1}{6} (\hat{q}_3 - \hat{q}_1 + \hat{q}_2 - \hat{q}_4) \\
&\quad - (\lambda + 2\mu) \frac{\Delta x_2 L_1}{6} (\hat{r}_3 - \hat{r}_1 + \hat{r}_4 - \hat{r}_2), \tag{3.101}
\end{aligned}$$

$$\begin{aligned}
B_4^{(I)} &= -i\omega \frac{\Delta x_2 \Delta x_3 L_1}{3} s\hat{\psi}_4 - \mu \frac{\Delta x_3 L_1}{6} (\hat{r}_3 - \hat{r}_1 + \hat{r}_2 - \hat{r}_4) \\
&\quad - \mu \frac{\Delta x_2 L_1}{6} (\hat{q}_3 - \hat{q}_1 + \hat{q}_4 - \hat{q}_2), \tag{3.102}
\end{aligned}$$

$$\begin{aligned}
B_5^{(I)} &= -i\omega \frac{\Delta x_2 \Delta x_3 L_1}{3} s\hat{\psi}_5 - \mu \frac{\Delta x_2 \Delta x_3}{4} \left( -\frac{i\bar{k}L_1}{3} - \frac{1}{4} \right) (\hat{r}_1 + \hat{r}_2 + \hat{r}_3 + \hat{r}_4) \\
&\quad - \mu \frac{\Delta x_2 L_1}{6} (\hat{p}_3 - \hat{p}_1 + \hat{p}_4 - \hat{p}_2), \tag{3.103}
\end{aligned}$$

$$\begin{aligned}
B_6^{(I)} &= -i\omega \frac{\Delta x_2 \Delta x_3 L_1}{3} s\hat{\psi}_6 - \mu \frac{\Delta x_2 \Delta x_3}{4} \left( -\frac{i\bar{k}L_1}{3} - \frac{1}{4} \right) (\hat{q}_1 + \hat{q}_2 + \hat{q}_3 + \hat{q}_4) \\
&\quad - \mu \frac{\Delta x_3 L_1}{6} (\hat{p}_3 - \hat{p}_1 + \hat{p}_2 - \hat{p}_4). \tag{3.104}
\end{aligned}$$

Now assuming, from equation (3.6), a form for the stretching function of

$$-i\omega s = -i\omega\alpha + \alpha\beta,$$

then taking inverse Fourier transforms in time of equations (3.93)-(3.98) gives, for each finite element,

$$\begin{aligned}\frac{B_1^{(F)}}{\Delta x_1 \Delta x_2 \Delta x_3} &= \dot{\psi}_1 - \frac{\lambda + 2\mu}{4\Delta x_1} (p_7 - p_1 + p_8 - p_2 + p_3 - p_5 + p_4 - p_6) \\ &\quad - \frac{\lambda}{4\Delta x_2} (q_7 - q_1 + q_2 - q_8 + q_3 - q_5 + q_6 - q_4) \\ &\quad - \frac{\lambda}{4\Delta x_3} (r_7 - r_1 + r_8 - r_2 + r_5 - r_3 + r_6 - r_4),\end{aligned}\quad (3.105)$$

$$\begin{aligned}\frac{B_2^{(F)}}{\Delta x_1 \Delta x_2 \Delta x_3} &= \dot{\psi}_2 - \frac{\lambda}{4\Delta x_1} (p_7 - p_1 + p_8 - p_2 + p_3 - p_5 + p_4 - p_6) \\ &\quad - \frac{\lambda + 2\mu}{4\Delta x_2} (q_7 - q_1 + q_2 - q_8 + q_3 - q_5 + q_6 - q_4) \\ &\quad - \frac{\lambda}{4\Delta x_3} (r_7 - r_1 + r_8 - r_2 + r_5 - r_3 + r_6 - r_4),\end{aligned}\quad (3.106)$$

$$\begin{aligned}\frac{B_3^{(F)}}{\Delta x_1 \Delta x_2 \Delta x_3} &= \dot{\psi}_3 - \frac{\lambda}{4\Delta x_1} (p_7 - p_1 + p_8 - p_2 + p_3 - p_5 + p_4 - p_6) \\ &\quad - \frac{\lambda}{4\Delta x_2} (q_7 - q_1 + q_2 - q_8 + q_3 - q_5 + q_6 - q_4) \\ &\quad - \frac{\lambda + 2\mu}{4\Delta x_3} (r_7 - r_1 + r_8 - r_2 + r_5 - r_3 + r_6 - r_4),\end{aligned}\quad (3.107)$$

$$\begin{aligned}\frac{B_4^{(F)}}{\Delta x_1 \Delta x_2 \Delta x_3} &= \dot{\psi}_4 - \frac{\mu}{4\Delta x_2} (r_7 - r_1 + r_2 - r_8 + r_3 - r_5 + r_6 - r_4) \\ &\quad - \frac{\mu}{4\Delta x_3} (q_7 - q_1 + q_8 - q_2 + q_5 - q_3 + q_6 - q_4),\end{aligned}\quad (3.108)$$

$$\begin{aligned}\frac{B_5^{(F)}}{\Delta x_1 \Delta x_2 \Delta x_3} &= \dot{\psi}_5 - \frac{\mu}{4\Delta x_1} (r_7 - r_1 + r_8 - r_2 + r_3 - r_5 + r_4 - r_6) \\ &\quad - \frac{\mu}{4\Delta x_3} (p_7 - p_1 + p_8 - p_2 + p_5 - p_3 + p_6 - p_4),\end{aligned}\quad (3.109)$$

$$\begin{aligned}\frac{B_6^{(F)}}{\Delta x_1 \Delta x_2 \Delta x_3} &= \dot{\psi}_6 - \frac{\mu}{4\Delta x_1} (q_7 - q_1 + q_8 - q_2 + q_3 - q_5 + q_4 - q_6) \\ &\quad - \frac{\mu}{4\Delta x_2} (p_7 - p_1 + p_2 - p_8 + p_3 - p_5 + p_6 - p_4),\end{aligned}\quad (3.110)$$

and taking inverse Fourier transforms in time of equations (3.99)-(3.104) gives, for

each infinite element,

$$\begin{aligned}
B_1^{(I)} &= \frac{\Delta x_2 \Delta x_3 L_1 \alpha}{3} \left( \dot{\psi}_1 + \beta \psi_1 \right) - \frac{(\lambda + 2\mu) \Delta x_2 \Delta x_3}{4} \left( \frac{L_1}{3\bar{c}} (\dot{p}_1 + \dot{p}_2 + \dot{p}_3 + \dot{p}_4) \right. \\
&\quad \left. - \frac{1}{4} (p_1 + p_2 + p_3 + p_4) \right) - \frac{\lambda \Delta x_3 L_1}{6} (q_3 - q_1 + q_2 - q_4) \\
&\quad - \frac{\lambda \Delta x_2 L_1}{6} (r_3 - r_1 + r_4 - r_2), \tag{3.111}
\end{aligned}$$

$$\begin{aligned}
B_2^{(I)} &= \frac{\Delta x_2 \Delta x_3 L_1 \alpha}{3} \left( \dot{\psi}_2 + \beta \psi_2 \right) - \frac{\lambda \Delta x_2 \Delta x_3}{4} \left( \frac{L_1}{3\bar{c}} (\dot{p}_1 + \dot{p}_2 + \dot{p}_3 + \dot{p}_4) \right. \\
&\quad \left. - \frac{1}{4} (p_1 + p_2 + p_3 + p_4) \right) - \frac{(\lambda + 2\mu) \Delta x_3 L_1}{6} (q_3 - q_1 + q_2 - q_4) \\
&\quad - \frac{\lambda \Delta x_2 L_1}{6} (r_3 - r_1 + r_4 - r_2), \tag{3.112}
\end{aligned}$$

$$\begin{aligned}
B_3^{(I)} &= \frac{\Delta x_2 \Delta x_3 L_1 \alpha}{3} \left( \dot{\psi}_3 + \beta \psi_3 \right) - \frac{\lambda \Delta x_2 \Delta x_3}{4} \left( \frac{L_1}{3\bar{c}} (\dot{p}_1 + \dot{p}_2 + \dot{p}_3 + \dot{p}_4) \right. \\
&\quad \left. - \frac{1}{4} (p_1 + p_2 + p_3 + p_4) \right) - \frac{\lambda \Delta x_3 L_1}{6} (q_3 - q_1 + q_2 - q_4) \\
&\quad - \frac{(\lambda + 2\mu) \Delta x_2 L_1}{6} (r_3 - r_1 + r_4 - r_2), \tag{3.113}
\end{aligned}$$

$$\begin{aligned}
B_4^{(I)} &= \frac{\Delta x_2 \Delta x_3 L_1 \alpha}{3} \left( \dot{\psi}_4 + \beta \psi_4 \right) - \frac{\mu \Delta x_3 L_1}{6} (r_3 - r_1 + r_2 - r_4) \\
&\quad - \frac{\mu \Delta x_2 L_1}{6} (q_3 - q_1 + q_4 - q_2), \tag{3.114}
\end{aligned}$$

$$\begin{aligned}
B_5^{(I)} &= \frac{\Delta x_2 \Delta x_3 L_1 \alpha}{3} \left( \dot{\psi}_5 + \beta \psi_5 \right) - \frac{\mu \Delta x_2 \Delta x_3}{4} \left( \frac{L_1}{3\bar{c}} (\dot{r}_1 + \dot{r}_2 + \dot{r}_3 + \dot{r}_4) \right. \\
&\quad \left. - \frac{1}{4} (r_1 + r_2 + r_3 + r_4) \right) - \frac{\mu \Delta x_2 L_1}{6} (p_3 - p_1 + p_4 - p_2), \tag{3.115}
\end{aligned}$$

$$\begin{aligned}
B_6^{(I)} &= \frac{\Delta x_2 \Delta x_3 L_1 \alpha}{3} \left( \dot{\psi}_6 + \beta \psi_6 \right) - \frac{\mu \Delta x_2 \Delta x_3}{4} \left( \frac{L_1}{3\bar{c}} (\dot{q}_1 + \dot{q}_2 + \dot{q}_3 + \dot{q}_4) \right. \\
&\quad \left. - \frac{1}{4} (q_1 + q_2 + q_3 + q_4) \right) - \frac{\mu \Delta x_3 L_1}{6} (p_3 - p_1 + p_2 - p_4). \tag{3.116}
\end{aligned}$$

For the infinite elements, both velocity and stress time derivatives appear so closer inspection is required of the system in order to find an explicit form. It must also be remembered that since the velocity equations will be recombined at a global level, whatever manipulation is done to the finite element equations

must also be done to the infinite element equations and vice versa. The system of equations (3.78)-(3.80) and (3.111)-(3.116) can be written in matrix form as

$$M_1 \dot{\mathbf{p}} = M_2 \mathbf{p} \quad (3.117)$$

where

$$M_1 = \begin{bmatrix} C_1 & 0 & 0 & 0 & 0 & 0 & 0 & 0 & 0 & 0 & 0 & 0 & 0 & C_2 & 0 & 0 & 0 & 0 & 0 & 0 \\ 0 & C_1 & 0 & 0 & 0 & 0 & 0 & 0 & 0 & 0 & 0 & 0 & 0 & C_2 & 0 & 0 & 0 & 0 & 0 & 0 \\ 0 & 0 & C_1 & 0 & 0 & 0 & 0 & 0 & 0 & 0 & 0 & 0 & 0 & C_2 & 0 & 0 & 0 & 0 & 0 & 0 \\ 0 & 0 & 0 & C_1 & 0 & 0 & 0 & 0 & 0 & 0 & 0 & 0 & 0 & C_2 & 0 & 0 & 0 & 0 & 0 & 0 \\ 0 & 0 & 0 & 0 & C_1 & 0 & 0 & 0 & 0 & 0 & 0 & 0 & 0 & 0 & 0 & 0 & 0 & 0 & C_2 & 0 \\ 0 & 0 & 0 & 0 & 0 & C_1 & 0 & 0 & 0 & 0 & 0 & 0 & 0 & 0 & 0 & 0 & 0 & 0 & 0 & C_2 \\ 0 & 0 & 0 & 0 & 0 & 0 & C_1 & 0 & 0 & 0 & 0 & 0 & 0 & 0 & 0 & 0 & 0 & 0 & 0 & C_2 \\ 0 & 0 & 0 & 0 & 0 & 0 & 0 & C_1 & 0 & 0 & 0 & 0 & 0 & 0 & 0 & 0 & 0 & 0 & 0 & C_2 \\ 0 & 0 & 0 & 0 & 0 & 0 & 0 & 0 & C_1 & 0 & 0 & 0 & 0 & 0 & 0 & 0 & 0 & 0 & 0 & C_2 \\ 0 & 0 & 0 & 0 & 0 & 0 & 0 & 0 & 0 & C_1 & 0 & 0 & 0 & 0 & 0 & 0 & 0 & 0 & 0 & C_2 \\ 0 & 0 & 0 & 0 & 0 & 0 & 0 & 0 & 0 & 0 & C_1 & 0 & 0 & 0 & 0 & 0 & 0 & 0 & 0 & C_2 \\ 0 & 0 & 0 & 0 & 0 & 0 & 0 & 0 & 0 & 0 & 0 & C_1 & 0 & 0 & 0 & 0 & 0 & 0 & 0 & C_2 \\ D_2 & D_2 & D_2 & D_2 & 0 & 0 & 0 & 0 & 0 & 0 & 0 & 0 & 0 & D_1 & 0 & 0 & 0 & 0 & 0 & 0 \\ D_3 & D_3 & D_3 & D_3 & 0 & 0 & 0 & 0 & 0 & 0 & 0 & 0 & 0 & D_1 & 0 & 0 & 0 & 0 & 0 & 0 \\ D_3 & D_3 & D_3 & D_3 & 0 & 0 & 0 & 0 & 0 & 0 & 0 & 0 & 0 & D_1 & 0 & 0 & 0 & 0 & 0 & 0 \\ 0 & 0 & 0 & 0 & 0 & 0 & 0 & 0 & 0 & 0 & 0 & 0 & 0 & 0 & 0 & 0 & D_1 & 0 & 0 & 0 \\ 0 & 0 & 0 & 0 & 0 & 0 & 0 & 0 & D_4 & D_4 & D_4 & D_4 & 0 & 0 & 0 & 0 & D_1 & 0 & 0 & 0 \\ 0 & 0 & 0 & 0 & D_4 & D_4 & D_4 & D_4 & 0 & 0 & 0 & 0 & 0 & 0 & 0 & 0 & 0 & 0 & 0 & D_1 \end{bmatrix}, \quad (3.118)$$

with

$$\begin{aligned} C_1 &= \rho \frac{\Delta x_2 \Delta x_3 L_1}{12} \alpha, \\ C_2 &= - \frac{\Delta x_2 \Delta x_3 L_1}{12 \bar{c}}, \\ D_1 &= \frac{\Delta x_2 \Delta x_3 L_1}{3} \alpha, \\ D_2 &= - \frac{\Delta x_2 \Delta x_3 L_1 (\lambda + 2\mu)}{12 \bar{c}}, \\ D_3 &= - \frac{\Delta x_2 \Delta x_3 L_1 \lambda}{12 \bar{c}}, \\ D_4 &= - \frac{\Delta x_2 \Delta x_3 L_1 \mu}{12 \bar{c}}, \end{aligned}$$

and where

$$M_2 = \begin{bmatrix} E_1 & 0 & 0 & 0 & 0 & 0 & 0 & 0 & 0 & 0 & 0 & 0 & E_2 & 0 & 0 & 0 & E_3 & E_4 \\ 0 & E_1 & 0 & 0 & 0 & 0 & 0 & 0 & 0 & 0 & 0 & 0 & E_2 & 0 & 0 & 0 & E_3 & -E_4 \\ 0 & 0 & E_1 & 0 & 0 & 0 & 0 & 0 & 0 & 0 & 0 & 0 & E_2 & 0 & 0 & 0 & -E_3 & -E_4 \\ 0 & 0 & 0 & E_1 & 0 & 0 & 0 & 0 & 0 & 0 & 0 & 0 & E_2 & 0 & 0 & 0 & -E_3 & E_4 \\ 0 & 0 & 0 & 0 & E_1 & 0 & 0 & 0 & 0 & 0 & 0 & 0 & 0 & E_4 & 0 & E_3 & 0 & E_2 \\ 0 & 0 & 0 & 0 & 0 & E_1 & 0 & 0 & 0 & 0 & 0 & 0 & 0 & -E_4 & 0 & E_3 & 0 & E_2 \\ 0 & 0 & 0 & 0 & 0 & 0 & E_1 & 0 & 0 & 0 & 0 & 0 & 0 & -E_4 & 0 & -E_3 & 0 & E_2 \\ 0 & 0 & 0 & 0 & 0 & 0 & 0 & E_1 & 0 & 0 & 0 & 0 & 0 & E_4 & 0 & -E_3 & 0 & E_2 \\ 0 & 0 & 0 & 0 & 0 & 0 & 0 & 0 & E_1 & 0 & 0 & 0 & 0 & 0 & E_3 & E_4 & E_2 & 0 \\ 0 & 0 & 0 & 0 & 0 & 0 & 0 & 0 & 0 & E_1 & 0 & 0 & 0 & 0 & E_3 & -E_4 & E_2 & 0 \\ 0 & 0 & 0 & 0 & 0 & 0 & 0 & 0 & 0 & 0 & E_1 & 0 & 0 & 0 & -E_3 & -E_4 & E_2 & 0 \\ 0 & 0 & 0 & 0 & 0 & 0 & 0 & 0 & 0 & 0 & 0 & E_1 & 0 & 0 & -E_3 & E_4 & E_2 & 0 \\ F_2 & F_2 & F_2 & F_2 & -F_3 & F_3 & F_3 & -F_3 & -F_4 & -F_4 & F_4 & F_4 & F_1 & 0 & 0 & 0 & 0 & 0 \\ F_5 & F_5 & F_5 & F_5 & -F_6 & F_6 & F_6 & -F_6 & -F_4 & -F_4 & F_4 & F_4 & 0 & F_1 & 0 & 0 & 0 & 0 \\ F_5 & F_5 & F_5 & F_5 & -F_3 & F_3 & F_3 & -F_3 & -F_7 & -F_7 & F_7 & F_7 & 0 & 0 & F_1 & 0 & 0 & 0 \\ 0 & 0 & 0 & 0 & -F_9 & -F_9 & F_9 & F_9 & -F_8 & F_8 & F_8 & -F_8 & 0 & 0 & 0 & F_1 & 0 & 0 \\ -F_9 & -F_9 & F_9 & F_9 & 0 & 0 & 0 & 0 & F_{10} & F_{10} & F_{10} & F_{10} & 0 & 0 & 0 & 0 & F_1 & 0 \\ -F_8 & F_8 & F_8 & -F_8 & F_{10} & F_{10} & F_{10} & F_{10} & 0 & 0 & 0 & 0 & 0 & 0 & 0 & 0 & 0 & F_1 \end{bmatrix}, \quad (3.119)$$

$$\mathbf{p}^T = \begin{bmatrix} p_1 & p_2 & p_3 & p_4 & q_1 & q_2 & q_3 & q_4 & r_1 & r_2 & r_3 & r_4 & \psi_1 & \psi_2 & \psi_3 & \psi_4 & \psi_5 & \psi_6 \end{bmatrix}, \quad (3.120)$$

with

$$\begin{aligned}
E_1 &= -\rho \frac{\Delta x_2 \Delta x_3 L_1}{12} \alpha \beta, \\
E_2 &= \frac{\Delta x_2 \Delta x_3}{16}, \\
E_3 &= \frac{\Delta x_2 L_1}{6}, \\
E_4 &= \frac{\Delta x_3 L_1}{6}, \\
F_1 &= -\frac{\Delta x_2 \Delta x_3 L_1}{3} \alpha \beta, \\
F_2 &= -\frac{\Delta x_2 \Delta x_3 (\lambda + 2\mu)}{16}, \\
F_3 &= \frac{\Delta x_3 L_1 \lambda}{6}, \\
F_4 &= \frac{\Delta x_2 L_1 \lambda}{6}, \\
F_5 &= -\frac{\Delta x_2 \Delta x_3 \lambda}{16}, \\
F_6 &= \frac{\Delta x_3 L_1 (\lambda + 2\mu)}{6}, \\
F_7 &= \frac{\Delta x_2 L_1 (\lambda + 2\mu)}{6}, \\
F_8 &= \frac{\Delta x_3 L_1 \mu}{6}, \\
F_9 &= \frac{\Delta x_2 L_1 \mu}{6}, \\
F_{10} &= -\frac{\Delta x_2 \Delta x_3 \mu}{16}.
\end{aligned}$$

In order to provide an explicit scheme, matrix  $M_1$  must be diagonalised. To do so, the entries must first be nondimensionalised. The first equation of the system (3.117) will be considered, with rows two to twelve following similarly. So

$$C_1 \dot{p}_1 + C_2 \dot{\psi}_1 = E_1 p_1 + E_2 \psi_1 + E_3 \psi_5 + E_4 \psi_6, \quad (3.121)$$

then taking the scalings

$$p_1 = \bar{c}\tilde{p}_1, \quad t = T\tilde{t}, \quad \psi_i = \mu\tilde{\psi}_i$$

so

$$\begin{aligned} \frac{\partial p_1}{\partial t} &= \frac{\partial(\bar{c}\tilde{p}_1)}{\partial(T\tilde{t})} = \frac{\bar{c}}{T} \frac{\partial\tilde{p}_1}{\partial\tilde{t}} = \frac{\bar{c}}{T}\tilde{p}'_1, \\ \frac{\partial\psi_i}{\partial t} &= \frac{\partial(\mu\tilde{\psi}_i)}{\partial(T\tilde{t})} = \frac{\mu}{T} \frac{\partial\tilde{\psi}_i}{\partial\tilde{t}} = \frac{\mu}{T}\tilde{\psi}'_i, \end{aligned}$$

where ' denotes  $\partial/\partial\tilde{t}$ . Then

$$C_1 \frac{\bar{c}}{T}\tilde{p}'_1 + C_2 \frac{\mu}{T}\tilde{\psi}'_1 = E_1\bar{c}\tilde{p}_1 + E_2\mu\tilde{\psi}_1 + E_3\mu\tilde{\psi}_5 + E_4\mu\tilde{\psi}_6. \quad (3.122)$$

Now the coefficients have dimensions

$$\begin{aligned} C_1 \frac{\bar{c}}{T} &= \frac{\rho\Delta x_2\Delta x_3 L_1\alpha\bar{c}}{12T} \sim \left[ \frac{ML^{-3}L^3LT^{-1}}{T} \right] = [MLT^{-2}], \\ C_2 \frac{\mu}{T} &= -\frac{\Delta x_2\Delta x_3\mu}{12\bar{c}T} \sim \left[ \frac{L^3ML^{-1}T^{-2}}{LT^{-1}T} \right] = [MLT^{-2}], \\ E_1\bar{c} &= -\frac{\rho\Delta x_2\Delta x_3 L_1\alpha\beta\bar{c}}{12} \sim [ML^{-3}L^3T^{-1}LT^{-1}] = [MLT^{-2}], \\ E_2\mu &= \frac{\Delta x_2\Delta x_3\mu}{16} \sim [L^2ML^{-1}T^{-2}] = [MLT^{-2}], \\ E_3\mu &= \frac{\Delta x_2 L_1\mu}{6} \sim [L^2ML^{-1}T^{-2}] = [MLT^{-2}], \\ E_4\mu &= \frac{\Delta x_3 L_1\mu}{6} \sim [L^2ML^{-1}T^{-2}] = [MLT^{-2}]. \end{aligned}$$

Then for diagonalisation,

$$\left| C_1 \frac{\bar{c}}{T} \right| \gg \left| C_2 \frac{\mu}{T} \right|$$

that is,

$$\alpha \gg \frac{\mu}{\rho \bar{c}^2} \quad (3.123)$$

and it can be noted that if  $\bar{c}$  is taken to be the shear wavespeed,  $c_s$ , then this condition becomes  $\alpha \gg 1$ . So equation (3.122) becomes

$$C_1 \frac{\bar{c}}{T} \tilde{p}'_1 = E_1 \bar{c} \tilde{p}_1 + E_2 \mu \tilde{\psi}_1 + E_3 \mu \tilde{\psi}_5 + E_4 \mu \tilde{\psi}_6$$

and redimensionalising gives

$$C_1 \dot{p}_1 = E_1 p_1 + E_2 \psi_1 + E_3 \psi_5 + E_4 \psi_6,$$

which is just equation (3.121) without the  $\dot{\psi}_1$  term but the nondimensionalisation provided the condition on  $\alpha$  given in equation (3.123).

The thirteenth row of the system (3.117) will now be considered, with rows fourteen to eighteen following similarly. From row thirteen,

$$D_2 (\dot{p}_1 + \dot{p}_2 + \dot{p}_3 + \dot{p}_4) + D_1 \dot{\psi}_1 = M_{2,13} \cdot \mathbf{p},$$

and nondimensionalising as before gives

$$D_2 \frac{\bar{c}}{T} (\tilde{p}'_1 + \tilde{p}'_2 + \tilde{p}'_3 + \tilde{p}'_4) + D_1 \frac{\mu}{T} \tilde{\psi}'_1 = M_{2,13} \cdot \tilde{\mathbf{p}}.$$

For diagonalisation, it is required that

$$\left| D_1 \frac{\mu}{T} \right| \gg \left| D_2 \frac{\bar{c}}{T} \right|,$$



that is

$$\alpha \gg \frac{\lambda + 2\mu}{4\mu}. \quad (3.124)$$

For physical considerations in mechanics,  $(\lambda + 2\mu)/\mu$  is equivalent to the ratio of  $(c_p/c_s)^2$ , that is to say, the ratio of the pressure wavespeed to the shear wavespeed. In steel for example  $c_p/c_s \approx 6000/3000 = 2$  which is a fairly typical ratio. So

$$\alpha \gg \frac{\lambda + 2\mu}{4\mu} = \frac{1}{4} \frac{(\lambda + 2\mu)/\rho}{\mu/\rho} = \frac{1}{4} \left( \frac{c_p}{c_s} \right)^2 \approx 1$$

as before. So the matrix  $M_1$  in equation (3.118) is now a diagonal matrix (with all diagonal entries non-zero) and hence it is trivially invertible. Then using Euler's method, from equation (3.78) with consideration to the diagonalisation just performed, an explicit form can be given by

$$A_{1i'}^{(I)} = C_1 \frac{p_{i'}^{(t+1)} - p_{i'}^{(t)}}{\delta t} - E_1 p_{i'}^{(t)} - E_2 \psi_1 + \chi_{i'}^{1,2} E_4 \psi_6 + \chi_{i'}^{0,2} E_3 \psi_5, \quad (3.125)$$

and similarly for the other velocity components

$$A_{2i'}^{(I)} = C_1 \frac{q_{i'}^{(t+1)} - q_{i'}^{(t)}}{\delta t} - E_1 q_{i'}^{(t)} - E_2 \psi_6 + \chi_{i'}^{1,2} E_4 \psi_2 + \chi_{i'}^{0,2} E_3 \psi_4, \quad (3.126)$$

and

$$A_{3i'}^{(I)} = C_1 \frac{r_{i'}^{(t+1)} - r_{i'}^{(t)}}{\delta t} - E_1 r_{i'}^{(t)} - E_2 \psi_5 + \chi_{i'}^{1,2} E_4 \psi_4 + \chi_{i'}^{0,2} E_3 \psi_3. \quad (3.127)$$

The convergence of this numerical scheme requires a Courant-Friedrichs-Lewy

(CFL) like condition and this is given by

$$\delta t < \min \Delta x_j / c_p$$

where the the compressional wavespeed is given by  $c_p = \sqrt{(\lambda + 2\mu)/\rho}$ . The physical need for this condition is that time it takes for the wave to travel to adjacent spatial grid points (so  $\Delta x/c_p$ ) must be greater than the discrete time used in the numerical algorithm ( $\delta t$ ) to update the values at each grid point. If this is violated then the numerical scheme becomes unstable and the solution blows up.

The stress equations can also now be formulated, with respect to the nondimensionalisation, from equations (3.111)-(3.116), using Euler's method to give

$$B_1^{(I)} = D_1 \frac{\psi_1^{(t+1)} - \psi_1^{(t)}}{\delta t} \tag{3.128}$$

$$- F_2(p_1 + p_2 + p_3 + p_4) - F_3(q_3 - q_1 + q_2 - q_4) - F_4(r_3 - r_1 + r_4 - r_2), \tag{3.129}$$

and similarly for the other stress components we have

$$B_2^{(I)} = D_1 \frac{\psi_2^{(t+1)} - \psi_2^{(t)}}{\delta t} \quad (3.130)$$

$$- F_5(p_1 + p_2 + p_3 + p_4) - F_6(q_3 - q_1 + q_2 - q_4) - F_4(r_3 - r_1 + r_4 - r_2), \quad (3.131)$$

$$B_3^{(I)} = D_1 \frac{\psi_3^{(t+1)} - \psi_3^{(t)}}{\delta t} \quad (3.132)$$

$$- F_5(p_1 + p_2 + p_3 + p_4) - F_3(q_3 - q_1 + q_2 - q_4) - F_7(r_3 - r_1 + r_4 - r_2), \quad (3.133)$$

$$B_4^{(I)} = D_1 \frac{\psi_4^{(t+1)} - \psi_4^{(t)}}{\delta t} - F_8(r_3 - r_1 + r_2 - r_4) - F_9(q_3 - q_1 + q_4 - q_2), \quad (3.134)$$

$$B_5^{(I)} = D_1 \frac{\psi_5^{(t+1)} - \psi_5^{(t)}}{\delta t} - F_{10}(r_1 + r_2 + r_3 + r_4) - F_9(p_3 - p_1 + p_4 - p_2), \quad (3.135)$$

and

$$B_6^{(I)} = D_1 \frac{\psi_6^{(t+1)} - \psi_6^{(t)}}{\delta t} - F_{10}(q_1 + q_2 + q_3 + q_4) - F_8(p_3 - p_1 + p_2 - p_4). \quad (3.136)$$

### 3.4.3 The final solution

The stress equations are calculated on an element by element basis therefore, from equations (3.105)-(3.110), applying Euler's method and rearranging to give an

explicit form, for each finite element

$$\begin{aligned}\psi_1^{(t+1)} = & \psi_1^{(t)} + \delta t \left( \frac{\lambda + 2\mu}{4\Delta x_1} (p_7 - p_1 + p_8 - p_2 + p_3 - p_5 + p_4 - p_6) \right. \\ & + \frac{\lambda}{4\Delta x_2} (q_7 - q_1 + q_2 - q_8 + q_3 - q_5 + q_6 - q_4) \\ & \left. + \frac{\lambda}{4\Delta x_3} (r_7 - r_1 + r_8 - r_2 + r_5 - r_3 + r_6 - r_4) \right),\end{aligned}\quad (3.137)$$

$$\begin{aligned}\psi_2^{(t+1)} = & \psi_2^{(t)} + \delta t \left( \frac{\lambda}{4\Delta x_1} (p_7 - p_1 + p_8 - p_2 + p_3 - p_5 + p_4 - p_6) \right. \\ & + \frac{\lambda + 2\mu}{4\Delta x_2} (q_7 - q_1 + q_2 - q_8 + q_3 - q_5 + q_6 - q_4) \\ & \left. + \frac{\lambda}{4\Delta x_3} (r_7 - r_1 + r_8 - r_2 + r_5 - r_3 + r_6 - r_4) \right),\end{aligned}\quad (3.138)$$

$$\begin{aligned}\psi_3^{(t+1)} = & \psi_3^{(t)} + \delta t \left( \frac{\lambda}{4\Delta x_1} (p_7 - p_1 + p_8 - p_2 + p_3 - p_5 + p_4 - p_6) \right. \\ & + \frac{\lambda}{4\Delta x_2} (q_7 - q_1 + q_2 - q_8 + q_3 - q_5 + q_6 - q_4) \\ & \left. + \frac{\lambda + 2\mu}{4\Delta x_3} (r_7 - r_1 + r_8 - r_2 + r_5 - r_3 + r_6 - r_4) \right),\end{aligned}\quad (3.139)$$

$$\begin{aligned}\psi_4^{(t+1)} = & \psi_4^{(t)} + \delta t \left( \frac{\mu}{4\Delta x_2} (r_7 - r_1 + r_2 - r_8 + r_3 - r_5 + r_6 - r_4) \right. \\ & \left. + \frac{\mu}{4\Delta x_3} (q_7 - q_1 + q_8 - q_2 + q_5 - q_3 + q_6 - q_4) \right),\end{aligned}\quad (3.140)$$

$$\begin{aligned}\psi_5^{(t+1)} = & \psi_5^{(t)} + \delta t \left( \frac{\mu}{4\Delta x_1} (r_7 - r_1 + r_8 - r_2 + r_3 - r_5 + r_4 - r_6) \right. \\ & \left. + \frac{\mu}{4\Delta x_3} (p_7 - p_1 + p_8 - p_2 + p_5 - p_3 + p_6 - p_4) \right),\end{aligned}\quad (3.141)$$

$$\begin{aligned}\psi_6^{(t+1)} = & \psi_6^{(t)} + \delta t \left( \frac{\mu}{4\Delta x_1} (q_7 - q_1 + q_8 - q_2 + q_3 - q_5 + q_4 - q_6) \right. \\ & \left. + \frac{\mu}{4\Delta x_2} (p_7 - p_1 + p_2 - p_8 + p_3 - p_5 + p_6 - p_4) \right),\end{aligned}\quad (3.142)$$

and from equations (3.129)-(3.136), for each infinite element

$$\begin{aligned} \psi_1^{(t+1)} = & \psi_1^{(t)} + \frac{\delta t}{\alpha} \left( -\frac{3(\lambda + 2\mu)}{16L_1}(p_1 + p_2 + p_3 + p_4) \right. \\ & \left. + \frac{\lambda}{2\Delta x_2}(q_3 - q_1 + q_2 - q_4) + \frac{\lambda}{2\Delta x_3}(r_3 - r_1 + r_4 - r_2) \right), \end{aligned} \quad (3.143)$$

$$\begin{aligned} \psi_2^{(t+1)} = & \psi_2^{(t)} + \frac{\delta t}{\alpha} \left( -\frac{3\lambda}{16L_1}(p_1 + p_2 + p_3 + p_4) \right. \\ & \left. + \frac{\lambda + 2\mu}{2\Delta x_2}(q_3 - q_1 + q_2 - q_4) + \frac{\lambda}{2\Delta x_3}(r_3 - r_1 + r_4 - r_2) \right), \end{aligned} \quad (3.144)$$

$$\begin{aligned} \psi_3^{(t+1)} = & \psi_3^{(t)} + \frac{\delta t}{\alpha} \left( -\frac{3\lambda}{16L_1}(p_1 + p_2 + p_3 + p_4) \right. \\ & \left. + \frac{\lambda}{2\Delta x_2}(q_3 - q_1 + q_2 - q_4) + \frac{\lambda + 2\mu}{2\Delta x_3}(r_3 - r_1 + r_4 - r_2) \right), \end{aligned} \quad (3.145)$$

$$\begin{aligned} \psi_4^{(t+1)} = & \psi_4^{(t)} + \frac{\delta t}{\alpha} \left( \frac{\mu}{2\Delta x_2}(r_3 - r_1 + r_2 - r_4) + \frac{\mu}{2\Delta x_3}(q_3 - q_1 + q_4 - q_2) \right), \end{aligned} \quad (3.146)$$

$$\begin{aligned} \psi_5^{(t+1)} = & \psi_5^{(t)} + \frac{\delta t}{\alpha} \left( -\frac{3\mu}{16L_1}(r_1 + r_2 + r_3 + r_4) + \frac{\mu}{2\Delta x_3}(p_3 - p_1 + p_4 - p_2) \right), \end{aligned} \quad (3.147)$$

and

$$\begin{aligned} \psi_6^{(t+1)} = & \psi_6^{(t)} + \frac{\delta t}{\alpha} \left( -\frac{3\mu}{16L_1}(q_1 + q_2 + q_3 + q_4) + \frac{\mu}{2\Delta x_2}(p_3 - p_1 + p_2 - p_4) \right). \end{aligned} \quad (3.148)$$

Now for the velocity equations, for each finite element, for example from equation (3.75),

$$A_{1i'}^{(F)} = \frac{\rho\Delta x_1\Delta x_2\Delta x_3}{8}\dot{p}_{i'} + \chi_{i'}^{0,2}\frac{\Delta x_2\Delta x_3}{4}\psi_1 + \chi_{i'}^{1,2}\frac{\Delta x_1\Delta x_3}{4}\psi_6 + \chi_{i'}^{0,4}\frac{\Delta x_1\Delta x_2}{4}\psi_5,$$

which leads to an explicit form (using Euler's method) of

$$A_{1i'}^{(F)} = \frac{\rho \Delta x_1 \Delta x_2 \Delta x_3}{8} \frac{p_{i'}^{(t+1)} - p_{i'}^{(t)}}{\delta t} + \chi_{i'}^{0,2} \frac{\Delta x_2 \Delta x_3}{4} \psi_1 + \chi_{i'}^{1,2} \frac{\Delta x_1 \Delta x_3}{4} \psi_6 + \chi_{i'}^{0,4} \frac{\Delta x_1 \Delta x_2}{4} \psi_5,$$

while for each infinite element, for example from equation (3.125),

$$A_{1i'} = \frac{\rho \Delta x_2 \Delta x_3 L_1 \alpha}{12} \frac{p_{i'}^{(t+1)} - p_{i'}^{(t)}}{\delta t} + \frac{\rho \Delta x_2 \Delta x_3 L_1 \alpha \beta}{12} p_{i'}^{(t)} - \frac{\Delta x_2 \Delta x_3}{16} \psi_1 + \chi_{i'}^{1,2} \frac{\Delta x_3 L_1}{6} \psi_6 + \chi_{i'}^{0,2} \frac{\Delta x_2 L_1}{6} \psi_5.$$

Now recombining the elements in order to calculate the velocities at a global level gives

$$\begin{aligned} & b_n^{(F)} \frac{\rho \Delta x_1 \Delta x_2 \Delta x_3}{8} \frac{p_n^{(t+1)} - p_n^{(t)}}{\delta t} \\ & + b_n^{(I)} \left( \frac{\rho \Delta x_2 \Delta x_3 L_1 \alpha}{12} \frac{p_n^{(t+1)} - p_n^{(t)}}{\delta t} + \frac{\rho \Delta x_2 \Delta x_3 L_1 \alpha \beta}{12} p_n^{(t)} \right) \\ & = \sum_{k=1}^{b_n^{(F)}} F^{(F)} + \sum_{l=1}^{b_n^{(I)}} F^{(I)} \end{aligned}$$

where  $b_n^{(F)}$  is the number of finite elements that share global node  $n$  as a vertex,  $b_n^{(I)}$  is the number of infinite elements that share global node  $n$  as a vertex,  $F^{(F)}$  is the combination of stress terms used in  $A_{1i'}^{(F)}$  when global node  $n$  is local node  $i'$  in a finite element, and  $F^{(I)}$  is the combination of stress terms used in  $A_{1i'}^{(I)}$  when

global node  $n$  is local node  $i'$  in an infinite element. So

$$\begin{aligned}
& \left( b_n^{(F)} \frac{\rho \Delta x_1 \Delta x_2 \Delta x_3}{8} + b_n^{(I)} \frac{\rho \Delta x_2 \Delta x_3 L_1 \alpha}{12} \right) p_n^{(t+1)} \\
&= \left( b_n^{(F)} \frac{\rho \Delta x_1 \Delta x_2 \Delta x_3}{8} + b_n^{(I)} \frac{\rho \Delta x_2 \Delta x_3 L_1 \alpha}{12} (1 - \beta \delta t) \right) p_n^{(t)} \\
&+ \delta t \left( \sum_{k=1}^{b_n^{(F)}} F^{(F)} + \sum_{l=1}^{b_n^{(I)}} F^{(I)} \right)
\end{aligned}$$

and letting

$$W^{(F)} = b_n^{(F)} \frac{\rho \Delta x_1 \Delta x_2 \Delta x_3}{8}, \quad W^{(I)} = b_n^{(I)} \frac{\rho \Delta x_2 \Delta x_3 L_1 \alpha}{12}, \quad (3.149)$$

then

$$\begin{aligned}
p_n^{(t+1)} &= \left( 1 - \beta \delta t \frac{W^{(I)}}{W^{(F)} + W^{(I)}} \right) p_n^{(t)} \\
&+ \frac{\delta t}{W^{(F)} + W^{(I)}} \left( \sum_{k=1}^{b_n^{(F)}} F^{(F)} + \sum_{l=1}^{b_n^{(I)}} F^{(I)} \right), \quad (3.150)
\end{aligned}$$

and in the same way, for the other components of velocity

$$\begin{aligned}
q_n^{(t+1)} &= \left( 1 - \beta \delta t \frac{W^{(I)}}{W^{(F)} + W^{(I)}} \right) q_n^{(t)} \\
&+ \frac{\delta t}{W^{(F)} + W^{(I)}} \left( \sum_{k=1}^{b_n^{(F)}} F^{(F)} + \sum_{l=1}^{b_n^{(I)}} F^{(I)} \right), \quad (3.151)
\end{aligned}$$

$$\begin{aligned}
r_n^{(t+1)} &= \left( 1 - \beta \delta t \frac{W^{(I)}}{W^{(F)} + W^{(I)}} \right) r_n^{(t)} \\
&+ \frac{\delta t}{W^{(F)} + W^{(I)}} \left( \sum_{k=1}^{b_n^{(F)}} F^{(F)} + \sum_{l=1}^{b_n^{(I)}} F^{(I)} \right). \quad (3.152)
\end{aligned}$$

## 3.5 Retaining a spatial dependency

### 3.5.1 The velocity equations

Since attention is restricted to a waveguide problem then the PML will only stretch the coordinates in the  $x_1$  direction. So we set  $s_2 = s_3 \equiv 1$ . Then from equations (3.28)-(3.30),

$$\begin{aligned}
& \sum_{j=1}^N \left\{ \int_{\Omega_F} -i\omega\rho N_i N_j d\Omega_F \hat{p}_j \right. \\
& + \int_{\Omega_F} \left\{ \frac{1}{s_1} \frac{\partial N_i}{\partial x_1} N_j \hat{\gamma}_{1j} + \frac{\partial N_i}{\partial x_2} N_j \hat{\gamma}_{6j} + \frac{\partial N_i}{\partial x_3} N_j \hat{\gamma}_{5j} \right\} d\Omega_F \left. \right\} \\
& = \sum_{j=1}^N \left\{ \frac{1}{\bar{c}} \left( \int_{\Gamma_X} \left( \frac{\lambda + 2\mu}{s_1^2} + 2\mu \right) w_i f_j g_i g_j d\Gamma_X \hat{p}_j \right. \right. \\
& + \int_{\Gamma_X} \frac{\lambda + \mu}{s_1} w_i f_j g_i g_j d\Gamma_X \hat{q}_j + \int_{\Gamma_X} \frac{\lambda + \mu}{s_1} w_i f_j g_i g_j d\Gamma_X \hat{r}_j \left. \right) \\
& + \frac{\epsilon}{-i\omega} \int_{\Gamma_X} \left( \frac{\lambda + 2\mu}{s_1^2} + 2\mu + \frac{2(\lambda + \mu)}{s_1} \right) w_i g_i d\Gamma_X \\
& - \int_{\Omega_I} \left\{ \frac{1}{s_1} \frac{\partial w_i}{\partial x_1} f_j g_i g_j \hat{\gamma}_{1j} + w_i f_j \frac{\partial g_i}{\partial x_2} g_j \hat{\gamma}_{6j} + w_i f_j \frac{\partial g_i}{\partial x_3} g_j \hat{\gamma}_{5j} \right\} d\Omega_I \\
& \left. - \int_{\Omega_I} -i\omega\rho w_i f_j g_i g_j d\Omega_I \hat{p}_j \right\} \quad (i = 1, \dots, N) \tag{3.153}
\end{aligned}$$



$$\begin{aligned}
& \sum_{j=1}^N \left\{ \int_{\Omega_F} -i\omega\rho N_i N_j d\Omega_F \hat{q}_j \right. \\
& + \int_{\Omega_F} \left\{ \frac{1}{s_1} \frac{\partial N_i}{\partial x_1} N_j \hat{\gamma}_{6j} + \frac{\partial N_i}{\partial x_2} N_j \hat{\gamma}_{2j} + \frac{\partial N_i}{\partial x_3} N_j \hat{\gamma}_{4j} \right\} d\Omega_F \left. \right\} \\
& = \sum_{j=1}^N \left\{ \frac{1}{\bar{c}} \left( \int_{\Gamma_X} \left( \frac{\mu}{s_1^2} + \lambda + 3\mu \right) w_i f_j g_i g_j d\Gamma_X \hat{q}_j \right. \right. \\
& + \int_{\Gamma_X} \frac{\lambda + \mu}{s_1} w_i f_j g_i g_j d\Gamma_X \hat{p}_j + \int_{\Gamma_X} (\lambda + \mu) w_i f_j g_i g_j d\Gamma_X \hat{r}_j \left. \right) \\
& + \frac{\epsilon}{-i\omega} \int_{\Gamma_X} \left( \frac{\mu}{s_1^2} + \frac{\lambda + \mu}{s_1} + 2\lambda + 4\mu \right) w_i g_i d\Gamma_X \\
& - \int_{\Omega_I} \left\{ \frac{1}{s_1} \frac{\partial w_i}{\partial x_1} f_j g_i g_j \hat{\gamma}_{6j} + w_i f_j \frac{\partial g_i}{\partial x_2} g_j \hat{\gamma}_{2j} + w_i f_j \frac{\partial g_i}{\partial x_3} g_j \hat{\gamma}_{4j} \right\} d\Omega_I \\
& \left. - \int_{\Omega_I} -i\omega\rho w_i f_j g_i g_j d\Omega_I \hat{q}_j \right\} \quad (i = 1, \dots, N) \tag{3.154}
\end{aligned}$$

$$\begin{aligned}
& \sum_{j=1}^N \left\{ \int_{\Omega_F} -i\omega\rho N_i N_j d\Omega_F \hat{r}_j \right. \\
& + \int_{\Omega_F} \left\{ \frac{1}{s_1} \frac{\partial N_i}{\partial x_1} N_j \hat{\gamma}_{5j} + \frac{\partial N_i}{\partial x_2} N_j \hat{\gamma}_{4j} + \frac{\partial N_i}{\partial x_3} N_j \hat{\gamma}_{3j} \right\} d\Omega_F \left. \right\} \\
& = \sum_{j=1}^N \left\{ \frac{1}{\bar{c}} \left( \int_{\Gamma_X} \left( \frac{\mu}{s_1^2} + \lambda + 3\mu \right) w_i f_j g_i g_j d\Gamma_X \hat{r}_j \right. \right. \\
& + \int_{\Gamma_X} \frac{\lambda + \mu}{s_1} w_i f_j g_i g_j d\Gamma_X \hat{p}_j + \int_{\Gamma_X} (\lambda + \mu) w_i f_j g_i g_j d\Gamma_X \hat{q}_j \left. \right) \\
& + \frac{\epsilon}{-i\omega} \int_{\Gamma_X} \left( \frac{\mu}{s_1^2} + \frac{\lambda + \mu}{s_1} + 2\lambda + 4\mu \right) w_i g_i d\Gamma_X \\
& - \int_{\Omega_I} \left\{ \frac{1}{s_1} \frac{\partial w_i}{\partial x_1} f_j g_i g_j \hat{\gamma}_{5j} + w_i f_j \frac{\partial g_i}{\partial x_2} g_j \hat{\gamma}_{4j} + w_i f_j \frac{\partial g_i}{\partial x_3} g_j \hat{\gamma}_{3j} \right\} d\Omega_I \\
& \left. - \int_{\Omega_I} -i\omega\rho w_i f_j g_i g_j d\Omega_I \hat{r}_j \right\} \quad (i = 1, \dots, N) \tag{3.155}
\end{aligned}$$

The basis functions are defined as before in equations (3.34)-(3.36), the test functions as in equations (3.37) and (3.38), and the mappings from the global coordinates again as shown in Figures 3.4 and 3.6. With the dimensionless  $s_1(x_1, \omega)$

given by equation (3.6), then from the left-hand side of equation (3.153) define for each finite element (in  $\Omega_F$ )  $A_{1i'}^{(F)}$ ,  $A_{2i'}^{(F)}$ , and  $A_{3i'}^{(F)}$  as before by the expressions given in equations (3.44)-(3.46). The finite element case then is identical to that presented in section 3.4. From the right-hand side of equation (3.153) (again taking the negative to emphasise the similarity to the finite element case) with  $s_1$  given by equation (3.6), define for each infinite element (in  $\Omega_I$ )

$$\begin{aligned}
A_{1i'}^{(I)} = & \sum_{j'=1}^4 \left\{ -i\omega\rho \int_{\Omega_{IE}} w_{i'} f_{j'} g_{i'} g_{j'} d\Omega_{IE} \hat{p}_{j'} \right. \\
& - \frac{1}{\bar{c}} \left( \left( \frac{\lambda + 2\mu}{(s_1(X_1))^2} + 2\mu \right) \hat{p}_{j'} + \frac{\lambda + \mu}{s_1(X_1)} \hat{q}_{j'} + \frac{\lambda + \mu}{s_1(X_1)} \hat{r}_{j'} \right) \int_{\Gamma_X} w_{i'} f_{j'} g_{i'} g_{j'} d\Gamma_X \\
& - \frac{\epsilon}{-i\omega} \left( \frac{\lambda + 2\mu}{(s_1(X_1))^2} + 2\mu + \frac{2(\lambda + \mu)}{s_1(X_1)} \right) \int_{\Gamma_X} w_{i'} g_{i'} d\Gamma_X \\
& \left. + \int_{\Omega_{IE}} \left\{ \frac{1}{s_1} \frac{\partial w_i}{\partial x_1} f_j g_i g_j \hat{\gamma}_{1j'} + w_{i'} f_{j'} \frac{\partial g_{i'}}{\partial x_2} g_{j'} \hat{\gamma}_{6j'} + w_{i'} f_{j'} \frac{\partial g_{i'}}{\partial x_3} g_{j'} \hat{\gamma}_{5j'} \right\} d\Omega_{IE} \right\} \\
& (i' = 1, \dots, 4), \tag{3.156}
\end{aligned}$$

$$\begin{aligned}
A_{2i'}^{(I)} = & \sum_{j'=1}^4 \left\{ -i\omega\rho \int_{\Omega_{IE}} w_{i'} f_{j'} g_{i'} g_{j'} d\Omega_{IE} \hat{q}_{j'} \right. \\
& - \frac{1}{\bar{c}} \left( \left( \frac{\mu}{(s_1(X_1))^2} + \lambda + 3\mu \right) \hat{q}_{j'} + \frac{\lambda + \mu}{s_1(X_1)} \hat{p}_{j'} + (\lambda + \mu) \hat{r}_{j'} \right) \int_{\Gamma_X} w_{i'} f_{j'} g_{i'} g_{j'} d\Gamma_X \\
& - \frac{\epsilon}{-i\omega} \left( \frac{\mu}{(s_1(X_1))^2} + \frac{\lambda + \mu}{s_1(X_1)} + 2(\lambda + 2\mu) \right) \int_{\Gamma_X} w_{i'} g_{i'} d\Gamma_X \\
& \left. + \int_{\Omega_{IE}} \left\{ \frac{1}{s_1} \frac{\partial w_{i'}}{\partial x_1} f_{j'} g_{i'} g_{j'} \hat{\gamma}_{6j'} + w_{i'} f_{j'} \frac{\partial g_{i'}}{\partial x_2} g_{j'} \hat{\gamma}_{2j'} + w_{i'} f_{j'} \frac{\partial g_{i'}}{\partial x_3} g_{j'} \hat{\gamma}_{4j'} \right\} d\Omega_{IE} \right\} \\
& (i' = 1, \dots, 4), \tag{3.157}
\end{aligned}$$

$$\begin{aligned}
A_{3i'}^{(I)} = & \sum_{j'=1}^4 \left\{ -i\omega\rho \int_{\Omega_{IE}} w_{i'} f_{j'} g_{i'} g_{j'} d\Omega_{IE} \hat{r}_{j'} \right. \\
& - \frac{1}{\bar{c}} \left( \left( \frac{\mu}{(s_1(X_1))^2} + \lambda + 3\mu \right) \hat{r}_{j'} + \frac{\lambda + \mu}{s_1(X_1)} \hat{p}_{j'} + (\lambda + \mu) \hat{q}_{j'} \right) \int_{\Gamma_X} w_{i'} f_{j'} g_{i'} g_{j'} d\Gamma_X \\
& - \frac{\epsilon}{-i\omega} \left( \frac{\mu}{(s_1(X_1))^2} + \frac{\lambda + \mu}{s_1(X_1)} + 2(\lambda + 2\mu) \right) \int_{\Gamma_X} w_{i'} g_{i'} d\Gamma_X \\
& \left. + \int_{\Omega_{IE}} \left\{ \frac{1}{s_1} \frac{\partial w_{i'}}{\partial x_1} f_{j'} g_{i'} g_{j'} \hat{\gamma}_{5j'} + w_{i'} f_{j'} \frac{\partial g_{i'}}{\partial x_2} g_{j'} \hat{\gamma}_{4j'} + w_{i'} f_{j'} \frac{\partial g_{i'}}{\partial x_3} g_{j'} \hat{\gamma}_{3j'} \right\} d\Omega_{IE} \right\} \\
& (i' = 1, \dots, 4), \tag{3.158}
\end{aligned}$$

where the  $X_1$  in the argument of the  $s_1$  indicates that it is being evaluated on  $\Gamma_X$  where  $x_1 = X_1$ .

The integrals that must be evaluated are then given by equations (3.50)-(3.59) with the exception of equation (3.57) which takes the slightly different form of

$$\begin{aligned}
\int_{\Omega_{IE}} \frac{1}{s_1} \frac{\partial w_{i'}}{\partial x_1} f_{j'} g_{i'} g_{j'} d\Omega_{IE} &= \lim_{X_1 \rightarrow \infty} \int_{L_1}^{X_1} \frac{1}{s_1} \frac{\partial w_{i'}}{\partial x_1} f_{j'} dx_1 \int_{-1}^1 \int_{-1}^1 g_{i'} g_{j'} \frac{\Delta x_2 \Delta x_3}{4} d\eta d\zeta \\
&= \frac{\Delta x_2 \Delta x_3}{16} \left( 1 + \frac{\eta_{i'} \eta_{j'}}{3} \right) \left( 1 + \frac{\zeta_{i'} \zeta_{j'}}{3} \right) \\
&\quad \times \lim_{X_1 \rightarrow \infty} \int_{L_1}^{X_1} \frac{1}{s_1} \left( \frac{L_1}{x_1} \right)^4 \left( i\bar{k} - \frac{1}{x_1} \right) dx_1, \tag{3.159}
\end{aligned}$$

in a similar manner to the integration in equation (3.57). Since the aim is to perform an inverse Fourier transform in time later on,  $\omega$  (or  $i\omega$ ) must be taken outside the integral. So

$$s_1(x_1) = \alpha_1(x_1) \left( 1 + \frac{i}{\omega} \beta_1(x_1) \right) = \alpha_1(x_1) \left( \frac{\omega + i\beta_1(x_1)}{\omega} \right)$$

therefore

$$\frac{1}{s_1(x_1)} = \frac{\omega}{\alpha_1(x_1) (\omega + i\beta_1(x_1))} = \frac{\omega^2 - i\omega\beta_1(x_1)}{\alpha_1(x_1) (\omega^2 + (\beta_1(x_1))^2)} = \frac{1 - i\beta_1(x_1)/\omega}{\alpha_1(x_1) (1 + (\beta_1(x_1))^2/\omega^2)}.$$

Now assuming

$$\omega \gg \beta_1(x_1) \quad (3.160)$$

then a Taylor series expansion (of order 1) can be used to give

$$\begin{aligned} \frac{1}{s_1(x_1)} &\approx \frac{1}{\alpha_1(x_1)} \left(1 - \frac{i}{\omega} \beta_1(x_1)\right) \left(1 - \frac{(\beta_1(x_1))^2}{\omega^2}\right) \\ &= \frac{1}{\alpha_1(x_1)} \left(1 - \frac{i}{\omega} \beta_1(x_1) - \frac{(\beta_1(x_1))^2}{\omega^2} + \frac{i}{\omega^3} (\beta_1(x_1))^3\right) \end{aligned}$$

Then in equation (3.159)

$$\begin{aligned} \int_{L_1}^{X_1} \frac{1}{s_1} \left(\frac{L_1}{x_1}\right)^4 \left(i\bar{k} - \frac{1}{x_1}\right) dx_1 &= \int_{L_1}^{X_1} \frac{1}{s_1} \left(\frac{L_1}{x_1}\right)^4 \left(\frac{i\omega}{\bar{c}} - \frac{1}{x_1}\right) dx_1 \\ &= \int_{L_1}^{X_1} \left(i\omega + \beta_1(x_1) - \frac{i}{\omega} (\beta_1(x_1))^2 - \frac{1}{\omega^2} (\beta_1(x_1))^3\right) \frac{1}{\alpha_1(x_1)\bar{c}} \left(\frac{L_1}{x_1}\right)^4 dx_1 \\ &\quad - \int_{L_1}^{X_1} \left(1 - \frac{i}{\omega} \beta_1(x_1) - \frac{(\beta_1(x_1))^2}{\omega^2} + \frac{i}{\omega^3} (\beta_1(x_1))^3\right) \frac{1}{\alpha_1(x_1)x_1} \left(\frac{L_1}{x_1}\right)^4 dx_1 \\ &= I_1^* + i\omega I_2^* - \frac{i}{\omega} I_3^* - \frac{1}{\omega^2} I_4^* - \frac{i}{\omega^3} I_5^* \end{aligned}$$

where

$$I_1^* = \lim_{X_1 \rightarrow \infty} \int_{L_1}^{X_1} \left(\frac{\beta_1(x_1)}{\bar{c}} - \frac{1}{x_1}\right) \frac{1}{\alpha_1(x_1)} \left(\frac{L_1}{x_1}\right)^4 dx_1 \quad (3.161)$$

$$I_2^* = \lim_{X_1 \rightarrow \infty} \int_{L_1}^{X_1} \frac{1}{\alpha_1(x_1)\bar{c}} \left(\frac{L_1}{x_1}\right)^4 dx_1 \quad (3.162)$$

$$I_3^* = \lim_{X_1 \rightarrow \infty} \int_{L_1}^{X_1} \left(\frac{(\beta_1(x_1))^2}{\bar{c}} - \frac{\beta_1(x_1)}{x_1}\right) \frac{1}{\alpha_1(x_1)} \left(\frac{L_1}{x_1}\right)^4 dx_1 \quad (3.163)$$

$$I_4^* = \lim_{X_1 \rightarrow \infty} \int_{L_1}^{X_1} \left(\frac{(\beta_1(x_1))^3}{\bar{c}} - \frac{(\beta_1(x_1))^2}{x_1}\right) \frac{1}{\alpha_1(x_1)} \left(\frac{L_1}{x_1}\right)^4 dx_1 \quad (3.164)$$

$$I_5^* = \lim_{X_1 \rightarrow \infty} \int_{L_1}^{X_1} \frac{(\beta_1(x_1))^3}{\alpha_1(x_1)x_1} \left(\frac{L_1}{x_1}\right)^4 dx_1 \quad (3.165)$$

and so from equation (3.159) we have

$$\int_{\Omega_{IE}} \frac{1}{s_1} \frac{\partial w_{i'}}{\partial x_1} f_{j'} g_{i'} g_{j'} d\Omega_{IE} = \frac{\Delta x_2 \Delta x_3}{16} \left(1 + \frac{\eta_{i'} \eta_{j'}}{3}\right) \left(1 + \frac{\zeta_{i'} \zeta_{j'}}{3}\right) \times \left(I_1^* + i\omega I_2^* - \frac{i}{\omega} I_3^* - \frac{1}{\omega^2} I_4^* - \frac{i}{\omega^3} I_5^*\right). \quad (3.166)$$

Note that the  $I_j^*$  are just constants but it must be ensured that the limits exist. To evaluate them, a choice for the dependency on  $x_1$  of  $\alpha_1$  and  $\beta_1$  has to be made. This will be discussed shortly. Now from equations (3.156)-(3.158) with integrals given by equations (3.54)-(3.56), (3.58), (3.59) and (3.166), for each infinite element

$$\begin{aligned} A_{1i'}^{(I)} = & \sum_{j'=1}^4 \left\{ -i\omega\rho \frac{\Delta x_2 \Delta x_3}{16} \left(1 + \frac{\eta_{i'} \eta_{j'}}{3}\right) \left(1 + \frac{\zeta_{i'} \zeta_{j'}}{3}\right) \frac{L_1}{3} \hat{p}_{j'} \right. \\ & + \frac{\Delta x_2 \Delta x_3}{16} \left(1 + \frac{\eta_{i'} \eta_{j'}}{3}\right) \left(1 + \frac{\zeta_{i'} \zeta_{j'}}{3}\right) \\ & \times \left(I_1^* + i\omega I_2^* - \frac{i}{\omega} I_3^* - \frac{1}{\omega^2} I_4^* - \frac{i}{\omega^3} I_5^*\right) \hat{\gamma}_{1j'} \\ & + \frac{L_1}{3} \frac{\Delta x_3}{8} \eta_{i'} \left(1 + \frac{\zeta_{i'} \zeta_{j'}}{3}\right) \hat{\gamma}_{6j'} \\ & \left. + \frac{L_1}{3} \frac{\Delta x_2}{8} \zeta_{i'} \left(1 + \frac{\eta_{i'} \eta_{j'}}{3}\right) \hat{\gamma}_{5j'} \right\} \quad (i' = 1, \dots, 4), \quad (3.167) \end{aligned}$$

$$\begin{aligned}
A_{2i'}^{(I)} = \sum_{j'=1}^4 \left\{ & -i\omega\rho \frac{\Delta x_2 \Delta x_3}{16} \left(1 + \frac{\eta_{i'} \eta_{j'}}{3}\right) \left(1 + \frac{\zeta_{i'} \zeta_{j'}}{3}\right) \frac{L_1}{3} \hat{q}_{j'} \right. \\
& + \frac{\Delta x_2 \Delta x_3}{16} \left(1 + \frac{\eta_{i'} \eta_{j'}}{3}\right) \left(1 + \frac{\zeta_{i'} \zeta_{j'}}{3}\right) \\
& \times \left( I_1^* + i\omega I_2^* - \frac{i}{\omega} I_3^* - \frac{1}{\omega^2} I_4^* - \frac{i}{\omega^3} I_5^* \right) \hat{\gamma}_{6j'} \\
& + \frac{L_1}{3} \frac{\Delta x_3}{8} \eta_{i'} \left(1 + \frac{\zeta_{i'} \zeta_{j'}}{3}\right) \hat{\gamma}_{2j'} \\
& \left. + \frac{L_1}{3} \frac{\Delta x_2}{8} \zeta_{i'} \left(1 + \frac{\eta_{i'} \eta_{j'}}{3}\right) \hat{\gamma}_{4j'} \right\} \quad (i' = 1, \dots, 4), \quad (3.168)
\end{aligned}$$

$$\begin{aligned}
A_{3i'}^{(I)} = \sum_{j'=1}^4 \left\{ & -i\omega\rho \frac{\Delta x_2 \Delta x_3}{16} \left(1 + \frac{\eta_{i'} \eta_{j'}}{3}\right) \left(1 + \frac{\zeta_{i'} \zeta_{j'}}{3}\right) \frac{L_1}{3} \hat{r}_{j'} \right. \\
& + \frac{\Delta x_2 \Delta x_3}{16} \left(1 + \frac{\eta_{i'} \eta_{j'}}{3}\right) \left(1 + \frac{\zeta_{i'} \zeta_{j'}}{3}\right) \\
& \times \left( I_1^* + i\omega I_2^* - \frac{i}{\omega} I_3^* - \frac{1}{\omega^2} I_4^* - \frac{i}{\omega^3} I_5^* \right) \hat{\gamma}_{5j'} \\
& + \frac{L_1}{3} \frac{\Delta x_3}{8} \eta_{i'} \left(1 + \frac{\zeta_{i'} \zeta_{j'}}{3}\right) \hat{\gamma}_{4j'} \\
& \left. + \frac{L_1}{3} \frac{\Delta x_2}{8} \zeta_{i'} \left(1 + \frac{\eta_{i'} \eta_{j'}}{3}\right) \hat{\gamma}_{3j'} \right\} \quad (i' = 1, \dots, 4). \quad (3.169)
\end{aligned}$$

As before, the assumption is made that the stress components at a local node  $i'$ , given by  $\hat{\gamma}_{ni'}$  for  $n = 1, \dots, 6$ , are equal to the stress components at local node  $j'$ , given by  $\hat{\gamma}_{nj'}$  for  $n = 1, \dots, 6$ , when nodes  $i'$  and  $j'$  belong to the same element. Therefore

$$\hat{\gamma}_{ni'} = \hat{\gamma}_{nj'} \equiv \hat{\psi}_n \quad i', j' \in \Omega_e$$

where  $\Omega_e$  is either a finite or infinite element. Then  $\hat{\gamma}_{ni'}$ , the stress components at a local node  $i'$ , can be replaced by  $\hat{\psi}_n$ , the stress component for the element under consideration. Now expanding the summations in equations (3.167)-(3.169) as before and mass lumping for the velocity coefficients yields, for each infinite element

$$A_{1i'}^{(I)} = \frac{\rho\Delta x_2\Delta x_3 L_1}{12}(-i\omega\hat{p}_{i'}) + \frac{\Delta x_2\Delta x_3}{4} \left( I_1^* + i\omega I_2^* - \frac{i}{\omega} I_3^* - \frac{1}{\omega^2} I_4^* - \frac{i}{\omega^3} I_5^* \right) \hat{\psi}_1 \\ + \chi_{i'}^{1,2} \frac{\Delta x_3 L_1}{6} \hat{\psi}_6 + \chi_{i'}^{0,2} \frac{\Delta x_2 L_1}{6} \hat{\psi}_5 \quad (i' = 1, \dots, 4), \quad (3.170)$$

$$A_{2i'}^{(I)} = \frac{\rho\Delta x_2\Delta x_3 L_1}{12}(-i\omega\hat{q}_{i'}) + \frac{\Delta x_2\Delta x_3}{4} \left( I_1^* + i\omega I_2^* - \frac{i}{\omega} I_3^* - \frac{1}{\omega^2} I_4^* - \frac{i}{\omega^3} I_5^* \right) \hat{\psi}_6 \\ + \chi_{i'}^{1,2} \frac{\Delta x_3 L_1}{6} \hat{\psi}_2 + \chi_{i'}^{0,2} \frac{\Delta x_2 L_1}{6} \hat{\psi}_4 \quad (i' = 1, \dots, 4), \quad (3.171)$$

$$A_{3i'}^{(I)} = \frac{\rho\Delta x_2\Delta x_3 L_1}{12}(-i\omega\hat{r}_{i'}) + \frac{\Delta x_2\Delta x_3}{4} \left( I_1^* + i\omega I_2^* - \frac{i}{\omega} I_3^* - \frac{1}{\omega^2} I_4^* - \frac{i}{\omega^3} I_5^* \right) \hat{\psi}_5 \\ + \chi_{i'}^{1,2} \frac{\Delta x_3 L_1}{6} \hat{\psi}_4 + \chi_{i'}^{0,2} \frac{\Delta x_2 L_1}{6} \hat{\psi}_3 \quad (i' = 1, \dots, 4). \quad (3.172)$$

For the infinite elements, when taking inverse Fourier transforms in time, the terms with  $\omega$  on the denominator in equations (3.170)-(3.172) will result in integrals, which would rather be avoided. Therefore, a form must be found for the stretching function  $s_1$ , such that the integrals in equations (3.163)-(3.165) tend to zero in the limit as  $X_1 \rightarrow \infty$ . In what follows it has been assumed that such a form has been found in order to maintain as general a derivation as possible. However, it would be wrong to blindly assume that this is possible so first an example is presented where a particular form has been chosen for the stretching function in order to show that these conditions can be satisfied.

Generalising the form found in [147],  $\alpha_1$  and  $\beta_1$  are taken to be of the form

$$\alpha_1(x_1) = 1 + \bar{\alpha}(x_1 - L_1)^m \quad (3.173)$$

$$\beta_1(x_1) = \bar{\beta}(x_1 - L_1)^n \quad (3.174)$$

where  $\bar{\alpha}$  and  $\bar{\beta}$  are independent of  $x_1$  with a form to be determined and  $m, n$  are constants. It is noted in [147] that this is a form that has been found to be effective despite a lack of rigorous methodology. Given that the aim is to eliminate integrals  $I_3^*, I_4^*, I_5^*$ , which all contain higher powers of  $\beta_1$  on the numerator, with  $\beta_1^3$  the highest power, and  $\alpha_1$  on the denominator, it seems prudent to choose  $m, n$ , such that  $m > 3n$ . Therefore the choice of  $m = 1, n = 1/4$  is made. With these parameters, with  $\alpha_1(x_1)$  given by equation (3.175) and  $\beta_1(x_1)$  given by equation (3.176), the integrals in equations (3.163)-(3.165) can be evaluated in Mathematica [151] (before taking the limit as  $X_1 \rightarrow \infty$ ). The results are complicated, but for brevity, with terms ordered by magnitude,

$$\begin{aligned} \int_{L_1}^{X_1} \frac{(\beta_1(x_1))^3}{\alpha_1(x_1)x_1} \left(\frac{L_1}{x_1}\right)^4 dx_1 &\sim \frac{\bar{\beta}^3}{\bar{\alpha}^5 X_1^{13/4}} + \dots + \frac{\bar{\beta}^3}{\bar{\alpha}} \ln(X_1), \\ \int_{L_1}^{X_1} \frac{(\beta_1(x_1))^3}{\bar{\alpha}\alpha_1(x_1)} \left(\frac{L_1}{x_1}\right)^4 dx_1 &\sim \frac{\bar{\beta}^3}{\bar{\alpha}^{15/4} X_1} + \dots + \frac{\bar{\beta}^3}{\bar{\alpha}} \ln(X_1), \\ \int_{L_1}^{X_1} \frac{(\beta_1(x_1))^2}{\alpha_1(x_1)x_1} \left(\frac{L_1}{x_1}\right)^4 dx_1 &\sim \frac{\bar{\beta}^2}{\bar{\alpha}^2 X_1^{7/2}} + \dots + \frac{\bar{\beta}^2}{\bar{\alpha}}, \\ \int_{L_1}^{X_1} \frac{(\beta_1(x_1))^2}{\bar{\alpha}\alpha_1(x_1)} \left(\frac{L_1}{x_1}\right)^4 dx_1 &\sim \frac{\bar{\beta}^2}{\bar{\alpha}^2 X_1^{5/2}} + \dots + \frac{\bar{\beta}^2}{\bar{\alpha}}, \\ \int_{L_1}^{X_1} \frac{\beta_1(x_1)}{\alpha_1(x_1)x_1} \left(\frac{L_1}{x_1}\right)^4 dx_1 &\sim \frac{\bar{\beta}}{\bar{\alpha}^5 X_1^{15/4}} + \dots + \frac{\bar{\beta}}{\bar{\alpha}} \ln(X_1), \\ \int_{L_1}^{X_1} \frac{\beta_1(x_1)}{\bar{\alpha}\alpha_1(x_1)} \left(\frac{L_1}{x_1}\right)^4 dx_1 &\sim \frac{\bar{\beta}}{\bar{\alpha}^4 X_1^{15/4}} + \dots + \frac{\bar{\beta}}{\bar{\alpha}} \ln(X_1), \end{aligned}$$

and the aim then is to have all but the last of these integrals to tend to zero in the



limit as  $X_1 \rightarrow \infty$  for a given choice of  $\bar{\alpha}$  and  $\bar{\beta}$ . Examining the possibilities where  $\bar{\alpha}$  and  $\bar{\beta}$  either tend to zero, infinity or a nonzero constant in the limit, it quickly becomes clear that no choice can be made to retain the last integral without also retaining the second to last. Therefore the decision is made to have the  $\bar{\beta}$  term tend to zero in the limit  $X_1 \rightarrow \infty$ , ensuring that only the parts of integrals  $I_1^*, \dots, I_5^*$ , involving  $\alpha_1$  alone remain, that is  $I_2^*$  and part of  $I_1^*$ . To achieve this the dimensions of  $\bar{\alpha}$  and  $\bar{\beta}$  must first be considered. By definition,  $\alpha_1$  must be nondimensional and  $\beta_1$  has dimensions  $[T^{-1}]$ , and therefore from equation (3.173),  $\bar{\alpha} \sim [L^{-m}]$ , and from equation (3.174),  $\bar{\beta} \sim [L^{-n}T^{-1}]$ . It must also hold that  $\bar{\beta}$  tends to zero, while  $\bar{\alpha}$  tends to a finite constant as  $X_1 \rightarrow \infty$ . So, in order to satisfy these conditions choose

$$\bar{\alpha} = \frac{\bar{\alpha}}{L_1^m} \frac{X_1}{X_1 - L_1}, \quad (3.175)$$

$$\bar{\beta} = \frac{\bar{c}}{(X_1 - L_1)^{n+1}}, \quad (3.176)$$

where  $\bar{\alpha}$  is some constant parameter that can be used to fine tune the PML.

With  $\alpha_1, \beta_1$ , given as in equations (3.173) and (3.174), and  $\bar{\alpha}, \bar{\beta}$ , given as in equations (3.175) and (3.176), and with  $m = 1, n = 1/4$ , the integrals  $I_1^*$  and  $I_2^*$  can be evaluated in Mathematica to give

$$I_1^* = \frac{12\bar{\alpha}^4 \ln\left(\frac{\bar{\alpha}}{L_1}\right) + 12\bar{\alpha}^4 \ln(L_1) - 25\bar{\alpha}^4 + 48\bar{\alpha}^3 - 36\bar{\alpha}^2 + 16\bar{\alpha} - 3}{12(\bar{\alpha} - 1)^5}, \quad (3.177)$$

$$I_2^* = \frac{L_1(-11\bar{\alpha}^3 + 6\bar{\alpha}^3 \ln(\bar{\alpha}) + 18\bar{\alpha}^2 - 9\bar{\alpha} + 2)}{6(\bar{\alpha} - 1)^4 \bar{c}}. \quad (3.178)$$

Inverse Fourier transforms in time can then be taken in order to proceed.

Returning now to the more general case (assuming a form has been found for the stretching function such that  $I_3^*, I_4^*, I_5^*$  tend to zero and  $I_1^*, I_2^*$  converge to a

non-zero constant as  $X_1 \rightarrow \infty$ ) and taking inverse Fourier transforms of equations (3.170)-(3.172) gives for each infinite element

$$A_{1i'}^{(I)} = \frac{\rho\Delta x_2\Delta x_3 L_1}{12} \dot{p}_{i'} - \frac{\Delta x_2\Delta x_3}{4} I_2^* \dot{\psi}_1 + \frac{\Delta x_2\Delta x_3}{4} I_1^* \psi_1 + \chi_{i'}^{1,2} \frac{\Delta x_3 L_1}{6} \psi_6 + \chi_{i'}^{0,2} \frac{\Delta x_2 L_1}{6} \psi_5 \quad (i' = 1, \dots, 4), \quad (3.179)$$

$$A_{2i'}^{(I)} = \frac{\rho\Delta x_2\Delta x_3 L_1}{12} \dot{q}_{i'} - \frac{\Delta x_2\Delta x_3}{4} I_2^* \dot{\psi}_6 + \frac{\Delta x_2\Delta x_3}{4} I_1^* \psi_6 + \chi_{i'}^{1,2} \frac{\Delta x_3 L_1}{6} \psi_2 + \chi_{i'}^{0,2} \frac{\Delta x_2 L_1}{6} \psi_4 \quad (i' = 1, \dots, 4), \quad (3.180)$$

and

$$A_{3i'}^{(I)} = \frac{\rho\Delta x_2\Delta x_3 L_1}{12} \dot{r}_{i'} - \frac{\Delta x_2\Delta x_3}{4} I_2^* \dot{\psi}_5 + \frac{\Delta x_2\Delta x_3}{4} I_1^* \psi_5 + \chi_{i'}^{1,2} \frac{\Delta x_3 L_1}{6} \psi_4 + \chi_{i'}^{0,2} \frac{\Delta x_2 L_1}{6} \psi_3 \quad (i' = 1, \dots, 4). \quad (3.181)$$

### 3.5.2 The stress equations

Now the same treatment is applied to the stress equation (3.10). With the solution expressed in terms of the basis function expansion in equations (3.24) and (3.25), with the basis functions and test functions given by equations (3.26) and (3.27), assuming as before that  $s = 1$  in  $\Omega_F$  and  $s_2 = s_3 \equiv 1$  in  $\Omega_I$ , from equations

(3.81)-(3.86)

$$\begin{aligned}
& \sum_{j=1}^N \left\{ \int_{\Omega_F} -i\omega N_i N_j \hat{\gamma}_{1j} d\Omega_F \right. \\
& \quad \left. - \int_{\Omega_F} \left\{ (\lambda + 2\mu) N_i \frac{\partial N_j}{\partial x_1} \hat{p}_j + \lambda N_i \frac{\partial N_j}{\partial x_2} \hat{q}_j + \lambda N_i \frac{\partial N_j}{\partial x_3} \hat{r}_j \right\} d\Omega_F \right\} \\
& = \sum_{j=1}^N \left\{ \int_{\Omega_I} \left\{ \frac{\lambda + 2\mu}{s_1} w_i \frac{\partial f_j}{\partial x_1} g_i g_j \hat{p}_j + \lambda w_i f_j g_i \frac{\partial g_j}{\partial x_2} \hat{q}_j + \lambda w_i f_j g_i \frac{\partial g_j}{\partial x_3} \hat{r}_j \right\} d\Omega_I \right. \\
& \quad \left. - \int_{\Omega_I} -i\omega w_i f_j g_i g_j \hat{\gamma}_{1j} d\Omega_I \right\} \quad (i = 1, \dots, N), \tag{3.182}
\end{aligned}$$

$$\begin{aligned}
& \sum_{j=1}^N \left\{ \int_{\Omega_F} -i\omega N_i N_j \hat{\gamma}_{2j} d\Omega_F \right. \\
& \quad \left. - \int_{\Omega_F} \left\{ \lambda N_i \frac{\partial N_j}{\partial x_1} \hat{p}_j + (\lambda + 2\mu) N_i \frac{\partial N_j}{\partial x_2} \hat{q}_j + \lambda N_i \frac{\partial N_j}{\partial x_3} \hat{r}_j \right\} d\Omega_F \right\} \\
& = \sum_{j=1}^N \left\{ \int_{\Omega_I} \left\{ \frac{\lambda}{s_1} w_i \frac{\partial f_j}{\partial x_1} g_i g_j \hat{p}_j + (\lambda + 2\mu) w_i f_j g_i \frac{\partial g_j}{\partial x_2} \hat{q}_j + \lambda w_i f_j g_i \frac{\partial g_j}{\partial x_3} \hat{r}_j \right\} d\Omega_I \right. \\
& \quad \left. - \int_{\Omega_I} -i\omega w_i f_j g_i g_j \hat{\gamma}_{2j} d\Omega_I \right\} \quad (i = 1, \dots, N), \tag{3.183}
\end{aligned}$$

$$\begin{aligned}
& \sum_{j=1}^N \left\{ \int_{\Omega_F} -i\omega N_i N_j \hat{\gamma}_{3j} d\Omega_F \right. \\
& \quad \left. - \int_{\Omega_F} \left\{ \lambda N_i \frac{\partial N_j}{\partial x_1} \hat{p}_j + \lambda N_i \frac{\partial N_j}{\partial x_2} \hat{q}_j + (\lambda + 2\mu) N_i \frac{\partial N_j}{\partial x_3} \hat{r}_j \right\} d\Omega_F \right\} \\
& = \sum_{j=1}^N \left\{ \int_{\Omega_I} \left\{ \frac{\lambda}{s_1} w_i \frac{\partial f_j}{\partial x_1} g_i g_j \hat{p}_j + \lambda w_i f_j g_i \frac{\partial g_j}{\partial x_2} \hat{q}_j + (\lambda + 2\mu) w_i f_j g_i \frac{\partial g_j}{\partial x_3} \hat{r}_j \right\} d\Omega_I \right. \\
& \quad \left. - \int_{\Omega_I} -i\omega w_i f_j g_i g_j \hat{\gamma}_{3j} d\Omega_I \right\} \quad (i = 1, \dots, N), \tag{3.184}
\end{aligned}$$

$$\begin{aligned}
& \sum_{j=1}^N \left\{ \int_{\Omega_F} -i\omega N_i N_j \hat{\gamma}_{4j} d\Omega_F - \int_{\Omega_F} \left\{ \mu N_i \frac{\partial N_j}{\partial x_2} \hat{r}_j + \mu N_i \frac{\partial N_j}{\partial x_3} \hat{q}_j \right\} d\Omega_F \right\} \\
&= \sum_{j=1}^N \left\{ \int_{\Omega_I} \left\{ \mu w_i f_j g_i \frac{\partial g_j}{\partial x_2} \hat{r}_j + \mu w_i f_j g_i \frac{\partial g_j}{\partial x_3} \hat{q}_j \right\} d\Omega_I \right. \\
&\quad \left. - \int_{\Omega_I} -i\omega w_i f_j g_i g_j \hat{\gamma}_{4j} d\Omega_I \right\} \quad (i = 1, \dots, N), \tag{3.185}
\end{aligned}$$

$$\begin{aligned}
& \sum_{j=1}^N \left\{ \int_{\Omega_F} -i\omega N_i N_j \hat{\gamma}_{5j} d\Omega_F - \int_{\Omega_F} \left\{ \mu N_i \frac{\partial N_j}{\partial x_1} \hat{r}_j + \mu N_i \frac{\partial N_j}{\partial x_3} \hat{p}_j \right\} d\Omega_F \right\} \\
&= \sum_{j=1}^N \left\{ \int_{\Omega_I} \left\{ \frac{\mu}{s_1} w_i \frac{\partial f_j}{\partial x_1} g_i g_j \hat{r}_j + \mu w_i f_j g_i \frac{\partial g_j}{\partial x_3} \hat{p}_j \right\} d\Omega_I \right. \\
&\quad \left. - \int_{\Omega_I} -i\omega w_i f_j g_i g_j \hat{\gamma}_{5j} d\Omega_I \right\} \quad (i = 1, \dots, N), \tag{3.186}
\end{aligned}$$

$$\begin{aligned}
& \sum_{j=1}^N \left\{ \int_{\Omega_F} -i\omega N_i N_j \hat{\gamma}_{6j} d\Omega_F - \int_{\Omega_F} \left\{ \mu N_i \frac{\partial N_j}{\partial x_1} \hat{q}_j + \mu N_i \frac{\partial N_j}{\partial x_2} \hat{p}_j \right\} d\Omega_F \right\} \\
&= \sum_{j=1}^N \left\{ \int_{\Omega_I} \left\{ \frac{\mu}{s_1} w_i \frac{\partial f_j}{\partial x_1} g_i g_j \hat{q}_j + \mu w_i f_j g_i \frac{\partial g_j}{\partial x_2} \hat{p}_j \right\} d\Omega_I \right. \\
&\quad \left. - \int_{\Omega_I} -i\omega w_i f_j g_i g_j \hat{\gamma}_{6j} d\Omega_I \right\} \quad (i = 1, \dots, N). \tag{3.187}
\end{aligned}$$

Then, given the choice of basis functions in equations (3.34)-(3.36) and test functions in equations (3.37) and (3.38), the integrals that will have to be evaluated are given by equations (3.50)-(3.59) with the exception of equation (3.57) which

has the slightly different form of

$$\begin{aligned}
\int_{\Omega_{IE}} \frac{1}{s_1} w_{i'} \frac{\partial f_{j'}}{\partial x_1} g_{i'} g_{j'} d\Omega_{IE} &= \lim_{X_1 \rightarrow \infty} \int_{L_1}^{X_1} \frac{1}{s_1} w_{i'} \frac{\partial f_{j'}}{\partial x_1} dx_1 \int_{-1}^1 \int_{-1}^1 g_{i'} g_{j'} \frac{\Delta x_2 \Delta x_3}{4} d\eta d\zeta \\
&= \frac{\Delta x_2 \Delta x_3}{16} \left(1 + \frac{\eta_{i'} \eta_{j'}}{3}\right) \left(1 + \frac{\zeta_{i'} \zeta_{j'}}{3}\right) \\
&\quad \times \lim_{X_1 \rightarrow \infty} \int_{L_1}^{X_1} \frac{1}{s_1} \left(\frac{L_1}{x_1}\right)^4 \left(-\frac{1}{x_1} - i\bar{k}\right) dx_1 \\
&= \frac{\Delta x_2 \Delta x_3}{16} \left(1 + \frac{\eta_{i'} \eta_{j'}}{3}\right) \left(1 + \frac{\zeta_{i'} \zeta_{j'}}{3}\right) \\
&\quad \times \left(I_6^* - i\omega I_2^* - \frac{i}{\omega} I_7^* - \frac{1}{\omega^2} I_8^* - \frac{i}{\omega^3} I_5^*\right) \quad (3.188)
\end{aligned}$$

where

$$I_6^* = \lim_{X_1 \rightarrow \infty} \int_{L_1}^{X_1} \left(-\frac{1}{x_1} - \frac{\beta_1(x_1)}{\bar{c}}\right) \frac{1}{\alpha_1(x_1)} \left(\frac{L_1}{x_1}\right)^4 dx_1 \quad (3.189)$$

$$I_7^* = \lim_{X_1 \rightarrow \infty} \int_{L_1}^{X_1} \left(-\frac{\beta_1(x_1)}{x_1} - \frac{(\beta_1(x_1))^2}{\bar{c}}\right) \frac{1}{\alpha_1(x_1)} \left(\frac{L_1}{x_1}\right)^4 dx_1 \quad (3.190)$$

$$I_8^* = \lim_{X_1 \rightarrow \infty} \int_{L_1}^{X_1} \left(-\frac{(\beta_1(x_1))^2}{x_1} - \frac{(\beta_1(x_1))^3}{\bar{c}}\right) \frac{1}{\alpha_1(x_1)} \left(\frac{L_1}{x_1}\right)^4 dx_1 \quad (3.191)$$

and assuming as before that  $\omega \gg \beta_1(x_1)$ . Then, from the right-hand side of equation (3.182) (taking the negative once more to emphasise the similarity to the finite element case), define for each infinite element

$$\begin{aligned}
B_{1i'}^{(I)} &= \sum_{j'=1}^4 \frac{\Delta x_2 \Delta x_3}{16} \left(1 + \frac{\eta_{i'} \eta_{j'}}{3}\right) \left(1 + \frac{\zeta_{i'} \zeta_{j'}}{3}\right) \frac{L_1}{3} (-i\omega \hat{\gamma}_{1j'}) \\
&\quad - (\lambda + 2\mu) \frac{\Delta x_2 \Delta x_3}{16} \left(1 + \frac{\eta_{i'} \eta_{j'}}{3}\right) \left(1 + \frac{\zeta_{i'} \zeta_{j'}}{3}\right) \\
&\quad \times \left(I_6^* - i\omega I_2^* - \frac{i}{\omega} I_7^* - \frac{1}{\omega^2} I_8^* - \frac{i}{\omega^3} I_5^*\right) \hat{p}_{j'} \\
&\quad - \lambda \frac{L_1}{3} \frac{\Delta x_3}{8} \eta_{j'} \left(1 + \frac{\zeta_{i'} \zeta_{j'}}{3}\right) \hat{q}_{j'} - \lambda \frac{L_1}{3} \frac{\Delta x_2}{8} \zeta_{j'} \left(1 + \frac{\eta_{i'} \eta_{j'}}{3}\right) \hat{r}_{j'} \quad (i' = 1, \dots, 4).
\end{aligned}$$

Again, in order to provide an explicit scheme, it is assumed that  $\hat{\gamma}_{ni'} = \hat{\gamma}_{nj'} \equiv \hat{\psi}_n$  when  $i', j'$  are nodes of the same element, and then expanding the summation in  $j'$  yields

$$\begin{aligned}
B_1^{(I)} = & -i\omega \frac{\Delta x_2 \Delta x_3 L_1}{3} \hat{\psi}_1 \\
& - \frac{(\lambda + 2\mu) \Delta x_2 \Delta x_3}{4} \left( I_6^* - i\omega I_2^* - \frac{i}{\omega} I_7^* - \frac{1}{\omega^2} I_8^* - \frac{i}{\omega^3} I_5^* \right) (\hat{p}_1 + \hat{p}_2 + \hat{p}_3 + \hat{p}_4) \\
& - \frac{\lambda \Delta x_3 L_1}{6} (\hat{q}_3 - \hat{q}_1 + \hat{q}_2 - \hat{q}_4) \\
& - \frac{\lambda \Delta x_2 L_1}{6} (\hat{r}_3 - \hat{r}_1 + \hat{r}_4 - \hat{r}_2), \tag{3.192}
\end{aligned}$$

and similarly from equations (3.183)-(3.187)

$$\begin{aligned}
B_2^{(I)} &= -i\omega \frac{\Delta x_2 \Delta x_3 L_1}{3} \hat{\psi}_2 \\
&\quad - \frac{\lambda \Delta x_2 \Delta x_3}{4} \left( I_6^* - i\omega I_2^* - \frac{i}{\omega} I_7^* - \frac{1}{\omega^2} I_8^* - \frac{i}{\omega^3} I_5^* \right) (\hat{p}_1 + \hat{p}_2 + \hat{p}_3 + \hat{p}_4) \\
&\quad - \frac{(\lambda + 2\mu) \Delta x_3 L_1}{6} (\hat{q}_3 - \hat{q}_1 + \hat{q}_2 - \hat{q}_4) \\
&\quad - \frac{\lambda \Delta x_2 L_1}{6} (\hat{r}_3 - \hat{r}_1 + \hat{r}_4 - \hat{r}_2), \tag{3.193}
\end{aligned}$$

$$\begin{aligned}
B_3^{(I)} &= -i\omega \frac{\Delta x_2 \Delta x_3 L_1}{3} \hat{\psi}_3 \\
&\quad - \frac{\lambda \Delta x_2 \Delta x_3}{4} \left( I_6^* - i\omega I_2^* - \frac{i}{\omega} I_7^* - \frac{1}{\omega^2} I_8^* - \frac{i}{\omega^3} I_5^* \right) (\hat{p}_1 + \hat{p}_2 + \hat{p}_3 + \hat{p}_4) \\
&\quad - \frac{\lambda \Delta x_3 L_1}{6} (\hat{q}_3 - \hat{q}_1 + \hat{q}_2 - \hat{q}_4) \\
&\quad - \frac{(\lambda + 2\mu) \Delta x_2 L_1}{6} (\hat{r}_3 - \hat{r}_1 + \hat{r}_4 - \hat{r}_2), \tag{3.194}
\end{aligned}$$

$$\begin{aligned}
B_4^{(I)} &= -i\omega \frac{\Delta x_2 \Delta x_3 L_1}{3} \hat{\psi}_4 \\
&\quad - \frac{\mu \Delta x_3 L_1}{6} (\hat{r}_3 - \hat{r}_1 + \hat{r}_2 - \hat{r}_4) - \frac{\mu \Delta x_2 L_1}{6} (\hat{q}_3 - \hat{q}_1 + \hat{q}_4 - \hat{q}_2), \tag{3.195}
\end{aligned}$$

$$\begin{aligned}
B_5^{(I)} &= -i\omega \frac{\Delta x_2 \Delta x_3 L_1}{3} \hat{\psi}_5 \\
&\quad - \frac{\mu \Delta x_2 \Delta x_3}{4} \left( I_6^* - i\omega I_2^* - \frac{i}{\omega} I_7^* - \frac{1}{\omega^2} I_8^* - \frac{i}{\omega^3} I_5^* \right) (\hat{r}_1 + \hat{r}_2 + \hat{r}_3 + \hat{r}_4) \\
&\quad - \frac{\mu \Delta x_2 L_1}{6} (\hat{p}_3 - \hat{p}_1 + \hat{p}_4 - \hat{p}_2), \tag{3.196}
\end{aligned}$$

$$\begin{aligned}
B_6^{(I)} &= -i\omega \frac{\Delta x_2 \Delta x_3 L_1}{3} \hat{\psi}_6 \\
&\quad - \frac{\mu \Delta x_2 \Delta x_3}{4} \left( I_6^* - i\omega I_2^* - \frac{i}{\omega} I_7^* - \frac{1}{\omega^2} I_8^* - \frac{i}{\omega^3} I_5^* \right) (\hat{q}_1 + \hat{q}_2 + \hat{q}_3 + \hat{q}_4) \\
&\quad - \frac{\mu \Delta x_3 L_1}{6} (\hat{p}_3 - \hat{p}_1 + \hat{p}_2 - \hat{p}_4). \tag{3.197}
\end{aligned}$$

For the infinite elements, before taking inverse Fourier transforms in time, as before, a form must be chosen for the stretching function such that  $I_7^*, I_8^*$  tend to zero and  $I_6^*$  converges to a non-zero constant as  $X_1 \rightarrow \infty$ . As before, an example problem is presented, taking  $\alpha_1(x_1)$  and  $\beta_1(x_1)$  to be given by equations

(3.173) and (3.174), with  $\bar{\alpha}$  and  $\bar{\beta}$  given by equations (3.175) and (3.176), and with  $m = 1, n = 1/4$ , in order to show that this goal can be achieved. Since  $I_6^* \approx I_1^*$ ,  $I_7^* \approx I_3^*$  and  $I_8^* \approx I_4^*$ , in the limit  $X_1 \rightarrow \infty$  we have  $I_7^* \rightarrow 0, I_8^* \rightarrow 0$  and

$$I_6^* \equiv I_1^* = \frac{12\bar{\alpha}^4 \ln\left(\frac{\bar{\alpha}}{L_1}\right) + 12\bar{\alpha}^4 \ln(L_1) - 25\bar{\alpha}^4 + 48\bar{\alpha}^3 - 36\bar{\alpha}^2 + 16\bar{\alpha} - 3}{12(\bar{\alpha} - 1)^5}. \quad (3.198)$$

Now, once again returning to the more general case where it is assumed that a form has been found for the stretching function such that  $I_7^*, I_8^*$  tend to zero and  $I_2^*, I_6^*$  converge as  $X_1 \rightarrow \infty$ , by taking inverse Fourier transforms in time of



equations (3.192)-(3.197), for each infinite element,

$$\begin{aligned}
B_1^{(I)} &= \frac{\Delta x_2 \Delta x_3 L_1}{3} \dot{\psi}_1 - \frac{(\lambda + 2\mu) \Delta x_2 \Delta x_3}{4} I_2^*(\dot{p}_1 + \dot{p}_2 + \dot{p}_3 + \dot{p}_4) \\
&\quad - \frac{(\lambda + 2\mu) \Delta x_2 \Delta x_3}{4} I_6^*(p_1 + p_2 + p_3 + p_4) - \frac{\lambda \Delta x_3 L_1}{6} (q_3 - q_1 + q_2 - q_4) \\
&\quad - \frac{\lambda \Delta x_2 L_1}{6} (r_3 - r_1 + r_4 - r_2), \tag{3.199}
\end{aligned}$$

$$\begin{aligned}
B_2^{(I)} &= \frac{\Delta x_2 \Delta x_3 L_1}{3} \dot{\psi}_2 - \frac{\lambda \Delta x_2 \Delta x_3}{4} I_2^*(\dot{p}_1 + \dot{p}_2 + \dot{p}_3 + \dot{p}_4) \\
&\quad - \frac{\lambda \Delta x_2 \Delta x_3}{4} I_6^*(p_1 + p_2 + p_3 + p_4) - \frac{(\lambda + 2\mu) \Delta x_3 L_1}{6} (q_3 - q_1 + q_2 - q_4) \\
&\quad - \frac{\lambda \Delta x_2 L_1}{6} (r_3 - r_1 + r_4 - r_2), \tag{3.200}
\end{aligned}$$

$$\begin{aligned}
B_3^{(I)} &= \frac{\Delta x_2 \Delta x_3 L_1}{3} \dot{\psi}_3 - \frac{\lambda \Delta x_2 \Delta x_3}{4} I_2^*(\dot{p}_1 + \dot{p}_2 + \dot{p}_3 + \dot{p}_4) \\
&\quad - \frac{\lambda \Delta x_2 \Delta x_3}{4} I_6^*(p_1 + p_2 + p_3 + p_4) - \frac{\lambda \Delta x_3 L_1}{6} (q_3 - q_1 + q_2 - q_4) \\
&\quad - \frac{(\lambda + 2\mu) \Delta x_2 L_1}{6} (r_3 - r_1 + r_4 - r_2), \tag{3.201}
\end{aligned}$$

$$\begin{aligned}
B_4^{(I)} &= \frac{\Delta x_2 \Delta x_3 L_1}{3} \dot{\psi}_4 - \frac{\mu \Delta x_3 L_1}{6} (r_3 - r_1 + r_2 - r_4) - \frac{\mu \Delta x_2 L_1}{6} (q_3 - q_1 + q_4 - q_2), \tag{3.202}
\end{aligned}$$

$$\begin{aligned}
B_5^{(I)} &= \frac{\Delta x_2 \Delta x_3 L_1}{3} \dot{\psi}_5 - \frac{\mu \Delta x_2 \Delta x_3}{4} I_2^*(\dot{r}_1 + \dot{r}_2 + \dot{r}_3 + \dot{r}_4) \\
&\quad - \frac{\mu \Delta x_2 \Delta x_3}{4} I_6^*(r_1 + r_2 + r_3 + r_4) - \frac{\mu \Delta x_2 L_1}{6} (p_3 - p_1 + p_4 - p_2), \tag{3.203}
\end{aligned}$$

$$\begin{aligned}
B_6^{(I)} &= \frac{\Delta x_2 \Delta x_3 L_1}{3} \dot{\psi}_6 - \frac{\mu \Delta x_2 \Delta x_3}{4} I_2^*(\dot{q}_1 + \dot{q}_2 + \dot{q}_3 + \dot{q}_4) \\
&\quad - \frac{\mu \Delta x_2 \Delta x_3}{4} I_6^*(q_1 + q_2 + q_3 + q_4) - \frac{\mu \Delta x_3 L_1}{6} (p_3 - p_1 + p_2 - p_4). \tag{3.204}
\end{aligned}$$

As before, for the infinite elements, both velocity and stress time derivatives appear so closer inspection of the system is required in order to find an explicit form. It must also be remembered that since the velocity equations will be recombined at a global level, whatever manipulations are performed on the finite element equations must also be performed on the infinite element equations and vice versa. The system of equations (3.179)-(3.181) and (3.199)-(3.204) can be

written in matrix form as follows,

$$M_3 \dot{\mathbf{p}} = M_4 \mathbf{p} \quad (3.205)$$

where

$$M_3 = \begin{bmatrix} C_1 & 0 & 0 & 0 & 0 & 0 & 0 & 0 & 0 & 0 & 0 & 0 & 0 & C_2 & 0 & 0 & 0 & 0 & 0 & 0 \\ 0 & C_1 & 0 & 0 & 0 & 0 & 0 & 0 & 0 & 0 & 0 & 0 & 0 & C_2 & 0 & 0 & 0 & 0 & 0 & 0 \\ 0 & 0 & C_1 & 0 & 0 & 0 & 0 & 0 & 0 & 0 & 0 & 0 & 0 & C_2 & 0 & 0 & 0 & 0 & 0 & 0 \\ 0 & 0 & 0 & C_1 & 0 & 0 & 0 & 0 & 0 & 0 & 0 & 0 & 0 & C_2 & 0 & 0 & 0 & 0 & 0 & 0 \\ 0 & 0 & 0 & 0 & C_1 & 0 & 0 & 0 & 0 & 0 & 0 & 0 & 0 & 0 & 0 & 0 & 0 & 0 & 0 & C_2 \\ 0 & 0 & 0 & 0 & 0 & C_1 & 0 & 0 & 0 & 0 & 0 & 0 & 0 & 0 & 0 & 0 & 0 & 0 & 0 & C_2 \\ 0 & 0 & 0 & 0 & 0 & 0 & C_1 & 0 & 0 & 0 & 0 & 0 & 0 & 0 & 0 & 0 & 0 & 0 & 0 & C_2 \\ 0 & 0 & 0 & 0 & 0 & 0 & 0 & C_1 & 0 & 0 & 0 & 0 & 0 & 0 & 0 & 0 & 0 & 0 & 0 & C_2 \\ 0 & 0 & 0 & 0 & 0 & 0 & 0 & 0 & C_1 & 0 & 0 & 0 & 0 & 0 & 0 & 0 & 0 & 0 & 0 & C_2 \\ 0 & 0 & 0 & 0 & 0 & 0 & 0 & 0 & 0 & C_1 & 0 & 0 & 0 & 0 & 0 & 0 & 0 & 0 & 0 & C_2 \\ 0 & 0 & 0 & 0 & 0 & 0 & 0 & 0 & 0 & 0 & C_1 & 0 & 0 & 0 & 0 & 0 & 0 & 0 & 0 & C_2 \\ 0 & 0 & 0 & 0 & 0 & 0 & 0 & 0 & 0 & 0 & 0 & C_1 & 0 & 0 & 0 & 0 & 0 & 0 & 0 & C_2 \\ D_2 & D_2 & D_2 & D_2 & 0 & 0 & 0 & 0 & 0 & 0 & 0 & 0 & 0 & D_1 & 0 & 0 & 0 & 0 & 0 & 0 \\ D_3 & D_3 & D_3 & D_3 & 0 & 0 & 0 & 0 & 0 & 0 & 0 & 0 & 0 & D_1 & 0 & 0 & 0 & 0 & 0 & 0 \\ D_3 & D_3 & D_3 & D_3 & 0 & 0 & 0 & 0 & 0 & 0 & 0 & 0 & 0 & D_1 & 0 & 0 & 0 & 0 & 0 & 0 \\ 0 & 0 & 0 & 0 & 0 & 0 & 0 & 0 & 0 & 0 & 0 & 0 & 0 & 0 & 0 & 0 & D_1 & 0 & 0 & 0 \\ 0 & 0 & 0 & 0 & 0 & 0 & 0 & 0 & D_4 & D_4 & D_4 & D_4 & 0 & 0 & 0 & 0 & D_1 & 0 & 0 & 0 \\ 0 & 0 & 0 & 0 & D_4 & D_4 & D_4 & D_4 & 0 & 0 & 0 & 0 & 0 & 0 & 0 & 0 & 0 & 0 & 0 & D_1 \end{bmatrix}, \quad (3.206)$$

with

$$\begin{aligned} C_1 &= \frac{\rho \Delta x_2 \Delta x_3 L_1}{12}, \\ C_2 &= -\frac{\Delta x_2 \Delta x_3}{4} I_2^*, \\ D_1 &= \frac{\Delta x_2 \Delta x_3 L_1}{3}, \\ D_2 &= -\frac{(\lambda + 2\mu) \Delta x_2 \Delta x_3}{4} I_2^*, \\ D_3 &= -\frac{\lambda \Delta x_2 \Delta x_3}{4} I_2^*, \\ D_4 &= -\frac{\mu \Delta x_2 \Delta x_3}{4} I_2^*, \end{aligned}$$

and where

$$M_4 = \begin{bmatrix} 0 & 0 & 0 & 0 & 0 & 0 & 0 & 0 & 0 & 0 & 0 & 0 & E_1 & 0 & 0 & 0 & E_3 & E_2 \\ 0 & 0 & 0 & 0 & 0 & 0 & 0 & 0 & 0 & 0 & 0 & 0 & E_1 & 0 & 0 & 0 & E_3 & -E_2 \\ 0 & 0 & 0 & 0 & 0 & 0 & 0 & 0 & 0 & 0 & 0 & 0 & E_1 & 0 & 0 & 0 & -E_3 & -E_2 \\ 0 & 0 & 0 & 0 & 0 & 0 & 0 & 0 & 0 & 0 & 0 & 0 & E_1 & 0 & 0 & 0 & -E_3 & E_2 \\ 0 & 0 & 0 & 0 & 0 & 0 & 0 & 0 & 0 & 0 & 0 & 0 & 0 & E_2 & 0 & 0 & E_3 & 0 \\ 0 & 0 & 0 & 0 & 0 & 0 & 0 & 0 & 0 & 0 & 0 & 0 & 0 & 0 & -E_2 & 0 & E_3 & 0 \\ 0 & 0 & 0 & 0 & 0 & 0 & 0 & 0 & 0 & 0 & 0 & 0 & 0 & 0 & -E_2 & 0 & -E_3 & 0 \\ 0 & 0 & 0 & 0 & 0 & 0 & 0 & 0 & 0 & 0 & 0 & 0 & 0 & 0 & E_2 & 0 & -E_3 & 0 \\ 0 & 0 & 0 & 0 & 0 & 0 & 0 & 0 & 0 & 0 & 0 & 0 & 0 & 0 & 0 & E_3 & E_2 & E_1 \\ 0 & 0 & 0 & 0 & 0 & 0 & 0 & 0 & 0 & 0 & 0 & 0 & 0 & 0 & 0 & E_3 & -E_2 & E_1 \\ 0 & 0 & 0 & 0 & 0 & 0 & 0 & 0 & 0 & 0 & 0 & 0 & 0 & 0 & 0 & -E_3 & -E_2 & E_1 \\ 0 & 0 & 0 & 0 & 0 & 0 & 0 & 0 & 0 & 0 & 0 & 0 & 0 & 0 & 0 & -E_3 & E_2 & E_1 \\ F_1 & F_1 & F_1 & F_1 & -F_2 & F_2 & F_2 & -F_2 & -F_3 & -F_3 & F_3 & F_3 & 0 & 0 & 0 & 0 & 0 & 0 \\ F_4 & F_4 & F_4 & F_4 & -F_5 & F_5 & F_5 & -F_5 & -F_3 & -F_3 & F_3 & F_3 & 0 & 0 & 0 & 0 & 0 & 0 \\ F_4 & F_4 & F_4 & F_4 & -F_2 & F_2 & F_2 & -F_2 & -F_6 & -F_6 & F_6 & F_6 & 0 & 0 & 0 & 0 & 0 & 0 \\ 0 & 0 & 0 & 0 & -F_7 & -F_7 & F_7 & F_7 & -F_8 & F_8 & F_8 & -F_8 & 0 & 0 & 0 & 0 & 0 & 0 \\ -F_7 & -F_7 & F_7 & F_7 & 0 & 0 & 0 & 0 & F_9 & F_9 & F_9 & F_9 & 0 & 0 & 0 & 0 & 0 & 0 \\ -F_8 & F_8 & F_8 & -F_8 & F_9 & F_9 & F_9 & F_9 & 0 & 0 & 0 & 0 & 0 & 0 & 0 & 0 & 0 & 0 \end{bmatrix}, \quad (3.207)$$

$$\mathbf{p}^T = \begin{bmatrix} p_1 & p_2 & p_3 & p_4 & q_1 & q_2 & q_3 & q_4 & r_1 & r_2 & r_3 & r_4 & \psi_1 & \psi_2 & \psi_3 & \psi_4 & \psi_5 & \psi_6 \end{bmatrix}, \quad (3.208)$$

with

$$\begin{aligned}
E_1 &= -\frac{\Delta x_2 \Delta x_3}{4} I_1^*, \\
E_2 &= \frac{\Delta x_3 L_1}{6}, \\
E_3 &= \frac{\Delta x_2 L_1}{6}, \\
F_1 &= \frac{(\lambda + 2\mu) \Delta x_2 \Delta x_3}{4} I_6^*, \\
F_2 &= \frac{\lambda \Delta x_3 L_1}{6}, \\
F_3 &= \frac{\lambda \Delta x_2 L_1}{6}, \\
F_4 &= \frac{\lambda \Delta x_2 \Delta x_3}{4} I_6^*, \\
F_5 &= \frac{(\lambda + 2\mu) \Delta x_3 L_1}{6}, \\
F_6 &= \frac{(\lambda + 2\mu) \Delta x_2 L_1}{6}, \\
F_7 &= \frac{\mu \Delta x_2 L_1}{6}, \\
F_8 &= \frac{\mu \Delta x_3 L_1}{6}, \\
F_9 &= \frac{\mu \Delta x_2 \Delta x_3}{4} I_6^*.
\end{aligned}$$

In order to provide an explicit scheme, matrix  $M_3$  must be diagonalised. To do so, the entries must first be nondimensionalised. The first equation of the system (3.205) will be considered, with rows two to twelve following similarly. So

$$C_1 \dot{p}_1 + C_2 \dot{\psi}_1 = E_1 \psi_1 + E_2 \psi_6 + E_3 \psi_5, \quad (3.209)$$

then taking the same scalings as before

$$p_1 = \bar{c} \tilde{p}_1, \quad t = T \tilde{t}, \quad \psi_i = \mu \tilde{\psi}_i, \quad (3.210)$$

so that

$$\frac{\partial p_1}{\partial t} = \frac{\bar{c}}{T} \tilde{p}'_1, \quad \frac{\partial \psi_i}{\partial t} = \frac{\mu}{T} \tilde{\psi}'_i, \quad (3.211)$$

where  $'$  denotes  $\partial/\partial \tilde{t}$ . Also, from equation (3.162), substituting  $\tilde{x}_1 = x_1/L_1$ , so that  $d\tilde{x}_1/dx_1 = 1/L_1$ , that is,  $dx_1 = L_1 d\tilde{x}_1$ , and for the limits when  $x_1 = L_1, \tilde{x}_1 = 1$  and when  $x_1 = X_1, \tilde{x}_1 = X_1/L_1$ , so that

$$\begin{aligned} I_2^* &= \frac{1}{\bar{c}} \lim_{X_1 \rightarrow \infty} \int_1^{X_1/L_1} \frac{1}{\alpha_1(L_1 \tilde{x}_1)} \left( \frac{1}{\tilde{x}_1} \right)^4 L_1 d\tilde{x}_1 \\ &= \frac{L_1}{\bar{c}} \lim_{X_1 \rightarrow \infty} \int_1^{X_1/L_1} \frac{1}{\alpha_1(L_1 \tilde{x}_1)} \left( \frac{1}{\tilde{x}_1} \right)^4 d\tilde{x}_1. \end{aligned}$$

By definition  $\alpha_1$  is nondimensional therefore  $I_2^* = L_1 \tilde{I}_2^*/\bar{c}$  and

$$I_2^* \sim [LTL^{-1}] = [T].$$

Similarly, from equation (3.161), using the substitution  $\tilde{x}_1 = x_1/L_1$  as before,

$$I_1^* = \lim_{X_1 \rightarrow \infty} \int_1^{X_1/L_1} \left( \frac{\beta_1(L_1 \tilde{x}_1)}{\bar{c}} - \frac{1}{L_1 \tilde{x}_1} \right) \frac{1}{\alpha_1(L_1 \tilde{x}_1)} \left( \frac{1}{\tilde{x}_1} \right)^4 L_1 d\tilde{x}_1.$$

By definition  $\beta_1$  has dimension  $[T^{-1}]$  therefore

$$I_1^* \sim \left[ \frac{T^{-1}TL}{L} \right],$$

that is to say  $I_1^*$  is nondimensional. Then

$$C_1 \frac{\bar{c}}{T} \tilde{p}'_1 + C_2 \frac{\mu}{T} \tilde{\psi}'_1 = E_1 \mu \tilde{\psi}_1 + E_2 \mu \tilde{\psi}_6 + E_3 \mu \tilde{\psi}_5. \quad (3.212)$$

Now the coefficients have dimensions

$$\begin{aligned}
C_1 \frac{\bar{c}}{T} &= \frac{\rho \Delta x_2 \Delta x_3 L_1 \bar{c}}{12T} \sim \left[ \frac{ML^{-3}L^3LT^{-1}}{T} \right] = [MLT^{-2}], \\
C_2 \frac{\mu}{T} &= -\frac{\Delta x_2 \Delta x_3 I_2^* \mu}{4T} \sim \left[ \frac{L^2 T M L^{-1} T^{-2}}{T} \right] = [MLT^{-2}], \\
E_1 \mu &= -\frac{\Delta x_2 \Delta x_3 I_1^* \mu}{4} \sim [L^2 M L^{-1} T^{-2}] = [MLT^{-2}], \\
E_2 \mu &= \frac{\Delta x_3 L_1 \mu}{6} \sim [L^2 M L^{-1} T^{-2}] = [MLT^{-2}], \\
E_3 \mu &= \frac{\Delta x_2 L_1 \mu}{6} \sim [L^2 M L^{-1} T^{-2}] = [MLT^{-2}].
\end{aligned}$$

Then for diagonalisation

$$\left| C_1 \frac{\bar{c}}{T} \right| \gg \left| C_2 \frac{\mu}{T} \right|,$$

that is,

$$I_2^* \ll \frac{\rho L_1 \bar{c}}{3\mu}. \tag{3.213}$$

So equation (3.212) becomes

$$C_1 \frac{\bar{c}}{T} \tilde{p}'_1 = E_1 \mu \tilde{\psi}_1 + E_2 \mu \tilde{\psi}_6 + E_3 \mu \tilde{\psi}_5,$$

and redimensionalising gives

$$C_1 \dot{p}_1 = E_1 \psi_1 + E_2 \psi_6 + E_3 \psi_5,$$

which is just equation (3.209) without the  $\dot{\psi}_1$  term but the nondimensionalisation provided the condition on  $I_2^*$  given in equation (3.213).

The thirteenth row of the system (3.205) will now be considered, with rows

fourteen to eighteen following similarly. From row thirteen,

$$D_2 (\dot{p}_1 + \dot{p}_2 + \dot{p}_3 + \dot{p}_4) + D_1 \dot{\psi}_1 = M_{4,13} \cdot \mathbf{p},$$

and nondimensionalising as before gives

$$D_2 \frac{\bar{c}}{T} (\tilde{p}'_1 + \tilde{p}'_2 + \tilde{p}'_3 + \tilde{p}'_4) + D_1 \frac{\mu}{T} \tilde{\psi}'_1 = M_{4,13} \cdot \tilde{\mathbf{p}}.$$

For diagonalisation, it is required that

$$\left| D_1 \frac{\mu}{T} \right| \gg \left| D_2 \frac{\bar{c}}{T} \right|,$$

that is,

$$I_2^* \ll \frac{4L_1\mu}{3\bar{c}(\lambda + \mu)}. \quad (3.214)$$

Then using Euler's method, from equation (3.179) with consideration to the diagonalisation just performed, an explicit form can be given by

$$A_{1i'}^{(I)} = C_1 \frac{p_{i'}^{(t+1)} - p_{i'}^{(t)}}{\delta t} - E_1 \psi_1 + \chi_{i'}^{1,2} E_2 \psi_6 + \chi_{i'}^{0,2} E_3 \psi_5, \quad (3.215)$$

and similarly for the other velocity components,

$$A_{2i'}^{(I)} = C_1 \frac{q_{i'}^{(t+1)} - q_{i'}^{(t)}}{\delta t} - E_1 \psi_6 + \chi_{i'}^{1,2} E_2 \psi_2 + \chi_{i'}^{0,2} E_3 \psi_4, \quad (3.216)$$

and

$$A_{3i'}^{(I)} = C_1 \frac{r_{i'}^{(t+1)} - r_{i'}^{(t)}}{\delta t} - E_1 \psi_5 + \chi_{i'}^{1,2} E_2 \psi_4 + \chi_{i'}^{0,2} E_3 \psi_3. \quad (3.217)$$

The stress equations can also now be formulated, with respect to the diagonalisation, from equations (3.199)-(3.204), using Euler's method to give

$$B_1^{(I)} = D_1 \frac{\psi_1^{(t+1)} - \psi_1^{(t)}}{\delta t} - F_1(p_1 + p_2 + p_3 + p_4) - F_2(q_3 - q_1 + q_2 - q_4) - F_3(r_3 - r_1 + r_4 - r_2), \quad (3.218)$$

and similarly for the other stress components we have

$$B_2^{(I)} = D_1 \frac{\psi_2^{(t+1)} - \psi_2^{(t)}}{\delta t} - F_4(p_1 + p_2 + p_3 + p_4) - F_5(q_3 - q_1 + q_2 - q_4) - F_3(r_3 - r_1 + r_4 - r_2), \quad (3.219)$$

$$B_3^{(I)} = D_1 \frac{\psi_3^{(t+1)} - \psi_3^{(t)}}{\delta t} - F_4(p_1 + p_2 + p_3 + p_4) - F_2(q_3 - q_1 + q_2 - q_4) - F_6(r_3 - r_1 + r_4 - r_2), \quad (3.220)$$

$$B_4^{(I)} = D_1 \frac{\psi_4^{(t+1)} - \psi_4^{(t)}}{\delta t} - F_8(r_3 - r_1 + r_2 - r_4) - F_7(q_3 - q_1 + q_4 - q_2), \quad (3.221)$$

$$B_5^{(I)} = D_1 \frac{\psi_5^{(t+1)} - \psi_5^{(t)}}{\delta t} - F_9(r_1 + r_2 + r_3 + r_4) - F_7(p_3 - p_1 + p_4 - p_2), \quad (3.222)$$

and

$$B_6^{(I)} = D_1 \frac{\psi_6^{(t+1)} - \psi_6^{(t)}}{\delta t} - F_9(q_1 + q_2 + q_3 + q_4) - F_8(p_3 - p_1 + p_2 - p_4). \quad (3.223)$$

### 3.5.3 The final solution

The stress equations can be calculated on an element by element basis, therefore, for each finite element, the stress components are given by equations (3.137)-



(3.142), while for each infinite element, from equations (3.224)-(3.229),

$$\begin{aligned} \psi_1^{(t+1)} = & \psi_1^{(t)} + \delta t \left( \frac{3(\lambda + 2\mu)I_6^*}{4L_1}(p_1 + p_2 + p_3 + p_4) \right. \\ & \left. + \frac{\lambda}{2\Delta x_2}(q_3 - q_1 + q_2 - q_4) + \frac{\lambda}{2\Delta x_3}(r_3 - r_1 + r_4 - r_2) \right), \end{aligned} \quad (3.224)$$

$$\begin{aligned} \psi_2^{(t+1)} = & \psi_2^{(t)} + \delta t \left( \frac{3\lambda I_6^*}{4L_1}(p_1 + p_2 + p_3 + p_4) \right. \\ & \left. + \frac{\lambda + 2\mu}{2\Delta x_2}(q_3 - q_1 + q_2 - q_4) + \frac{\lambda}{2\Delta x_3}(r_3 - r_1 + r_4 - r_2) \right), \end{aligned} \quad (3.225)$$

$$\begin{aligned} \psi_3^{(t+1)} = & \psi_3^{(t)} + \delta t \left( \frac{3\lambda I_6^*}{4L_1}(p_1 + p_2 + p_3 + p_4) \right. \\ & \left. + \frac{\lambda}{2\Delta x_2}(q_3 - q_1 + q_2 - q_4) + \frac{\lambda + 2\mu}{2\Delta x_3}(r_3 - r_1 + r_4 - r_2) \right), \end{aligned} \quad (3.226)$$

$$\psi_4^{(t+1)} = \psi_4^{(t)} + \delta t \left( \frac{\mu}{2\Delta x_2}(r_3 - r_1 + r_2 - r_4) + \frac{\mu}{2\Delta x_3}(q_3 - q_1 + q_4 - q_2) \right), \quad (3.227)$$

$$\psi_5^{(t+1)} = \psi_5^{(t)} + \delta t \left( \frac{3\mu I_6^*}{4L_1}(r_1 + r_2 + r_3 + r_4) + \frac{\mu}{2\Delta x_3}(p_3 - p_1 + p_4 - p_2) \right), \quad (3.228)$$

and

$$\psi_6^{(t+1)} = \psi_6^{(t)} + \delta t \left( \frac{3\mu I_6^*}{4L_1}(q_1 + q_2 + q_3 + q_4) + \frac{\mu}{2\Delta x_2}(p_3 - p_1 + p_2 - p_4) \right). \quad (3.229)$$

Now for the velocity equations, for each finite element, for example from equation (3.75),

$$A_{1i'}^{(F)} = \frac{\rho\Delta x_1\Delta x_2\Delta x_3}{8}\dot{p}_{i'} + \chi_{i'}^{0,2}\frac{\Delta x_2\Delta x_3}{4}\psi_1 + \chi_{i'}^{1,2}\frac{\Delta x_1\Delta x_3}{4}\psi_6 + \chi_{i'}^{0,4}\frac{\Delta x_1\Delta x_2}{4}\psi_5,$$

which leads to an explicit form (using Euler's method) of

$$\begin{aligned} A_{1i'}^{(F)} = & \frac{\rho\Delta x_1\Delta x_2\Delta x_3}{8} \frac{p_{i'}^{(t+1)} - p_{i'}^{(t)}}{\delta t} \\ & + \chi_{i'}^{0,2}\frac{\Delta x_2\Delta x_3}{4}\psi_1 + \chi_{i'}^{1,2}\frac{\Delta x_1\Delta x_3}{4}\psi_6 + \chi_{i'}^{0,4}\frac{\Delta x_1\Delta x_2}{4}\psi_5, \end{aligned}$$

while for each infinite element, for example from equation (3.215),

$$A_{1i'} = \frac{\rho \Delta x_2 \Delta x_3 L_1 \alpha}{12} \frac{p_{i'}^{(t+1)} - p_{i'}^{(t)}}{\delta t} + \frac{\Delta x_2 \Delta x_3 I_2^* \lambda}{4} \psi_1 + \chi_{i'}^{1,2} \frac{\Delta x_3 L_1}{6} \psi_6 + \chi_{i'}^{0,2} \frac{\Delta x_2 L_1}{6} \psi_5.$$

Now recombining the elements in order to calculate the velocities at a global level gives

$$\begin{aligned} & b_n^{(F)} \frac{\rho \Delta x_1 \Delta x_2 \Delta x_3}{8} \frac{p_n^{(t+1)} - p_n^{(t)}}{\delta t} \\ & + b_n^{(I)} \frac{\rho \Delta x_2 \Delta x_3 L_1}{12} \frac{p_n^{(t+1)} - p_n^{(t)}}{\delta t} \\ & = \sum_{k=1}^{b_n^{(F)}} F^{(F)} + \sum_{l=1}^{b_n^{(I)}} F^{(I)} \end{aligned}$$

where  $b_n^{(F)}$  is the number of finite elements that share global node  $n$  as a vertex,  $b_n^{(I)}$  is the number of infinite elements that share global node  $n$  as a vertex,  $F^{(F)}$  is the combination of stress terms used in  $A_{1i'}^{(F)}$  when global node  $n$  is local node  $i'$  in a finite element, and  $F^{(I)}$  is the combination of stress terms used in  $A_{1i'}^{(I)}$  when global node  $n$  is local node  $i'$  in an infinite element. So

$$\begin{aligned} & \left( b_n^{(F)} \frac{\rho \Delta x_1 \Delta x_2 \Delta x_3}{8} + b_n^{(I)} \frac{\rho \Delta x_2 \Delta x_3 L_1}{12} \right) p_n^{(t+1)} \\ & = \left( b_n^{(F)} \frac{\rho \Delta x_1 \Delta x_2 \Delta x_3}{8} + b_n^{(I)} \frac{\rho \Delta x_2 \Delta x_3 L_1}{12} \right) p_n^{(t)} \\ & + \delta t \left( \sum_{k=1}^{b_n^{(F)}} F^{(F)} + \sum_{l=1}^{b_n^{(I)}} F^{(I)} \right) \end{aligned}$$

and letting

$$W^{(F)} = b_n^{(F)} \frac{\rho \Delta x_1 \Delta x_2 \Delta x_3}{8}, \quad W^{(I)} = b_n^{(I)} \frac{\rho \Delta x_2 \Delta x_3 L_1}{12}, \quad (3.230)$$

then

$$p_n^{(t+1)} = p_n^{(t)} + \frac{\delta t}{W^{(F)} + W^{(I)}} \left( \sum_{k=1}^{b_n^{(F)}} F^{(F)} + \sum_{l=1}^{b_n^{(I)}} F^{(I)} \right), \quad (3.231)$$

and in the same way, for the other components of velocity

$$q_n^{(t+1)} = q_n^{(t)} + \frac{\delta t}{W^{(F)} + W^{(I)}} \left( \sum_{k=1}^{b_n^{(F)}} F^{(F)} + \sum_{l=1}^{b_n^{(I)}} F^{(I)} \right), \quad (3.232)$$

$$r_n^{(t+1)} = r_n^{(t)} + \frac{\delta t}{W^{(F)} + W^{(I)}} \left( \sum_{k=1}^{b_n^{(F)}} F^{(F)} + \sum_{l=1}^{b_n^{(I)}} F^{(I)} \right). \quad (3.233)$$

### 3.6 Implementation

The new combined perfectly matching layer and infinite element formulation for the elastodynamic wave equation was implemented in Fortran for the test problem of a semi-infinite rectangular wave guide. A simple pseudocode is presented here.

```

BEGIN
  Define number of nodes in each direction
  Initialise variables
  Set material properties
  Set infinite element wavespeed parameter given by  $\bar{c}$ 
  if constant stretching then
    set stretching parameters  $\alpha$  and  $\beta$ 
    if  $\alpha$  violates conditions (3.123) or (3.124) then
      STOP
    end if
  else if spatially dependent stretching then

```

```

set stretching parameter  $\bar{\alpha}$ 
if  $I_2^*$  given by equation (3.178) violates conditions (3.214) or (3.213) then
    STOP
end if
end if
Initialise velocities, nodal weightings and stresses at all nodes
Define the mass of a finite element as in equation (3.149)
if constant stretching then
    Define the mass of an infinite element as in equation (3.149)
else if spatially dependent stretching then
    Define the mass of an infinite element as in equation (3.230)
end if
for  $K = 1, \dots, N3 - 1$  do
     $\triangleright$  where  $N3$  is the number of nodes in the  $x_3$  direction
    for  $J = 1, \dots, N2 - 1$  do
         $\triangleright$  where  $N2$  is the number of nodes in the  $x_2$  direction
        for  $I = 1, \dots, N1 - 1$  do
             $\triangleright$  where  $N1$  is the number of nodes in the  $x_1$  direction
            Assign weights to all the nodes of the finite elements using the local
coordinate index as shown in figures 3.2-3.4
        end for
            Assign weights to all the nodes of the infinite elements using the local
coordinate index as shown in figures 3.5 and 3.6
        end for
    end for
for timesteps from 1 to 1400 do

```

Increase the time by  $\delta t$

**for**  $I = 1, \dots, NNOD$  **do**

▷ where  $NNOD$  is the total number of nodes in the waveguide

**if** constant stretching **then**

Update velocities at node  $I$  using equations (3.150)-(3.152)

**else if** spatially dependent stretching **then**

Update velocities at node  $I$  using equations (3.231)-(3.233)

**end if**

**for**  $I = 1, \dots, NNOD$  **do**

Set stresses to zero

**end for**

**end for**

Apply an initial sinusoidal wave in the  $x_1$  direction only for the first 35 timesteps

**for**  $K = 1, \dots, N3 - 1$  **do**

**for**  $J = 1, \dots, N2 - 1$  **do**

**for**  $I = 2, \dots, N1$  **do**

Set elastic constants to be equal throughout the nodes

▷ this allows scope for heterogeneous materials

**end for**

Convert global node numbering to a local node index for the finite elements

**for**  $I = 1, \dots, N1 - 1$  **do**

Calculate stresses on finite elements using equations (3.137)-(3.142)

**end for**

Convert global node numbering to a local node index for the infinite

elements

**if** constant stretching **then**

    Calculate stresses on infinite elements using equations (3.143)-  
(3.147)

**else if** spatially dependent stretching **then**

    Calculate stresses on infinite elements using equations (3.224)-  
(3.228)

**end if**

**end for**

**end for**

    Find a strand in the middle of the waveguide and find the maximum velocity  
in the  $x_1$  direction and the position at which this occurs on the strand

    Find the reflection coefficient at a specified node in the middle of the waveguide and write to a file

**end for**

    Find the runtime and write this to a file

END

## 3.7 Results

Having derived PML+IE formulations with constant stretching and spatially dependent stretching, each case was implemented in an explicit finite element code using Fortran. A comparison was then made between the PML+IE formulation and the FE only implementation (without an infinite boundary in the  $x_1$  direction) using a reflection coefficient measure. The reflection coefficient,  $p_{refl}$ , is defined as the ratio of the reflected wave to the incident wave, measured at a node in the

centre of the waveguide. It is given by

$$p_{refl} = \frac{p_{max}^{(2)}}{p_{max}^{(1)}}, \quad (3.234)$$

where, for a node in the middle of the waveguide at position  $x^* = (a\Delta x_1, b\Delta x_2, b\Delta x_3)$ , then

$$p_{max}^{(1)} = \max_{t \in [t_i - \delta t_n, t_i + \delta t_n]} |p(t)|,$$

$$p_{max}^{(2)} = \max_{t \in [t_r - \delta t_n, t_r + \delta t_n]} |p(t)|,$$

where  $t_i$  is the number of timesteps taken for the incident wave to first reach this node and  $t_r$  is the number of timesteps taken for the reflected wave to return to this node. The  $p_{max}$  values are calculated over a window in time of size  $2\delta t$  centred at time  $t_{i/r}$  to ensure that the arrival time of the maximum amplitude of the wavefront is accurately captured.

The reflection coefficient is used to find values of the stretching function parameters that maximise the reduction in the reflected wave. In the example below a steel waveguide that has  $n_2 = 5$  nodes in width,  $n_2 = 5$  nodes in height and  $n_1 = 201$  nodes in length (see Figure 3.2) is used, where the nodes are equally spaced (that is  $\Delta x_1 = \Delta x_2 = \Delta x_3 = 1 \times 10^{-5}$ m). Each simulation was run for 1400 timesteps where the timestep was given by  $\delta t = 0.6\Delta x_1/c_p$ , and  $a = 99$ ,  $b = 3$ ,  $t_i = 99\Delta x_1/(\delta t c_E)$  and  $t_r = (2(n_1 - 1) - 99)\Delta x_1/(\delta t c_E)$  where  $c_E = \sqrt{E/\rho}$ , with E denoting Young's modulus.

### 3.7.1 Constant Stretching

In the case of constant stretching in the PML function, there are two parameters to optimise, namely  $\alpha$  and  $\beta$  from equation (3.6). Figure 3.8 shows the first velocity component ( $p$ ) along a horizontal line in the centre of the waveguide at a fixed point in time. This time is chosen as the point immediately after reflection from the end of the waveguide for both the FE only formulation and the PML+IE formulation with constant stretching with  $\alpha = 1.0001$  and  $\beta = 10$ . It can be seen that the reflected wave has a greater amplitude for the FE only case (around 1) than for the PML+IE case (close to 0.55), demonstrating that the PML+IE formulation is successful in reducing the reflection from the boundary. The oscillations apparent in this figure are artefacts of the coarseness of the mesh used.

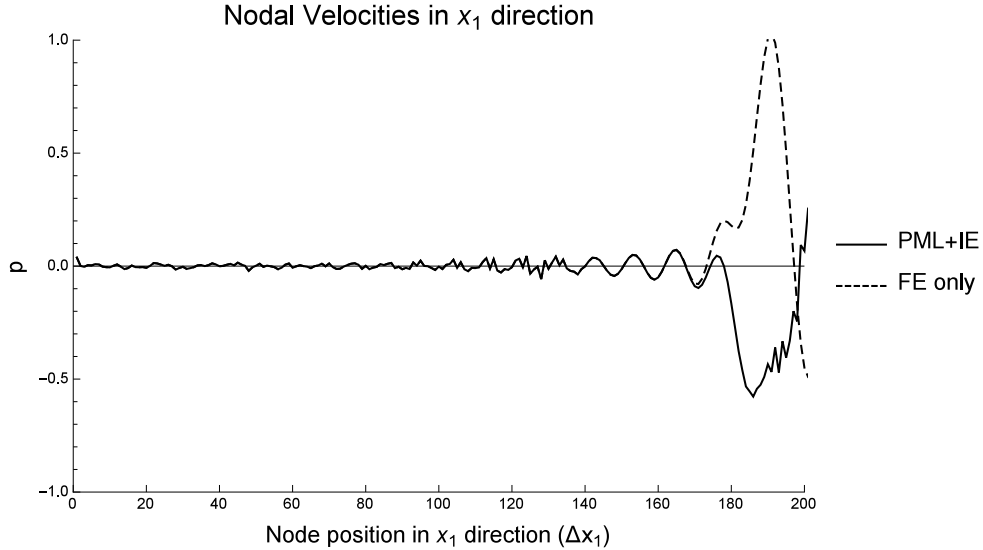


Figure 3.8: Plot of the amplitude of  $p$ , the velocity in the  $x_1$  direction at a fixed point in time, for a horizontal line of nodes in the middle of a  $n_1 = 201$  node long waveguide (with  $n_2 = n_3 = 5$ ) and with the parameters in equation (3.6) given by  $\alpha = 1.0001$  and  $\beta = 10$ . The plot shows the time immediately after the wave has reached the end of the waveguide and is reflected back into it.

The effect of the stretching function parameter  $\alpha$  is assessed in Figure 3.9. Since  $\alpha$  appears in the infinite element weighting  $W^{(l)}$  in equation (3.149), it is assumed





Figure 3.9: The effect of the stretching function parameter  $\alpha$  in equation (3.6) on the reflection coefficient calculated via equation (3.234) for both the FE only formulation (dashed line) and the PML+IE formulation (full line) with constant stretching for a steel waveguide,  $n_1 = 201$  nodes in length, with the stretching function parameter  $\beta = 10$ .

that it should be of the order  $\Delta x_1/L_1$  so that  $W^{(I)}$  is similar to  $W^{(F)}$ . However, from the condition in equation (3.124) and given that the material parameters of the test waveguide are those of steel,  $\alpha > 1$  must hold. Therefore small values close to unity are tested and Figure 3.9 shows that the reflection coefficient increases as  $\alpha$  increases so the best choice for the stretching function parameter  $\alpha$  is given by a value close to 1 and so  $\alpha = 1.0001$  is chosen.

The effect of the other stretching function parameter  $\beta$  is assessed in Figure 3.10. Since  $\beta$  appears in the velocity update in equations (3.150)-(3.152), it is assumed that the coefficient of  $p_n^{(t)}$ ,  $q_n^{(t)}$ , and  $r_n^{(t)}$ , should be between 0 and 1. From Figure 3.10, it is clear that smaller values of  $\beta$  produce the lowest reflection coefficients and so  $\beta = 10$  is chosen.

Taking the stretching parameters to be  $\alpha = 1.0001$  and  $\beta = 10$ , Figure 3.11 shows that for both the FE only formulation and the PML+IE formulation, the

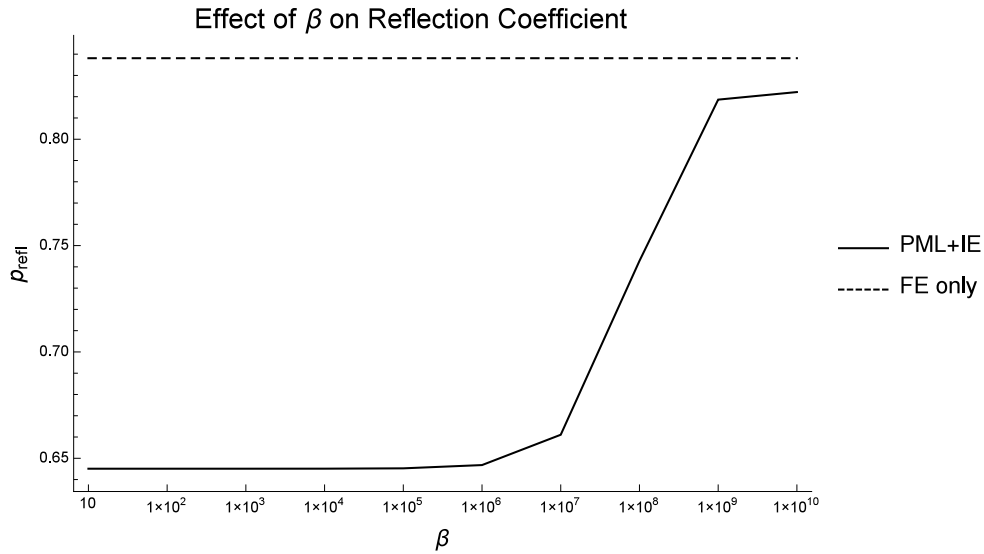


Figure 3.10: The effect of the stretching function parameter  $\beta$  (from equation (3.6)) on the reflection coefficient ( $p_{refl}$  given by equation (3.234)) for both the FE only formulation and the PML+IE formulation with constant stretching for a steel waveguide,  $n_1 = 201$  nodes in length, with the stretching function parameter  $\alpha = 1.0001$ .

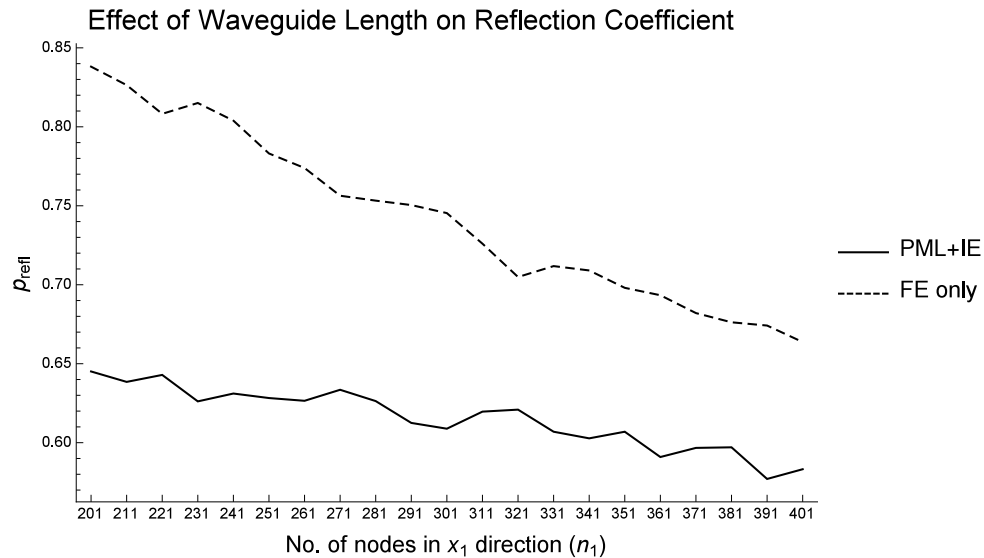


Figure 3.11: The effect of the length of the waveguide on the reflection coefficient ( $p_{refl}$  given by equation (3.234)) for both the FE only implementation and the PML+IE implementation with constant stretching for a steel waveguide with the stretching function parameters in equation (3.6) given by  $\alpha = 1.0001$  and  $\beta = 10$ .

greater the length of the waveguide, the smaller the reflection coefficient as is expected. Figure 3.12 shows that the time taken to run the simulations increases

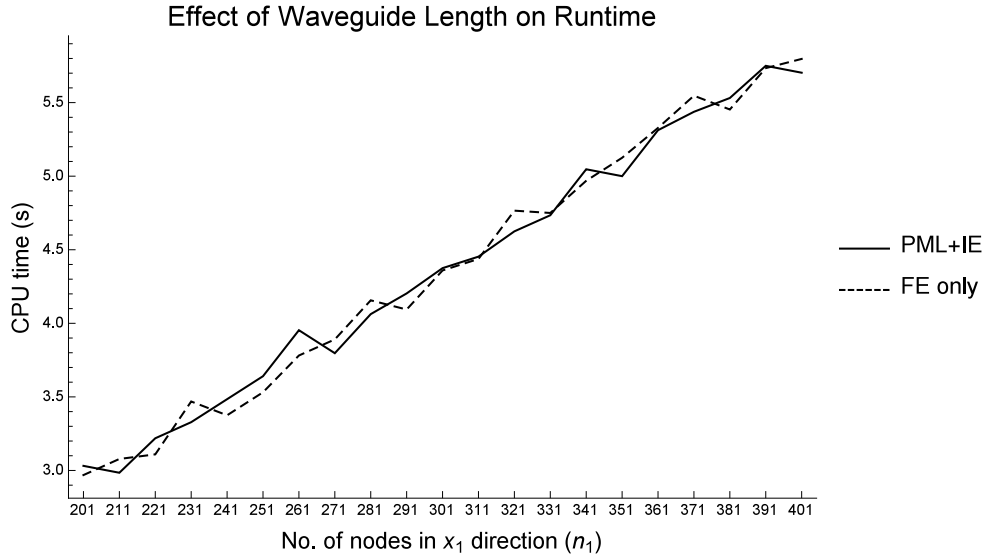


Figure 3.12: The effect of the length of the waveguide on the runtime for both the FE only implementation and the PML+IE implementation with constant stretching for a steel waveguide with the stretching function parameters in equation (3.6) given by  $\alpha = 1.0001$  and  $\beta = 10$ .

with the length of the waveguide, again as expected, but importantly showing that there is little to no difference in runtime between the FE only formulation and the PML+IE formulation. It also shows that the runtime scales linearly with the length of the waveguide as expected.

Looking at Figures 3.11 and 3.12 together, it can be seen that the PML+IE formulation can produce a reflection coefficient equal to that of the FE only formulation by using less than half the number of nodes (memory) and taking around the half the time to run the simulation.

### 3.7.2 Spatially Dependent Stretching

In the case of nonconstant stretching in the PML stretching function, in order to proceed with the formulation, a choice was made for the form of the stretching

function in equations (3.173) and (3.174), with equations (3.175) and (3.176), and with  $m = 1$  and  $n = 1/4$ . Therefore there is only one degree of freedom in the parameters to explore, namely  $\bar{\alpha}$ . Figure 3.13 shows the first velocity component ( $p$ ) along a horizontal line in the centre of the waveguide at a fixed point in time. This time is chosen as the point immediately after reflection from the end of the waveguide for both the FE only formulation and the PML+IE formulation with spatially dependent stretching with  $\bar{\alpha} = 2$ . It can be seen that the reflected wave has a greater amplitude for the FE only case (around 1) than for the PML+IE case (close to 0.55), demonstrating that the PML+IE formulation is successful in reducing the reflection from the boundary.

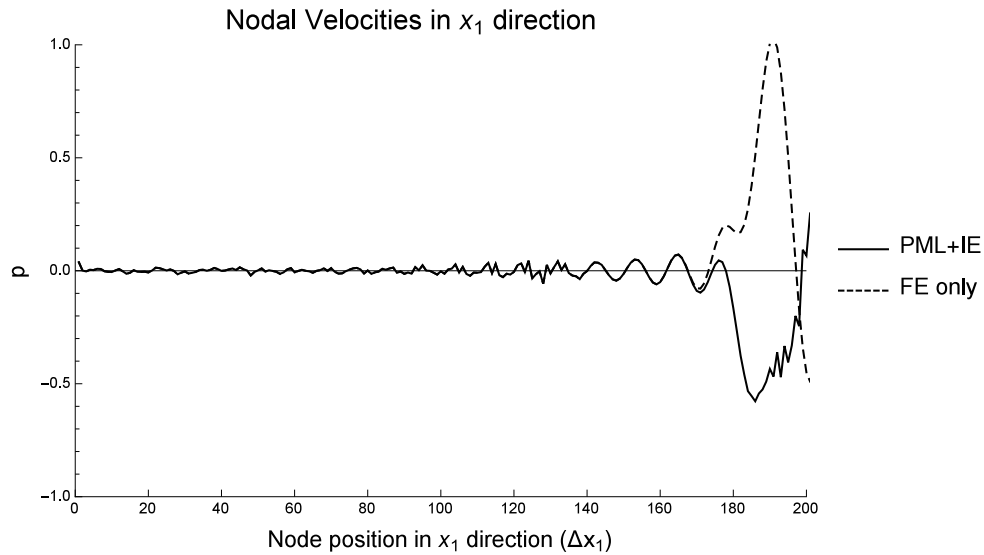


Figure 3.13: Plot of the amplitude of  $p$ , the velocity in the  $x_1$  direction at a fixed point in time, for a horizontal line of nodes in the middle of a  $n_1 = 201$  node long waveguide (with  $n_2 = n_3 = 5$ ) with  $\bar{\alpha} = 2$ ,  $m = 1$  and  $n = 1/4$ . The plot shows the time immediately after the wave has reached the end of the waveguide and is reflected back into it.

The effect of the stretching function parameter  $\bar{\alpha}$  on the reflection coefficient is assessed in Figures 3.14 and 3.15. Since  $\bar{\alpha}$  appears in the expressions given by equations (3.177) and (3.178) it can be seen immediately that there will be a

singularity where  $\bar{\alpha} = 1$ . Away from this value, these expressions are small and have little impact on the system. Therefore values close to this singularity are explored for  $\bar{\alpha}$ , with values approaching one from the negative side ( $1^-$ ) shown in Figure 3.14 and values approaching one from the positive side ( $1^+$ ) shown in Figure 3.15. The values shown examine the behaviour of the reflection coefficient when  $\bar{\alpha}$  is as close to unity as possible without breaching the conditions given by equations (3.214) and (3.213). It can be seen from both figures that values close to one in fact produce larger reflection coefficients (for the case with  $m = 1$  and  $n = 1/4$ ) so  $\bar{\alpha} = 2$  is chosen.

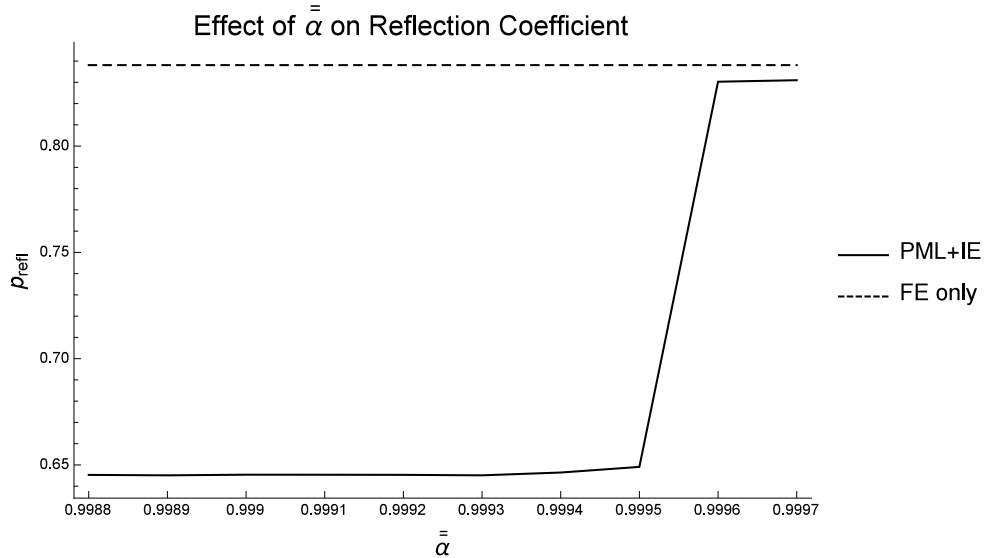


Figure 3.14: The effect of the stretching function parameter  $\bar{\alpha}$ , given in equation (3.175), on the reflection coefficient for both the FE only formulation and the PML+IE formulation with spatially dependent stretching for a steel waveguide of  $n_1 = 201$  nodes in length, with  $m = 1$  and  $n = 1/4$  in equations (3.175) and (3.176).

With this value for  $\bar{\alpha}$ , Figure 3.16 shows that for both the FE only formulation and the PML+IE formulation, the greater the length of the waveguide, the smaller the reflection coefficient as is expected. Figure 3.17 shows that the time taken to run the simulations increases with the length of the waveguide, again as expected,

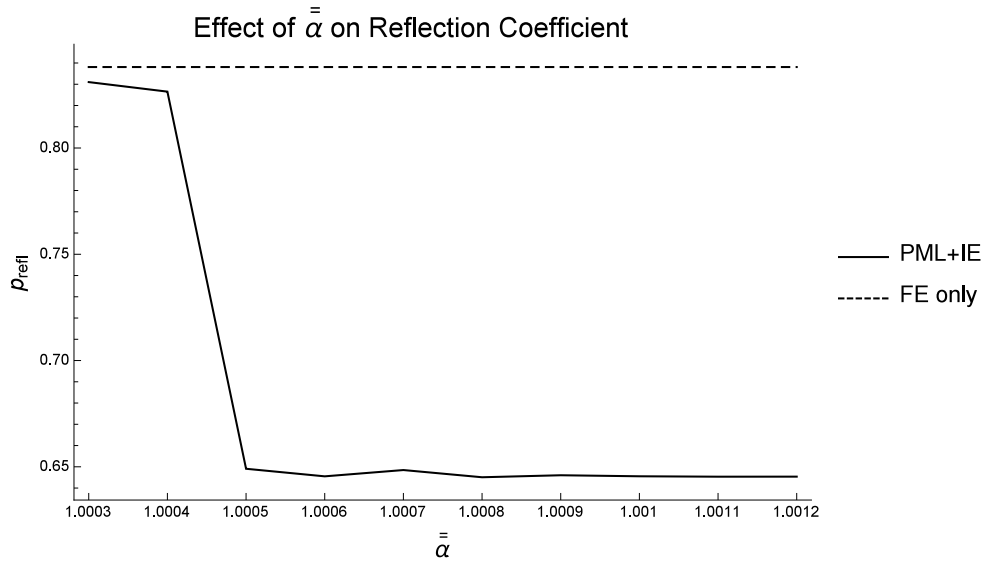


Figure 3.15: The effect of the stretching function parameter  $\bar{\alpha}$ , given in equation (3.175), on the reflection coefficient for both the FE only formulation and the PML+IE formulation with spatially dependent stretching for a steel waveguide of 201 nodes in length, with  $m = 1$  and  $n = 1/4$ .

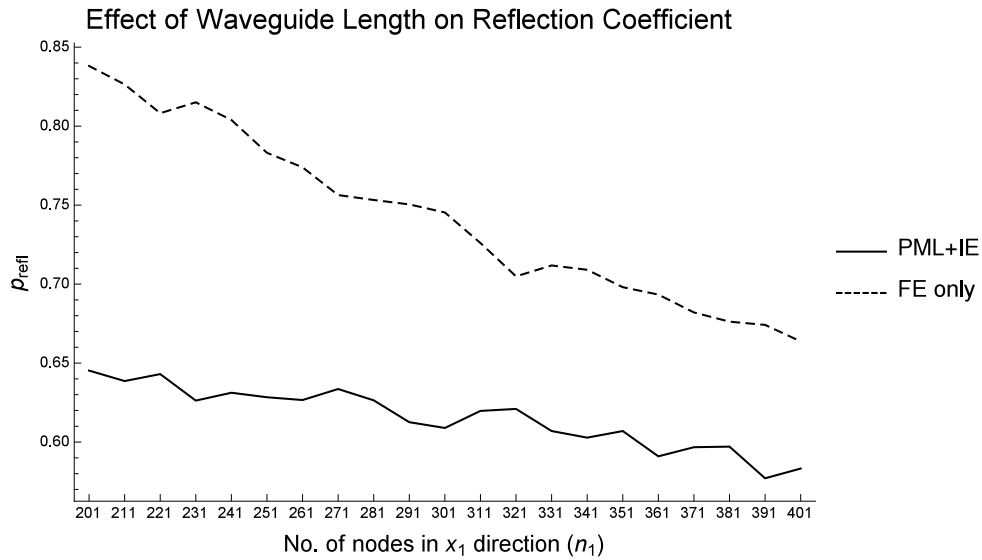


Figure 3.16: The effect of the length of the waveguide on the reflection coefficient for both the FE only implementation and the PML+IE implementation with spatially dependent stretching for a steel waveguide with the stretching function parameter in equation (3.175) given by  $\bar{\alpha} = 2$ , with  $m = 1$  and  $n = 1/4$ .

while showing there is little to no difference in runtime between the FE only formulation and the PML+IE formulation.

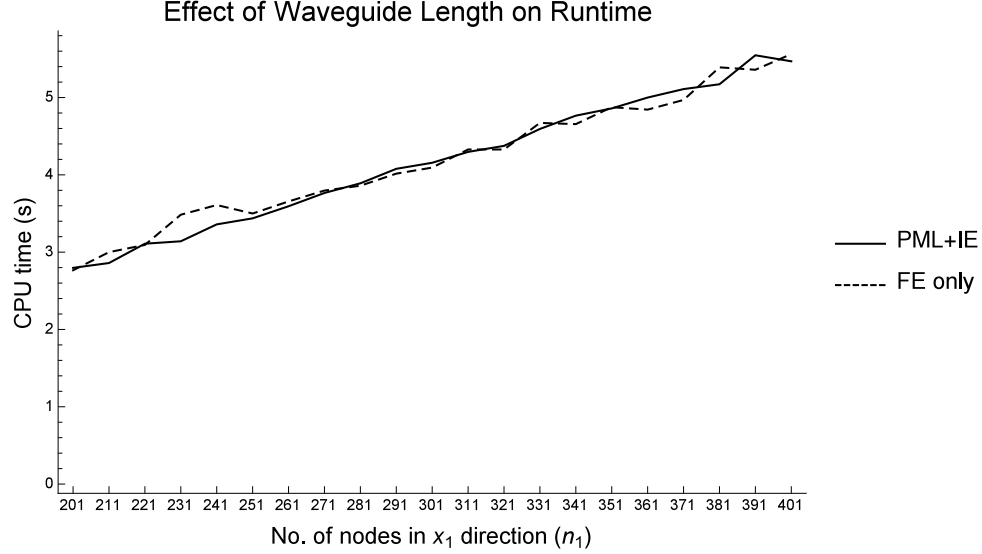


Figure 3.17: The effect of the length of the waveguide on the runtime for both the FE only implementation and the PML+IE implementation with spatially dependent stretching for a steel waveguide with the stretching function parameter in equation (3.175) given by  $\bar{\alpha} = 2$ , with  $m = 1$  and  $n = 1/4$ .

Looking at Figures 3.16 and 3.17 together, it can be seen that the PML+IE formulation can produce a reflection coefficient equal to that of the FE only formulation by using less than half the number of nodes and taking around the half the time to run the simulation.

In both the constant stretching case and the spatially dependent stretching case, the reflection coefficient could not be improved beyond  $p_{refl} = 0.645$  for the examples shown. In terms of CPU time, both cases exhibited very similar results, with a runtime of around 2.8s for a waveguide with  $n_1 = 201$  nodes, increasing linearly to around 6.25s in the constant stretching case and 5.75s in the spatially dependent stretching case for a waveguide with  $n_1 = 401$  nodes.

## 3.8 Conclusion

An Infinite Element has been successfully combined with a Perfectly Matching Layer to produce a new boundary condition for unbounded wave problems in the time domain. Through the example problem of a semi-infinite elastic waveguide that is locally isotropic, a formulation has been devised for an explicit finite element approach using the new PML+IE combination. Two cases have been considered: the first where the PML stretching function has constant coefficients, and the second where a spatial dependency is retained. Both cases have been implemented in an explicit FE code and a comparison made to the FE only approach. By using a reflection coefficient as a measure of accuracy, it has been found that in both the case with constant stretching and the case with spatially dependent stretching, the new combined PML+IE is successful in improving accuracy, reducing the reflection coefficient by up to 20%. It has been shown that using finite elements only would take double the memory and twice the CPU time to run to achieve the same reflection coefficient as this new PML+IE formulation.

While it would be useful to make comparisons between the PML+IE formulation and IE only or PML only formulations, it is not possible to simply switch off one of these components in this formulation. In the case of the infinite element, this is embedded in the formulation through the form of the test function  $w_i$  in equation (3.38), permeating the entire derivation. In the case of the PML, setting the parameters  $\alpha = 1$ ,  $\beta = 0$  in equation (3.6) would eliminate stretching, however this would cause a singularity where  $\alpha$  appears in a denominator, as in equations (3.143)-(3.148).



# Chapter 4

## Conclusions

### 4.1 Introduction

Infinite domains arise in a variety of real world situations, but when modelling these domains, numerical methods are restricted by memory and processor limitations. A number of boundary conditions exist to handle these unbounded domains, but each has its own strengths and weaknesses. The focus of this thesis has been to develop a new perfectly matching layer and infinite element combination for use in unbounded wave problems, for both the frequency domain and the time domain, in order to improve existing finite element techniques for modelling ultrasound devices and systems. The combination of a coordinate stretching transformation for the PML, and infinite element basis functions in the variational formulation achieved this new method for the acoustic wave equation and the elastic wave equation. A framework for assessing the impact of the stretching function choice was also presented through comparison with the exact solution in the frequency domain case, and with a reflection coefficient in the time domain case.

For the acoustic wave equation in the frequency domain, the problem of a

vibrating sphere was considered. The existence of an exact solution provided a measure with which to assess the accuracy of the new PML+IE method. The acoustic response was used to derive the inertia and resistance which were then used as a measure of accuracy. A variational formulation was used to introduce the infinite elements through test functions, while a complex coordinate stretching enabled the perfectly matching layer to be introduced in this derivation for the first time. Three types of infinite element were then considered in turn: the unconjugated Burnett element, the conjugated Burnett element and the Astley-Leis element. The infinite element only formulation was then shown to be a particular case of the PML+IE formulation, achieved by choosing  $z = r$  for the stretching function. The difference between the PML+IE formulation and the exact solution was introduced as an error measure for both the inertia and resistance, and integrated over a range of wavelengths for a number of acoustic modes. A set of stretching function parameters was then assessed to demonstrate that greater accuracy can be achieved using the new PML+IE method than by using the IE only method.

In the case of the elastodynamic wave equation, a three dimensional, heterogeneous volume was constructed with a new PML+IE formulation at its boundary. The special case of a semi-infinite, locally isotropic, homogeneous waveguide was then examined to allow an empirical comparison of the proposed method to the infinite element only approach. To do so, Fourier transforms of the elastodynamic wave equation were taken in time to introduce the complex coordinate stretching function. The variational formulation was then followed as before, introducing the infinite elements through test functions in the exterior domain, while the interior was modelled by traditional hexahedral finite elements. The case with a constant PML stretching function in all three directions was considered first, then the case

with stretching in only one direction with a spatial dependency. Mass lumping and diagonalisation were then necessary to allow an explicit scheme to be implemented. A reflection coefficient was introduced to compare the new PML+IE method with the FE only implementation and to find parameter values for the PML stretching function that could maximise the reduction in the reflected wave.

## 4.2 Results

The use of a combined perfectly matching layer and infinite element formulation for the acoustic wave equation was assessed via the exact solution of the acoustic response of a breathing sphere, in particular the inertia and resistance in Chapter 2. By introducing the difference between the exact solution and the PML+IE formulation as an error measure, the proposed combination was shown to have an improvement upon the infinite element only formulation over a range of acoustic modes for large wavelengths. In section 2.5, the error was plotted as a function of the perfectly matching layer stretching function parameters for a range of values, in turn, for the unconjugated Burnett element, the conjugated Burnett element and the Astley-Leis element. For all three types of infinite element, a range of values for the stretching function parameters was found to exist. This demonstrated that the proposed new combined method could result in an improvement in accuracy. Solution plots for the exact solution, the infinite element only solution and the PML+IE solution were also generated for each type of infinite element using the parameter values obtained, with plots produced for a number of acoustic modes. From the values found for the overall error function  $Q(\alpha^*, \beta^*)$  given by equation (2.45), it is possible to quantify the improvement in accuracy by noting that  $Q(\alpha^*, \beta^*) + E_{\mu, \nu}$  is the difference between the PML+IE solution and the exact

solution, while  $E_{\mu,\nu}$  is the difference between the IE only solution and the exact solution. Therefore  $(Q(\alpha^*, \beta^*) + E_{\mu,\nu})/E_{\mu,\nu}$  gives a measure of the improvement using each type of infinite element in the PML+IE formulations. Using this measure, the unconjugated Burnett element results in an improvement in accuracy of around 90%, the conjugated Burnett element results in an improved accuracy of around 91%, and the Astley-Leis element results in an increase in accuracy of around 88%.

In Chapter 3, this new PML+IE formulation was shown to be possible for the time dependent elastic wave equation. A case with constant stretching in the perfectly matching layer and another with spatially dependent stretching were considered. Both cases were implemented in an explicit finite element code and compared to the FE only approach using a reflection coefficient. In the case with constant stretching, there were two parameters to optimise in the perfectly matching layer coordinate stretching function. Plots were created of the velocity in the  $x_1$  direction (the infinite direction of the waveguide) at a fixed point in time for a horizontal line of nodes in the centre of the waveguide. The plots showed the timestep immediately after the wave reached the end of the waveguide and was reflected back into it. The effect of the stretching parameters on the reflection coefficient were then plotted to find optimal parameters. The effect of the length of the waveguide on the reflection coefficient and on the running time of the simulation were also plotted. The same process was followed for the case with spatially dependent stretching in the  $x_1$  direction, but with only one parameter to be optimised. In both cases, the new formulation was found to be successful in improving accuracy, reducing the reflection by up to 20%. Using the PML+IE formulations had very little difference in runtime to using FE only, meaning implementation would not encumber processing. It was also found that

a reflection coefficient equal that of the FE only case could be found with the PML+IE formulations, using less than half the number of nodes and taking around half the time to run.

### 4.3 Future Work

While the possibility of combining perfectly matching layers and infinite elements was demonstrated, the benefits of this method were unable to be fully explored. There are a number of avenues of exploration available to advance this work further, including:

1. Optimisation of the form of the perfectly matching layer stretching function. The form taken in the frequency domain problem was informed by the outcome of the time domain problem, but this is not necessarily the best choice. Further exploration of the coordinate transformation could lead to significant improvement in performance, both in terms of accuracy and in terms of efficiency.
2. Comparison of PML+IE and other boundary methods within an explicit time domain implementation. As there was no simple method of implementing the PML only or IE only formulations in the time domain, the reflection coefficient measure was used to give an indication of accuracy, however a comparison to current techniques would help to benchmark any improvement that may be gained using the new PML+IE formulation.
3. Other boundary conditions. In the elastodynamic case, all boundaries except the infinite facing surface had stress-free conditions imposed. Further studies could investigate the effects of different boundary conditions in the  $x_2$  and  $x_3$  directions.

4. Exploration of the method in other materials. The present study dealt only with locally isotropic homogeneous materials. It would be interesting to study the application of the PML+IE formulation in materials that are locally anisotropic, or again in materials that are heterogeneous, with changing material constants.

## 4.4 Concluding Remarks

This thesis has presented a new combined perfectly matching layer and infinite element formulation for the first time. It has been shown to be possible in both the frequency and time domains and has been implemented in an explicit finite element code. It is hoped that further work can be done to optimise the choice of PML stretching function and to show an improvement over existing boundary methods.

# List of Figures

2.1	A schematic showing the domain $\Omega_e$ where the Perfectly Matching Layer and Infinite Element formulation is applied. . . . .	12
2.2	Plots of the error $Q(\alpha, \beta)$ given by equation (2.45) for the PML+IE formulation using the unconjugated Burnett element with varying $\alpha$ and $\beta = 0.01$ . A negative value for $Q(\alpha, \beta)$ indicates that the PML+IE formulation has more agreement with the exact solution than does the IE only formulation. . . . .	42
2.3	Plots of the error $Q(\alpha, \beta)$ given by equation (2.45) for the PML+IE formulation using the unconjugated Burnett element with varying $\beta$ and $\alpha = -0.07$ . A negative value for $Q(\alpha, \beta)$ indicates that the PML+IE formulation has more agreement with the exact solution than does the IE only formulation. . . . .	43
2.4	Plots of the specific inertia for the exact solution, $S_\mu^{exact}$ given by equation (2.12) (solid line), and the numerical values of the specific inertia for the infinite element only formulation, $S_\mu^{IE}$ (dashed), and for the PML+IE formulation using the unconjugated Burnett element, $S_\mu^{PML+IE}$ (dotted) given by equation (2.37) with $(\alpha, \beta) = (-0.07, 0.01)$ , where $kR$ is plotted on a logarithmic scale. . . . .	44

2.5 Plots of the specific resistance for the exact solution,  $R_{\mu}^{exact}$  given by equation (2.7) (solid line), and the numerical values of the specific resistance for the infinite element only formulation,  $R_{\mu}^{IE}$  (dashed), and for the PML+IE formulation using the unconjugated Burnett element,  $R_{\mu}^{PML+IE}$  (dotted) given by equation (2.38) with  $(\alpha, \beta) = (-0.07, 0.01)$ , where  $kR$  is plotted on a logarithmic scale. . . . . 45

2.6 Plots of the error  $Q(\alpha, \beta)$  given by equation (2.45) for the PML+IE formulation using the conjugated Burnett element with varying  $\alpha$  and  $\beta = 0.01$ . A negative value for  $Q(\alpha, \beta)$  indicates that the PML+IE formulation has more agreement with the exact solution than does the IE only formulation. . . . . 47

2.7 Plots of the error  $Q(\alpha, \beta)$  given by equation (2.45) for the PML+IE formulation using the conjugated Burnett element with varying  $\beta$  and  $\alpha = 0.07$ . A negative value for  $Q(\alpha, \beta)$  indicates that the PML+IE formulation has more agreement with the exact solution than does the IE only formulation. . . . . 48

2.8 Plots of the specific inertia for the exact solution,  $S_{\mu}^{exact}$  (solid line), given by equation (2.12), and the numerical values for the specific inertia for the infinite element only formulation,  $S_{\mu}^{IE}$  (dashed), and for the PML+IE formulation using the conjugated Burnett element,  $S_{\mu}^{PML+IE}$  (dotted), given by equation (2.37), with  $(\alpha, \beta) = (0.07, 0.01)$ , where  $kR$  is plotted on a logarithmic scale. . . . . 49



2.9	Plots of the specific resistance for the exact solution, $R_\mu^{exact}$ (solid line), given by equation (2.7), and the numerical values of the specific resistance for the infinite element only formulation, $R_\mu^{IE}$ (dashed), and for the PML+IE formulation using the conjugated Burnett element, $R_\mu^{PML+IE}$ (dotted), given by equation (2.38), with $(\alpha, \beta) = (0.07, 0.01)$ , where $kR$ is plotted on a logarithmic scale. . . . .	50
2.10	Plots of the error $Q(\alpha, \beta)$ given by equation (2.45), for the PML+IE formulation using the Astley-Leis element with varying $\alpha$ and $\beta = 0.01$ . . . . .	51
2.11	Plots of the error $Q(\alpha, \beta)$ given by equation (2.45), for the PML+IE formulation using the Astley-Leis element with varying $\beta$ and $\alpha = -0.02$ . . . . .	52
2.12	Plots of the specific inertia for the exact solution, $S_\mu^{exact}$ (solid line), given by equation (2.12), and the numerical values of the specific inertia for the infinite element only formulation, $S_\mu^{IE}$ (dashed), and for the PML+IE formulation using the Astley-Leis element, $S_\mu^{PML+IE}$ (dotted), given by equation (2.37), with $(\alpha, \beta) = (-0.02, 0.01)$ , where $kR$ is plotted on a logarithmic scale. . . . .	53
2.13	Plots of the specific resistance for the exact solution, $R_\mu^{exact}$ (solid line), given by equation (2.7), and the numerical values of the specific resistance for the infinite element only formulation, $R_\mu^{IE}$ (dashed), and for the PML+IE formulation using the Astley-Leis element, $R_\mu^{PML+IE}$ (dotted), given by equation (2.38), with $(\alpha, \beta) = (-0.02, 0.01)$ , where $kR$ is plotted on a logarithmic scale. . . . .	55

3.1	The geometry of the semi-infinite rectangular waveguide. The interior domain $\Omega_F$ is of fixed length $L_1$ and is meshed using standard finite elements. The exterior domain $\Omega_I$ is the semi-infinite part of the domain and uses the PML/IE combination. The face $\Gamma_X$ at $x_1 = X_1$ is a notional face that will later be allowed to tend to infinity.	59
3.2	The global node numbering scheme (in $\Omega_F$ ) is illustrated where $n_1$ , $n_2$ , and $n_3$ , are the number of nodes in the $x_1$ , $x_2$ , and $x_3$ directions respectively. The numbering sequence begins at the bottom front corner of the waveguide (position 1 above) where $(x_1, x_2, x_3) = (0, 0, 0)$ and traverses the $x_1$ direction first, the $x_2$ direction second, and the $x_3$ direction third.	68
3.3	The global node numbers for a finite element $e$ (in $\Omega_F$ ) are shown, where $k$ , $l$ , and $m$ are indices rather than coordinates, and where $n_1$ , $n_2$ , and $n_3$ , again denote the number of nodes in the $x_1$ , $x_2$ , and $x_3$ directions respectively.	69
3.4	The mapping of the finite elements (in $\Omega_F$ ) in global coordinates $(x_1, x_2, x_3)$ to local coordinates $(\xi, \eta, \zeta)$ with node numbering indicated as shown. The local node numbering $i' = 1, \dots, 8$ , is used in the figure on the left.	69
3.5	The global node numbers for an infinite element $e$ (in $\Omega_I$ ) are shown, where $l$ and $m$ are indices rather than coordinates, and where $n_1$ , $n_2$ , and $n_3$ , again denote the number of nodes in the $x_1$ , $x_2$ , and $x_3$ directions respectively.	70

3.6	The mapping of the infinite elements (in $\Omega_I$ ) in global coordinates $(x_2, x_3)$ to local coordinates $(\eta, \zeta)$ with node numbering indicated as shown. The local node numbering $i' = 1, \dots, 4$ , is used in the figure on the left and the $x_1$ direction (the infinite element direction) points out of the plane of the page. . . . .	70
3.7	Local coordinate $\xi$ is plotted as a function of global coordinate $x_1$ . The other local coordinates $\eta(x_2)$ and $\zeta(x_3)$ follow similarly. . . . .	71
3.8	Plot of the amplitude of $p$ , the velocity in the $x_1$ direction at a fixed point in time, for a horizontal line of nodes in the middle of a $n_1 = 201$ node long waveguide (with $n_2 = n_3 = 5$ ) and with the parameters in equation (3.6) given by $\alpha = 1.0001$ and $\beta = 10$ . The plot shows the time immediately after the wave has reached the end of the waveguide and is reflected back into it. . . . .	138
3.9	The effect of the stretching function parameter $\alpha$ in equation (3.6) on the reflection coefficient calculated via equation (3.234) for both the FE only formulation (dashed line) and the PML+IE formulation (full line) with constant stretching for a steel waveguide, $n_1 = 201$ nodes in length, with the stretching function parameter $\beta = 10$ . . . . .	139
3.10	The effect of the stretching function parameter $\beta$ (from equation (3.6)) on the reflection coefficient ( $p_{refl}$ given by equation (3.234)) for both the FE only formulation and the PML+IE formulation with constant stretching for a steel waveguide, $n_1 = 201$ nodes in length, with the stretching function parameter $\alpha = 1.0001$ . . . . .	140

3.11	The effect of the length of the waveguide on the reflection coefficient ( $p_{refl}$ given by equation (3.234)) for both the FE only implementation and the PML+IE implementation with constant stretching for a steel waveguide with the stretching function parameters in equation (3.6) given by $\alpha = 1.0001$ and $\beta = 10$ . . . . .	140
3.12	The effect of the length of the waveguide on the runtime for both the FE only implementation and the PML+IE implementation with constant stretching for a steel waveguide with the stretching function parameters in equation (3.6) given by $\alpha = 1.0001$ and $\beta = 10$ . . . . .	141
3.13	Plot of the amplitude of $p$ , the velocity in the $x_1$ direction at a fixed point in time, for a horizontal line of nodes in the middle of a $n_1 = 201$ node long waveguide (with $n_2 = n_3 = 5$ ) with $\bar{\alpha} = 2$ , $m = 1$ and $n = 1/4$ . The plot shows the time immediately after the wave has reached the end of the waveguide and is reflected back into it. . . . .	142
3.14	The effect of the stretching function parameter $\bar{\alpha}$ , given in equation (3.175), on the reflection coefficient for both the FE only formulation and the PML+IE formulation with spatially dependent stretching for a steel waveguide of $n_1 = 201$ nodes in length, with $m = 1$ and $n = 1/4$ in equations (3.175) and (3.176). . . . .	143
3.15	The effect of the stretching function parameter $\bar{\alpha}$ , given in equation (3.175), on the reflection coefficient for both the FE only formulation and the PML+IE formulation with spatially dependent stretching for a steel waveguide of 201 nodes in length, with $m = 1$ and $n = 1/4$ . . . . .	144

3.16 The effect of the length of the waveguide on the reflection coefficient for both the FE only implementation and the PML+IE implementation with spatially dependent stretching for a steel waveguide with the stretching function parameter in equation (3.175) given by  $\bar{\alpha} = 2$ , with  $m = 1$  and  $n = 1/4$ . . . . . 144

3.17 The effect of the length of the waveguide on the runtime for both the FE only implementation and the PML+IE implementation with spatially dependent stretching for a steel waveguide with the stretching function parameter in equation (3.175) given by  $\bar{\alpha} = 2$ , with  $m = 1$  and  $n = 1/4$ . . . . . 145

# Appendix A

## The stiffness tensor

Given that

$$C = \begin{bmatrix} C_{1111} & C_{1122} & C_{1133} & C_{1123} & C_{1131} & C_{1112} \\ C_{2211} & C_{2222} & C_{2233} & C_{2223} & C_{2231} & C_{2212} \\ C_{3311} & C_{3322} & C_{3333} & C_{3323} & C_{3331} & C_{3312} \\ C_{2311} & C_{2322} & C_{2333} & C_{2323} & C_{2331} & C_{2312} \\ C_{3111} & C_{3122} & C_{3133} & C_{3123} & C_{3131} & C_{3112} \\ C_{1211} & C_{1222} & C_{1233} & C_{1223} & C_{1231} & C_{1212} \end{bmatrix} = \begin{bmatrix} C_{11} & C_{12} & C_{13} & C_{14} & C_{15} & C_{16} \\ C_{21} & C_{22} & C_{23} & C_{24} & C_{25} & C_{26} \\ C_{31} & C_{32} & C_{33} & C_{34} & C_{35} & C_{36} \\ C_{41} & C_{42} & C_{43} & C_{44} & C_{45} & C_{46} \\ C_{51} & C_{52} & C_{53} & C_{54} & C_{55} & C_{56} \\ C_{61} & C_{62} & C_{63} & C_{64} & C_{65} & C_{66} \end{bmatrix},$$

and for an isotropic material, the only nonzero entries are given by

$$C_{11} = C_{22} = C_{33} = \lambda + 2\mu,$$

$$C_{12} = C_{13} = C_{23} = C_{21} = C_{31} = C_{32} = \lambda,$$

$$C_{44} = C_{55} = C_{66} = \mu,$$

then, with  $\hat{\mathbf{v}} = (p, q, r)$ , for  $i = 1$

$$\begin{aligned}
\frac{C_{ijkl}}{s_j s_l} \hat{v}_k &= \frac{C_{1111}}{s_1 s_1} \hat{p} + \frac{C_{1122}}{s_1 s_2} \hat{q} + \frac{C_{1133}}{s_1 s_3} \hat{r} + \frac{C_{1212}}{s_2 s_2} \hat{p} + \frac{C_{1221}}{s_2 s_1} \hat{q} + \frac{C_{1313}}{s_3 s_3} \hat{p} + \frac{C_{1331}}{s_3 s_1} \hat{r} \\
&= \frac{C_{11}}{s_1^2} \hat{p} + \frac{C_{12}}{s_1 s_2} \hat{q} + \frac{C_{13}}{s_1 s_3} \hat{r} + \frac{C_{66}}{s_2^2} \hat{p} + \frac{C_{66}}{s_2 s_1} \hat{q} + \frac{C_{55}}{s_3^2} \hat{p} + \frac{C_{55}}{s_3 s_1} \hat{r} \\
&= \frac{\lambda + 2\mu}{s_1^2} \hat{p} + \frac{\lambda}{s_1 s_2} \hat{q} + \frac{\lambda}{s_1 s_3} \hat{r} + \frac{\mu}{s_2^2} \hat{p} + \frac{\mu}{s_2 s_1} \hat{q} + \frac{\mu}{s_3^2} \hat{p} + \frac{\mu}{s_3 s_1} \hat{r},
\end{aligned}$$

for  $i = 2$

$$\begin{aligned}
\frac{C_{ijkl}}{s_j s_l} \hat{v}_k &= \frac{C_{2112}}{s_1 s_2} \hat{p} + \frac{C_{2121}}{s_1 s_1} \hat{q} + \frac{C_{2211}}{s_2 s_1} \hat{p} + \frac{C_{2222}}{s_2 s_2} \hat{q} + \frac{C_{2233}}{s_2 s_3} \hat{r} + \frac{C_{2323}}{s_3 s_3} \hat{q} + \frac{C_{2332}}{s_3 s_2} \hat{r} \\
&= \frac{C_{66}}{s_1 s_2} \hat{p} + \frac{C_{66}}{s_1^2} \hat{q} + \frac{C_{12}}{s_2 s_1} \hat{p} + \frac{C_{22}}{s_2^2} \hat{q} + \frac{C_{23}}{s_2 s_3} \hat{r} + \frac{C_{44}}{s_3^2} \hat{q} + \frac{C_{44}}{s_3 s_2} \hat{r} \\
&= \frac{\mu}{s_1 s_2} \hat{p} + \frac{\mu}{s_1^2} \hat{q} + \frac{\lambda}{s_2 s_1} \hat{p} + \frac{\lambda + 2\mu}{s_2^2} \hat{q} + \frac{\lambda}{s_2 s_3} \hat{r} + \frac{\mu}{s_3^2} \hat{q} + \frac{\mu}{s_3 s_2} \hat{r},
\end{aligned}$$

and for  $i = 3$

$$\begin{aligned}
\frac{C_{ijkl}}{s_j s_l} \hat{v}_k &= \frac{C_{3113}}{s_1 s_3} \hat{p} + \frac{C_{3131}}{s_1 s_1} \hat{r} + \frac{C_{3223}}{s_2 s_3} \hat{q} + \frac{C_{3232}}{s_2 s_2} \hat{r} + \frac{C_{3311}}{s_3 s_1} \hat{p} + \frac{C_{3322}}{s_3 s_2} \hat{q} + \frac{C_{3333}}{s_3 s_3} \hat{r} \\
&= \frac{C_{55}}{s_1 s_3} \hat{p} + \frac{C_{55}}{s_1^2} \hat{r} + \frac{C_{44}}{s_2 s_3} \hat{q} + \frac{C_{44}}{s_2^2} \hat{r} + \frac{C_{31}}{s_3 s_1} \hat{p} + \frac{C_{32}}{s_3 s_2} \hat{q} + \frac{C_{33}}{s_3^2} \hat{r} \\
&= \frac{\mu}{s_1 s_3} \hat{p} + \frac{\mu}{s_1^2} \hat{r} + \frac{\mu}{s_2 s_3} \hat{q} + \frac{\mu}{s_2^2} \hat{r} + \frac{\lambda}{s_3 s_1} \hat{p} + \frac{\lambda}{s_3 s_2} \hat{q} + \frac{\lambda + 2\mu}{s_3^2} \hat{r}.
\end{aligned}$$

# Bibliography

- [1] J. Dominguez and T. Meise. On the use of the BEM for wave propagation in infinite domains. *Engineering Analysis with Boundary Elements*, 8(3):132–138, 1991.
- [2] S. V. Tsynkov. Numerical solution of problems on unbounded domains. A review. *Applied Numerical Mathematics*, 27(4):465–532, 1998.  
(Special Issue on Absorbing Boundary Conditions).
- [3] S. Song, H. J. Shin, and Y. H. Jang. Development of an ultrasonic phased array system for nondestructive tests of nuclear power plant components. *Nuclear Engineering and Design*, 214(1):151–161, 2002.
- [4] C. Meola, G. M. Carlomagno, A. Squillace, and A. Vitiello. Non-destructive evaluation of aerospace materials with lock-in thermography. *Engineering Failure Analysis*, 13(3):380–388, 2006.
- [5] G. Dhatt, E. Lefrançois, and G. Touzot. *Finite Element Method*. ISTE. Wiley, London, 2012.
- [6] O. C. Zienkiewicz, C. Emson, and P. Bettess. A novel boundary infinite element. *International Journal for Numerical Methods in Engineering*, 19(3):393–404, 1983.



- [7] R. Clayton and B. Engquist. Absorbing boundary conditions for acoustic and elastic wave equations. *Bulletin of the Seismological Society of America*, 67(6):1529–1540, 1977.
- [8] J.P. Berenger. A perfectly matched layer for the absorption of electromagnetic waves. *Journal of Computational Physics*, 114:185–200, 1994.
- [9] P. Bettess. *Infinite Elements*. Penshaw Press, Sunderland, 1992.
- [10] M.F. Davis. Audio and Electroacoustics. In T. Rossing, editor, *Springer Handbook of Acoustics*, chapter 18, pages 779–817. Springer-Verlag, New York, 2nd edition, 2014.
- [11] A.D. Grinnell, E. Gould, and M.B. Fenton. A History of the Study of Echolocation. In M.B. Fenton, A.D. Grinnell, A.N. Popper, and R.R. Fay, editors, *Bat Bioacoustics*, chapter 1, pages 1–24. Springer, New York, 2016.
- [12] J.F.C. Windmill, J.C. Jackson, E.J. Tuck, and D. Robert. Keeping up with Bats: Dynamic Auditory Tuning in a Moth. *Current Biology*, 16(24):2418–2423, 2006.
- [13] B. Møhl. Target detection by echolocating bats. In *Animal sonar*, pages 435–450. Springer, 1988.
- [14] L.G. Barrett-Lennard, J.K.B. Ford, and K.A. Heise. The mixed blessing of echolocation: differences in sonar use by fish-eating and mammal-eating killer whales. *Animal Behaviour*, 51(3):553–565, 1996.
- [15] C. Lees, J. Abramowicz, C. Brezinka, K. Salvesen, G. ter Haar, K. Marsal, and S.F. Axell, R. and Smith. Ultrasound from Conception to 10<sup>+0</sup> Weeks of Gestation. *Royal College of Obstetricians and Gynaecologists Scientific Impact Paper No.49*, 2015.

- [16] T. Grau, R.W. Leipold, R. Conradi, E. Martin, and J. Motsch. Efficacy of ultrasound imaging in obstetric epidural anesthesia. *Journal of Clinical Anesthesia*, 14(3):169–175, 2002.
- [17] V. Catanzarite, C. Maida, W. Thomas, A. Mendoza, L. Stanco, and K.M. Picquadio. Prenatal sonographic diagnosis of vasa previa: ultrasound findings and obstetric outcome in ten cases. *Ultrasound in Obstetrics & Gynecology*, 18(2):109–115, 2001.
- [18] B. Kallam, A. Abuhamad, J. Hermida, F. Nesi, M.L. Joseph, E. Fiekowsky, and L. Noguchi. Development of obstetric ultrasound service delivery assessment tools in the context of the zika virus epidemic in five USAID priority countries. *American Journal of Obstetrics and Gynecology*, 217(6):724–725, 2017.
- [19] E.C. Smith, K.I. Xixis, G.A. Grant, and S.A. Grant. Assessment of obstetric brachial plexus injury with preoperative ultrasound. *Muscle & Nerve*, 53(6):946–950, 2016.
- [20] G. Leech. Physical Principals and the Basic Exam. In P. Nihoyannopoulos and J. Kisslo, editors, *Echocardiography*, chapter 1, pages 3–30. Springer, London, 2009.
- [21] B.N. Potkin, A.L. Bartorelli, J.M. Gessert, R.F. Neville, Y. Almagor, W.C. Roberts, and M.B. Leon. Coronary artery imaging with intravascular high-frequency ultrasound. *Circulation*, 81(5):1575–1585, 1990.
- [22] P.A. Blanco and T.F. Cianciulli. Pulmonary edema assessed by ultrasound: impact in cardiology and intensive care practice. *Echocardiography*, 33(5):778–787, 2016.

- [23] N.E. Hasselberg and T. Edvardsen. Ultrasound/echocardiography. In *Advanced Cardiac Imaging*, pages 15–46. Elsevier, 2015.
- [24] R. Arntfield, J. Pace, M. Hewak, and D. Thompson. Focused transesophageal echocardiography by emergency physicians is feasible and clinically influential: observational results from a novel ultrasound program. *Journal of Emergency Medicine*, 50(2):286–294, 2016.
- [25] K.R. Erikson, F.J. Fry, and J.P. Jones. Ultrasound in medicine-a review. *IEEE Transactions On Sonics and Ultrasonics*, SU-21, No.3:144–170, 1974.
- [26] P.G. Newman and G.S. Rozycki. The history of ultrasound. *Surgical Clinics of North America*, 78(2):179–195, 1998.
- [27] D. Kane, W. Grassi, R. Sturrock, and P.V. Balint. A brief history of musculoskeletal ultrasound: From bats and ships to babies and hips. *Rheumatology*, 43(7):931–933, 2004.
- [28] R.G. Stein, D. Wollschläger, R. Kreienberg, W. Janni, M. Wischnewsky, J. Diessner, T. Stüber, C. Bartmann, M. Krockenberger, J. Wischhusen, et al. The impact of breast cancer biological subtyping on tumor size assessment by ultrasound and mammography-a retrospective multicenter cohort study of 6543 primary breast cancer patients. *BMC Cancer*, 16(1):459, 2016.
- [29] R. Guo, G. Lu, B. Qin, and B. Fei. Ultrasound imaging Technologies for Breast Cancer Detection and Management: a review. *Ultrasound in Medicine and Biology*, 44(1):37–70, 2018.
- [30] C.C. Riedl, N. Luft, C. Bernhart, M. Weber, M. Bernathova, M.M. Tea, M. Rudas, C.F. Singer, and T.H. Helbich. Triple-modality screening trial for familial breast cancer underlines the importance of magnetic resonance

- imaging and questions the role of mammography and ultrasound regardless of patient mutation status, age, and breast density. *Journal of Clinical Oncology*, 33(10):1128–1135, 2015.
- [31] L. Medina-Valdés, M. Pérez-Liva, J. Camacho, J.M. Udías, J.L. Herraiz, and N. González-Salido. Multi-modal ultrasound imaging for breast cancer detection. *Physics Procedia*, 63:134–140, 2015.
- [32] C.F. Njeh, C.M. Boivin, and C.M. Langton. The role of ultrasound in the assessment of osteoporosis: a review. *Osteoporosis International*, 7(1):7–22, 1997.
- [33] A. Saverino, M. Del Sette, M. Conti, D. Ermirio, M. Ricca, G. Rovetta, and C. Gandolfo. Hyperechoic plaque: an ultrasound marker for osteoporosis in acute stroke patients with carotid disease. *European Neurology*, 55(1):31–36, 2006.
- [34] K. Thomsen, J. Ryg, A.P. Hermann, L. Matzen, and T. Masud. Calcaneal quantitative ultrasound and Phalangeal radiographic absorptiometry alone or in combination in a triage approach for assessment of osteoporosis: a study of older women with a high prevalence of falls. *BMC geriatrics*, 14(1):143, 2014.
- [35] I. Ghozlani, A. El Maataoui, M. Ghazi, A. Kherrab, and R. Niamane. AB0836 Performance of quantitative ultrasound and six osteoporosis risk indexes in menopausal women: validation and comparative evaluation study, 2017.
- [36] N. Petterson, E. van Disseldorp, F. van de Vosse, M. van Sambeek, and R. Lopata. Improved ultrasound-based mechanical characterization of ab-

- dominal aortic aneurysms. In *2017 IEEE International Ultrasonics Symposium*, Washington, DC, 2017. IEEE.
- [37] J.M. Guirguis-Blake, T.L. Beil, C.A. Senger, and E.P. Whitlock. Ultrasonography screening for abdominal aortic aneurysms: a systematic evidence review for the US Preventive Services Task Force. *Annals of Internal Medicine*, 160(5):321–329, 2014.
- [38] N.C. Batagini, C.A.P. Ventura, M.L. Raghavan, M.C. Chammas, A. Tachibana, and E.S. da Silva. Volumetry and biomechanical parameters detected by 3D and 2D ultrasound in patients with and without an abdominal aortic aneurysm. *Vascular Medicine*, 21(3):209–216, 2016.
- [39] A. Wittek, C. Blase, W. Derwich, T. Schmitz-Rixen, and C. Fritzen. Characterization of the mechanical behavior and pathophysiological state of abdominal aortic aneurysms based on 4D ultrasound strain imaging. In *Optical Methods for Inspection, Characterization, and Imaging of Biomaterials III*, volume 10333, page 1033303. International Society for Optics and Photonics, 2017.
- [40] D.A. Hernandez, V.H. Contreras, L. Leija, A. Vera, D. Martinez-Fong, and M.I. Gutierrez. Acoustic field simulation for focused ultrasound on skull with craniotomy for drug delivery in rat brain. In *2017 Global Medical Engineering Physics Exchanges/Pan American Health Care Exchanges*, pages 1–5, Tuxtla-Gutierrez, Mexico, 2017. IEEE.
- [41] H. Liu, M. Hua, P. Chen, P. Chu, C. Pan, H. Yang, C. Huang, J. Wang, T. Yen, and K. Wei. Blood-brain barrier disruption with focused ultrasound enhances delivery of chemotherapeutic drugs for glioblastoma treatment. *Radiology*, 255(2):415–425, 2010.

- [42] V. Krishna, F. Sammartino, and A. Rezai. A Review of the Current Therapies, Challenges, and Future Directions of Transcranial Focused Ultrasound Technology: Advances in Diagnosis and Treatment. *JAMA neurology*, 75(2):246–254, 2018.
- [43] C. Fan, C. Ting, Y. Chang, K. Wei, H. Liu, and C. Yeh. Drug-loaded bubbles with matched focused ultrasound excitation for concurrent blood-brain barrier opening and brain-tumor drug delivery. *Acta Biomaterialia*, 15:89–101, 2015.
- [44] J. de Ruijter, F. van de Vosse, M. van Sambeek, and R. Lopata. Mechanical characterization of vascular tissue using ultrasound. In *2017 IEEE International Ultrasonics Symposium*, Washington, DC, 2017. IEEE.
- [45] B. Mahmood, C. Ewertsen, J. Carlsen, and M.B. Nielsen. Ultrasound Vascular Elastography as a Tool for Assessing Atherosclerotic Plaques—A Systematic Literature Review. *Ultrasound International Open*, 2(4):E106, 2016.
- [46] J. N. Ramalho and M. Castillo, editors. Wiley-Blackwell, Hoboken, New Jersey.
- [47] E. Picano and M. Paterni. Ultrasound tissue characterization of vulnerable atherosclerotic plaque. *International Journal of Molecular Sciences*, 16(5):10121–10133, 2015.
- [48] W.W. Roberts, T.L. Hall, K. Ives, J.S. Wolf, J.B. Fowlkes, and C.A. Cain. Pulsed cavitation ultrasound: a noninvasive technology for controlled tissue ablation (histotripsy) in the rabbit kidney. *Journal of Urology*, 175(2):734–738, 2006.

- [49] A.D. Maxwell, C.A. Cain, A.P. Duryea, L. Yuan, H.S. Gurm, and Z. Xu. Noninvasive thrombolysis using pulsed ultrasound cavitation therapy–histotripsy. *Ultrasound in Medicine and Biology*, 35(12):1982–1994, 2009.
- [50] K. Kieran, T.L. Hall, J.E. Parsons, J.S. Wolf, J.B. Fowlkes, C.A. Cain, and W.W. Roberts. Refining histotripsy: defining the parameter space for the creation of nonthermal lesions with high intensity, pulsed focused ultrasound of the in vitro kidney. *Journal of Urology*, 178(2):672–676, 2007.
- [51] K. Lin, Y. Kim, A.D. Maxwell, T. Wang, T.L. Hall, Z. Xu, J.B. Fowlkes, and C. Cain. Histotripsy beyond the intrinsic cavitation threshold using very short ultrasound pulses: Microtripsy. *IEEE Transactions on Ultrasonics, Ferroelectrics, and Frequency Control*, 61(2):251–265, 2014.
- [52] T. Ikeda, S. Yoshizawa, N. Koizumi, M. Mitsuishi, and Y. Matsumoto. Focused ultrasound and lithotripsy. In *Therapeutic Ultrasound*, pages 113–129. Springer, 2016.
- [53] P.C. May, W. Kreider, A.D. Maxwell, Y.N. Wang, B.W. Cunitz, P.M. Blomgren, C.D. Johnson, J.S.H. Park, M.R. Bailey, D. Lee, J.D. Harper, and M.D. Sorensen. Detection and evaluation of renal injury in burst wave lithotripsy using ultrasound and magnetic resonance imaging. *Journal of Endourology*, 31(8):786–792, 2017.
- [54] H.E. Smith, D.A. Bryant, J. KooNg, R.A. Chapman, and G. Lewis. Extracorporeal shockwave lithotripsy without radiation: Ultrasound localization is as effective as fluoroscopy. *Urology Annals*, 8(4):454, 2016.

- [55] A.D. Maxwell, B.W. Cunitz, W. Kreider, O.A. Sapozhnikov, R.S. Hsi, J.D. Harper, M.R. Bailey, and M.D. Sorensen. Fragmentation of urinary calculi in vitro by burst wave lithotripsy. *Journal of Urology*, 193(1):338–344, 2015.
- [56] A.D. Walmsley. Ultrasonics in dentistry. *Physics Procedia*, 63:201–207, 2015.
- [57] J. Marotti, S. Heger, J. Tinschert, P. Tortamano, F. Chuembou, K. Radermacher, and S. Wolfart. Recent advances of ultrasound imaging in dentistry—a review of the literature. *Oral Surgery, Oral Medicine, Oral Pathology and Oral Radiology*, 115(6):819–832, 2013.
- [58] S.K. Karumuri, T. Rastogi, K. Beeraka, M.R. Penumatcha, and S.R. Olepu. Ultrasound: a revenant therapeutic modality in dentistry. *Journal of Clinical and Diagnostic Research*, 10(7):ZE08, 2016.
- [59] R. Vayron, V.H. Nguyen, S. Naili, and G. Haiat. Ultrasound Assessment of Dental Implant Stability: Finite Element Analysis of Wave Propagation. In *International Conference on the Development of Biomedical Engineering in Vietnam*, pages 387–392. Springer, 2017.
- [60] P. Akermann. *Encyclopedia of British Submarines 1901-1955*. Periscope Publishing, Limited, 2002.
- [61] A. D’Amico and R. Pittenger. A brief history of active sonar. Technical report, Space and Naval Warfare Systems Center, San Diego CA, 2009.
- [62] S. Zhang, C. Xia, and N. Fang. Broadband acoustic cloak for ultrasound waves. *Physical Review Letters*, 106(2):024301, 2011.
- [63] W.S. Gan. Underwater Acoustical Cloaking. In *New Acoustics Based on Metamaterials*, pages 259–275. Springer, 2018.



- [64] S.A. Cummer and D. Schurig. One path to acoustic cloaking. *New Journal of Physics*, 9(3):45, 2007.
- [65] F. Chemat, N. Rombaut, A. Sicaire, A. Meullemiestre, A. Fabiano-Tixier, and M. Abert-Vian. Ultrasound assisted extraction of food and natural products. Mechanisms, techniques, combinations, protocols and applications. A review. *Ultrasonics Sonochemistry*, 34:540–560, 2017.
- [66] T.J. Mason, F. Chemat, and M. Vinatoru. The extraction of natural products using ultrasound or microwaves. *Current Organic Chemistry*, 15(2):237–247, 2011.
- [67] V. Sivakumar, J. Vijaeeswarri, and J.L. Anna. Effective natural dye extraction from different plant materials using ultrasound. *Industrial Crops and Products*, 33(1):116–122, 2011.
- [68] M.D. Esclapez, J.V. García-Pérez, A. Mulet, and J.A. Cárcel. Ultrasound-assisted extraction of natural products. *Food Engineering Reviews*, 3(2):108, 2011.
- [69] F. Bot, S. Plazzotta, and M. Anese. Treatment of Food Industry Wastewater With Ultrasound: A Big Opportunity for the Technology. In *Ultrasound: Advances for Food Processing and Preservation*, pages 391–408. Elsevier, 2017.
- [70] F.G. Kootenaei, N. Mehrdadi, G.N. Bidhendi, and H.A. Rad. Application of Ultrasound waves for Sludge Dewatering. *International Journal of Life Sciences*, 9(4):6–9, 2015.

- [71] S.K. Khanal, D. Grewell, S. Sung, and J. Van Leeuwen. Ultrasound applications in wastewater sludge pretreatment: a review. *Critical Reviews in Environmental Science and Technology*, 37(4):277–313, 2007.
- [72] P.C. Sangave and A.B. Pandit. Ultrasound pre-treatment for enhanced biodegradability of the distillery wastewater. *Ultrasonics Sonochemistry*, 11(3-4):197–203, 2004.
- [73] S. Palma, B. Zhou, and H. Feng. Fresh Produce Treated by Power Ultrasound. In *Ultrasound: Advances for Food Processing and Preservation*, pages 201–213. Elsevier, 2017.
- [74] I.J. Seymour, D. Burfoot, R.L. Smith, L.A. Cox, and A. Lockwood. Ultrasound decontamination of minimally processed fruits and vegetables. *International Journal of Food Science & Technology*, 37(5):547–557, 2002.
- [75] H. Sagong, S. Lee, P. Chang, S. Heu, S. Ryu, Y. Choi, and D. Kang. Combined effect of ultrasound and organic acids to reduce *Escherichia coli* O157:H7, *Salmonella* Typhimurium, and *Listeria monocytogenes* on organic fresh lettuce. *International Journal of Food Microbiology*, 145(1):287–292, 2011.
- [76] J.F.B. São José and M.C.D. Vanetti. Effect of ultrasound and commercial sanitizers in removing natural contaminants and *Salmonella enterica* Typhimurium on cherry tomatoes. *Food Control*, 24(1-2):95–99, 2012.
- [77] K.J. Wu, T.S. Gregory, J. Moore, B. Hooper, D. Lewis, and Z.T.H. Tse. Development of an indoor guidance system for unmanned aerial vehicles with power industry applications. *IET Radar, Sonar & Navigation*, 11(1):212–218, 2016.

- [78] G. Sposito, C. Ward, P. Cawley, P.B. Nagy, and C. Scruby. A review of non-destructive techniques for the detection of creep damage in power plant steels. *NDT & E International*, 43(7):555–567, 2010.
- [79] M.H. Skjelvareid, Y. Birkelund, and Y. Larsen. Internal pipeline inspection using virtual source synthetic aperture ultrasound imaging. *NDT & E International*, 54:151–158, 2013.
- [80] D.K. Hsu. Non-destructive evaluation (NDE) of aerospace composites: ultrasonic techniques. In V.M. Karbhari, editor, *Non-Destructive Evaluation (NDE) of Polymer Matrix Composites*, Woodhead Publishing Series in Composites Science and Engineering, chapter 15, pages 397–422. Woodhead Publishing, 2013.
- [81] X. Guan, J. Zhang, E.M. Rasselkorde, W.A. Abbasi, and S.K. Zhou. Material damage diagnosis and characterization for turbine rotors using three-dimensional adaptive ultrasonic NDE data reconstruction techniques. *Ultrasonics*, 54(2):516–525, 2014.
- [82] S. Gholizadeh. A review of non-destructive testing methods of composite materials. *Procedia Structural Integrity*, 1:50–57, 2016.
- [83] M.R. Jolly, A. Prabhakar, B. Sturzu, K. Hollstein, R. Singh, S. Thomas, P. Foote, and A. Shaw. Review of Non-destructive Testing (NDT) Techniques and their Applicability to Thick Walled Composites. In *Proceedings of the 4th International Conference on Through-life Engineering Services*, volume 38, pages 129–136, Cranfield, UK, 2015.

- [84] G. Dobie, R. Summan, S. G. Pierce, W. Galbraith, and G. Hayward. A Noncontact Ultrasonic Platform for Structural Inspection. *IEEE Sensors Journal*, 11(10):2458–2468, Oct 2011.
- [85] L.L. Thompson and P.M. Pinsky. A space-time finite element method for structural acoustics in infinite domains part 1: Formulation, stability and convergence. *Computer Methods in Applied Mechanics and Engineering*, 132(3-4):195–227, 1996.
- [86] D. Givoli and S. Vigdergauz. Artificial boundary conditions for 2D problems in geophysics. *Computer methods in applied mechanics and engineering*, 110(1-2):87–101, 1993.
- [87] Y.M. Shen, Y.H. Zheng, and Y.G. You. On the radiation and diffraction of linear water waves by a rectangular structure over a sill. Part I. Infinite domain of finite water depth. *Ocean Engineering*, 32(8):1073–1097, 2005.
- [88] J.P. Boyd. Orthogonal rational functions on a semi-infinite interval. *Journal of Computational Physics*, 70(1):63–88, 1987.
- [89] C. Pescatore and G. Spiga. Functional analysis of integral transport equations in linear rarefied gas dynamics. *Meccanica*, 12(3):134–137, 1977.
- [90] S.S. Saini, P. Bettess, and O.C. Zienkiewicz. Coupled hydrodynamic response of concrete gravity dams using finite and infinite elements. *Earthquake Engineering & Structural Dynamics*, 6(4):363–374, 1978.
- [91] Q. Chen and A. Konrad. A review of finite element open boundary techniques for static and quasi-static electromagnetic field problems. *IEEE Transactions on Magnetics*, 33(1):663–676, 1997.

- [92] D. Givoli. *Numerical Methods for Problems in Infinite Domains*, volume 33 of *Studies in Applied Mechanics*. Elsevier Science Publishers B.V., Amsterdam, 1992.
- [93] I. Harari. A survey of finite element methods for time-harmonic acoustics. *Computer Methods in Applied Mechanics and Engineering*, 195:1594–1607, 2006.
- [94] L.L. Thompson. A review of finite element methods for time-harmonic acoustics. *Journal of the Acoustical Society of America*, 119:1315–1330, 2006.
- [95] U. Basu. Perfectly matched layers for acoustic and elastic waves: Theory, finite-element implementation and application to earthquake analysis of dam-water-foundation rock systems. *Dam Safety Research Program, US Department of the Interior, Bureau of Reclamation*, 2008. Report DSO-07-02.
- [96] I. Harari, M. Slavutin, and E. Turkel. Analytical and numerical studies of a finite element PML for the Helmholtz equation. *Journal of Computational Acoustics*, 8(01):121–137, 2000.
- [97] A. Bermudez, L. Hervella-Nieto, A. Prieto, and R. Rodríguez. An optimal finite-element/PML method for the simulation of acoustic wave propagation phenomena. In E. Taroco, E.A. de Souza Neto, and A.A. Novotny, editors, *Variational Formulation in Mechanics: Theory and Applications*, pages 43–54. CIMNE, Barcelona, Spain, 2007.
- [98] Y. Li and O. Bou Matar. Convolutional perfectly matched layer for elastic second-order wave equation. *The Journal of the Acoustical Society of America*, 127(3):1318–1327, 2010.

- [99] P. Rajagopal, M. Drozdz, E.A. Skelton, M.J.S. Lowe, and R.V. Craster. On the use of absorbing layers to simulate the propagation of elastic waves in unbounded isotropic media using commercially available finite element packages. *NDT & E International*, 51:30–40, 2012.
- [100] M.B. Drozdz. *Efficient finite element modelling of ultrasound waves in elastic media*. PhD thesis, Imperial College London, 2008.
- [101] K. Hasegawa and T. Shimada. Perfectly Matched Layer for Finite Element Analysis of Elastic Waves in Solids. In F. Ebrahimi, editor, *Finite Element Analysis - Applications in Mechanical Engineering*, chapter 8. InTech, Rijeka, Croatia, 2012.
- [102] J. Kocbach. *Finite element modeling of ultrasonic piezoelectric transducers*. PhD thesis, University of Bergen, 2000.
- [103] N.N. Abboud, G.L. Wojcik, D.K. Vaughan, J. Mould Jr, D.J. Powell, and L. Nikodym. Finite element modeling for ultrasonic transducers. In *Medical Imaging '98*, pages 19–42. International Society for Optics and Photonics, 1998.
- [104] M.W. Nygren. Finite element modeling of piezoelectric ultrasonic transducers. Master's thesis, Norwegian University of Science and Technology, 2011.
- [105] O. Al-Hattamleh, J. Cho, R.F. Richards, D.F. Bahr, and C.D. Richards. The effect of design and process parameters on electromechanical coupling for a thin-film PZT membrane. *Journal of microelectromechanical systems*, 15(6):1715–1725, 2006.

- [106] S.Y. Wang. A finite element model for the static and dynamic analysis of a piezoelectric bimorph. *International Journal of Solids and Structures*, 41(15):4075–4096, 2004.
- [107] W. Hwang and H.C. Park. Finite element modeling of piezoelectric sensors and actuators. *AIAA journal*, 31(5):930–937, 1993.
- [108] F. Akasheh, T. Myers, J.D. Fraser, S. Bose, and A. Bandyopadhyay. Development of piezoelectric micromachined ultrasonic transducers. *Sensors and Actuators A: Physical*, 111(2):275–287, 2004.
- [109] PZFlex. <http://www.pzflex.com/>. Accessed: 11th April 2018.
- [110] Engquist, B. and Majda, A. Radiation boundary conditions for acoustic and elastic wave calculations. *Communications on Pure and Applied Mathematics*, 32(3):313–357, 1979.
- [111] A. Bayliss, M. Gunzburger, and E. Turkel. Boundary conditions for the numerical solution of elliptic equations in exterior regions. *SIAM Journal on Applied Mathematics*, 42(2):430–451, 1982.
- [112] F. Collino. High order absorbing boundary conditions for wave propagation models. In Kleinman, editor, *Proceedings of the 2nd International Conference on Mathematical and Numerical Aspects of Wave Propagation*, pages 161–171. SIAM, Philadelphia, 1993.
- [113] J. Keller and D. Givoli. Exact non-reflecting boundary conditions. *Journal of Computational Physics*, 82:172–192, 1989.
- [114] A.H.-D. Cheng and D.T. Cheng. Heritage and early history of the boundary element method. *Engineering Analysis with Boundary Elements*, 29(3):268–302, mar 2005.

- [115] W.C. Chew and Q.H. Liu. Perfectly matched layers for elastodynamics: a new absorbing boundary condition. *Journal of Computational Acoustics*, 4(4):341–359, 1996.
- [116] M.R. Lyons, A.C. Polycarpou, and C.A. Balanis. On the accuracy of perfectly matched layers using a finite element formulation. In *IEEE Microwave Theory and Techniques Society International Symposium Digest*, volume 1, pages 205–208, San Francisco, California, June 1996.
- [117] Q.H. Liu and J. Tao. The perfectly matched layer for acoustic waves in absorptive media. *Journal of the Acoustical Society of America*, 102(4):2072–2082, 1997.
- [118] Q. Qi and T.L. Geers. Evaluation of the perfectly matched layer for computational acoustics. *Journal of Computational Physics*, 139:166–183, 1998.
- [119] E. Turkel and A. Yefet. Absorbing PML boundary layers for wave-like equations. *Applied Numerical Mathematics*, 27:533–557, 1998.
- [120] U. Basu and A.K. Chopra. Perfectly matched layers for time-harmonic elastodynamics of unbounded domains: theory and finite-element implementation. *Computer Methods in Applied Mechanics and Engineering*, 192:1337–1375, 2003.
- [121] C. Michler, L. Demkowicz, J. Kurtz, and D. Pardo. Improving the performance of Perfectly Matched Layers by means of hp-adaptivity. Technical report, Institute for Computational Engineering and Sciences, The University of Texas at Austin, 201 East 24th Street, ACES Building, Austin, TX, 78712, USA, 2006.



- [122] Z. Chen and H. Wu. An adaptive finite element method with perfectly matched absorbing layers for the wave scattering by periodic structures. *SIAM Journal on Numerical Analysis*, 41(3):799–826, 2003.
- [123] D. Correia and J.M. Jin. On the development of a higher-order PML. *IEEE Transactions on Antennas and Propagation*, 53(12):4157–4163, 2005.
- [124] X. Yuan, D. Borup, J.W. Wiskin, M. Berggren, R. Eidsens, and S.A. Johnson. Formulation and validation of Berenger’s PML absorbing boundary for the FDTD simulation of acoustic scattering. *IEEE Transactions on Ultrasonics, Ferroelectrics, and Frequency Control*, 44(4):816–822, 1997.
- [125] R.J. Astley. Infinite elements for wave problems: a review of current formulations and an assessment of accuracy. *International Journal of Numerical Methods in Engineering*, 49:951–976, 2000.
- [126] D. Dreyer and O. Von Estorff. Improved conditioning of infinite elements for exterior acoustics. *International Journal for Numerical Methods in Engineering*, 58(6):933–953, 2003.
- [127] K. Gerdes. A summary of infinite element formulations for exterior Helmholtz problems. *Computer methods in applied mechanics and engineering*, 164(1-2):95–105, 1998.
- [128] L. Cremers and K.R. Fyfe. On the use of variable order infinite wave envelope elements for acoustic radiation and scattering. *The Journal of the Acoustical Society of America*, 97(4):2028–2040, 1995.
- [129] L. Demkowicz and J. Shen. A few new (?) facts about infinite elements. *Computer methods in applied mechanics and engineering*, 195(29):3572–3590, 2006.

- [130] J.A. Bettess and P. Bettess. A new mapped infinite wave element for general wave diffraction problems and its validation on the ellipse diffraction problem. *Computer methods in applied mechanics and engineering*, 164(1-2):17–48, 1998.
- [131] R.J. Astley and J.P. Coyette. The performance of spheroidal infinite elements. *International Journal for Numerical Methods in Engineering*, 52(12):1379–1396, 2001.
- [132] R.J. Astley and J.P. Coyette. Conditioning of infinite element schemes for wave problems. *International Journal for Numerical Methods in Biomedical Engineering*, 17(1):31–41, 2001.
- [133] D. Dreyer, S. Petersen, and O. von Estorff. Effectiveness and robustness of improved infinite elements for exterior acoustics. *Computer Methods in Applied Mechanics and Engineering*, 195(29):3591–3607, 2006.
- [134] R.J. Astley. Transient wave envelope elements for wave problems. *Journal of Sound and Vibration*, 192(1):245–261, 1996.
- [135] R.J. Astley, J.P. Coyette, and L. Cremers. Three-dimensional wave-envelope elements of variable order for acoustic radiation and scattering. Part II. Formulation in the time domain. *The Journal of the Acoustical Society of America*, 103(1):64–72, 1998.
- [136] J.L. Cipolla and M.J. Butler. Infinite elements in the time domain using a prolate spheroidal multipole expansion. *International Journal for Numerical Methods in Engineering*, 43(5):889–908, 1998.

- [137] R.J. Astley and J.A. Hamilton. The stability of infinite element schemes for transient wave problems. *Computer Methods in Applied Mechanics and Engineering*, 195(29):3553–3571, 2006.
- [138] M. Ross. Modeling methods for silent boundaries in infinite media. *Fluid-Structure Interaction, Aerospace Engineering Sciences – University of Colorado at Boulder*, pages 5519–006, 2004.
- [139] C. Zhao and S. Valliappan. Transient infinite elements for contaminant transport problems. *International Journal for Numerical Methods in Engineering*, 37(7):1143–1158, 1994.
- [140] C. Zhao. *Dynamic and transient infinite elements: theory and geophysical, geotechnical and geoenvironmental applications*. Springer Science & Business Media, 2009.
- [141] A. Sommerfeld. *Partial differential equations in physics*, volume 1. Academic Press, 1949.
- [142] P.M. Morse and K.U. Ingard. *Theoretical Acoustics*. Princeton University Press, Princeton, New Jersey, 1968.
- [143] I. Harari and R. Djellouli. Analytical study of the effect of wave number on the performance of local absorbing boundary conditions for acoustic scattering. *Applied Numerical Mathematics*, 50:15–47, 2004.
- [144] M. Abramowitz and I.A. Stegun. *Handbook of Mathematical Functions*. US Department of Commerce, National Bureau of Standards, Washington, DC, 1964.

- [145] D.S. Burnett. Three-dimensional acoustic infinite element based on a prolate spheroidal multipole expansion. *Journal of the Acoustical Society of America*, 96:2798–2816, 1994.
- [146] D.S. Burnett and R.L. Holford. Prolate and oblate spheroidal acoustic infinite elements. *Computer Methods in Applied Mechanics and Engineering*, 158(1):117–141, 1998.
- [147] H. Assi and R. S. Cobbold. Compact second-order time-domain perfectly matched layer formulation for elastic wave propagation in two dimensions. *Mathematics and Mechanics of Solids*, 22(1):20–37, 2017.
- [148] J.L. Cipolla. Design for a hybrid absorbing element in the time domain using PML and Infinite Element concepts. In *Proceedings of the ASME 2014 International Mechanical Engineering Conference and Exposition*, page V013T16A011, Montreal, Quebec, Canada, November 2014.
- [149] J.S. Pettigrew, A.J. Mulholland, J.L. Cipolla, J. Mould, and R. Banks. A combined Perfectly Matching Layer and Infinite Element formulation for unbounded wave problems in the frequency domain. In *Proceedings of the ASME 2014 International Mechanical Engineering Conference and Exposition*, page V013T16A013, Montreal, Quebec, Canada, November 2014.
- [150] J.L. Rose. *Ultrasound waves in solid media*. Cambridge University Press, Cambridge, 1999.
- [151] Wolfram Research Inc. Mathematica. Version 9.0, 2012. Champaign, Illinois.